# CHARACTERIZATION OF GLYCEROL METABOLISM AND RELATED METABOLIC PATHWAYS IN THE HALOARCHAEAON *Haloferax volcanii*

By

KATHERINE SHERWOOD RAWLS

A DISSERTATION PRESENTED TO THE GRADUATE SCHOOL
OF THE UNIVERSITY OF FLORIDA IN PARTIAL FULFILLMENT
OF THE REQUIREMENTS FOR THE DEGREE OF
DOCTOR OF PHILOSOPHY

UNIVERSITY OF FLORIDA

2010

To my husband, Colin Rawls, who has been my guiding light, and to my parents, Steve and Francy Sherwood, for their unconditional love and support

ACKNOWLEDGMENTS

I express my deepest gratitude to my academic advisor, Dr. Julie Maupin-Furlow, for challenging my intellectual capabilities and for expanding my scientific curiosity. Her guidance during my graduate career has been crucial toward successful completion of my degree. I also wish to thank the additional members of my graduate supervisory committee, Drs. Linda Bloom, Graciela Lorca, Lonnie Ingram and K.T. Shanmugam for their project insight and for generous use of their equipment.

Special thanks are extended to current and former graduate students, post-doctoral students, laboratory technicians, and undergraduate researchers of the Maupin-Furlow research laboratory for creating a stimulating, pleasant environment in which to work. Specifically, I would like to acknowledge David Cano for his help in generating the glycerol kinase mutant; Shalane Yacovone and Mario Corro for their assistance in generating several knockout strains including the phosphotransferase system mutants, the dihydroxyacetone kinase mutants, and the GlpR repressor mutant; and Mayra Souza for her additional assistance in generating the GlpR repressor mutant as well as the transcriptional promoter-reporter fusion constructs. Also, I wish to thank Gosia Gil-Ramadas for her guidance as my undergraduate research mentor. Special thanks are also extended to Dr. Sivakumar Uthandi and Nikita Nembhard for their insightful advice and support, especially during my last semester of graduate school.

Thank you to all graduate funding agencies including the University of Florida Alumni Foundation, the Doris Lowe and Verna and Earl Lowe Scholarship Fund, the National Institute of Health, and the Department of Energy for their financial support of my dissertation project.

I finally wish to acknowledge my immediate family members: my parents, Francy and Steve Sherwood; my sister, Kelley Sherwood; my niece, Reagan Timmons; my grandmothers Johnnie Sherwood and Helen Glenn; and my late grandfathers Jim Sherwood and Bill Glenn, who have always graciously provided their moral and financial support throughout my academic career. I most importantly thank my husband, Colin Rawls, for providing unwavering love and encouragement throughout this challenging process.

TABLE OF CONTENTS

LIST OF TABLES

LIST OF FIGURES

## LIST OF ABBREVIATIONS

| | |
|---|---|
| Å | Angstrom |
| $A_{260}$ | Absorbance at 260 nm |
| $A_{280}$ | Absorbance at 280 nm |
| $A_{340}$ | Absorbance at 340 nm |
| $A_{405}$ | Absorbance at 405 nm |
| $A_{595}$ | Absorbance at 595 nm |
| $AAA^{+}$ | ATPase associated with diverse cellular activities |
| ABC | ATP binding cassette |
| AC | Adenylate cyclase |
| ADP | Adenosine-5’-diphosphate |
| Amp | Ampicillin |
| AP | Antarctic phosphatase |
| AR | Activating region |
| ATP | Adenosine-5’-triphosphate |
| ATCC | American type culture collection |
| BFD | Bacterioferritin-associated ferredoxin |
| BLAST | Basic local alignment search tool |
| °C | Degrees Celsius |
| C- | Carboxyl |
| CA | Casamino acids |
| cAMP | Cyclic AMP |
| cAMP-CRP | cAMP complexed with CRP |
| CFU | Colony forming units |
| cm | Centimeter |

| | |
|---|---|
| COG | Clusters of orthologous groups |
| *cre* | Catabolite responsive element |
| Crh | Catabolite repression protein Hpr |
| CRP | cAMP receptor protein |
| CSPD | Disodium 3-(4-methoxyspiro{1,2-dioxetane-3,2'-(5'-chloro)tricyclo[3.3.1.$1^{3,7}$]decan}-4-yl) phenyl phosphate |
| $C_T$ | Threshold count |
| Da | Dalton |
| DBD | DNA binding domain |
| DEPC | Diethylpyrocarbonate |
| DHA | Dihydroxyacetone |
| DHAK | Dihydroxyacetone kinase |
| DHAP | Dihydroxyacetone phosphate |
| DIG-11-dUTP | 2'-deoxyuridine-5'-triphosphate coupled by an 11-atom spacer to digoxigenin |
| DMSO | Dimethyl sulfoxide |
| DNA | Deoxyribonucleic acid |
| dNTP | Deoxyribonucleotide triphosphate |
| EI | Enzyme I of the PEP:PTS |
| EII | Enyzme II of the PEP:PTS |
| $EIIA^{Glc}$ | Glucose-specific phosphocarrier EII protein of the PEP:PTS |
| $E_a$ | Energy of activation (kcal·$mol^{-1}$) |
| ED | Entner-Doudoroff |
| EMP | Embden-Meyerhof-Parnas |
| EDTA | Ethylenediaminetetraacetic acid |
| F1P | Fructose-1-phosphate |

| | |
|---|---|
| FAD | Oxidized Flavin adenine dinucleotide |
| FADH | Reduced Flavin adenine dinucleotide |
| FBP | Fructose-1,6-bisphosphate |
| fg | Femtogram |
| FOA | 5-Fluoroorotic acid |
| Fru | Fructose |
| *g* | Gravitational force |
| G1P | Glycerol-1-phosphate |
| G3P | Glycerol-3-phosphate |
| G3PDH | Glycerol-3-phosphate dehydrogenase |
| G3PP | Glycerol-3-phosphate phosphatase |
| GD | Glycerol dehydratase |
| GDH | Glycerol dehydrogenase |
| GK | Glycerol kinase |
| Glu | Glucose |
| Gly | Glycerol |
| HPA | 3-Hydroxypropionaldehyde |
| HPLC | High performance liquid chromatography |
| Hpr | Histidine-containing phosphorylatable protein of the PTS |
| Hpt | Histidine-containing phosphotransfer domain |
| HTH | Helix-turn-helix |
| in | Inch |
| $K_{av}$ | Gel phase distribution coefficient |
| kcal | Kilocalorie |
| Kd | Binding dissociation constant |

| | |
|---|---|
| kDa | Kilodalton |
| KDG | 2-keto-3-deoxygluconate |
| KDGK | KDG kinase |
| KDPG | 2-keto-3-deoxy-6-phosphogluconate |
| $K_m$ | Michaelis Menten constant ($mol \cdot l^{-1}$) |
| LB | Luria-Bertani medium |
| lb | Pound |
| LDH | Lactate dehydrogenase |
| M | Molar ($mol \cdot liter^{-1}$) |
| MFS | Major facilitator superfamily |
| mg | Milligram |
| µg | Microgram |
| µM | Micromolar ($\mu mol \cdot liter^{-1}$) |
| min | Minutes |
| MIP | Major intrinsic protein |
| ml | Milliliter |
| MM | Minimal medium |
| mM | Millimolar ($mmol \cdot liter^{-1}$) |
| MOPS | 3-(N-Morpholino)propanesulfonic acid, 4-Morpholinepropanesulfonic acid |
| N- | Amino |
| $NAD^+$ | Oxidized Nicotinamide adenine dinucleotide |
| NADH | Reduced Nicotinamide adenine dinucleotide |
| n.d. | Not determined |
| nm | Nanometer |
| NMR | Nuclear magnetic resonance |

| | |
|---|---|
| Nv | Novobiocin |
| $OD_{600}$ | Optical density at 600 nm |
| ONPG | *o*-nitrophenyl-β-D-galactopyranoside |
| OR | Oxidoreductase |
| ORF | Open reading frame |
| PAGE | Polyacrylamide gel electrophoresis |
| PCR | Polymerase chain reaction |
| PDH | 1,3-Propanediol dehydrogenase |
| PEP | Phosphoenolpyruvate |
| PFK | Phosphofructokinase |
| PFL | Pyruvate formate lyase |
| PMSF | Phenylmethylsulfonyl fluoride |
| PNK | Polynucleotide kinase |
| PRD | PEP carbohydrate PTS regulatory domain |
| PTS | Phosphotransferase system |
| qRT-PCR | Quantitative reverse-transcriptase polymerase chain reaction |
| $R^2$ | Coefficient of determination |
| rRNA | Ribosomal RNA |
| RNA | Ribonucleic acid |
| RPM | Revolutions per minute |
| RT | Reverse transcriptase |
| s | Seconds |
| SAM | *S*-adenosyl methionine |
| SD | Standard deviation |
| SDS | Sodium dodecyl sulfate |

| | |
|---|---|
| SSC | Saline sodium citrate |
| TBP | TATA binding protein |
| TFB | Transcription factor B |
| TIM | Triosephosphate isomerase |
| TM | Transmembrane |
| Tris | N-tris(hydroxylmethyl)aminomethane |
| U | Enzyme activity unit [$\mu mol \cdot min^{-1} \cdot (mg\ protein)^{-1}$] |
| UV | Ultraviolet |
| V | Volt |
| v | Volume (in ml) |
| $V_o$ | Void volume of the column (ml) |
| $V_C$ | Geometric bed volume (ml) |
| $V_{max}$ | Maximal velocity ($mol \cdot l^{-1} s^{-1}$) |
| $V_R$ | Retention (elution) volume of the protein (ml) |
| w | Weight (grams) |
| YPC | Yeast peptone casamino acids medium |

Abstract of Dissertation Presented to the Graduate School
of the University of Florida in Partial Fulfillment of the
Requirements for the Degree of Doctor of Philosophy

CHARACTERIZATION OF GLYCEROL METABOLISM AND RELATED METABOLIC PATHWAYS IN THE HALOARCHAEAON *Haloferax volcanii*

By

Katherine Sherwood Rawls

December 2010

Chair: Julie Maupin-Furlow
Major: Microbiology and Cell Science

The molecular mechanisms surrounding carbon utilization and its regulation are not well characterized in haloarchaea. Glycerol is a readily-abundant energy source for halophilic, heterotrophic communities as a result of its large-scale production by the halotolerant green algae *Dunaliella sp.* This study sought to characterize glycerol catabolism in the model haloarchaeon *Haloferax volcanii*. This work provides evidence that glycerol is a preferred carbon source over glucose and that the former is metabolized through chromosomally-encoded glycerol kinase (*glpK*) and glycerol-3-phosphate dehydrogenase (*gpdA1B1C1*). Both *glpK* and *gpdA1* transcripts were glycerol-inducible, and the enzymatic activity of their gene products was not inhibited by glucose. Furthermore, *glpK* and *gpdA1B1C1* are under the control of a strong, glycerol-inducible promoter. The glycerol metabolic operon also includes a putative glycerol facilitator as well as a homolog of the bacterial phosphotransferase system (PTS) protein Hpr. Additional bacterial PTS homologs EI and EII are encoded in the *H. volcanii* genome and preliminary evidence suggests that these EI and $EIIB^{Fru}$ homologs may be involved in *H. volcanii* fructose metabolism. This work also examines the regulation of haloarchaeal carbon metabolism in *H. volcanii*, including the characterization of a

DeoR/GlpR-type transcriptional repressor of glucose and fructose metabolic enzymes. The putative DeoR/GlpR-type protein encoded by *glpR* is transcriptionally-linked to *pfkB* encoding phosphofructokinase (PFK). Based on qRT-PCR, enzyme activity, and transcriptional reporter analyses, GlpR is likely a transcriptional repressor of genes encoding PFK and 2-keto-3-deoxygluconate kinase, two key enzymes of haloarchaeal fructose and glucose metabolism, respectively. This GlpR protein purified as a tetramer by gel filtration chromatography under both high and low salt and is postulated to use a phosphorylated intermediate of either glucose and/or fructose metabolism as its ligand. A putative repressor binding motif consisting of an inverted hexameric repeat was identified adjacent to characterized archaeal promoter consensus motifs upstream of the *kdgK1* and *glpR-pfkB* genes. Taken together, our results provide insight into the carbon metabolic pathways of various investigated heterotrophic haloarchaea.

# CHAPTER 1
# LITERATURE REVIEW

## Introduction

This literature review is designed to present the most relevant, primary scientific literature concerning glycerol, glucose, and fructose metabolism and their regulation in the three domains of life. The review will highlight characterized glycerol metabolic enzymes, regulation of glycerol metabolism, glycerol transport across the biological membrane, and the biological relevance of glycerol including its industrial and medical applications. This review will additionally focus on glucose and fructose metabolism in haloarchaea with regards to metabolic enzymes, regulation, and sugar transport across the biological membrane.

## An Overview of Glycerol Metabolism

Glycerol is a ubiquitous molecule that serves as an important biosynthetic precursor. Glycerol is the structural component of many lipids, and glycerol derivatives glycerol-1-phosphate (G1P) or its enantiomer glycerol-3-phosphate (G3P) are used as the backbone for archaeal or bacterial and eukaryotic biological membrane lipids, respectively (Kates, 1978). Glycerol is also the principal compatible solute produced in response to decreased extracellular water activity by yeast (Brown and Simpson, 1972; Blomberg and Adler, 1989) as well as algae (Craigie and McLachlan, 1964; Ben Amotz and Avron, 1973b; Borowitzka and Brown, 1974; Ben Amotz and Avron, 1979). Glycerol also serves as a cryoprotective agent and contributes to inorganic phosphate recycling as well as energy production, neoglucogenesis, and redox balance (Brisson et al., 2001). In fungi, glycerol is primarily produced from dihydroxyacetone phosphate (DHAP) through G3P dehydrogenase (G3PDH, encoded by *gpdABC* or *glpABC*) and G3P

phosphatase (G3PP). There are two characterized routes of aerobic glycerol catabolism: i) through glycerol kinase (GK, encoded by *glpK*) and G3PDH or ii) through glycerol dehydrogenase (GDH) and dihydroxyacetone kinase (DHAK, encoded by *dhaKLM*) (either phosphoenolpyruvate:phosphotransferase system (PEP:PTS)-linked or ATP-dependent). Glycerol can also be fermented to 1,3-propanediol as a major product through the action of glycerol dehydratase (GD) and 1,3-propanediol dehydrogenase (1,3-PDH), and for this reason has been widely used as a feedstock in bioconversion. Glycerol can pass through the cell membrane by facilitated diffusion, simple diffusion, or through active transport, and regulation of glycerol metabolism occurs both transcriptionally and post-translationally and at different steps in the metabolic pathway. Each of these aspects of glycerol metabolism is discussed.

**Biosynthesis of Glycerol**

Glycerol is produced by eukaryotes and has osmoregulatory, biosynthetic, and/or redox balancing functions. Fungal glycerol production has been best characterized with regards to biochemistry and cellular physiology where glycerol is involved in many important cellular functions including osmoregulation during low water activity (Blomberg and Adler, 1992) and maintenance of redox balance during fermentation of glucose to ethanol (Ansell et al., 1997; Björkqvist et al., 1997; Nissen et al., 2000). Glycerol is cytosolically synthesized by *Saccharomyces cerevisiae* from DHAP as catalyzed by *GPD1* and *GPD2*-encoded G3PDH and the *GPP1P* and *GPP2P*-encoded G3PP. Both *GPD1P* and *GPP2P* are osmotically-induced, whereas their isoenzymes (*GPD2P* and *GPP1P*) are induced during anaerobic metabolism (Albertyn et al., 1994; Ohmiya et al., 1995; Norbeck et al., 1996; Ansell et al., 1997; Björkqvist et al., 1997). *Dunaliella tertiolecta* also contains multiple isoenzymes for glycerol synthesis that are

differentially-induced. The mode of induction depends on the ultimate function of the glycerol molecule, specifically whether it will be further modified for lipid synthesis or will be used directly as an osmoprotectant.

**Glycerol-3-phosphate dehydrogenase**

G3PDH [*sn*-G3P : nicotinamide adenine dinucleotide ($NAD^+$) 2-oxidoreductase (OR), EC 1.1.1.8] catalyzes the reversible reduction of DHAP to G3P and is distributed throughout all domains of life. In higher plants and algae, G3PDH is often referred to as DHAP reductase because at physiological pH and substrate concentrations, the enzyme is essentially inactive as a dehydrogenase (Gee et al., 1988a; Gee et al., 1988b; Gee et al., 1989). Interestingly, certain yeasts including *S. cerevisiae* and *Schizosaccharomyces pombe* encode two isoenzymes of G3PDH which modulate different cellular activities (*GPD1P* and *GPD2P*). While *GPD1P* is osmotically-induced and appears to increase glycerol synthesis in response to osmotic stress, *GPD2P* is induced under anoxic conditions (Albertyn et al., 1994; Ohmiya et al., 1995; Norbeck et al., 1996; Ansell et al., 1997; Björkqvist et al., 1997). Overproduction of either GPD1 or GPD2 in *S. cerevisiae* increases glycerol production, indicating that DHAP reduction may be a rate-limiting step in glycerol synthesis (Nevoigt and Stahl, 1996; Remize et al., 2001). Similarly, the microalgae *D. tertiolecta* also has multiple isoforms of G3PDH which are differentially-located and differentially-induced (Gee et al., 1989; Gee et al., 1993; Ghoshal et al., 2002). Two major G3PDH isoenzymes are located in the chloroplast, and a minor form is located in the cytoplasm. One of the major isoenzymes is thought to be involved in lipid synthesis on the basis of its constitutive enzymatic activity and its sensitivity toward detergents, lipids, and long-chain acyl CoA derivates. The other major species is thought to be involved in osmotic-stress response based on

its stimulation during growth on high salt. The minor form of the enzyme is believed to contribute to lipid synthesis based on its constitutive nature.

**Glycerol-3-phosphate phosphatase**

G3PP (G3P phosphohydrolase, EC 3.1.3.21) catalyzes the hydrolysis of G3P to glycerol and phosphate. *S. cerevisiae* encodes two isoenzymes of G3PP which are differentially expressed under either anaerobiosis or salt stress. Although both G3PP isoenzymes (Gpp1 and Gpp2) are induced during hyperosmotic conditions (Påhlman et al., 2001), only the expression of *GPP1* is induced under anaerobic conditions (Påhlman et al., 2001). Mutants lacking both *GPP1* and *GPP2* are devoid of G3PP activity and produce only small amounts of glycerol, confirming the essential role of G3PP in glycerol biosynthesis (Påhlman et al., 2001). Unlike G3PDH, overproduction of either Gpp1 or Gpp2 does not enhance glycerol production in yeast, indicating that G3P hydrolysis is not a rate-limiting step in glycerol synthesis (Påhlman et al., 2001).

**Glycerol Dissimilation to Dihydroxyacetone Phosphate**

There are two characterized routes of glycerol dissimilation to DHAP: i) through GK and G3PDH [flavin adenine dinucleotide (FAD)-dependent or $NAD(P)^+$-dependent] or ii) through $NAD(P)^+$-dependent GDH and DHAK (ATP-or PEP:PTS-dependent). A number of yeasts including *S. cerevisiae* (Sprague and Cronan, 1977), *Debaryomyces hansenii* (Blomberg and Adler, 1989), and *Candida glycerinogenes* (Chen et al., 2008) metabolize glycerol primarily through the former route. In this route, glycerol is first converted to G3P by GK. G3P can either serve as a precursor for lipid biosynthesis or can be subsequently converted into the glycolytic intermediate DHAP by G3PDH. *S. cerevisiae* cells deficient in either *GUT1*-encoded GK or *GUT2*-encoded G3PDH are unable to utilize glycerol as a sole carbon source (Sprague and Cronan, 1977). In

contrast, some yeasts such as *S. pombe* solely metabolize glycerol through GDH (Gancedo et al., 1986; Matsuzawa et al., 2010) and DHAK (Gancedo et al., 1986; Kimura et al., 1998). Interestingly, the yeasts *S. cerevisiae* (Norbeck and Blomberg, 1997), *D. hanseii* (Blomberg and Adler, 1989), and *Zygosaccharomyces rouxii* (Wang et al., 2002) metabolize glycerol through either route; however, the latter route (through GDH and DHAK) is more commonly activated during osmotic stress. Higher eukaryotes also encode GK and G3PDH enzymes of glycerol dissimilation that are highly conserved in amino acid sequence (Ayala et al., 1996; Brisson et al., 2001). GDHs and DHAKs are also found in higher eukaryotes, although the latter are based on sequence similarity to bacterial DHAKs. GK and G3PDH homologs are widely distributed in archaea with the exception of autotrophic methanogenic archaea which are unable to utilize glycerol as an energy source (Nishihara et al., 1999). GDH and DHAK homologs are not as common as GK and G3PDH homologs in archaea, with distribution limited to haloarchaea. Specifically, GDH enzyme activity has only been detected in *Halobacterium salinarium* and *Halobacterium cutirubrum* which are not known to metabolize glycerol (Rawal et al., 1988), and DHAK has only recently been identified in archaea based on genome sequences (Bolhuis et al., 2006; Hartman et al., 2010; Benson et al., 2010). GK and G3PDH are widely distributed in bacteria, although several bacterial GDHs and DHAKs have also been characterized, especially in *Enterobacteriaceae* (Bouvet et al., 1995). Some bacteria including certain strains of *Enterococcus faecalis* can metabolize glycerol to DHAP using either route (Bizzini et al., 2010).

**Glycerol kinase**

GK (ATP : glycerol phosphotransferase, EC 2.7.1.30) catalyzes the transfer of the gamma-phosphoryl group of adenosine-5'-triphosphate (ATP) to glycerol to form G3P. GK is a ubiquitous member of the ribonuclease H-like family of kinases, a protein superfamily whose members are composed of two domains with an intervening cleft containing the ATPase catalytic site (Cheek et al., 2005).

The crystal structure of *Escherichia coli* GK reveals that adenosine-5'-diphosphate (ADP) binds in the intercleft site and that glycerol binds directly below ADP in the interdomain cleft (Hurley et al., 1993). Glycerol binding is stabilized by arginine-83, glutamate-184, tyrosine-135, and aspartate-245 residues which form hydrogen bonds with the hydroxyl groups of glycerol, and through van der Waals interactions between typtophan-103, phenylalanine-270, and the glycerol carbon backbone. The aspargaine-10 and aspartate-245 residues are thought to serve as the $Mg^{2+}$ binding sites, the former of which is also proposed to be involved in ATP-hydrolysis. Kinetic and biochemical evidence suggests that *E. coli* GK exists in equilibrium between functional dimeric and tetrameric forms (de Riel and Paulus, 1978a), the latter of which can be inactivated by allosteric regulators.

GK is known to be a rate-limiting and regulated step of glycerol metabolism in many bacteria. GK is primarily regulated to limit glycerol metabolism when more preferable carbon sources such as glucose are available. In *E. coli*, GK regulation also prevents toxic accumulation of methylgloxyl during growth on glycerol (Freedberg et al., 1971). GK catalytic activity is allosterically inhibited by the small molecule fructose 1,6-bisphosphate (FBP) in both Gram-negative and Gram-positive bacteria. Additionally, the glucose-specific phosphocarrier protein of the PEP:PTS ($EIIA^{Glc}$) inhibits GK activity

solely in Gram-negative bacteria (Görke and Stülke, 2008) and GK activity is activated through an enzyme I (EI)-dependent phosphorylation by heat-stable histidine phosphorylatable protein (Hpr) exclusively in Gram-positive bacteria (Görke and Stülke, 2008). Furthermore, the *E. coli* glycerol facilitator protein GlpF may increase GK activity as evidenced by the significant increase in the Michaelis Menten constant ($K_m$) and decrease in maximal velocity ($V_{max}$) of GK upon deletion of *glpF* (Thorner and Paulus, 1973; Voegele et al., 1993). GK is also regulated at the transcriptional level through a variety of proteins including members of the CRP/FNR superfamily (specifically, CRP and Ers), CcpA (a LacI/GalR superfamily member), and GlpR (a DeoR/GlpR superfamily member).

**Glycerol-3-phosphate dehydrogenase**

G3PDHs are either $NAD^+$-(*sn*-G3P : $NAD^+$ 2-OR, EC 1.1.1.8), FAD- (*sn*-G3P: cytochrome OR, EC 1.1.5.3), or $NADP^+$-dependent (*sn*-G3P : $NADP^+$ 1-OR, EC 1.1.1.177) enzymes which catalyze the reversible conversion of G3P to DHAP. Despite cofactor differences, G3PDHs are conserved with greater than 45% protein sequence identity across all domains of life (Yeh et al., 2008). While $NAD^+$-dependent G3PDHs are cytosolically located, FAD-dependent G3PDHs are localized to the cytoplasmic membrane in bacteria (Walz et al., 2002) and are tightly bound to the outer surface of the inner mitochondrial membrane in eukaryotes (Lin, 1977). In eukaryotes, FAD-dependent G3PDH, together with its cytosolic counterpart, form the G3P shuttle. This shuttle is responsible for the re-oxidation of NADH by the mitochondrial electron transport chain (Ansell et al., 1997; Larsson et al., 1998). $NADP^+$-dependent G3PDHs are more limited in distribution compared to either $NAD^+$- or FAD-dependent G3PDHs,

with the only biochemically characterized representative in the hyperthermophilic archaeon *Archaeoglobus fulgidus* (Sakasegawa et al., 2004).

The *E. coli* genome encodes two G3PDH which are differentially expressed depending upon oxygen availability. Under oxygen-rich conditions, a membrane-associated homodimeric protein encoded by *glpD* is produced (Schryvers et al., 1978). Under anaerobic conditions, the *glpABC* operon is preferentially expressed. This membrane-associated, anaerobic G3PDH consists of a tri-heteromeric complex which utilizes fumarate or nitrate as the external electron acceptor (Cole et al., 1988; Varga and Weiner, 1995). Catalytic activity is carried by the soluble GlpAC dimer and membrane-associated GlpB mediates electron transfer from the GlpAC dimer to the terminal electron acceptor fumarate through the membrane-bound menaquinone pool (Cole et al., 1988; Varga and Weiner, 1995). GlpA binds FAD cofactor noncovalently, GlpC binds flavin mononucleotide, and GlpB contains two iron-sulfur clusters (Cole et al., 1988). Seven fully active structures of *E. coli* GlpD, both native and substrate analogue-bound, have been solved to 1.75 Å resolution (Yeh et al., 2008). GlpD is composed of both a soluble, extramembranous C-terminal ‘cap’ domain as well as a cytoplasmic membrane-associated N-terminal domain. Binding of the N-terminus of the protein to the membrane is mediated by the exposure of a basic amphipathic helix that inserts into the hydrophobic-core regions of membrane lipids (Walz et al., 2002). In addition to serving as the anchor for GlpD, the N-terminus of the protein contains the substrate as well as the cofactor binding domains, and is thought to contain a ubiquinone-docking site (Yeh et al., 2008).

**Glycerol dehydrogenase**

GDHs are either $NAD^+$- (glycerol : $NAD^+$ 2-OR, EC 1.1.1.6) or $NADP^+$-dependent (glycerol : $NADP^+$ 2-OR, EC 1.1.1.72) enzymes which catalyze the pH-dependent, reversible oxidation of glycerol to DHA. While $NAD^+$-dependent GDHs are widespread, $NADP^+$-dependent GDHs are primarily found in fungi (Jennings, 1984), halophilic algae (Borowitzka et al., 1977), higher eukaryotes (Toews, 1967; Kormann et al., 1972), and the bacterium *Gluconobacter sp*. (Adachi et al., 2008; Richter et al., 2009). The directionality of the redox reaction is pH-dependent; the oxidation of glycerol occurs under basic conditions (optimum at pH 10), and the reduction of DHA occurs under slightly acidic conditions (optimum at pH 6). Although glycerol dissimilation to DHAP usually occurs through GK in *E. coli*, GDH may be alternatively used upon GK inactivation (St Martin et al., 1977). The *E. coli* GDH exhibits broad substrate specificity, acting on 1,2-propanediol and its analogs, and is activated by ammonium, potassium, and rubidium ions and is strongly inhibited by N-ethylmalemide, 8-hydroxyquinoline, 1,10-phenanthroline, and cupric or calcium ions (Tang et al., 1979).

**Dihydroxyacetone kinase**

DHAKs (glycerone kinases, EC 2.7.1.29) are a family of amino acid sequence-conserved enzymes which utilize either ATP (eukaryotes and bacteria) or PEP (bacteria) as the source of the high-energy phosphoryl group (Bächler et al., 2005a). DHAKs display wide distribution in eukaryotes and bacteria, and the recent sequencing of haloarchaeal genomes have led to the identification of DHAK homologs in archaea (Bolhuis et al., 2006). The DHAK family can be divided into four distinct groups: i) single subunit ATP-dependent DHAKs (found in *Citrobacter freundii*, yeasts, plants, and animals), ii) PEP-dependent DHAKs consisting of DhaK, DhaL, and a single-domain

DhaM subunit (distributed throughout bacteria), iii) PEP-dependent DHAKs consisting of DhaK, DhaL, and a multi-domain DhaM subunit (found in *Corynebacterium diphtheriae*, *E. coli*, *Desulfovibrio vulgaris*, and other Proteobacteria as well as some Actinobacteria), and iv) incomplete DHAKs including two subunit DHAKs encoded by discistronic operons without DhaM and DHAKs whose function resembles ATP-dependent DHAKs, but whose sequence is more PEP:PTS-dependent-like (often found in bacterial species such as *Yersinia pestis*, *Burkholderia pseudomallei*, and *Sinorhizobium meliloti* which encode a reduced PTS that often does not contain carbohydrate transporters) (Erni et al., 2006).

DHAK crystal structures have been solved for the PEP:PTS-dependent DHAKs of *E. coli* (Siebold et al., 2003b; Oberholzer et al., 2006) and *Lactococcus lactis* (Zurbriggen et al., 2008) and for the ATP-dependent DHAK of *C. freundii* (Siebold et al., 2003a). While ATP-dependent DHAKs consist of a single polypeptide with two-domains (DhaK and DhaL), PEP:PTS-dependent DHAKs consist of three subunits (DhaK, DhaL, and DhaM). The DhaK subunits from ATP- and PEP:PTS-dependent DHAKs have similar topology, consisting of an N-terminal domain resembling the mannose family of transporters and a C-terminal domain which is structurally similar to FtsZ, a cell-division protein. DhaK binds DHA covalently between the carbonyl carbon of DHA and the imidazole ring (Nε2) on the active site histidine residue which is stabilized through hydrogen bonding. This hemiaminal linkage between the substrate and DhaK is not involved in catalysis but instead allows for chemical discrimination between short-chain carbonyl compounds which are capable of forming such linkages (such as DHA) and polyols which cannot form the covalent interaction (such as glycerol). This chemical

discrimination allows DHAKs to retain activity, even in the presence of molar quantities of glycerol (Erni et al., 2006). DhaL topology is conserved between ATP- and PEP:PTS-dependent DHAKs, although the surface potential of these proteins differs significantly (Oberholzer et al., 2006). DhaL contains a novel fold consisting of an eight-helix barrel of regular up-down topology, a hydrophobic core, and a capped nucleotide-binding site in a shallow depression at the narrow end of the barrel (Bächler et al., 2005a; Oberholzer et al., 2006). ADP is coordinated by two magnesium ($Mg^{2+}$) ions which are in turn complexed by three gamma-carboxyl groups from invariant aspartate residues. Water molecules help to complete the octahedral coordination sphere. Although the DhaL topology between ATP- and PEP:PTS-dependent DHAKs is conserved, the bound nucleotide assumes a different role in each case. In ATP-dependent DHAKs, ADP serves a catalytic substrate of the reaction, similar to the nucleotide role in other kinases. In contrast, the nucleotide in PEP:PTS-dependent DHAKs serves as a coenzyme which is not exchanged for ATP, but is instead re-phosphorylated *in situ* by DhaM (Bächler et al., 2005a). Treatment of *E. coli* DhaL with a chelating agent destabilizes nucleotide binding, thus decreasing the thermal unfolding temperature of DhaL significantly (Bächler et al., 2005a). In most bacterial PEP:PTS-dependent DHAKs, DhaM consists of a single domain which is homologous to the PTS mannose-specific transporter, $IIAB^{Man}$ (Erni et al., 2006; Zurbriggen et al., 2008). Occasionally, DhaM contains of additional domains which are homologous to the general carrier PTS proteins, Hpr and EI (Gutknecht et al., 2001).

**Anaerobic Glycerol Dissimilation Pathways**

Several members of the *Enterobacteriaceae* including *Klebsiella pneumoniae*, *E. coli*, and *Enterobacter sp*., and many Firmicutes such as *Clostridium pasteurianum*,

*Clostridium butyricum*, *C. freundii*, and *Lactobacillus reuteri* are capable of anaerobic growth on glycerol as the sole source of carbon and energy (Bouvet et al., 1995). As a result, their fermentative pathways have been more extensively studied and these microorganisms have often been used as microbial powerhouses for the anaerobic conversion of glycerol to more valuable chemical products. In the absence of an external oxidant, glycerol is converted by *Enterobacteriaceae* members to 1,3-propanediol through the action of GD and 1,3-PDH. 1,3-propanediol is the major anaerobic conversion product, accounting for 50-60% of the glycerol consumed, although minor products including ethanol, 2,3-propanediol, acetic acid, and lactic acid are also formed (Daniel et al., 1998).

**Glycerol dehydratase**

GD (glycerol hydrolyase, EC 4.2.1.30) catalyzes the coenzyme B12- (most GDs) or *S*-andenosyl methionine (SAM)-dependent (*C. butyricum* GD) dehydration of glycerol to form 3-hydroxypropionaldehyde (3-HPA). Coenzyme B12-dependent GDs are widespread in Firmicutes and *Enterobacteriaceae*, and have been biochemically characterized from many representatives including *Citrobacter*, *Klebsiella*, *Clostridium*, and *Propionibacter* (Toraya et al., 1980). SAM-dependent GD has only more recently been described in *C. butyricum* (Raynaud et al., 2003; O'Brien et al., 2004).

Coenzyme B12-dependent GDs have similar biochemical properties to diol dehydratases; however their substrate specificity, subunit composition, monovalent cation selection, and cofactor affinity differ (Toraya, 2000). Both diol dehydratases and coenzyme B12-dependent GDs proceed through a radical mechanism in which an adenosyl radical forms in the active site through homolytic cleavage of the cofactor cobalamin (Co)-carbon (C) bond which triggers substrate activation by abstraction of a

hydrogen atom (Toraya, 2003). Due to the nature of the biochemical reaction, GDs are easily inactivated by both substrate and cofactor analogs (Bachovchin et al., 1977); thus, the genomes of GD-containing members often encode reactivase enzymes. Upon inactivation of GD holoenzyme in *K. pneumoniae*, the enzyme-bound coenzyme loses the adenine moiety from its upper axial ligand through irreversible cleavage of the Co-C bond (Mori and Toraya, 1999). The reactivating factor (encoded by *gdrAB*) mediates the ATP-dependent exchange of the enzyme-bound, modified cobalamin for coenzyme containing the adenine moiety. The modified coenzyme is released from the active site and is converted back to its adenylated form through reductive adenosylation. In *C. freundii*, the structural genes of GD encoded by *dhaBCE* are part of the *dha* regulon which also encodes genes for reactivation of inactivated GD (*dhaFG*) as well as additional genes of the pathway (*dhaDKT*) (Seifert et al., 2001). This regulon is under the control of the transcriptional activator DhaR which induces expression under anaerobic conditions when either glycerol or DHA are present.

SAM-dependent GD is similar in tertiary structure to SAM-dependent pyruvate formate lyase (PFL), and, also like *E. coli* PFL, crystallizes as a dimer (Becker et al., 1999; O'Brien et al., 2004). As a result of the structural homology between SAM-dependent GD and PFL, SAM-dependent GD is thought to proceed through a radical mechanism similar to SAM-dependent PFL in which reductive cleavage of SAM results in the transient formation of a 5‘-deoxyadenosyl radical (Frey et al., 1994; Wagner et al., 1999). While this mechanism is reminiscent of the coenzyme B12-dependent GD mechanism, the exact chemical details are not well understood due to the highly transient nature of the SAM radical (O'Brien et al., 2004).

### 1,3-Propanediol dehydrogenase

1,3-PDH (1,3-propanediol oxidoreductase, EC 1.1.1.202) catalyzes the NADH-dependent dehydrogenation of 3-HPA to 1,3-propanediol. Although 1,3-propanediol cannot be metabolized further by glycerol-fermenting microorganisms without genetic manipulation (Zhu et al., 2002), the $NAD^+$ generated during the reduction of 3-HPA can be used by GDH to support oxidative glycerol metabolism.

The biochemical properties of 1,3-PDHs from *Lactobacilli sp.* and *K. pneumoniae* have been elucidated. The tetrameric 1,3-PDH from *L. reuteri* reduces acetol and DHA in addition to 3-HPA, and oxidizes glycerol and propanediol (Talarico et al., 1990). These properties are in contrast to the 1,3-PDH enzymes from *K. pneumoniae*, *Lactobacillus brevis*, and *Lactobacillus buchneri* which purify as either an octomer or a hexamer and are unable to utilize glycerol as an oxidative substrate (Johnson and Lin, 1987; Veiga-da-Cunha and Foster, 1992). Many 1,3-PDHs are inactivated by both metal chelaters and oxygen (Johnson and Lin, 1987; Daniel et al., 1995). In *C. butyricum*, the *dhaT* gene encoding 1,3-PDH is under the control of a two-component signal transduction system, DhaAS/DhaA, which activates gene expression in response to cellular physiological parameters such as redox potential, similar to the DhaR protein found in other 1,3-propandiol generating bacteria (Seo et al., 2009).

## Glycerol Transport Across a Biological Membrane

Two types of membrane transport systems have been distinguished for small molecules, active and passive transport. Active transport systems are characterized as those requiring metabolic energy to move a substance across a biological membrane against an electrochemical gradient. By contrast, passive transport systems are energy-independent. Passive transport can occur with (facilitated diffusion) or without (simple

diffusion) the help of facilitator proteins. Bacteria and eukaryotes utilize passive transport with respect to glycerol transport, while fungi can also employ active glycerol transport mechanisms. Glycerol transport in archaea has not been characterized at the molecular level, although bioinformatic analysis predicts the presence of at least GlpF-like proteins in some archaea based on primary amino acid sequence identity. Due to the absence of information on archaeal glycerol transport, this section will only focus on glycerol transport in bacteria and eukaryotes.

**Intrinsic Permeability**

The small size and uncharged nature of glycerol allows cells to be intrinsically permeable to this molecule. *Shigella flexneri* and *E. coli* mutants deficient in glycerol facilitator protein GlpF are able to grow on glycerol as a sole carbon source (Richey and Lin, 1972). Both mutants exhibit a calculated maximal glycerol equilibration half life of 20 to 40 s compared to the 2 s equilibration half life of their parental strains. Thus, although glycerol equilibration can proceed through simple diffusion, facilitated diffusion enables much more rapid uptake of glycerol. Glycerol is much less permeable through the membranes of yeast and algae which accumulate the molecule as an osmoprotectant (Brown et al., 1982; Karlgren et al., 2005). Gated glycerol export channels allow yeast cells to rapidly control and fine-tune their glycerol content (Van Aelst et al., 1991). Despite limited glycerol permeability under standard conditions, *Dunaliella sp.* display increased glycerol permeability in response to environmental factors such as increased temperature (Wegmann et al., 1980; Elevi Bardavid et al., 2008) and osmotic stress (Fujii and Hellebust, 1992).

## Aquaglyceroporins

The major intrinsic protein (MIP) family of integral membrane proteins is a ubiquitous family whose members serve as transmembrane (TM) channels that conduct water as well as linear polyalcohols by energy-independent mechanisms (Reizer et al., 1993). Members of this family include aquaporins which facilitate water flux across the membrane. This family also includes aquaglyceroporins which are highly selective for small molecules such as glycerol and other aldols, and not ions and charged solutes which would otherwise dissipate the electrochemical potential across the cell membrane. Given the specificity of aquaglyceroporins for small molecules, it is without question that they serve important roles in nutrient uptake, osmoregulation, and probably other cellular processes. Aquaglyceroporins are distributed throughout bacteria, filamentous fungi, yeast, and some archaea (Reizer et al., 1993). Representatives from all but the archaeal domain have been characterized at the biochemical level. The structures of various members of the MIP family have been determined (Fu et al., 2000; Sui et al., 2000; Froger et al., 2001; Andrews et al., 2008), revealing a conserved right-handed bundle of six TM α-helices. Symmetry in the N-and C-terminal halves of the protein structure suggests that the aquaglyceroporins originated from a tandem, intragenic duplication event of an ancestral protein containing three TM domains (Wistow et al., 1991). GlpF and Fpsp1 are the best characterized aquaglyceroporins in bacteria and eukaryotes, respectively. Additional aquaglyceroporins AQP3, AQP7, and AQP9 in mammals, Yfl054-like in yeast, and others are also discussed.

**Glycerol facilitator protein GlpF**

Glycerol facilitator protein (GlpF) is an MIP that catalyzes the equilibration of glycerol between the intracellular and extracellular spaces in bacteria (Duchesne et al., 2001). GlpF has been best characterized in *E. coli*, where it was first described as a channel protein due to i) its substrate specificity which is dependent on molecular weight, not chemical structure, and ii) its temperature-insensitivity with regards to diffusion (Heller et al., 1980). Like other genes of the *glp* regulon in *E. coli*, the gene encoding GlpF is induced by G3P (Sanno et al., 1968) and provides a strong growth advantage when extracellular glycerol is limiting (Richey and Lin, 1972). Upon internalization of extracellular glycerol, intracellular glycerol is subsequently converted into G3P by GK. This metabolic conversion provides the chemical potential difference of glycerol uptake. Due to the inability of GlpF to use G3P as a substrate for transport, an imbalance of glycerol concentration across the membrane is created, and G3P remains trapped intracellularly where it is further metabolized (Heller et al., 1980). Although G3P cannot be transported out of the cytoplasm by GlpF, G3P can be transported into the cell through the facilitator GlpT (Hayashi et al., 1964), a member of the major facilitator superfamily (MFS) of transporters. Upon internalization, G3P is oxidized to DHAP by G3PDH.

Similar to other aquaglyceroporins, GlpF is strictly selective for non-ionic compounds and has reduced conductivity for water compared to aquaporins (Fu et al., 2000). In addition to glycerol, GlpF conducts linear polyalcohols (alditols) and urea derivatives, for which it is stereo- and enantio-selective (Fu et al., 2000). The influx of glycerol as mediated by GlpF requires low energy of activation ($E_a$ 4.5 kcal·mol$^{-1}$) (Heller et al., 1980) and is non-saturable at more than 200 mM glycerol (Fu et al., 2000).

The crystal structure of an *E. coli* GlpF tetramer has been determined at 2.2 Å resolution, with each channel containing three glycerol molecules (Fu et al., 2000). The glycerol molecules proceed through an amphipathic channel with a radius of 15 Å on the periplasmic side that constricts to a "selectivity filter region" with a radius of <3.5 Å extending 28 Å in length to the cytoplasmic surface. Due to the constrictions in the "selectivity filter region", glycerol and related alditols are predicted to pass through this region in single file. Two conserved aspartic acid-proline-alanine motifs comprise a key interface between the duplicated three-and-one-half membrane-spanning α-helices (M1 through M8) that form a right-handed helical bundle around each channel. Two $Mg^{2+}$ ions are located in the center of the tetramer near the periplasmic face of the protein; the outer $Mg^{2+}$ ion is coordinated through the side chain of glutamate-43 and water, and the inner $Mg^{2+}$ ion is coordinated through tryptophan-42 and water. Site-directed mutagenesis suggests that glutamate-43 but not tryptophan-42 is critical for proper oligomerization, channel function, and *in vivo* stability of the GlpF protein (Cymer and Schneider, 2010).

**Fps1p**

In *S. cerevisiae*, the Fps1p aquaglyceroporin mediates glycerol export and, therefore, plays a crucial role in osmoregulation (Van Aelst et al., 1991). Genome-wide homology searches suggest that Fps1p-like proteins are restricted to yeasts (Hohmann, 2002). During hyper-osmotic conditions, yeast cells activate glycerol biosynthetic genes through an elaborate signaling system involving a mitogen-activated protein kinase cascade and the high-osmolarity glycerol pathway as a precondition for glycerol accumulation (Hohmann, 2002; Dihazi et al., 2004). In order for glycerol to accumulate as an organic osmotic solute, Fps1p activity drastically reduces within seconds after

exposure to the hyper-osmotic stress. Fps1p is reactivated after sufficient glycerol accumulation or once the cells have been shifted to hypo-osmotic conditions (Tamás et al., 1999).

Regulation and proper functioning of Fps1p are essential if cells are to maintain proper osmoregulation. Deletion of *FPS1* renders cells sensitive to hypo-osmotic shock due to the inability of these mutant cells to reduce excessive turgor pressure (Tamás et al., 1999). Hyperactive Fps1p results in sensitivity to hyper-osmotic stress due to the inability of cells to restore lost turgor pressure (Tamás et al., 1999). To mediate proper glycerol export, Fps1p is regulated by short C-terminal (Hedfalk et al., 2004) and N-terminal (Tamás et al., 2003) domains within the protein, which are required for retention of cellular glycerol under hypertonic stress. These Fps1p regulatory domains were initially identified through truncation analysis (Tamás et al., 2003; Hedfalk et al., 2004), and their importance has been confirmed through random genetic screens for hyperactive Fps1p-containing cells (Karlgren et al., 2004). The N-terminal regulatory domain consists of a cytoplasmic extension near the first TM domain and the C-terminal domain is located downstream of the sixth TM domain (Tamás et al., 2003; Hedfalk et al., 2004). The positioning of several critical amino acid residues of these domains are highly conserved in orthologs from other yeast species (Tamás et al., 2003; Hedfalk et al., 2004). The N-terminal regulatory domain has an amphiphilic character, and structural predictions indicate that it may fold into the membrane bilayer (Tamás et al., 2003). The N-terminal domain consists of a well-conserved motif (LYQNPQTPTVLP) which is part of an approximately 25-mer stretch of amino acids constituting a conserved sequence (Tamás et al., 2003). The intervening, conserved 20 amino acid

distance between the N-terminal regulatory domain and the first TM domain is important for proper channel regulation (Tamás et al., 2003). The dodecahedral motifs (amino acid residues 535–546) which constitute the C-terminal regulatory domain consist of a well-conserved first-half (HESPVN) and a variable latter half (Hedfalk et al., 2004). Fsp1p is also regulated by the paralogs Rgc1 and Rgc2 as evidenced by increased cell wall turgor pressure and elevated intracellular glycerol levels following gene deletion of both *RGC1* and *RGC2* (Beese et al., 2009). The exact mechanism through which this regulation occurs is still unknown.

The biological function of Fsp1p has been recently expanded to include arsenic flux as evidenced by modulation of Fps1p intracellular levels (Maciaszczyk-Dziubinska et al., 2010). Overexpression of Fps1p in *S. cerevisiae* increases arsenite tolerance while deletion of *FPS1* increases arsenite sensitivity (Maciaszczyk-Dziubinska et al., 2010). This study further determined that arsenite treatment increases the abundance of transcript specific for *FPS1* whose gene product localizes to the membrane, and transport experiments revealed that Fps1p in concert with the arsenite transporter Acr3p mediates arsenite efflux in *S. cerevisiae*.

**Additional Aquaglyceroporins**

In addition to the aquaglyceroporins GlpF and Fps1p which are well described, additional aquaglyceroporins which have not been characterized as extensively are discussed including: i) the fungal-specific Yfl054-like aquaglyceroporins, ii) a group of fungal aquaglyceroporins whose members are neither Fps1p- nor Yfl054-like, iii) the mammalian aquaglyceroporins (AQP3, AQP7, AQP9, and AQP10) and iv) nodulin-26-like aquaglyceroporins in plants.

Yfl054 is a fungal-specific aquaglyceroporin originally identified from the *S. cerevisiae* genome sequence (Hohmann et al., 2000). Additional homologs of Yfl054-like proteins have been identified in other yeast as well as filamentous fungi. Yfl054-like proteins are structurally distinguished from Fps1p as containing a long (approximately 350 amino acids in length) N-terminal extension and a 50 amino acid C-terminal extension. The core TM is highly sequence-conserved among Yfl054-like aquaglyceroporins, while the long N-terminal extension is variable, with the exception of a highly-conserved PVWSLNQPLPV motif (Pettersson et al., 2005). The biological function of Yfl054 has not been fully elucidated; however, one study has loosely implicated Yfl054 in glycerol flux based on slight differences in glycerol transport in parental and mutant strains (either Δ*FSP1* or Δ*FSP1* Δ*YFL054*) in the presence of ethanol (Oliveira et al., 2003). Due to differences in ethanol sensitivity and glycerol permeability, the authors suggested that Yfl054 may serve a different cellular function from Fps1p.

A third group of aquaglyceroporins has been solely identified in filamentous fungi as being neither Fsp1p-like nor Yfl054-like and whose members share limited sequence similarity and often differ in molecular size (Pettersson et al., 2005). Several members of this group have long N-terminal extensions similar to Yfl054. However, these proteins differ in their primary sequence from Yfl054-like proteins. Biochemical or genetic characterizations of members from this group of proteins has not been performed.

In mammals, thirteen aquaporins have been characterized (AQP0 – AQP12) (Ecelbarger et al., 1995; Lee et al., 1996; Lu et al., 1996; Ishibashi et al., 1998; Kuriyama et al., 2002; Mobasheri and Marples, 2004; Ishibashi, 2009). Of these, four

have been classified as aquaglyceroporins: AQP3, AQP7, AQP9, and AQP10. These aquaglyceroporins describe a new class of water channels which are permeable to glycerol, but to a lesser degree than bacterial GlpF. Phylogenetic analysis reveals that these proteins cluster more closely with bacterial GlpF than with additional eukaryotic aquaporins (Ishibashi, 2009). In humans, these aquaglyceroporins are localized in different tissues; AQP3 and AQP9 in the kidney (Kuriyama et al., 2002), AQP7 in adipose tissue (Kuriyama et al., 2002), and AQP10 in the gastrointestinal tract (Ishibashi, 2009). Although AQP10 is related to AQP7 based on amino acid sequence identity (Zardoya, 2005), AQP10 is more closely related to AQP3 in function. Neither AQP10 nor AQP3 are capable of transporting arsenite, whereas AQP7 and AQP9 are known arsenite transporters (Liu et al., 2004).

The nodulin 26-like intrinsic protein subfamily is a highly-conserved, plant-specific protein family whose members transport a variety of uncharged solutes ranging from water to ammonia to glycerol. Two members in particular, nodulin-26 and LIMP2, specifically transport glycerol as well as other uncharged polyols and have a low intrinsic water permeability (Wallace et al., 2002). The primary sequences of nodulin-like protein subfamily members consist of a hybrid of amino acid residues conserved in aquaglyceroporins as well as aquaporins and contain some residues unique to the nodulin-like family (Wallace et al., 2002). Subfamily members are often subject to post-translational phosphorylation in response to environmental cues which can stimulate transport activity (Weaver and Roberts, 1992). Phosphorylation is common in both plant and animal MIPs, and this modification often occurs within the cytosolic termini and loop regions of the proteins, resulting in modulation of their localization, regulation, or

transport activity (Chaumont et al., 2005). Nodulin-like proteins are generally expressed at low levels in the plant compared to other MIPs, and several exhibit tissue-specific localization and are spatially- or temporally-regulated (Wallace et al., 2006). The biological significance of the glycerol transport behavior by nodulin-26-like family members is less well understood, since there is no apparent role for glycerol transport in metabolism or osmoregulation (Wallace et al., 2006).

**Active Transport of Glycerol**

Although not yet described in bacteria, several yeasts and some fungi can accumulate glycerol through active, proton symport (Ferreira et al., 2005). In *S. cerevisiae* and *Candida albicans*, Stl1p is responsible for mediating active glycerol / $H^+$ symport (Ferreira et al., 2005; Kayingo et al., 2009). Stl1p is a member of the sugar permease family of the MFS (Nelissen et al., 1997) and was implicated in glycerol / $H^+$ symporter in *S. cerevisiae* based on the following arguments: i) *STL1* mutants do not efficiently utilize or accumulate glycerol as a sole carbon and energy source, ii) active uptake of glycerol is absent in *STL1* mutants, iii) microarray and proteomic data correlate the expression of *STL1* and the presence of its gene product directly with glycerol uptake activity, iv) the localization of Stl1p in the plasma membrane and its glucose-dependent inactivation are fully consistent with its function as a transporter, v) heterologous expression of Stl1p in yeast cells without an active uptake mechanism enables the active uptake of glycerol, and vi) glycerol accumulation in the heterologous system is sensitive to the dissipation of proton motive force through the action of the protonophores and ionophores carbonyl cyanide 3-chlorophenylhydrazone and carbonyl cyanide 4-(trifluoromethoxy)phenylhydrazone (Ferreira et al., 2005). Stl1p transport activity appears to be negligible when wild-type *S. cerevisiae* cells are actively growing

in glucose-based complex media, regardless of salt concentration, but becomes measurable upon glucose exhaustion during salt stress (Lages and Lucas, 1997; Ferreira et al., 2005) or in response to increased temperature (Ferreira and Lucas, 2007).

## Transcriptional and Post-Translational Control of Glycerol Metabolism

Glycerol metabolism is controlled both transcriptionally and post-translationally and at different steps in catabolism. Gram-positive bacteria generally use Hpr as a central regulatory unit for carbon metabolism, whereas Gram-negative bacteria, specifically enteric bacteria, utilize $EIIA^{Glc}$ as the key regulatory unit (Deutscher et al., 2006). In addition to regulation by PTS components, glycerol metabolism is also regulated by non-PTS proteins including FNR, GlpR, DhaR, ArcA and ArcB, cAMP-CRP, CcpA, GlpP, Ers, and $\sigma^B$, as well as small molecules such as FBP.

### Transcriptional Regulators of Glycerol Metabolism

Gram-positive and Gram-negative bacterial genomes encode different transcriptional regulators of glycerol metabolism. Gram-negative bacteria use cAMP-CRP to regulate secondary carbon metabolism. The cAMP-CRP levels are subject to regulation by adenylate cyclase (AC, 3',5'-cyclic AMP synthetase, EC 4.61.1) encoded by *cya* which catalyzes the synthesis of cAMP from ATP. In contrast, Firmicutes typically do not encode AC, and the ability of these organisms to take up cAMP from the environment is unknown. Instead, Firmicutes use catabolite control protein A (CcpA) which binds to phosphorylated Hpr as the effector molecule to mediate catabolite repression. Most of the glycerol transcriptional regulators that have been characterized from Gram-positive bacteria were done so in *Bacillus subtilis*, whereas most of the Gram-negative regulators have been characterized in *E. coli*. As there are a large

number of possible glycerol transcriptional regulators, only a handful will be addressed within the scope of this literature review. Regulation by FNR, GlpR, DhaR, ArcA and ArcB, cAMP-CRP, CcpA, GlpP, Ers, and $\sigma^B$ will be discussed.

**cAMP-cAMP receptor protein**

The cAMP-CRP complex is a global regulator of transcription that is widespread in bacteria excluding Firmicutes where it is not predicted based on the absence of *cya* encoding AC (Deutscher et al., 2006). Many of regulatory targets of cAMP-CRP are involved in secondary carbon catabolism (Zubay et al., 1970). However, cAMP-CRP also controls other metabolic processes including but not limited to: osmoregulation (Landis et al., 1999), the stringent response (Johansson et al., 2000), nitrogen assimilation (Mao et al., 2007), biofilm formation (Jackson et al., 2002), iron uptake (Zhang et al., 2005), and multidrug resistance to antibiotics (Nishino et al., 2008). CRP is a member of the CRP-FNR superfamily of transcription factors whose members are generally transcriptional activators or, less likely, repressors of metabolic genes in facultative or strictly anaerobic bacteria (Körner et al., 2003). Proteins belonging to the CRP-FNR superfamily respond to a broad spectrum of both intracellular and extracellular signals including cAMP (Kolb et al., 1993), anoxia (Hutchings et al., 2002), redox state (Zeilstra-Ryalls and Kaplan, 1996), nitric oxide (Van Spanning et al., 1999), carbon monoxide (Aono et al., 1996), temperature (Dramsi et al., 1993), and 2-oxoglutarate (Muro-Pastor et al., 2001). This response occurs either through i) intrinsic sensory molecules which allow for the binding of an allosteric effector molecule or through ii) prosthetic groups which interact with the signal molecule (Körner et al., 2003). CRP is activated by binding its allosteric effector, cAMP (Blaszczyk et al., 2001), and is transcriptionally repressed by Fis (González-Gil et al., 1998), a small DNA

binding protein which regulates the expression of several genes needed for catabolism of sugars and nucleic acids.

The crystal structures of cAMP-CRP with (Passner and Steitz, 1997; Benoff et al., 2002) and without (Passner et al., 2000) bound DNA and apo-CRP (Sharma et al., 2009) have been solved. CRP is a homodimer consisting of two domains: a C-terminal α-helical DNA binding domain (DBD) and an N-terminal dimerization domain. The N-terminal domain consists of β-sheets which contain a hydrophobic pocket for cAMP binding that is connected by a linker region to the C-terminal domain. In the apo-form, the CRP C-terminal domain dimerizes with the DNA recognition helix F buried within its core. Upon binding cAMP, a reorientation occurs which liberates the DNA recognition helix (Sharma et al., 2009). Activated CRP then binds to a 22-bp palindromic region of DNA which induces severe DNA bending upon binding (Ebright et al., 1989). This bending mechanism allows for two regions of CRP, activation regions 1 (Zhou et al., 1993) and 2 (Niu et al., 1996) located in the C- and N-termini, respectively, to interact with RNA polymerase.

cAMP-CRP levels are subject to regulation by AC, which is in turn regulated by $EIIA^{Glc}$, and by both positive (Hanamura and Aiba, 1992) and negative (Aiba, 1983) auto-regulatory mechanisms. cAMP-CRP activates promoters that are grouped as class I, class II, or class III, depending on how many activation units (molecules of cAMP-CRP) are required and by the nature of the cAMP-CRP interaction with RNA polymerase. In addition to activation, CRP represses transcription by promoter exclusion, exclusion of activator protein, interaction with repressor protein, or hindering promoter clearance.

In *E. coli*, several glycerol metabolic genes are subject to regulation by cAMP-CRP complex. As evidenced by DNaseI footprinting, the cAMP-CRP dimer binds two regions centered at 60.5- and 37.5-bp upstream of the *E. coli glpFK* transcriptional start site, which also overlaps the GlpR binding site (Weissenborn et al., 1992). Furthermore, monomeric cAMP-CRP binds in regions centered at 41.5-, 91.5-, and 131.5-bp upstream of the *E. coli glpTQ* transcriptional start sites and regions centered at 0.5-, 40.5-, and 90.5-bp upstream of the *E. coli glpABC* transcriptional start site, each overlapping the GlpR and FNR binding sites (Larson et al., 1992). Additional cAMP-CRP sites were centered 63.5-bp upstream of the transcriptional start site of *glpD* and 58.5-bp upstream of the transcriptional start site for *glpEGR*, although these sites do not appear to overlap additional regulatory sites (Ye and Larson, 1988; Yang and Larson, 1998). The occurrence of tandem operators for cAMP-CRP and GlpR as opposed to overlapping operator regions may explain why *glpD* displays the greatest sensitivity to GlpR-dependent repression.

**FNR**

FNR is a member of the CRP/FNR superfamily of transcription factors which mediates the transition from aerobic to anaerobic growth in a number of bacteria (Körner et al., 2003). FNR activates genes involved in anaerobic metabolism, acid resistance, chemotaxis, cell structure, and molecular biosynthesis and transport. FNR also represses genes associated with aerobic metabolism (Salmon et al., 2003; Kang et al., 2005). FNR is composed of i) an N-terminal sensory domain containing four essential cysteine residues which link the $[4Fe\text{-}4S]^{2+}$ cluster, ii) a C-terminal helix-turn-helix (HTH) DBD, and iii) a dimerization motif located between the N- and C-termini (Green et al., 1993; Bates et al., 2000; Körner et al., 2003). In the absence of oxygen,

FNR purifies as a homodimer and the oxygen-sensitive $[4Fe\text{-}4S]^{2+}$ cluster promotes dimerization (Moore and Kiley, 2001). Oxygen destabilizes and inactivates the dimeric FNR complex through oxidation of the $[4Fe\text{-}4S]^{2+}$ cluster to two $[2Fe\text{-}2S]^{2+}$-containing monomers (Lazazzera et al., 1996; Khoroshilova et al., 1997). Prolonged oxygen exposure returns FNR to an apoprotein state through loss of the two $[2Fe\text{-}2S]^{2+}$ clusters (Sutton et al., 2004). Nitric oxide also inactivates FNR through nitrosylation of the $[4Fe\text{-}4S]^{2+}$ cluster (Cruz-Ramos et al., 2002). Molecules of apoFNR are degraded by ClpXP protease which binds to motifs located in the N- and C-termini of FNR (Mettert and Kiley, 2005).

In its activated form, FNR homodimer binds to a highly-conserved, dyad consensus DNA sequence, TTGAT-$N_4$-ATCAA (where N represents A, T, C, or G) (Eiglmeier et al., 1989), through contacts with serine-212 and glutamate-209 (Spiro et al., 1990). FNR activates transcription from both class I and class II promoters at locations 61-, 71-, 82-, or 92-bp upstream and at an average distance of 41.5-bp upstream of the transcriptional start site of the affected gene or operon, respectively (Wing et al., 1995). As a repressor, FNR often binds at sites located near the transcriptional start site of the affected gene or operon. Three activating regions (AR), AR1, AR2, and AR3, contact RNA polymerase through the α-subunit, $\sigma^{70}$, and the α N-terminal domain of RNA polymerase, thus promoting transcription (Lee et al., 2000; Lamberg et al., 2002; Blake et al., 2002). *E. coli* glycerol metabolic genes whose transcription is activated by FNR during anaerobiosis include *glpABC* (Kuritzkes et al., 1984) and *glpTQ* (Yang et al., 1997). Although the FNR binding sites have not been directly demonstrated, FNR is predicted to bind 0.5- and 40.5-bp upstream of the

transcriptional start site of *E. coli glpABC* and 91.5- and 131.5-bp upstream of the transcriptional start site of *E. coli glpTQ* based on sequence analysis (Eiglmeier et al., 1989).

**CcpA**

Many low-G+C Gram-positive bacteria such as *B. subtilis* do not encode AC, and were thus predicted to use a mode of regulation other than cAMP-CRP for catabolite repression. In Firmicutes, carbon catabolite repression is mediated by CcpA and Hpr (Deutscher et al., 2006). CcpA is a pleiotropic transcription factor that is a member of the LacI/GalR family of repressors (Henkin et al., 1991). The phosphorylation status at serine-46 of general PTS carrier protein Hpr and its homolog, catabolite repression protein Hpr (Crh), affect the ability of CcpA to regulate transcription of a variety of metabolic genes including *glpK* (Deutscher et al., 1994; Galinier et al., 1997). Thus, in Gram-positive bacteria, Hpr participates both in sugar translocation and serves as a co-repressor for metabolic enzymes. Although both Hpr and its homolog Crh contain the regulatory serine-46 residue, the histidine-15 residue is not conserved, indicating that Crh is not implicated in sugar transport.

Hpr phosphorylation is catalyzed by homohexameric ATP-dependent Hpr kinase (HprK), which is triggered by the availability of glycolytic intermediates such as FBP (Deutscher et al., 1995) and is inhibited by inorganic phosphate (Reizer et al., 1998). HprK phosphorylates Hpr in an ATP-dependent manner at the regulatory residue serine-46 which inhibits EI-dependent histidine-15 phosphorylation up to 600-fold (Stülke et al., 1998). In the presence of inorganic phosphate, HprK can also serve as a phosphorylase, catalyzing dephosphorylation at serine-46 (Galinier et al., 1998). HprK is also present in Gram-negative, non-enteric bacteria; however, due to the absence of

CcpA in these organisms, HprK is thought to mediate different processes (Deutscher et al., 2005). Gram-negative HprKs are suggested to mediate pathogenesis as HprKs often cluster with transcriptional regulators of virulence genes (Deutscher et al., 2005) and inactivation of *Neisseria meningentitis hprK* leads to decreased cellular adhesion of the pathogen to human epithelial cells (Boël et al., 2003). Two molecules of phosphorylated Hpr serve as the effector for the dimeric CcpA (Jones et al., 1997). Binding of these phosphorylated Hpr effector molecules to the CcpA C-terminal domain triggers a slight rotational movement of the CcpA core which brings the N-terminal DBD into a position that is competent for DNA binding (Schumacher et al., 2004). The CcpA-cofactor complex then binds to specific palindromic operator sequences in the promoter regions of catabolic operons known as catabolite responsive elements (*cre*) sites. In *B. subtilis*, the *cre* site overlaps the -35 promoter region of *glpFK* (Miwa et al., 2000).

**GlpR**

GlpR is a member of the DeoR/GlpR protein family whose members are widespread among bacteria. Amino acid sequence similarity search results indicate that some archaea also encode DeoR/GlpR homologs. DeoR/GlpR-type proteins often serve as transcriptional repressors (Munch-Petersen and Jensen, 1990; Weissenborn et al., 1992; Zeng and Saxild, 1999; Ray and Larson, 2004; Barrière et al., 2005; Haghjoo and Galán, 2007) or activators (Zhu and Lin, 1986; Gaurivaud et al., 2001) of either sugar or nucleoside metabolism. DeoR/GlpR-type regulators are comprised of approximately 250 amino acids, with a HTH DBD near the N-terminus and a C-terminal domain that often binds a sugar phosphate effector molecule of the relevant metabolic pathway (Zeng et al., 1996). In general, DeoR/GlpR family members display i) a conserved HTH motif with respect to the second helix, ii) a C-terminal oligomerization domain, and iii) an inducer-

binding domain. The first two amino acid residues of the recognition helix (the first helix in the HTH motif) of DeoR/GlpR-type repressors are thought to confer specificity for binding to the DNA sequence of the operator site. DeoR/GlpR-type repressors typically regulate transcription through operator binding and concomitant DNA looping (Amouyal et al., 1989; Larson et al., 1992).

GlpR has been implicated as a repressor of glycerol metabolism in *E. coli* (Cozzarelli et al., 1968) as well as *P. aeruginosa* (Schweizer and Po, 1996). The GlpR proteins exhibit significant similarity (79.4% similarity and 49% identity at the primary amino acid level) (Schweizer and Po, 1996); however, only *E. coli* GlpR has been biochemically characterized. A study involving *E. coli* GlpR purified to near-homogeneity revealed that under non-denaturing conditions, active GlpR exists as a tetramer with a subunit molecular weight of 30 kDa (Larson et al., 1987). GlpR specifically binds: i) DNA-harboring operator sites in a cooperative fashion and ii) G3P (Kd 20 - 50 μM), the latter of which diminishes transcriptional repression of the *glp* operon (Hayashi and Lin, 1965; Larson et al., 1987). Flow dialysis experiments indicated that each GlpR tetrameric subunit binds one molecule of G3P (Larson et al., 1987). Binding specificity of G3P for GlpR was evidenced through competition assays involving the binding of unlabelled compounds (≥ 500 μM) to radioactively labeled G3P (28 μm) and GlpR (1.4 μg) (Larson et al., 1987). Glycerol-2-phosphate, glycerol, PEP, and glucose-6-phosphate have no apparent effect on G3P binding to GlpR. Compounds more closely resembling G3P, such as DHAP and glycerophosphodiesters, have a small yet significant impact on binding which increases significantly when competing compounds are included at concentrations greater than 1 mM. Addition of G3P (5 mM) dissociates

GlpR (300 nM) from the *glpK* operator (1.5 nM). This concentration of G3P (5 mM) was not sufficient to dissociate GlpR from the promoter regions upstream of the *glpD*, *glpABC*, or *glpTQ* regulons, indicating that the affinities of the GlpR-operator complexes for G3P may vary depending on the operator sequence. Higher concentrations (> 5 mM) of G3P were not examined for the additional operator complexes. For *E. coli*, the GlpR operator consensus sequence is determined as 5'-WATKYTCGWW·AWCGAACATW-3' (where W is A or T, K is G or T, Y is C or T, and the dot represents the center of symmetry) (Zhao et al., 1994).

In *E. coli*, the *glp* regulon comprises five operons located at three different positions in the chromosome: i) *glpTQ* and *glpABC* operons are transcribed divergently from *glpEGR* located near 51 min of the linkage map, ii) *glpD* is located near the 77 min linkage map, and iii) *glpFKX* is located near the 89 min linkage map (Zeng et al., 1996). Each operon is negatively controlled by GlpR to varying extent, and repression is relieved by the inducer, G3P. G3P permease and glycerophosphodiesterase (encoded by *glpTQ*) and the subunits of G3PDH (encoded by *glpABC*) are divergently transcribed from a common control region containing five operator binding sites for GlpR (Larson et al., 1992). Transcriptional repression is thought to occur through DNA looping, similar to other characterized DeoR/GlpR regulators (Larson et al., 1992). The *glpD* operon encoding aerobically-expressed G3PDH and the *glpFKX* operon encoding GlpF, GK, and fructose-1,6-bisphosphatase II are tightly controlled by GlpR. GlpR binds both upstream of the *glpFKX* operon as well as internal to *glpK* (Weissenborn et al., 1992) and controls *glpD* expression through binding at one of four operator sites. Two operator sites are internal to the gene, one overlaps the -10 promoter element, and one

is located 30-bp downstream of the transcriptional start site (Yang and Larson, 1996). The *glpE* and *glpG* genes encoding the uncharacterized proteins GlpE and GlpG display sequence homology to the minor thiosulfate sulfurtransferase and an intramembrane serine protease cluster with *glpR* and are transcribed divergently from the neighboring *glpD* gene. Multiple promoter elements control the transcription of the *glpEGR* operon, allowing for differential expression of its gene products. The *glpEGR* operon is not subject to autoregulation (Yang and Larson, 1998). The order of glycerol metabolic operon sensitivity to GlpR repression from greatest to least sensitive is *glpD*, *glpTQ*, and *glpFKX* (Freedberg and Lin, 1973).

One study has implicated *P. aeruginosa* GlpR as a transcriptional repressor of glycerol metabolic genes (Schweizer and Po, 1996). The *P. aeruginosa glpR* gene is located upstream of *glpD* encoding G3PDH. Inactivation of *glpR* results in constitutive expression of glycerol transport activity as evidenced by $^{14}$C-glycerol uptake. GlpR also represses transcription from the *glpT* (encoding G3P permease) and *glpD* (encoding G3PDH) promoters as evidenced by transcriptional promoter-reporter fusion assays

**DhaR**

DhaR is a member of the enhancer-binding protein family and controls expression of the *E. coli dha* regulon through direct interaction with $\sigma^{70}$ of RNA polymerase and DNA looping (Rappas et al., 2005; Bächler et al., 2005b). DhaR consists of three domains: i) a C-terminal DBD (5 kDa), ii) a central $AAA^+$ (ATPase associated with diverse cellular activities) ATPase domain (24 kDa), and iii) an N-terminal receiver domain for ligands (37 kDa). The N-terminal sensing domain of DhaR consists of both GAF (cyclic GMP, adenylyl cyclase, FhlA) and PAS (Per-ARNT-Sim) domains, which are the ligand and protein interaction domains of two-component system sensor kinases

(Ponting and Aravind, 1997; Hurley, 2003). The central $AAA^+$ domain consists of seven highly conserved sequence motifs which are shared among $AAA^+$ proteins (Morett and Segovia, 1993).

The molecular mechanism concerning DhaR regulation of the *dha* operon has only been described by one study in *E. coli* (Bächler et al., 2005b). DhaR stimulates transcription of the *dha* regulon from a $\sigma^{70}$ promoter (the exact binding site of DhaR is unknown) and autorepresses transcription of *dhaR*. DhaK and DhaL serve as co-repressor and co-activator of DhaR. In the presence of DHA, a phosphoryl group is transferred from the ATP-bound DhaL subunit to DHA, allowing ADP-bound DhaL to bind to DhaR in the receiver domain. This binding in turn activates expression of the *dha* regulon. DhaK directly competes with ADP-bound DhaL for DhaR. DHA binding to DhaK reduces the affinity of DhaK as a co-repressor of DhaR binding. Based on gel filtration chromatography following co-purification, DhaR is proposed to bind as a dimer to either monomeric DhaL or dimeric DhaK. In the absence of DHA, DhaL is re-phosphorylated *in situ* by DhaM, and is therefore incapable of binding DhaR. DhaR orthologs encoded near *dha* operons are found in other bacteria including *C. freundii*, *K. pneumoniae*, and *Vibrio parahaemolyticus*, although none have been characterized in detail. Interestingly, DhaR from *C. freundii* can compliment an *E. coli dhaR* mutant, allowing for regulation of the *dha* operon (Bächler et al., 2005b).

**ArcA/ArcB**

The global ArcA/ArcB two-component regulatory system is used to reduce the expression of many aerobic genes under anaerobic conditions (Iuchi and Lin, 1988; Iuchi et al., 1989). Cytoplasmically-located ArcA is a member of the OmpR/PhoB subfamily of response regulators and contains an N-terminal receiver domain and a C-

terminal DBD. ArcB is membrane-associated tripartite protein consisting of i) an N-terminal primary transmitter domain, ii) a central receiver domain, and iii) a C-terminal histidine-containing phosphotransfer domain (HPt). ArcB serves as the sensor-histidine kinase which is autophosphorylated at histidine-292 under anaerobic conditions (Iuchi and Lin, 1992). Histidine-292 is predominantly in a phosphorylated state in response to fermentative, metabolic effectors such as D-lactate, pyruvate, and acetate (Georgellis et al., 1999). During autophosphorylation, the phosphoryl group is relayed from histidine-292 in the transmitter domain of ArcB, to the aspartate-576 residue in the receiver domain of ArcB, to the histidine-717 of ArcB Hpt, and finally to aspartate-54 in the receiver domain of ArcA, leading to the activation of ArcA as a DNA-binding protein (Georgellis et al., 1997; Jeon et al., 2001). However, under aerobic conditions, this autophosphorylation reaction is inhibited (Georgellis et al., 2001) and dephosphorylation of ArcA by reverse phosphorelay is promoted (Georgellis et al., 1998).

Physiological evidence has implicated the ArcA/ArcB two-component regulatory system as a transcriptional repressor of aerobically-expressed *glpD* encoding G3PDH in *E. coli* (Freedberg and Lin, 1973; Iuchi et al., 1990). G3PDH specific activity is reduced in an *E. coli* strain deficient in both *glpR* and *glpA* mutants under anaerobic conditions compared to oxygenic conditions (Freedberg and Lin, 1973). This anoxic-dependent reduction in G3PDH activity is compensated by deletion of either *arcA* or *arcB* (Iuchi et al., 1990). Thus, in *E. coli*, the global ArcA/ArcB two-component regulatory system is proposed to reduce the expression of *glpD* encoding the aerobic G3PDH during anoxic conditions. However, the molecular mechanisms surrounding repression including the ArcA/ArcB binding site are yet to be described.

**Additional transcriptional regulators of glycerol metabolism**

Given that there are several transcriptional regulators of glycerol metabolism, all of them cannot be covered in the scope of this review. Therefore, only a few additional activators will be further discussed including GlpP, Ers, and $\sigma^B$.

GlpP is a member of the G3P-responive antiterminator family which serves as an antiterminator for the *glp* regulon. In *B. subtilis*, GlpP activates the expression of the *glpFK*, *glpD*, and *glpTQ* transcriptional units through G3P-activated antitermination (Holmberg and Rutberg, 1991; Beijer et al., 1993; Nilsson et al., 1994). Activation of GlpP by G3P (Holmberg and Rutberg, 1991) facilitates binding to an inverted repeat element located in the leader region of *glpD* (Glatz et al., 1998). GlpP also presumably binds to the *glpFK* and *glpTQ* leader regions based on sequence similarity. In addition to antitermination, GlpP also serves to stabilize *glpD* message stability (Glatz et al., 1996). GlpP is widely distributed in Firmicutes; however, none of these additional proteins have been characterized.

Ers is a member of the CRP/FNR family and serves as a pleiotropic activator of virulence as well as metabolism in *E. faecalis* (Giard et al., 2006). Ers shares common CRP/FNR family characteristics including a HTH motif, a cyclic nucleotide binding domain, and several conserved amino acid residues (Riboulet-Bisson et al., 2009b). More recently, Ers was demonstrated to control glycerol metabolism of *E. faecalis* through positive regulation of both *ef0082* encoding a putative transporter protein and the *glpKOF* operon encoding GK, G3P oxidase, and GlpF (Riboulet-Bisson et al., 2009a). Although the mechanism by which Ers serves as an activator is unknown, it is proposed to be indirect based on DNaseI footprint analysis (Riboulet-Bisson et al., 2009a). Ers distribution appears to be limited to Firmicutes.

*Lysteria monocytogenes* transcriptionally regulates genes involved in stress-related functions by employing an alternative sigma factor, $\sigma^B$. Mutants lacking $\sigma^B$ display increased sensitivity to a wide range of stresses including osmotic pressure (Becker et al., 1998), acidic conditions (Wiedmann et al., 1998), temperature (Ferreira et al., 2001), and oxidative stress (Ferreira et al., 2001). More recently, $\sigma^B$ has been implicated as a regulator for virulence. Proteomic profiling of cells deficient in $\sigma^B$ identified proteins encoding putative DHAK subunits whose abundance was severely diminished compared to the parental strain (Abram et al., 2008). Growth analysis confirmed a reduction in the growth rate of a $\sigma^B$ mutant compared to the parental strain when grown on glycerol as the sole carbon source (Abram et al., 2008). Although proteomic and phenotypic evidence appears to suggest a role for $\sigma^B$ as a regulator of glycerol metabolism, molecular evidence is still lacking.

**Allosteric and Post-translational Regulation of Glycerol Kinase Activity**

In addition to its transcriptional regulation, bacterial GK activity is also regulated allosterically through the glycolytic intermediate FBP as well as general and sugar-specific PTS components and through post-translational modification. Specifically, GKs from Firmicutes are activated through phosphorylation at a conserved histidine residue by Hpr in the absence of preferred PTS substrates. Although Gram-positive and Gram-negative GKs contain 50 to 60% sequence identity, this phosphorylatable histidine residue which is highly conserved in Firmicutes is noticeably absent from Gram-negative bacterial proteins (Charrier et al., 1997). In contrast, enteric bacteria rely upon unphosphorylated $EIIA^{Glc}$ to mediate allosteric inhibition of GK activity (Novotny et al., 1985; de Boer et al., 1986). In addition to regulation by PTS components, both Gram-positive and Gram-negative bacterial GKs are allosterically regulated by FBP (Novotny

et al., 1985; de Boer et al., 1986). Both FBP and $EIIA^{Glc}$ exhibit positive cooperativity with respect to bacterial GKs and optimally inhibit these enzymes at pH 6.5 (Novotny et al., 1985). Each of these aspects will be discussed within this section.

**Hpr- and EI-dependent phosphorylation of glycerol kinase**

In Gram-positive bacteria such as *Enterococcus sp.* (Charrier et al., 1997), Hpr serves as an activator of GK activity through reversible phosphorylation (Deutscher and Sauerwald, 1986). In the presence of PTS substrates, EI phosphorylates Hpr which transfers the phosphate moiety to sugar-specific permeases which, in turn, phosphorylate the incoming PTS substrate. However, in the absence of preferable PTS substrates such as glucose, a phosphoryl residue is transferred from the N3-position of the histidine-15 residue of Hpr to GK, allowing for subsequent 10-15 fold activation (Yeh et al., 2004). The site of GK phosphorylation in *E. faecalis* was determined as a conserved histidine-232 residue (Charrier et al., 1997). Although Hpr-dependent phosphorylation is a dominant form of GK regulation for many Gram-positive bacteria, not all members are subject to this type of regulation. Glycerol is one of the few carbon sources that *Mycoplasma pneumoniae* is able to metabolize (Hames et al., 2009). As a result, *M. pneumoniae* genes encoding glycerol metabolic enzymes are constitutively expressed, and GK enzyme activity is not subject to activation by Hpr-dependent phosphorylation (Hames et al., 2009).

In addition to transferring phosphoryl moieties to GK, Hpr proteins can also donate phosphoryl groups to transcriptional regulators containing PEP-carbohydrate PTS regulatory domains (PRDs) (Stülke and Hillen, 1998). Phosphorylation of PRDs by Hpr is required for activation of these regulators. Several operon-specific transcriptional regulators in both Gram-positive and Gram-negative bacteria, including antiterminators

and activators, contain duplicate PRDs (Stülke et al., 1998). These PRD-containing regulators often serve as activators of enzymes involved either in the catabolism or generation of sugars transported by the PTS (Stülke et al., 1998). Antiterminator-containing PRDs have been demonstrated for regulators controlling β-glucosidase (Amster-Choder and Wright, 1992), sucrose (Crutz et al., 1990), glucose (Stülke et al., 1997), and lactose metabolism (Alpert and Siebers, 1997).

**Fructose 1,6-bisphosphate**

FBP is a key intermediary metabolite of glycolysis that regulates the activity of many metabolic enzymes including lactate dehydrogenase (Cameron et al., 1994), pyruvate kinase (Mellati et al., 1992), and GK (Thorner and Paulus, 1973). FBP allosterically binds to both tetrameric GK (Kd 0.79 ± 0.63 mM) as well as dimeric GK (Kd 19 ± 5 mM) (Yu and Pettigrew, 2003), and promotes tetramerization by 2 to 4 orders of magnitude (de Riel and Paulus, 1978a; de Riel and Paulus, 1978b). FBP-mediated inhibition of GK activity is dependent on GK concentration, with desensitization occurring with diluted GK (Yu and Pettigrew, 2003). FBP displays noncompetitive inhibition and negative cooperativity with respect to ATP concentration and uncompetitive inhibition with respect to glycerol (Thorner and Paulus, 1973; Ormö et al., 1998).

The crystal structure of FBP-bound *E. coli* GK has been solved, and the allosteric binding site of FBP determined (Ormö et al., 1998; Yu and Pettigrew, 2003). *E. coli* GK tetramer binds two molecules of FBP between two glycine-arginine loops (residues 224-236), where one-half of the binding site is donated by each monomer at the regulatory interface. Ionic interactions occur between the phosphate moieties of FBP and the GK residue arginine-236 (in the guanidinium loop). Hydrogen bonding between the GK

residue glycine-234 (in the amide hydrogen) and the 6-phosphate moiety of FBP stabilizes the structure of FBP-bound to the allosteric site of GK. Site-directed mutagenesis of the *E. coli* GK arginine-236 residue to alanine drastically reduces FBP inhibition, but does not prevent FBP-mediated GK tetramer association (Ormö et al., 1998). In addition to site-directed mutagenesis, hydroxylamine mutagenesis has been used to generate colonies which exhibited reduced catabolite repression of glycerol metabolism (Liu et al., 1994; Pettigrew, 2009). Sequencing of the *glpK* gene of these *E. coli* colonies revealed that an alanine-65 to threonine mutation perturbs GK oligomerization and eliminates FBP inhibition while an aspartate-72 to asparagine mutation decreases the affinity of FBP for GK (Liu et al., 1994; Pettigrew, 2009). Neither mutation, however, showed significant change of either GK catalytic activity or inhibition by $EIIA^{Glc}$.

**$EIIA^{Glc}$**

$EIIA^{Glc}$ (also called $III^{Glc}$ in older literature) is the central regulatory element of the PEP:PTS in enteric bacteria, serving as a signal for the availability of extracellular glucose. $EIIA^{Glc}$ recognizes and binds in a phosphorylation status-dependent manner to at least 10 different target proteins including lactose, melibiose, and maltose transport components as well as GK (Postma et al., 1993). Specifically, $EIIA^{Glc}$ modulates *glp* expression through both inducer exclusion and regulation of cAMP-CRP. Both mechanisms of action are dependent on the phosphorylation status of $EIIA^{Glc}$, especially at histidine-90, which in turn is dependent on both the availability of PTS substrates as well as the ratio of PEP to pyruvate. $EIIA^{Glc}$ is preferentially dephosphorylated when cells are exposed to readily-metabolized PTS substrates or when the ratio of PEP to pyruvate is low. In its non-phosphorylated state, $EIIA^{Glc}$ directly binds to and inactivates

metabolic enzymes and transporters of secondary carbon sources. Specifically, $EIIA^{Glc}$ binds to and inactivates GK, preventing *glp* inducer formation (Novotny et al., 1985). $EIIA^{Glc}$ can also modulate *glp* operon expression through regulation of AC. In the absence of readily-metabolized carbon sources (such as glucose), phosphorylated $EIIA^{Glc}$ activates AC. As a result, levels of cAMP and cAMP-CRP are elevated, leading to the activation of secondary metabolic operons such as the *glp* regulon. The inducer molecule (G3P) is subsequently produced which binds to and inactivates $EIIA^{Glc}$, preventing inducer exclusion. In its dephosphorylated state, $EIIA^{Glc}$ is unable to activate AC, thus decreasing cAMP and cAMP-CRP levels.

The crystal structure of $EIIA^{Glc}$-bound to GK in the allosteric site has been solved for *E. coli* proteins (Hurley et al., 1993). The interaction of $EIIA^{Glc}$ with GK occurs in the C-terminal domain about 30 Å from the glycerol binding site (Hurley et al., 1993) and is stimulated by the presence of $Zn^{2+}$ ions (Pettigrew et al., 1998). Site-directed mutagenesis of the $EIIA^{Glc}$ phosphoryl acceptor (histidine-90) and the adjoining histidine-75 residues to glutamine results in a loss of $EIIA^{Glc}$ regulatory function and severely impairs $EIIA^{Glc}$ phosphorylation, respectively (Presper et al., 1989; Meadow and Roseman, 1996). X-ray crystallography, differential scanning calorimetry, and nuclear magnetic resonance (NMR) reveal slight structural differences between the $EIIA^{Glc}$ mutant and parent protein structures (Pelton et al., 1996). Specifically, the histidine-90 to glutamate mutant protein contained additional coordinated water molecules and the histidine-75 to glutamate mutant protein had a reduced phospho-$EIIA^{Glc}$ hydrogen bond network.

## Industrial and Biological Significance of Glycerol

Glycerol has been considered “a neglected variable in biological processes”, due to its importance as a biosynthetic precursor, as a compatible solute, and/or as an organic carbon and energy source in all domains of life (Brisson et al., 2001). Glycerol is of extreme biological significance to halophilic communities, where it serves as an osmoprotectant for the primary producer *Dunaliella* and as the primary energy source for heterotrophic community members. In addition to its neglect with respect to biological processes, glycerol has also been considered an underutilized feedstock for bioconversion. Its low cost, ease of its production, and the highly reduced nature of its carbon atoms makes glycerol an attractive feedstock for bioconversion. Natural glycerol fermenters as well as heterologous systems have recently gained attention for the conversion of glycerol-rich waste streams generated from the biodiesel industry into more valuable products. Glycerol has also gained importance for its properties in the treatment and diagnosis of disease. Given the scope of this review, only the biological relevance of glycerol, in particular to halophilic ecosystems and the biotechnological and medical applications of glycerol will be discussed.

### Glycerol as a Feedstock for Bioconversion

Glycerol can be produced either by microbial fermentation, recovered as a by-product of saponification, or can be chemically synthesized from petrochemical feedstocks. Glycerol has been of recent interest as a feedstock for bioconversion due to the low costs associated with its production as a result of the biofuels industry. Biodiesel is produced through base-catalyzed esterification of vegetable oil and animal fats (triacylglycerols) with short-chain alcohols such as methanol or ethanol. The principal by-product [10% weight (w) / volume (v)] obtained through such reactions is glycerol

(Papanikolaou et al., 2002; González-Pajuelo et al., 2004; Mu et al., 2006). Once considered a valuable co-product from biodiesel production, crude glycerol is now considered a costly waste stream with high disposal costs (Yazdani and Gonzalez, 2007). As a result of the highly reduced nature of the carbon atoms and the low production cost, glycerol is gaining increasing interest as a feedstock for bioconversion. Purified glycerol as well as its conversion products are used in a variety of commercial products including but not limited to those produced by the cosmetics, paints, automotive, food, tobacco, pharmaceutical, pulp and paper, leather, and textile industries (Wang et al., 2001).

Fermentative glycerol conversion pathways have been studied extensively in naturally fermentative species including *Enterobacter sp.* (Barbirato et al., 1997), *C. freundii*, *Clostridium sp*. (Forsberg, 1987), *Lactobacillus sp*. (Schütz and Radler, 1984), *Bacillus welchii* (González-Pajuelo et al., 2004), and *K. pneumoniae* (Biebl et al., 1998), and many of these organisms have been used for the conversion of glycerol to the primary fermentative product, 1,3-propanediol. Conversion of a glycerol feedstock to products other than 1,3-propanediol can be achieved through modulating culture conditions and/or genetic manipulation (Forsberg, 1987). Alternative glycerol fermentation products include DHA (Hu et al., 2010), hydrogen (Ito et al., 2005; Sakai and Yagishita, 2007; Sabourin-Provost and Hallenbeck, 2009), ethanol (Ito et al., 2005; Sakai and Yagishita, 2007), succinic acid (Lee et al., 2001), propionic acid (Liu et al., 2010), butanol (Biebl, 2001), 2,3-butanediol (Biebl et al., 1998; Petrov and Petrova, 2009), and biosurfactants such as rhamnolipids (Santa Anna et al., 2001). Due to i) the pathogenicity, ii) the requirement of strict anaerobiosis, iii) the need for rich nutrient

supplementation, and iv) the difficulty of genetic manipulation of the abovementioned glycerol-fermenting species, acidic glycerol fermentation by *E. coli* has also been recently investigated (Yazdani and Gonzalez, 2007). *E. coli* has been used for the anaerobic conversion of glycerol to 1,2-propanediol, hydrogen, lactate, formic acid, acetate, succinate, and ethanol (Dharmadi et al., 2006; Gonzalez et al., 2008; Murarka et al., 2008).

**Therapeutic and Diagnostic Uses of Glycerol**

In addition to its chemical and metabolic conversion, glycerol has also been widely used directly in a number of therapeutics, ranging from cancer treatment to rehydrating agents. The viscosity of glycerol enables its use as a softener in cough syrups, emollients, and ointments (Brisson et al., 2001). Due to its osmoregulatory properties, glycerol is used as a purgative and for the treatment of cerebral edemas, glaucoma, intracranial hypertension, and acute strokes (McCurdy et al., 1966; Bayer et al., 1987; Brisson et al., 2001). Glycerol can also serve as a hydrating agent, facilitating water adsorption in the kidneys and intestines and has been used to treat acute gastrointestinal diseases and constipation (Brisson et al., 2001). Furthermore, glycerol has shown potential as an anti-cancer agent since glycerol functions as a chemical chaperone and may help in correcting p53-dependent apoptosis (Ohnishi et al., 1999).

Glycerol also has implications in diagnostics. Increased median hemolytic time in 0.3 M glycerol solution serves as an indicator for various red blood cell disorders such as sickle-cell anemia, sickle-thalassemia, and β-thalassemia (Gottfried and Robertson, 1974). Additionally, the levels of serum glucose following glycerol administration can serve as an indicator for glucose intolerance (Senior and Loridan, 1968), and abnormal

glycerol levels in the kidney may serve as an indicator of renal disease (Brisson et al., 2001).

**Biological Relevance of Glycerol to Halophilic Communities**

Aside from its bioindustrial uses, glycerol is an important biological molecule for halophilic communities. High salt environments such as the Dead Sea, the Great Salt Lakes, and salterns are dominated by i) halophilic archaea, ii) halophilic, rod-shaped bacteria of the genus *Salinibacter*, and iii) the unicellular green alga *Dunaliella sp.* which serves as the primary producer for heterotrophic community members. In order to withstand osmotic stresses, *Dunaliella sp.* produces molar quantities of glycerol as an osmotic solute (Figure 1-1). Permeability studies indicate that this glycerol is available to heterotrophic members, especially as a result of external stresses such as increased temperature or hypertonic conditions (Wegmann et al., 1980; Fujii and Hellebust, 1992; Elevi Bardavid et al., 2008) (Figure 1-1). Thus, glycerol is often postulated to be one of the most important energy sources for heterotrophic prokaryotes in hypersaline ecosystems. This section will review the osmoprotectant nature of glycerol, the production and release of glycerol by *Dunaliella sp.*, and glycerol metabolism by heterotrophic community members. The importance of DHA as a potentially key substrate in the saltern ecosystem will additionally be addressed.

**Osmoprotectant properties of glycerol**

Halophilic and halotolerant microorganisms have adapted different mechanisms to withstand the high osmotic pressure exerted by their surrounding hypersaline environment. Most halophilic archaea as well as bacterial species from the anaerobic, fermentative order *Halanaerobiales* and the aerobic, halotolerant genus *Salinibacter* maintain a high intracellular cation concentration equal to that of the surrounding

environment (Lanyi, 1974). In the case of *Halanaerobiales*, the 'salt-in' strategy is the only feasible means of haloadaptation, since very little energy is obtained from fermentative pathways and the massive production of organic compatible solutes would leave insufficient energy for other cellular functions (Oren, 1999). Interestingly, *Salinibacter sp.*, which coexist with *Halobacteriaceae* members in hypersaline environments, have archaeal-like properties including an acidic proteome and similarities in genomic composition, suggesting horizontal gene transfer occurred between the two heterotrophic community members (Oren, 2008; Ánton et al., 2008). In general, cells which employ a 'salt-in' strategy accumulate $K^+$, $Mg^{2+}$, and $Cl^-$ ions and exclude $Na^+$ ions (Christian and Waltho, 1962). This salt protects halophilic proteins that tend to contain an excess of acidic amino acids through charge shielding (Lanyi, 1974). As a result, most intracellular proteins require high salt to retain activity (Lanyi, 1974).

Many halophilic bacteria, osmophilic yeast, and the halotolerant algae *Dunaliella sp.* exclude intracellular salts and instead accumulate compatible solutes. Interestingly, methanogenic archaea both accumulate salt and synthesize organic osmotic solutes such as glycine betaine and β-amino acids (Oren, 2008). The term 'compatible solute' was invoked while observing that intracellular polyols accumulate in large quantities in osmophilic yeast and enable these cells to tolerate environments with low water activity (Brown and Simpson, 1972). 'Compatible solute' is now generally used to describe a low molecular weight solute accumulating at high concentration which, by virtue of being a poor enzyme inhibitor, protects enzymes against inhibition which would otherwise occur under low water activity. A variety of compatible solutes including amino acids and their derivatives, sugar alcohols, and sugars have been described in halophilic and

halotolerant microorganisms. Individual chemical classes of compatible solutes can be widely distributed or limited to members of particular a phylogenetic group. Glycine betaine is a widely distributed compatible solute used by both halophilic methanogens and a number of bacteria, although few prokaryotes are capable of *de novo* synthesis of this compound (Oren, 2008). More widespread in bacteria are cyclic amino acid derivatives ectoine and hydroxyectoine, the former of which is synthesized by a number of aerobic, heterotrophic bacteria (Oren, 2008). In contrast, the distribution of compatible solutes glucosylglycerol and Nε-acetyl-α-lysine is more limited; the former is found nearly exclusively in moderate to highly halophilic cyanobacteria while the latter is found only in aerobic Firmicutes (Oren, 2008). Polyols such as glycerol are employed as compatible solutes almost exclusively by eukaryotes, although *Pseudomonas putida* uses mannitol (Kets et al., 1996). Glycerol, in particular, is the principal compatible solute produced in response to decreased extracellular water activity by yeast (Brown and Simpson, 1972; Blomberg and Adler, 1989) as well as algae (Craigie and McLachlan, 1964; Ben Amotz and Avron, 1973b; Borowitzka and Brown, 1974; Ben Amotz and Avron, 1979).

**Glycerol production by the halotolerant green algae *Dunaliella***

Glycerol accumulates in molar quantities as a compatible solute in the green, halotolerant algae *Dunaliella sp.* in response to increasing salt concentrations (Craigie and McLachlan, 1964; Ben Amotz and Avron, 1973b; Borowitzka and Brown, 1974). The mechanisms surrounding glycerol synthesis have not been well elucidated. The available data suggests that glycerol is primarily produced from starch reserves in the chloroplast which are converted to DHAP through glycolysis with consumption of reducing equivalents which are supplemented by the pentose phosphate pathway

(Chitlaru and Pick, 1991). In *Dunaliella salina*, it is proposed that G3P is produced from DHAP through an $NAD^+$-dependent G3PDH and is transported into the cytoplasm by a phosphate translocator in exchange for an inorganic phosphate molecule. Once in the cytoplasm, G3P is hydrolyzed by G3PP to form glycerol. Excess glycerol is returned to cellular metabolism by oxidation to DHA through an $NADP^+$-dependent GDH. Subsequent phosphorylation of DHA by an ATP-dependent DHAK generates DHAP which is transported back into the chloroplast. In *D. tertiolecta* photosynthesis also contributes to glycerol synthesis as evidenced by $^{14}CO_2$-flux to glycerol; however, its carbon contribution relative to starch degradation decreases with increasing osmotic stress (Goyal, 2007). Proteomic evidence for the involvement of both starch catabolism and photoassimilation of carbon dioxide in glycerol synthesis has also been reported in *D. salina* (Liska et al., 2004), in which key enzymes involved in the Calvin cycle, starch mobilization, and energy production are more abundant in a salt-induced proteome as identified by mass spectrometry.

Several factors contribute to the regulation of glycerol synthesis including i) intracellular pH, ii) PFK activity, and iii) cellular levels of ATP and inorganic phosphate. Cytoplasmic alkalinization following hyperosmotic shock of *Dunaliella* is proposed to activate glycerol synthesis based on the pH-dependence of starch-catabolizing enzymes in this alga (Goyal et al., 1987; Kuchitsu et al., 1989). PFK is implicated in regulating glycerol synthesis from starch, as it is a classical checkpoint for glycolysis. ATP and photoassimilation products such as phosphoglyceric acid inhibit PFK activity (and subsequent glycerol production), while inorganic phosphate activates PFK activity and glycerol synthesis (Chitlaru and Pick, 1991). $NAD^+$-dependent DHA reductase

activity has been reported in *Dunaliella parva* (Ben Amotz and Avron, 1973a) as well as *D. tertiolecta* (Gee et al., 1989), with the former having very weak $NAD^+$-dependent G3PDH activity, suggesting that glycerol may also be synthesized from DHA.

Due to the fact that glycerol is essential to the haloadaptibility of *Dunaliella sp.*, glycerol is several orders of magnitude less permeable to the biological membrane of this type of microalgae when compared to other organisms (Brown et al., 1982). Thus, glycerol release from lysed algal cells is an important means by which this organic carbon and energy source becomes available to halophilic, heterotrophic community members. Aside from glycerol release from lysed cells, *Dunaliella* cells can leak glycerol, especially at temperatures above 45 °C (Wegmann et al., 1980; Elevi Bardavid et al., 2008). Significant release of intracellular glycerol has also be observed in the marine alga *D. tertiolecta* as a result of hypotonic stress (Fujii and Hellebust, 1992). Thus, glycerol appears to be a significant organic carbon and energy source for members of halophilic communities. In addition to glycerol, DHA derived from the glycerol cycle is a substrate of potential interest to heterotrophic community members, although the extent to which DHA is permeable to the algal membrane is currently unknown (Elevi Bardavid and Oren, 2008).

**Glycerol metabolism in halophilic bacteria**

Aside from the primary producer *Dunaliella sp.*, the saltern community is also dominated by heterotrophic members including the halophilic bacterium *Salinibacter sp.* and various haloarchaea. As a result of its production and release in *Dunaliella sp*., glycerol has been reported to be one of the most available and rapidly turned over organic substrates in saltern communities (Sher et al., 2004). *Salinibacter* is proposed to metabolize glycerol solely through a glycerol-inducible GK based on enzymatic

activity assays for which no significant $NAD^+$-dependent GDH activity has been detected in cell lysate (Sher et al., 2004). Unlike haloarchaea, *Salinibacter* does not appear to produce organic acids following incomplete oxidation of glycerol (Sher et al., 2004). Instead, DHA has been detected as an overflow product of glycerol metabolism on the basis of a non-specific colorimetric assay and a specific, enzyme activity assay (Elevi Bardavid and Oren, 2008). DHA production can account for up to 20% of the glycerol metabolized (Elevi Bardavid and Oren, 2008). Interestingly, in the absence of glycerol, *Salinibacter* consumes DHA (Elevi Bardavid and Oren, 2008). The molecular mechanisms surrounding this DHA production and metabolism are currently unknown.

**Glycerol metabolism in haloarchaea**

Archaeal glycerol metabolism has been widely uncharacterized at the molecular level, especially in haloarchaea. Most of the current knowledge concerning haloarchaeal glycerol metabolism is based on enzyme activity analysis (Wassef et al., 1970; Rawal et al., 1988; Oren, 1994; Oren and Gurevich, 1994a). Similar to bacteria, archaea are believed to metabolize glycerol through either i) GK and G3PDH or ii) GDH and DHAK. GK enzymatic activity has been detected in many haloarchaea (Rawal et al., 1988). GDH has only been detected in *H. salinarium* and *H. cutirubrum* (Rawal et al., 1988) which are non-utilizers of carbohydrates. GK is noticeably absent from those halophilic archaea that cannot use glycerol as an energy source, such as autotrophic methanogens (Nishihara et al., 1999). Thus, GK is not thought to be involved in the synthesis of the backbone of archaeal phospholipids which is instead mediated by *sn*-G1P dehydrogenase (Nishihara et al., 1999). Putative GKs (*glpK*) often cluster on the genome with putative G3PDH (*gpdABC*) as well as putative glycerol facilitators (*glpX*, *glpF*) (Figure 3-1). Although most of the glycerol consumed by haloarchaea as an

energy source is respired to carbon dioxide, some glycerol is incompletely oxidized to organic acids such as acetate, pyruvate, and lactate in *Haloferax* and *Haloarcula sp.*, possibly due to the low oxygen dissolution under high salt (Oren and Gurevich, 1994b).

Aside from glycerol, DHA is also proposed to be a significant organic carbon source for members of the halophilic, heterotrophic community (Elevi Bardavid et al., 2008). *Haloquadratum walsbyi* metabolizes DHA as evidenced by colorimetric and specific enzymatic activity assays when cells are grown in complex media with DHA supplemented at 5 mM (Elevi Bardavid and Oren, 2008). Along with *H. walsbyi* (Bolhuis et al., 2006), bioinformatics predicts that *Halobacterium lacusprofundi* (Schneider et al., 2006) and *H. volcanii* (Hartman et al., 2010) encode homologs of each of the PEP:PTS DHAK components, although there is currently no evidence supporting the metabolism of DHA by the latter two organisms. Interestingly, DHA is produced both in *Salinibacter* and *Dunaliella sp.* and is consumed over time in saltern communities (Elevi Bardavid and Oren, 2008). However, the source of DHA turnover is complicated by the fact that: i) *Dunaliella sp.* encode a functional DHAK (Lerner and Avron, 1977; Lerner et al., 1980) and ii) DHA transporters and its permeability has not been characterized for any of halophilic community members.

**An Overview of Glucose and Fructose Metabolism in Haloarchaea**

Although glycerol is widely used by haloarchaea as a primary energy source, only a limited number of haloarchaea metabolize sugars such as glucose and fructose. For instance, although *H. volcanii* utilizes both glucose and fructose as sole carbon and energy sources, *Halobacterium sp.* are not able to utilize either carbohydrate (Gochnauer and Kushner, 1969). Haloarchaeal fructose and glucose dissimilation pathways have been somewhat characterized; however, knowledge concerning the

mechanisms through which these pathways are regulated and the means by which the sugar is transported into the cell remain limited. This section will focus on the transport of glucose and fructose, characterized pathways of glucose and fructose metabolism, and key regulators of sugar metabolic enzymes in haloarchaea.

## Transport of Fructose and Glucose Across a Biological Membrane

Data on sugar transport is limited in archaea, especially in halophilic archaea. Bioinformatics predicts that PTS sugar-specific permeases and general phosphocarrier components are encoded within archaeal genomes including various haloarchaea and *Thermofilum pendens*. However, none of these PTS homologs have been characterized. ABC transporters and secondary transport systems utilizing an electrochemical gradient of $Na^+$ ions have been described in the translocation of fructose and glucose across the membrane. Each of these transport systems, including an overview of the bacterial PTS, will be discussed in detail within this section.

### Overview of the Phosphotransferase System

The PTS catalyzes the concomitant phosphorylation and transport of sugar substrates in bacteria. The PTS consists of three essential catalytic entities which can be fused or encoded separately: cytoplasmic general energy-coupling proteins EI and Hpr and membrane-associated sugar specific permease enzyme II (EII) (Postma et al., 1993). The EII complexes generally consist of three proteins or protein domains (EIIA, EIIB, and EIIC); however, the mannose permease family consists of an additional domain (EIID). The EIIA and EIIB domains are involved in phosphorylation, while EIIC functions as a membrane-bound permease. Phosphoryl relay proceeds from phosphoenolpyruvate (PEP) as generated by enolase, to the N3 position of histidine-189 of EI (Weigel et al., 1982a), to the N1 position of histidine-15 of Hpr (Weigel et al.,

1982b), to a phosphorylatable histidine residue in family-specific EIIA, to a phosphorylatable histidine residue within permease-specific EIIB, and finally to the sugar substrate transported by sugar-specific permease EIIC. All phosphoryl transfer reactions between PTS proteins are reversible, and the phosphorylation status of various PTS proteins is determined by both PTS transport activity and the PEP:pyruvate ratio, reflecting flux through glycolysis (Kotrba et al., 2001). The dynamic phosphorylation status of PTS proteins in response to nutritional conditions and the metabolic state of the cell serves as the basis for PTS-mediated regulation of diverse metabolic processes. These processes include the transport and metabolism of non-PTS carbon sources, cell division, chemoreception, carbon storage and metabolism, non-carbon compound transport, pathogenicity, cellular motility, cell physiology, gene expression, nitrogen metabolism, and switching between fermentative and respiratory metabolism (Barabote and Saier, Jr., 2005; Deutscher et al., 2006).

PTS components are widely distributed in bacteria (Barabote and Saier, Jr., 2005) and uncharacterized homologs are additionally present in archaea. High G + C Gram-positive bacteria generally have a partial PTS, although complete transport systems for glucose, fructose, and ascorbate have been described in some members including *Corynebacterium.* Most Firmicutes contain the general carrier components Hpr and EI as well as the regulatory enzyme HprK and sugar specific permeases for glucose, fructose, and lactose. Spirochetes and α-proteobacteria often lack PTS components or contain only the general carrier phosphoproteins; whereas, the β- and gamma-proteobacteria encode more complete PTS components. Furthermore, many gamma-proteobacteria encode paralogs of EI, Hpr, and fructose-specific IIA proteins which

function as a phosphorelay system, contributing to nitrogen regulation (Powell et al., 1995). Each of these PTS components will be discussed.

**General carrier protein EI**

EI is a highly-conserved, soluble protein which, in *E. coli*, exists in equilibrium between a functional homodimer and a non-phosphorylatable monomer (subunit molecular mass 59 to 64 kDa) (Chauvin et al., 1994). Only the dimeric EI accepts the phosphoryl moiety from PEP, and the relatively slow EI monomer to dimer transition appears to be the rate-limiting step during *in vitro* phosphotransfer (Chauvin et al., 1996). Transfer of the phosphate moiety from PEP to EI requires the presence of $Mg^{2+}$ ions, although subsequent phosphotransfer to Hpr does not require this additional cofactor (Weigel et al., 1982a). The amino acid sequence of EI exhibits 30% similarity with pyruvate phosphate dikinase and PEP synthase which autophosphorylate at their respective active-site histidine residues using ATP or PEP as a phosphoryl donor (Pocalyko et al., 1990; Kotrba et al., 2001). The EI monomer is composed of two functional domains of equal size as determined by high-sensitivity differential scanning calorimetry in *Salmonella typhimurium* (LiCalsi et al., 1991). The N-terminal domain contains both the active site histidine residue which is located within a conserved signature motif of PEP-utilizing enzymes and the Hpr interaction site (Kotrba et al., 2001). The EI C-terminus binds PEP and is necessary for self-dimerization (Chauvin et al., 1996). Biophysical analysis of the *Streptomyces coelicolor* EI with several effectors indicates that EI is partly unfolded under acidic conditions and that PEP induces structural changes in this protein (Hurtado-Gomez et al., 2006).

**General carrier protein Hpr**

Hpr is a soluble, general carrier protein consisting of a single domain of approximately 9 kDa of variable amino acid sequence (Postma et al., 1993). Despite sequence variability, the site of phosphorylation involved in sugar transport, histidine-15, is well-conserved among Hpr proteins and is within a common consensus motif. The tertiary structure of Hpr is highly conserved, consisting of an arrangement of three α-helices and four overlaying β-sheets (Klevit and Waygood, 1986). The histidine-15 residue is located within the amino terminus of the first α-helix. The NMR solution structures of Hpr complexed with EI (Garrett et al., 1999) and $EIIA^{Glc}$ (Wang et al., 2000) do not exhibit significant changes in the chemical shift values, indicating that Hpr does not undergo large conformational changes with different binding partners. Most low-G + C Gram-positive bacterial and a few Gram-negative bacterial Hpr proteins can also be phosphorylated at serine-46 by an ATP-dependent HprK. This regulatory phosphorylation does not participate in sugar transport, although it inhibits EI-dependent histidine-15 phosphorylation by up to 600-fold (Stülke et al., 1998).

**Sugar-specific component EII**

EII components are multi-domain proteins or protein complexes consisting of a family-specific phosphoryl donor EIIA, a permease specific phosphoryl donor EIIB, a sugar specific permease/receptor EIIC, and, in the case of mannose permeases, an auxiliary protein EIID (Barabote and Saier, Jr., 2005). The EIIAB components consist of two peripheral proteins or domains of similar size, while the EIICD are integral proteins or domains (Kotrba et al., 2001). The EIIABC can exist as separate proteins or can be fused. There are seven characterized PTS permease families including: i) the glucose family that transports glucose, *N*-acetylglucosamine, maltose, glucosamine, glucosides,

sucrose, trehalose, and *N*-acetylmuramic acid, ii) the fructose family that transports fructose, mannitol, mannose, and 2-*O*-α-mannosyl D-glycerate, iii) the lactose family that transports lactose, aromatic β-glucosides, cellobiose, N,N'-diacetylchitobiose, and lichenan oligosaccharides, iv) the glucitol family that transports glucitol and 2-methyl-D-erythitol, v) the galactitol family that transports galactitol and D-arabinol, vi) the mannose family that transports glucose, mannose, sorbose, fructose, glucosomaine, galactosamine, *N*-acetylglucosamine, and other related compounds, and vii) the ascorbate family that transports L-ascorbate (Barabote and Saier, Jr., 2005). A non-transporting, soluble EII complex (DhaMLK) phosphorylates DHA at the expense of PEP with the aid of Hpr and EI (Gutknecht et al., 2001).

**ATP Binding Cassette Transporters**

ATP binding cassette (ABC) transporters, which appear to be widespread in archaea (Saier, Jr., 2000), have been biochemically characterized in all domains of life. ABC transporters are a ubiquitous class of proteins involved in varying cellular processes such as substrate uptake or export, osmosensing and osmoregulation, and antigen processing (Holland and Blight, 1999). ABC transporters consist of two integral membrane permease proteins and an ATPase, the latter of which drives the substrate translocation event through ATP hydrolysis. In eukaryotes, each of these functional components is contained within a single polypeptide, whereas in prokaryotes, single proteins constitute these activities (Albers et al., 2004). ABC transporters often have a very high affinity for their substrate, and have even been reported as low as the sub-nanomolar range for archaea (Xavier et al., 1996; Woodson et al., 2005). This high affinity provides an advantage for organisms that inhabit nutrient-deprived ecological niches. The ATPase components are generally conserved at several motifs including

Walker A and B sites, a helical domain, a linker peptide, and a switch region. The permease components typically consist of five to six membrane-spanning helices and an EAA-loop located 100 amino acids from the C-terminus.

Prokaryotic ATP transporters function through extracellular substrate-binding proteins which bind the substrate and deliver it to the permease domains. Upon docking to the permeases, the substrate is released from the substrate-binding protein and is subsequently translocated across the membrane. Prokaryotic substrate-binding proteins are structurally conserved and consist of two distinct globular domains which are drawn nearer to each other in a hinge-bending mechanism upon substrate binding within the cleft region (Quiocho and Ledvina, 1996). Unlike their bacterial counterparts, archaeal substrate-binding proteins are often glycosylated (Koning et al., 2001; Elferink et al., 2001; Koning et al., 2002), although this modification is not required for substrate binding based on heterologous protein production studies in *E. coli* (Horlacher et al., 1998; Koning et al., 2001; Koning et al., 2002). Glycosylation is proposed to stabilize these extracellular substrate-binding proteins against proteolysis, influence their interaction with the cell membrane, and/or alter their thermostability (Albers et al., 2004). Many archaeal ABC transporters have been characterized from hyperthermophiles (Xavier et al., 1996; Horlacher et al., 1998; Albers et al., 1999; Koning et al., 2001; Koning et al., 2002; Bevers et al., 2006), although genetic evidence for ABC transporters in methanogenic (Jovell et al., 1996; Schmidt et al., 2007; Chan et al., 2010) and halophilic archaea (Wanner and Soppa, 1999; Woodson et al., 2005) has been demonstrated.

### Secondary Transporters

Secondary transporters depend on the electrochemical gradient of sodium ions or protons to translocate the substrate across the cytoplasmic membrane. This group of transporters is widely used in mammals for amino acid as well as glucose and fructose transport (MacDonald et al., 1977; Lerner, 1987). *H. volcanii* transports both glucose (Tawara and Kamo, 1991; Severina et al., 1991) and fructose (Takano et al., 1995) through a sodium-dependent electrochemical gradient which is induced by the respective hexoses. Interestingly, inhibitors of mammalian glucose transport such as phloridzen and forskolin inhibit the *H. volcanii* glucose transporter (Tawara and Kamo, 1991), despite the somewhat low (26%) primary amino acid sequence identity.

## Fructose and Glucose Metabolism and Their Regulation in Haloarchaea

Various haloarchaeal species including those of the genera *Halobacterium*, *Haloarcula*, *Haloferax*, and *Halococcus*, are able to utilize glucose and fructose as sole carbon and energy sources (Rawal et al., 1988). Some notable non-carbohydrate utilizers include *H. salinarum* and *H. cutirubrum* (Rawal et al., 1988). While basic carbon metabolic pathways such as the Entner-Doudoroff (ED) pathway are conserved in eukaryotes and eubacteria, archaea have diverse central metabolic networks. These highly variable central metabolic pathways of carbohydrate include modifications to the ED pathway as well as the Embden-Meyerhof-Parnas pathway (EMP pathway, glycolysis) (Siebers and Schönheit, 2005). Unlike bacteria which primarily degrade hexoses through a classical EMP pathway, haloarchaea such as *Halococcus saccharolyticus*, *Haloferax mediterranei*, and *Haloarcula vallismortis* catabolize the isomeric hexoses fructose and glucose through functionally separated, inducible pathways (Altekar and Rangaswamy, 1990; Altekar and Rangaswamy, 1992;

Rangaswamy and Altekar, 1994; Johnsen et al., 2001). $^{13}$C-NMR during fermentative growth, enzymatic studies, and DNA microarray analyses revealed that glucose is degraded only by way of a modified 'semi-phosphorylative' ED pathway in *Halobacterium saccharovorum*, *H. mediterranei*, *H. saccharolyticus*, *H. volcanii* and *H. vallismortis* (Tomlinson and Hochstein, 1972; Rawal et al., 1988; Johnsen et al., 2001; Zaigler et al., 2003) (Figure 1-2), whereas fructose is almost completely metabolized by way of a modified EMP pathway in *H. vallismortis* and *H. saccharolyticus* (Altekar and Rangaswamy, 1990; Johnsen et al., 2001) (Figure 1-3). Although the isomeric hexoses are catabolized by separate pathways according to $^{13}$C-NMR, enzymatic activities for proteins involved in both pathways were detectable in cells grown in either sugar, although not to the same extent as pathway-specific enzymes (Johnsen et al., 2001). As in the case of glycerol, haloarchaea including *Haloferax sp.* and *Haloarcula sp.* incompletely oxidize sugars to organic acids such as lactate, pyruvate, and acetate (Tomlinson and Hochstein, 1972; Oren and Gurevich, 1994b; Bräsen and Schönheit, 2001). To date, the knowledge concerning regulators of archaeal sugar metabolism has been limited. However, pairs of general transcription factors TATA-binding protein (TBP) and transcription factor B (TFB) contribute toward the expression of many genes including those involved in hexose metabolism (Facciotti et al., 2007; Coker and DasSarma, 2007). Aspects of each pathway including regulation are discussed.

**Glucose Degradation through a Modified Entner-Doudoroff Pathway**

Glucose degradation to pyruvate through a modified ED pathway by haloarchaea was first proposed for *H. saccharovorum* based on detectable enzymatic activities for glucose dehydrogenase and gluconate dehydratase and the absence of detectable activity for glucose-6-phosphate dehydrogenase and 6-phosphogluconate dehydrase

activities in crude cell extract (Hochstein, 1974). Evidence for a modified ED in glucose metabolism was subsequently reported for *H. mediterranei* and *H. vallismortis* based on a higher observed enzymatic activity of glucose dehydrogenase (8.3 to 29.8 mU) than glucose-6-phosphate dehydrogenase (0.6 to 3.7 mU) in glucose-grown cells (Rawal et al., 1988). More recently, radioisotope labeling experiments coupled with $^{13}C$-NMR and specific enzyme activity assays for glucose dehydrogenase, gluconate dehydratase, 2-keto-3-deoxygluconate kinase (KDGK), and 2-keto-3-deoxy-6-phosphogluconate (KDPG) aldolase has confirmed the degradation of glucose through a semi-phosphorylative ED pathway in *H. saccharolyticus* (Johnsen et al., 2001) and DNA microarray analysis of *H. volcanii* confirmed significant upregulation of gene transcripts encoding glucose dehydrogenase and KDGK during growth on glucose-containing media (Zaigler et al., 2003).

Unlike the classical ED pathway which begins with phosphorylation of either glucose or its oxidized derivative gluconate, the semi-phosphorylative ED pathway does not contain phosphorylated intermediates prior to KDPG (Figure 1-2). Instead, glucose is first oxidized to gluconate through an $NADP^+$-dependent glucose dehydrogenase. Following oxidation, gluconate dehydratase catalyzes the conversion of gluconate to 2-keto-3-deoxygluconate (KDG) which is then phosphorylated by a unique KDG kinase (KDGK) to KDPG. A subsequent cleavage of KDPG occurs by KDPG aldolase, yielding pyruvate and glyceraldehyde 3-phosphate. The latter compound is oxidized to pyruvate through a conventional process involving glyceraldehyde-3-phosphate dehydrogenase, phosphoglycerate kinase, phosphoglycerate mutase, enolase, and pyruvate kinase.

**Fructose Degradation through a Modified Embden-Meyerhof-Parnas Pathway**

Analysis of fructose degradation in *H. vallismortis* revealed that fructose is degraded to pyruvate through a modified EMP pathway based on measurement of ketohexokinase and phosphofructokinase (PFK) enzyme activities in fructose-grown cells (Altekar and Rangaswamy, 1990). As with glucose metabolism, radioisotope labeling experiments coupled with $^{13}$C-NMR and specific enzyme activity assays for ketohexokinase, PFK, as well as “classical” fructose catabolic enzymes have confirmed the degradation of fructose through a modified EMP pathway in *H. saccharolyticus* (Johnsen et al., 2001) (Figure 1-3).

This modified EMP pathway differs from the “classical” fructose degradation pathways of bacteria only in the mechanisms of fructose 1-phosphate (F1P) formation. Most bacteria phosphorylate fructose during transport by the PEP:PTS. However, in *H. vallismortis* and *H. saccharolyticus*, F1P is formed through ketohexokinase-dependent phosphorylation of fructose (Rangaswamy and Altekar, 1994; Johnsen et al., 2001). F1P is phosphorylated to FBP through PFK and is subsequently converted to two pyruvate molecules through the conventional enzymes of the EM pathway (Altekar and Rangaswamy, 1990; Johnsen et al., 2001). Some haloarchaea including *H. volcanii*, *Haloterrigena turkmenica*, and *Haloarcula marismortui* encode PTS general carrier components EI and Hpr as well as fructose-specific permeases, providing a possibility that fructose phosphorylation may proceed through the PTS, similar to many bacteria (Figure 1-3). However, functional characterization of these proteins has not been performed.

## Regulation of Glucose and Fructose Metabolism in Haloarchaea

Currently, very little data is available concerning the regulation of glucose and fructose metabolism in archaea, especially in haloarchaea. Although preferential utilization of glucose over fructose was demonstrated for *H. saccharolyticus*, the molecular basis of this catabolite repression has not described (Johnsen et al., 2001). The majority of characterized archaeal regulators of carbon metabolism are transcription factors from hyperthermophiles (Lee et al., 2003; Lee et al., 2005; Kanai et al., 2007), although a few of haloarchaeal regulators have also been characterized (Facciotti et al., 2007; Coker and DasSarma, 2007; Schmid et al., 2009). Specifically, in *H. salinarum*, pairs of general transcription factors TBP and TFB as well as the transcription factor TrmB control gene clusters (Facciotti et al., 2007; Coker and DasSarma, 2007); however, this haloarchaeon is not able to metabolize either glucose or fructose (Rawal et al., 1988). No regulators of sugar metabolism have been characterized in the model haloarchaeon *H. volcanii*, although homologs of characterized transcription factors are predicted based on primary sequence similarity.

### TrmB

TrmB is a transcriptional regulator that governs the expression of a wide array of genes in response to cellular redox and energy status. TrmB is conserved across many archaeal and some bacterial species (primarily Firmicutes); however, TrmB orthologs have not been characterized to date in bacteria (Lee et al., 2008). TrmB-like proteins regulate maltose and glucose usage in thermophilic archaea (Lee et al., 2003; Lee et al., 2005; Kanai et al., 2007; Lee et al., 2008) and in nutrient limitation in halophilic archaea (Schmid et al., 2009).

TrmB was originally identified in *Thermococcus litoralis* (Lee et al., 2003), where TrmB was implicated in regulating trehalose and maltose metabolism *in vitro*. In the absence of trehalose or maltose, TrmB blocks transcription of the trehalose and maltose ABC transporter operon, which also encodes *trmB*, through direct binding of its promoter region. Dissociation of TrmB from its operator sequence occurs upon binding of sugar ligands, resulting in subsequent transcriptional initiation. A recent *in vitro* analysis of *P. furiosus* TrmB suggested that the maltodextrin-specific ABC transporter is also under the control of TrmB (Lee et al., 2005). Maltodextrin and sucrose were found to relieve the TrmB-repression of maltodextrin transport, whereas glucose increased transcriptional repression of the ABC transporters.

More recently, *H. salinarium* TrmB has been implicated in coordinating the transcription of various genes including those involved in cofactor synthesis in response to nutrient limitation (Schmid et al., 2009). Microarray analysis of both parent and *trmB*-deficient strains grown in complex medium in the presence or absence of sugars (glucose or glycerol) indicated the differential transcription of 182 or 113 genes, respectively, whose gene products are linked to carbohydrate, amino acid, cofactor, vitamin, and purine biosynthetic pathways, many of which are incomplete. TrmB homologs can be found in most haloarchaea, but whether these homologs control similar gene clusters is unclear.

**General transcription factors TATA binding protein and transcription factor B**

General transcription factors are used for global gene regulation in all domains of life. Bacteria generally accomplish large-scale transcriptional regulation through σ factors which respond to environmental stimuli. On the other hand, eukaryotes utilize multi-subunit general transcription complexes to initiate large-scale changes in

transcription from various promoters. Despite the fact that many archaeal regulatory proteins resemble bacterial regulators, the transcriptional machinery is more eukaryotic-like (Geiduschek and Ouhammouch, 2005). In addition to a multi-subunit RNA polymerase, archaeal genomes contain the basal transcription factors TBP and TFB, which are orthologous to the eucaryal TBP and TFIIB proteins and are necessary and sufficient for initiating basal transcription (Zillig et al., 1979; Soppa, 1999; Bell and Jackson, 2001).

In haloarchaea, these general transcription factors are often present in multiple copies, with *H. salinarum* encoding six TBPs and seven TFB proteins (Baliga et al., 2000). Due to the interaction of TBP and TFB to recruit RNA polymerase and given the large number of orthologs present, there are several combinations of TBPs and TFBs which may drive transcription from an equally diverse set of promoters. Through gene knockout of general transcription factor orthologs and subsequent transcriptome analysis of mutant strains, a large regulatory network which includes genes encoding putative sugar metabolic enzymes was discovered (Facciotti et al., 2007; Coker and DasSarma, 2007). Co-immunoprecipitation analysis identified roughly 37% of all promoters (over 1,000) as being bound by a single transcription factor, whereas the majority of promoters are associated with multiple general transcription factors (Facciotti et al., 2007). Gene knockout and subsequent transcriptome analysis revealed that 20% of the total genes regulated by general transcription factors are regulated by TbpD and TfbA (Coker and DasSarma, 2007). Although target promoters of general transcription factors have been identified, the molecular mechanisms of the interactions are still unclear.

## Project Rationale and Design

The primary objective of this study was to characterize haloarchaeal carbon metabolism, specifically focusing on glycerol, glucose, and fructose metabolism, using *H. volcanii* as a model system. Although glycerol is thought to be a primary energy source for heterotrophic members of halophilic communities, the molecular mechanism surrounding its degradation and regulation has not been characterized. Thus, this study sought to elucidate the molecular mechanism surrounding glycerol metabolism in *H. volcanii.* Similarly, data concerning the regulation of haloarchaeal glucose and fructose metabolic enzymes is severely limited. Thus, this study also sought to characterize regulators of haloarchaeal glucose and fructose metabolism, specifically focusing on a DeoR/GlpR-type transcriptional regulator from *H. volcanii. H. volcanii* was chosen as a model haloarchaeon within which to study these pathways and their regulation based on the relevance of these carbon sources to this organism's ecology, the limited knowledge concerning these metabolic pathways and their regulation within the model organism, the ease with which *H. volcanii* is genetically manipulated, the availability of the genome sequence, and the availability of proteomic tools. After identifying homologs of bacterial glycerol metabolic enzymes in *H. volcanii*, involvement of each gene in glycerol catabolism was confirmed through gene deletion and subsequent phenotypic and carbon utilization studies. The biochemical properties, organization, and regulation of each of these genes and their gene products was determined through specific enzyme activity assays, (q)RT-PCRs, and transcriptional promoter-reporter fusion assays. A bioinformatic approach to identify regulators of glucose and fructose metabolism led to the discovery of a DeoR/GlpR-type repressor of glucose and fructose metabolic enzymes. The *glpR* gene clustered chromosomally with genes encoding sugar

metabolic enzymes. The physiological role of this regulatory protein was determined through gene deletion and subsequent qRT-PCRs, enzymatic activity assays, and transcriptional promoter-reporter fusion assays. A putative GlpR binding site for each target promoter region was identified by bioinformatic analysis, and a preliminary mode of regulation is suggested.

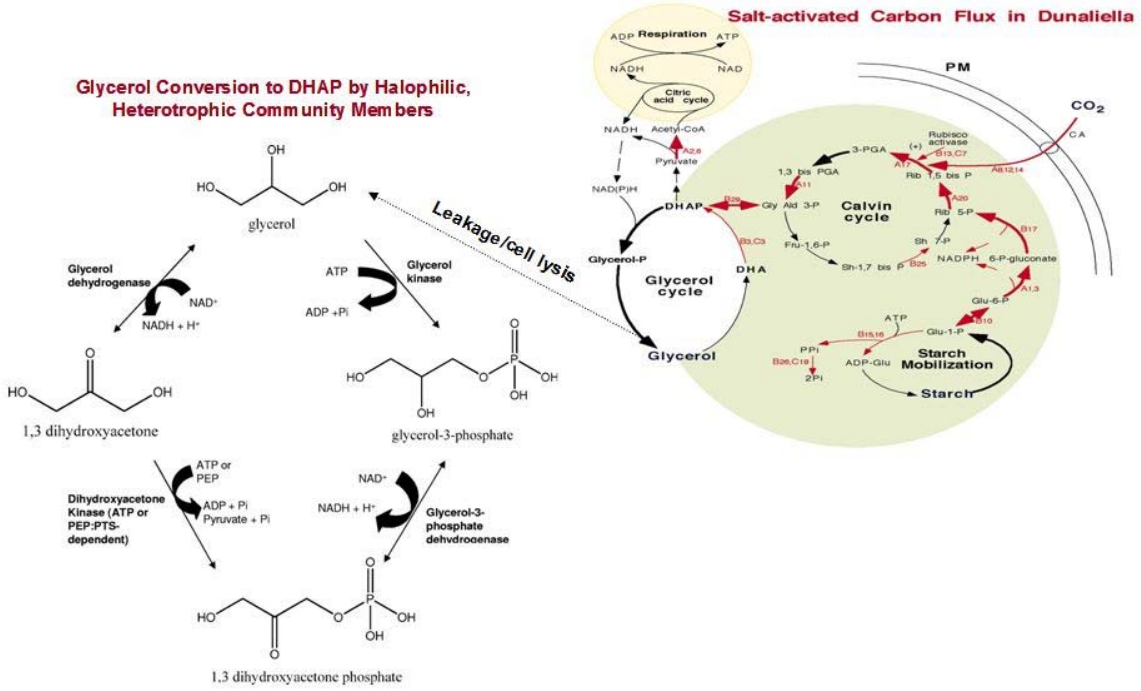


Figure 1-1. Glycerol synthesis, release, and catabolism in halophilic ecosystems. Glycerol is produced by *Dunaliella sp*. as an organic osmotic solute in response to salt stress through both degradation of starch reserves and by enhancement of photosynthesis. Glycerol is released into the environment either through algal cell lysis or by leakage which occurs in response to increased temperatures (above 45 °C) or hypotonic stress where it becomes a readily-available organic carbon source for heterotrophic community members. Halophilic, heterotrophic microorganisms can then convert glycerol into DHAP through one of two pathways: i) through GK and G3PDH or ii) through GDH and ATP- or PEP:PTS-dependent DHAK. The portion of the figure displaying salt-activated carbon flux in *Dunaliella* was modified from (Liska et al., 2004). Abbreviations: PM, plasma membrane; CA, carbonic anhydrase; PEP:PTS, phosphoenolpyruvate-linked phosphotransferase system.

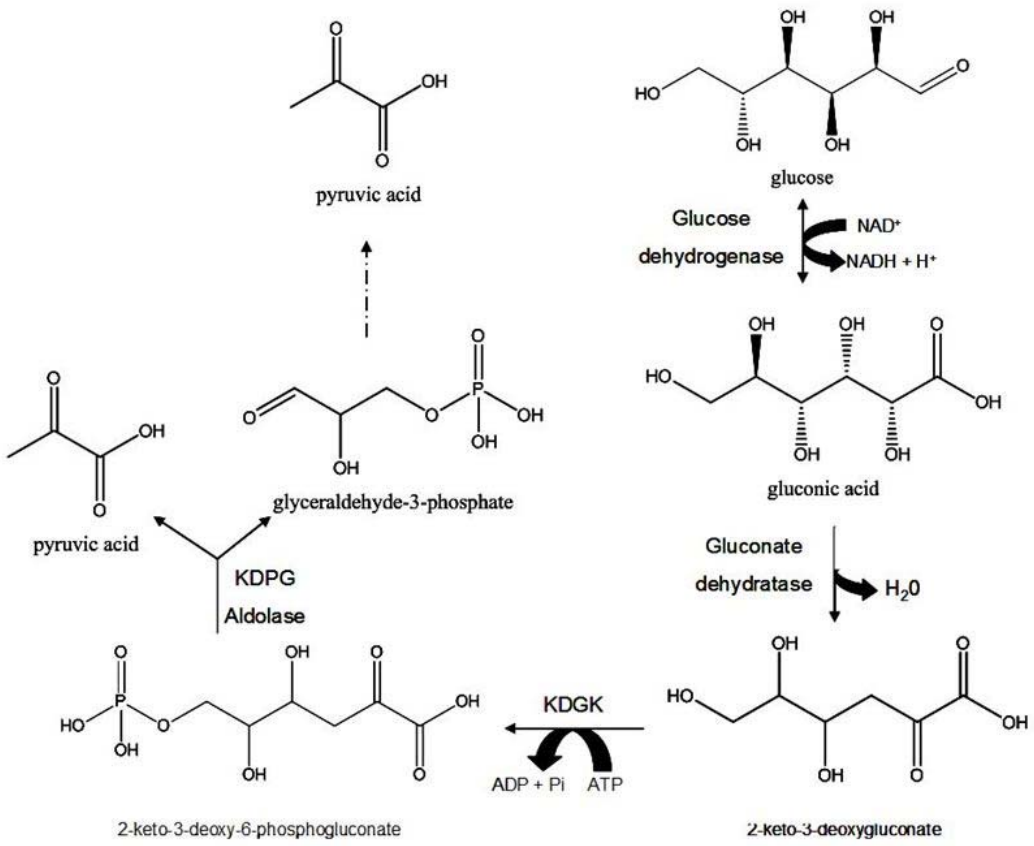


Figure 1-2. Metabolic conversion of glucose to pyruvic acid in haloarchaea. Glucose is metabolized by a modified Entner-Doudoroff Pathway in a variety of haloarchaea including *H. volcanii*, *H. saccharovorum*, *H. mediterranei*, *Haloarcula vallismortis*, and *H. saccharolyticus* as evidenced by proteomic data, $^{13}$C-NMR, and enzyme activity assays (Hochstein, 1974; Rawal et al., 1988; Johnsen et al., 2001; Zaigler et al., 2003). Dashed arrow indicates multiple conversion steps to pyruvic acid including conversions by "classical" enzymes glyceraldehyde-3-phosphate dehydrogenase, 3-phosphoglycerate kinase, phosphoglycerate mutase, enolase, and pyruvate kinase. Abbreviations: KDGK, 2-keto-3-deoxygluconate kinase; KDPG, 2-keto-3-deoxy-6-phosphogluconate.

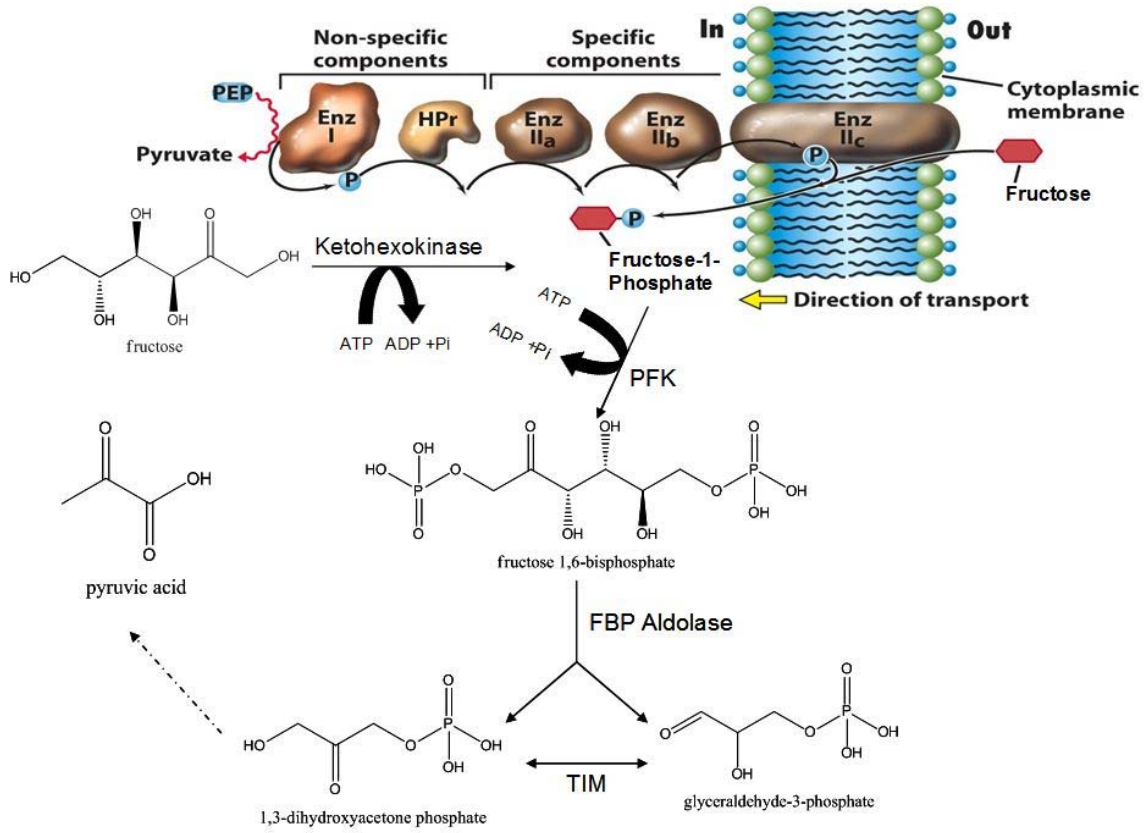


Figure 1-3. Potential routes for the metabolic conversion of fructose to pyruvic acid by haloarchaea. Conversion of fructose to F1P is catalyzed by ketohexokinase in *H. vallismortis* and *H. saccharolyticus* as evidenced by $^{13}$C-NMR and enzyme activity analysis (Rangaswamy and Altekar, 1994; Johnsen et al., 2001). Homologs of PTS general carrier components and fructose-specific PTS permease components are found in *H. volcanii*, *H. turkmenica*, and *H. marismortui*, although it is unclear whether these components are functional. The PTS portion of the figure was modified from (Madigan et al., 2006). Dashed arrow indicates multiple conversion steps to pyruvic acid including conversions by "classical" enzymes glyceraldehyde-3-phosphate dehydrogenase, 3-phosphoglycerate kinase, phosphoglycerate mutase, enolase, and pyruvate kinase. Abbreviations: PFK, phosphofructokinase; FBP, fructose-1,6-bisphosphate; and TIM, triosephosphate isomerase.

# CHAPTER 2
# METHODS AND MATERIALS

## Chemicals, Media, and Strains

### Chemicals and Reagents

Biochemicals and commercial enzymes were purchased from Sigma-Aldrich (St. Louis, MO). Other organic and inorganic analytical-grade chemicals were purchased from Fisher Scientific (Atlanta, GA) and Bio-Rad Laboratories (Hercules, CA). Desalted oligonucleotides were from Integrated DNA Technologies (Coralville, IA). 2'-Deoxyuridine-5'-triphosphate coupled by an 11-atom spacer to digoxigenin (DIG-11-dUTP), alkaline phosphatase-conjugated antibody raised against DIG, disodium 3-(4-methoxyspiro{1,2-dioxetane-3,2'-(5'-chloro)tricyclo[3.3.1.1$^{3,7}$]decan}-4-yl) phenyl phosphate (CSPD), DIG-labeled RNA molecular weight standard I (0.3 - 6.9 kb), and other DIG-related biochemicals were purchased from Roche Applied Science (Indianapolis, IN). Positively-charged nylon membranes (Bright-Star Plus) used for Southern hybridizations were from Ambion, Inc. (Austin, TX). Phusion and *Taq* DNA polymerases, restriction enzymes, deoxyribonucleotide triphosphates (dNTPs), T4 polynucleotide kinase (PNK), T4 DNA ligase, Antarctic Phosphatase (AP), and Quick-Load® 100 bp molecular weight standards were purchased from New England Biolabs (Ipswich, MA). Agarose, Precision Plus Protein™ Kaleidoscope molecular mass markers, and iQ™ SYBR® Green Supermix and iScript™ cDNA synthesis kit used for (quantitative) reverse transcriptase-polymerase chain reactions [(q)RT-PCRs] were purchased from Bio-Rad Laboratories. Hi-Lo DNA molecular weight standards were from Minnesota Molecular, Inc. (Minneapolis, MN). StrepTactin Superflow resin was purchased from Qiagen (Valenia, CA).

**Strains, Plasmids, and Culture Conditions**

Strains, oligonucleotide primers used for cloning and screening of mutant strains, and plasmids are listed in Tables 2-1 through 2-6. *Escherichia coli* strains DH5α or Top10 (Life Technologies, Carlsbad, California) was used for routine, recombinant DNA experiments. *E. coli* strain GM2163 (New England Biolabs) was used for isolation of plasmids lacking methylation for transformation into *H. volcanii* strains (Cline et al., 1989). Liquid cultures were aerated with orbital shaking at 200 revolutions per minute (RPM). *E. coli* strains were grown at 37 °C in Luria-Bertani (LB) medium (Bertani, 1951) supplemented with ampicillin (100 $mg \cdot l^{-1}$) as needed. *H. volcanii* strains were grown at 42 °C in various media including yeast extract-peptone-casamino acids (YPC), American Type Culture Collection (ATCC) 974, casamino acids (CA), YPC supplemented with glucose (Glu) or fructose (Fru), and minimal medium (MM) supplemented with glycerol (Gly), Glu, Fru, succinate (Suc), and various combinations of these carbon sources. Medium formulae were according to *The Halohandbook* (Dyall-Smith, 2008) with the following exception: Suc, Gly, Fru, and/or Glu were included at 20 mM each where indicated. Biodiesel waste was received from Douglas Renk at the University of Florida, Department of Chemical Engineering. Glycerol content of the biodiesel waste was analyzed by high performance liquid chromatography (HPLC) using a Bio-Rad Aminex® HPX-87H column (300 x 7.8 mm) and a refractive index detector with 4 mM $H_2SO_4$ as eluent (flow rate was set to 0.4 $ml^{-1}min^{-1}$). Biodiesel waste was then provided as the sole carbon source in the minimal medium to a final concentration of 20 mM glycerol. Media were supplemented as needed with novobiocin (0.1 $\mu g \cdot ml^{-1}$), 5-fluoroorotic acid (5-FOA) (50 $\mu g \cdot ml^{-1}$), tryptophan (820 $\mu g \cdot ml^{-1}$), and uracil (10 and 50 $\mu g \cdot ml^{-1}$ for growth in the presence and absence of 5-FOA,

respectively). Uracil and 5-FOA were dissolved in 100% [volume (v)/v for 5-FOA or weight (w)/v for uracil] dimethyl sulfoxide (DMSO) at 50 $mg \cdot ml^{-1}$ prior to addition to the growth medium.

For growth assays, cells were grown in media as indicated within Chapter 3 through Chapter 7. Cells were inoculated from –80 °C glycerol stocks onto appropriate solid media. Cells were thrice subcultured during logarithmic-phase growth and used as an inoculum for final growth analysis under various conditions as described below. Each subculture was started at an initial optical density at 600 nm ($OD_{600}$) of 0.03 to 0.04. For determination of growth rate, cell yield, and carbon utilization, cells were grown in 20 ml of medium in 250-ml baffled Erlenmeyer flasks. For GK enzyme activity assays, cells were grown in 100 ml of medium in 1000-ml flasks. For G3PDH, PFK, and KDGK enzyme activity assays and for RNA preparation, cells were grown in 25 ml of medium in 250-ml flasks. For β-galactosidase activity measurements, cells were grown in 3 ml of medium in 13 × 100 mm culture tubes. Cell growth was monitored by an increase in $OD_{600}$ [where 1 $OD_{600}$ unit equals approximately $1 \times 10^9$ colony forming units (CFU)$\cdot ml^{-1}$ for all strains used in this study]. All experiments were performed at least in triplicate and the means ± standard deviations (SD) of the results were calculated. For purification of C-terminally labeled StrepII-tagged proteins, cells were grown in 500 ml of YPC in 1000 ml flasks and pooled prior to protein purification.

**High Performance Liquid Chromatography**

At various time points during growth, 1 ml culture samples of parent (H26), GK *glpK* mutant (KS4), transcriptional repressor *glpR* mutant (KS8), and a mutant deficient in both *glpK* and *glpR* (KS10) were withdrawn and centrifuged (10 min, 10 000 × *g*, 4 ºC). Supernatant fractions were filtered using a 0.2 µm-pore size filters (Nalge Nunc

International, Rochester, NY) and subsequently analyzed by HPLC using a Bio-Rad Aminex® HPX-87H column (300 x 7.8 mm) and a refractive index detector with 4 mM $H_2SO_4$ as eluent (flow rate was set to 0.4 $ml^{-1}min^{-1}$). All experiments were performed at least in triplicate and the means ± SD of the results were calculated.

## DNA Procedures

### DNA Isolation and Analysis

Plasmid DNA was isolated from *E. coli* strains by use of the QIAprep spin miniprep kit (Qiagen). PCR products were purified by MinElute (Qiagen) prior to modification by restriction enzymes (BamHI, HindIII, KpnI, BlpI, BspHI, XbaI, HpaI, or NdeI), T4 PNK, or T4 DNA ligase. When applicable, plasmids were purified from agarose slices by QIAquick gel extraction kit (Qiagen). For rapid PCR screening, template DNA was extracted from *H. volcanii* mutant and parent strains and recombinant *E. coli* strains as described previously (Zhou et al., 2008). For Southern blots, *H. volcanii* genomic DNA was isolated from 5 ml cultures by DNA spooling (Dyall-Smith, 2008). The fidelities of all cloned PCR amplified products as well as mutant strains were confirmed by Sanger automated DNA sequencing using an Applied Biosystems model 3130 genetic analyzer (DNA Sequencing Facilities, Interdisciplinary Center for Biotechnology Research, University of Florida). DNA was separated by gel electrophoresis using 0.8% (w/v) or 2.0% (w/v) agarose gels in 1× TAE electrophoresis buffer [40 mM N-tris(hydroxymethyl) aminomethane (Tris)-acetate (pH 8.5) and 2 mM ethylenediaminetetraacetic acid (EDTA)] (Aaij and Borst, 1972). Hi-Lo (Minnesota Molecular, Inc.) or Quick-Load 100 bp (New England Biolabs) molecular weight standards were used for product size estimation. Gels were photographed with a Mini visionary imaging system (FOTODYNE, Hartland, WI) after staining with ethidium bromide (0.5 $\mu g \cdot ml^{-1}$).

**Polymerase Chain Reactions**

High-fidelity, double-stranded DNA PCR products used for construction of the plasmids listed in the Tables 2-1, 2-3, 2-5, and 2-7 were amplified using Phusion DNA polymerase. *Taq* DNA polymerase was used for screening transformants, for the generation of DIG-labeled double-stranded DNA probes that were used for Southern blotting, and for (q)RT-PCRs. All PCRs were performed according to the Supplier's instructions with the following modifications: 3% (v/v) DMSO was included and 0.1 mM dNTP mix was added to the standard DIG-labeling reaction mixture which included 1× DIG dNTP (Roche Applied Science). Primer pairs and template DNA used for the PCRs are outlined in the Tables 2-2, 2-4, 2-6, 2-8. PCRs were performed using an iCycler or GeneCycler (Bio-Rad Laboratories).

**Cloning**

Product inserts, vectors, and genomic DNA were digested using restriction enzymes (BamHI, HindIII, KpnI, BlpI, BspHI, XbaI, HpaI, SphI, MluI, ClaI, or NdeI) according to Manufacturer's specifications. Digested vector DNAs were treated with AP for 45 min at 37 ˚C followed by heat inactivation at 65 ˚C for 15 minutes prior to purification and subsequent ligation. For blunt-end cloning, Vent polymerase was used to resolve overhangs according to the Manufacturer's instructions. For inverse PCRs, the resulting products were treated with T4 PNK according to the Supplier's recommendations (New England Biolabs). Ligation reactions were performed using T4 DNA ligase at 16 ˚C for 12 - 16 hours according to the Supplier's recommendations.

**Construction of *H. volcanii* Deletion Strains**

Several genes were targeted for markerless deletion from the chromosome of *H. volcanii* H26 using the *pyrE2*-based "pop-in/pop-out" method (Bitan-Banin et al., 2003;

Allers et al., 2004). Briefly, the open reading frame (ORF) of the targeted gene along with 500-bp of flanking region was cloned into pTA131 digested with BamHI and HindIII. After ligation, the resulting plasmid was transformed into *E. coli* Top10, and screened for the presence of the insert. After confirming sequence fidelity, inverse PCR was performed to remove the coding region of the targeted gene, and the subsequent PCR product was treated with T4 PNK prior to ligation to generate the new plasmid construct. This plasmid was transformed into *E. coli* GM2163 before transformation into H26 Δ*pyrE2* which is a uracil auxotroph. *H. volcanii* transformants were plated onto CA medium without uracil and growth was counter-selected on media containing 5-FOA, allowing for either deletion of the target gene or restoration of the wild-type gene copy. Colonies were screened for the absence of a readily-generated PCR product by use of internal primers specific for the ORF of the target gene ('Negative-Forward' and 'Negative-Reverse' primer pairs). Colonies that did not yield this PCR product were confirmed to be mutant strains by Southern blotting and PCR with 'Confirm-Forward' and 'Confirm-Reverse' primer pairs that anneal within the target flanking regions cloned into the suicide plasmids. These latter PCR products were separated by gel electrophoresis and sequenced to confirm DNA fidelity.

**Southern Blot Analysis**

*H. volcanii* parent H26 and mutant strains were subjected to Southern blotting to confirm mutation as described previously (Zhou et al., 2008). Briefly, *H. volcanii* genomic DNA (10 µg) was isolated from 5 ml cultures by DNA spooling (Dyall-Smith, 2008) and subjected to restriction digestion for 6-8 hours. DNA was separated on a 0.8% (w/v) gel (20V, 12 - 16 h) and transferred (12 - 16 h) to a positively charged nylon membrane through capillary action. DNA was then cross-linked to the membrane using

a UV Stratalinker 2400 (Stratagene) and hybridized to a DIG-labeled probe specific for the region flanking the 5' or 3'-end of the target coding region (65 ºC, 12 - 16 h). Primers used for the construction of DIG-labeled probes are included in Tables 2-2, 2-4, and 2-8. Hybridization species were detected by CSPD-mediated chemiluminescence as recommended by the Supplier (Roche Applied Science) with the following modifications: an increase in stringency from 0.5x saline sodium citrate (SSC) [1x SSC is 0.15 M NaCl with 0.015 M sodium citrate (pH 7.0)] supplemented with 0.1% (w/v) sodium dodecyl sulfate (SDS) to 0.1x SSC supplemented with 0.1% (w/v) SDS was included in the washing of the membranes at 65 °C after hybridizations as needed. The DNA fragment sizes were estimated by methylene blue staining of the Hi-Lo DNA molecular weight markers on the membrane.

**Construction of Promoter-Reporter Fusion Constructs**

A plasmid-based reporter system was used to analyze transcription (Delmas et al., 2009) in which promoter regions of haloarchaeal operons/genes were fused to the *Haloferax alicantei*-derived *bgaH* gene encoding β-galactosidase. The *bgaH* gene was amplified from pTA102 (the primers used for cloning of the insert are provided in Table 2-6 and 2-8) and cloned into pJAM202 using NdeI and BlpI which fused the *bgaH* gene downstream of the strong rRNA P2 promoter of *H. cutirubrum* to generate pJAM2678. The regions upstream of *glpR-pfkB*, *kdgK1*, *kdgK2*, *glpK*, *gpdA1*, and *trpA* were amplified from *H. volcanii* genomic DS70 DNA using the primers listed in Tables 2-6 and 2-8, and were fused with *bgaH* using XbaI and NdeI digestion to generate pJAM2689 (188-bp *glpR-pfkB*-promoter region), pJAM2705 (89-bp *kdgK1*-promoter region), pJAM2706 (524-bp *kdgK1*-promoter region), pJAM2702 (232-bp *kdgK2*-promoter region), pJAM2703 (122-bp HVO_A0327-*kdgK2* promoter region), pJAM2679 (354-bp

*glpK*-promoter region), pJAM2780 (310-bp *gpdA1*-promoter region), and pJAM2712 (321-bp *trpA*-promoter region) (where bp represent the region upstream of the translational start codon of the first gene listed for each construct). Plasmid constructs were purified from *E. coli* strains Top10 and GM2163 prior to transformation of *H. volcanii* parent or *glpR* mutant strains. Promoter sequences were predicted upstream of *glpR-pfkB*, *kdgK1*, *kdgK2*, *glpK*, and *gpdA1* according to methods previously described (Schneider et al., 2006). Plasmid controls pJAM2714 and pJAM2715 were constructed using pJAM2678 by removal of the *H. cutirubrum* rRNA P2 promoter and the Shine-Dalgarno sequence (using XbaI and NdeI) or removal of only the rRNA P2 promoter (using XbaI and BamHI), respectively.

## RNA procedures

### RNA Isolation and Analysis

Total RNA used for (q)RT-PCRs was isolated from *H. volcanii* parent H26 and *glpR* mutant KS8 strains (exponential phase; $OD_{600}$ 0.3 - 0.5) using the RNeasy RNA purification columns (Qiagen). RNA was treated with amplification grade DNaseI according to the Supplier's recommendations (Sigma-Aldrich), with the following modifications: 3 units (U) of enzyme were added per µg RNA and the mixture was incubated for 45 min at room temperature. RNA integrity was determined by gel electrophoresis. RNA concentration was determined by measuring the absorbance at 260 nm ($A_{260}$) using a Nanovue Plus Spectrometer instrument (GE Healthcare Life Sciences, Uppsala, Sweden).

### (q)RT-PCRs

(q)RT-PCRs were performed using *H. volcanii* total RNA as a template (0.1 µg), appropriate primers (listed in Tables 2-4, 2-6, or 2-8), iQ™ SYBR® Green Supermix

(Bio-Rad Laboratories) (for qRT-PCRs), and an iCycler (Bio-Rad Laboratories) according to the Supplier's instructions (Bio-Rad Laboratories). RNA was reverse transcribed into cDNA using iScript™ (Bio-Rad Laboratories) according to the Manufacturer's instructions. After cDNA synthesis (25 ºC, 5 min; 42 ºC, 30 min; 85 ºC, 5 min), qRT-PCRs were preheated to 95 °C (4 min) followed by 40 amplification cycles consisting of denaturation (95 °C, 30 s), annealing (temperatures listed in Tables 2-4, 2-6, and 2-8, 1 min), and elongation (72 °C, 17 s). For RT-PCRs, reactions were preheated to 95 °C (4 min), followed by 35 amplification cycles consisting of denaturation (95 °C, 30 s), annealing (temperatures listed in Tables 2-4, 2-6, and 2-8, 1 min), and elongation (72 °C, 41 s), after which a final extension was performed at 72 °C (10 min). For each primer pair, negative and positive controls were included to exclude genomic DNA contamination and confirm primer pair function, respectively. For the controls, reactions were identical with the following exceptions: the sample was maintained on ice during the reverse-transcription step for the negative control, and *H. volcanii* genomic DNA prepared as previously described (Ng et al., 1995) was used as a template for the positive control reactions. PCR products from RT-PCRs were sequenced as described above to confirm specificity.

For qRT-PCRs, absolute (Rutledge and Côté, 2003) and/or relative (Pfaffl, 2001) quantification was performed for each transcript according to methods previously described. Transcript specific for the *H. volcanii* ribosomal protein L10 gene (*ribL)* was used as an internal control based on a previous study (Brenneis et al., 2007) and our confirmation by qRT-PCR that the N-fold induction of transcripts specific for *ribL* was close to 1.0 when parent H26 or *glpR* mutant KS8 was grown in minimal media. Varying

dilutions of cDNA samples were subjected to qRT-PCR, and the threshold counts ($C_T$) which fell within the linear range of *H. volcanii* genomic DNA standards ($R^2 > 0.99$ for the linear regressions of all standards tested) were used for transcript quantification. Experiments were performed in triplicate and the means ± SD of the results were calculated.

## Protein Procedures

### Protein Isolation and Analysis

C-terminally StrepII-tagged (Trp-Ser-His-Pro-Gln-Phe-Glu-Lys) proteins were purified by StrepTactin chromatography followed by gel filtration chromatography as detailed below. Purified protein fractions and molecular weight standards were analyzed by reducing 12% SDS–polyacrylamide gel electrophoresis (PAGE) (200 V, 50 - 60 min) (Laemmli, 1970). Protein fractions (20 µl) and Precision Plus Protein™ Kaleidoscope molecular mass marker (diluted at a ratio of 1:20 according to the Supplier's recommendations) were prepared for electrophoresis by boiling for 10 min in 20 µl of SDS–PAGE buffer [100 mM Tris-HCl (pH 6.8) with 10% (v/v) β-mercaptoethanol, 2% (w/v) SDS, 10% (v/v) glycerol, and 0.6 mg $ml^{-1}$ bromophenol blue]. Gels were stained with Coomassie Blue and imaged on a Bio-Rad XR imager according to Manufacturer's protocol (Bio-Rad Laboratories).

### StrepTactin Chromatography

Cells were harvested from two 500 ml cultures by centrifugation (20 min, 4,300 × *g*, 4 ºC), washed once with buffer W [100 mM Tris-HCl (pH 8.0) with 2 M NaCl], and resuspended in 20 ml of buffer W containing 10 mM phenylmethylsulfonyl fluoride (PMSF). Cells were passed four times through a chilled French pressure cell at 20,000 $lb \cdot in^{-2}$. Cell lysate was centrifuged twice to remove cell debris (14,000 × *g*, 15 min, 4 °C).

The filtrate obtained with a 0.45 µm pore-size filter (Nalge Nunc International) was applied to a StrepTactin column (Qiagen) (1 ml column volume and 3 mg protein·$ml^{-1}$ binding capacity) equilibrated with 10 ml of buffer W. The column was loaded with lysate (440 mg protein), and washed with 40 ml of buffer W. Protein was eluted with 10 ml of buffer E [100 mM Tris-HCl (pH 8.0) containing 2 M NaCl and 12.5 mM desthiobiotin] into 1 ml fractions. Protein fractions (770 µg) were pooled and further purified by gel filtration chromatography (details presented below). StrepTactin column resin was regenerated by washing the column with 15 ml of buffer R [100 mM Tris-HCl (pH 8.0) containing 150 mM NaCl, 1 mM EDTA, and 1 mM hydroxy-azophenyl-benzoic acid].

**Gel Filtration Chromatography**

After StrepTactin chromatography, samples (230 µg in 0.5 ml per run) were applied to a Superdex 200 HR 10/30 gel filtration column (GE Healthcare Life Sciences) equilibrated in buffer W or buffer L [100 mM Tris-HCl (pH 8.0) with 150 mM NaCl] at a flow-rate of 0.1 – 0.3 $ml^{-1}min^{-1}$. Molecular mass standards for gel filtration included cytochrome C (12 kDa), carbonic anhydrase (29 kDa), serum albumin (66 kDa), alcohol dehydrogenase (150 kDa), β-amylase (200 kDa), thyroglobulin (669 kDa), and Blue Dextran (2,000 kDa) (Sigma). Protein elution was monitored by UV absorbance at 280 nm ($A_{280}$) and quantified by Bradford assay (Bradford, 1976). Molecular mass was estimated from the linear regression ($R^2 > 0.99$) generated from plotting the logarithmic values of molecular mass against $K_{av}$ and the equation $K_{av}=(V_R - V_o)/(V_c - V_o)$ where $K_{av}$ is the gel phase distribution coefficient, $V_R$ is the retention (elution) volume of the protein, $V_c$ is the geometric bed volume, and $V_o$ is the void volume of the column. Column volume was calculated based on the measured column height of 29.94 cm and

the column radius of 10 cm. Experiments were performed at least in triplicate and the means ± SD of the results were calculated.

**Protein Quantification**

Protein concentrations were determined by the Bradford method (Bradford, 1976) with bovine serum albumin (Bio-Rad Laboratories) as the standard with the following modifications: the reaction volume for the colorimetric assay was scaled down to 200 µl and performed in a 96-well microplate reader at room temperature. Briefly, Bradford reagent (40 µl) was added to the protein sample and incubated for 5 minutes at room temperature, after which the absorbance at 595 nm ($A_{595}$) was determined for 100 µl of sample reaction. The assay was linear between 0 and 400 $\mu g \cdot ml^{-1}$ of protein.

**Glycerol Kinase Activity Assay**

Exponential growth phase cells (0.3 – 0.5 $OD_{600}$) were harvested by centrifugation (15 min, 6 000 × *g*, 4 ºC), washed once with 20 ml buffer K [100 mM potassium phosphate buffer (pH 7.4) with 3 M KCl], resuspended in 1 ml of buffer K, and broken by sonication (4 × 20 s at 140 W). Debris was removed by centrifugation (10 min, 12 000 × *g*, 4 ºC). Protein concentration was estimated using the Bradford assay and cell extract was used as the crude enzyme preparation. GK (ATP : glycerol 3-phosphotransferase, EC 2.7.1.30) activity was determined at 42 ºC in a coupled photometric reaction as described previously (Sher et al., 2004) with the following modifications: assay buffer was supplemented with 3 M KCl, negative controls lacked ATP, glycerol, or were performed using boiled parent cell lysate, and time points (after incubation at 42 ºC) for which samples were withdrawn included 10, 20, 30 35, 40, 45, 50, 60, and 90 min intervals. Briefly, GK activity was coupled to the formation of α-glycerophosphate which was quantified in the presence of $NAD^+$ and commercially available α-glycerophosphate

dehydrogenase. The reaction mixture (5 ml) contained 1 ml of cell extract (0.9 – 1 mg protein·ml$^{-1}$), 30 µmol ATP, 100 µmol L-cysteine, and buffer K, and was initiated with addition of 125 µmol glycerol. Sample reactions were incubated at 42 ºC for varying amounts of time (described above) after which 1 ml samples were withdrawn and the reaction terminated with addition of an equal volume of 0.2 N $H_2PO_4$. Samples were centrifuged (10 min, 12,000 × *g*) to remove precipitated proteins and the α-glycerophosphate content of 250 µl portions were quantified in a total reaction volume of 2.27 ml containing 0.011 N NaOH, 1.1 mM $NAD^+$, 0.66 M hydrazine sulfate, 1% (w/v) nicotinamide-sodium carbonate buffer, and 8 U of α-glycerophosphate dehydrogenase from rabbit muscle (Sigma, EC 1.1.1.8). After 1 hour of incubation at 30 ºC, the absorbance at 340 nm ($A_{340}$) was measured. Product formation was quantified by linear regression analysis ($R^2 > 0.99$) using standards which were linear between 0 and 10 mM α-glycerophosphate.

**PFK and KDGK Activity Assays**

Exponential growth phase cells (0.3 – 0.5 $OD_{600}$) were harvested by centrifugation (20 min, 4,300 × *g*, 4 ºC), washed once with 20 ml buffer A [100 mM Tris-HCl (pH 7.5) with 2 M NaCl], resuspended in 1 ml of buffer A containing 1 mM PMSF, and lysed by sonication (4 × 20 s at 140 W). Cell debris was removed by centrifugation (10 min, 12,000 × *g*, 4 ºC). Protein concentration was estimated using the Bradford assay. PFK and KDGK activity assays were carried out as previously detailed (Johnsen et al., 2001) with the following exceptions: all enzyme activities were carried out aerobically at 37 °C in a 96-well microplate reader filled with 0.1 ml of assay mixture (the path length for a 100 µl reaction was calculated as 0.2825 cm$^{-1}$). It was ensured that in coupled enzymatic assays, the auxiliary enzymes were not rate-limiting. Background change in

$A_{340}$ for reactions containing no substrate was subtracted from reactions in which substrate was included to yield the overall change in absorbance. Reactions containing boiled enzyme and no NADH were also included as controls. All experiments were performed in triplicate, and the means ± SD of the results were calculated. One U of enzyme activity is defined as 1 µmol substrate consumed or product formed per min with a molar extinction coefficient for NADH of 6,220 $M^{-1} \cdot cm^{-1}$.

PFK (EC.2.7.1.56) specific activity was determined at 37 °C by measuring the ATP-dependent formation of FBP from F1P, which was coupled to the oxidation of NADH by FBP aldolase, triosephosphate isomerase (TIM), and G3PDH. The assay mixture contained 100 mM Tris-HCl (pH 8.5) with 30 mM $MgCl_2$, 1 M KCl, 10 mM F1P sodium salt, 2 mM ATP, 0.3 mM NADH, 0.54 U FBP-aldolase, 2 U TIM, 0.34 U G3PDH, and cell extract (1 to 3 µg protein).

KDGK (EC 2.7.1.45) specific activity was determined at 37 °C by measuring the ATP- and gluconate-dependent formation of pyruvate, which was coupled to the oxidation of NADH by lactate dehydrogenase (LDH). The assay mixture contained 100 mM Tris-HCl (pH 8.5) with 1 M KCl, 10 mM $MgCl_2$, 2 mM ATP, 0.3 mM NADH, 10 mM sodium gluconate, 11 U LDH, and cell extract (5 µg protein).

**β-Galactosidase Assay**

Promoter activity for each transcriptional reporter fusion construct was assessed quantitatively by assaying β-galactosidase activity as previously described (Holmes and Dyall-Smith, 2000). Briefly, cells were grown in 3 ml of appropriate media and harvested at exponential growth phase (0.3 to 0.5 $OD_{600}$) by centrifugation (15 min, 6,000 × *g*, 4°C). Cell pellets were washed once in buffer B [50 mM Tris-HCl (pH 7.2) with 2.5 M NaCl and 10 µM $MnCl_2$], resuspended in 300 µl of buffer C [buffer B supplemented with

0.1% (w/v) β-mercaptoethanol] and lysed using 150 µl of 2 % (v/v) Triton X-100. Debris was removed by centrifugation (10 min, 6,000 × *g*, 4°C), and the protein concentration in the cell extract was determined using the Bradford assay. Cell lysates were assayed at 25 ºC for β-galactosidase specific activity by measuring the increase in absorbance at 405 nm ($A_{405}$) due to the liberation of *o*-nitrophenol from *o*-nitrophenyl-β-D-galactopyranoside (ONPG). The assay mixture (100 µl) contained 20 µl of cell lysate (3 to 5 µg protein), 70 µl of buffer C, and 2.66 mM ONPG (stock solution 8 $mg \cdot ml^{-1}$ in 100 mM potassium phosphate buffer, pH 7.2). Negative controls included cells carrying pJAM2714 and pJAM2715 (the *bgaH*-reporter plasmids devoid of promoter elements). Background values in which no substrate (ONPG) was added to the reaction were subtracted from reactions containing substrate for each lysate tested. All experiments were performed in triplicate, and the means ± SD of the results were calculated. One unit of β-galactosidase activity is defined as the amount of enzyme catalyzing the hydrolysis of 1 µmol ONPG$\cdot min^{-1}$ with a molar extinction coefficient for *o*-nitrophenol of 3,300 $M^{-1} \cdot cm^{-1}$.

**Genome Analysis and Construction of Phylogenetic Trees**

Ninety-two archaeal genomes (Benson et al., 2010) were searched for homologs of PTS general carrier and sugar-specific proteins with the BLASTP (Altschul et al., 1997) and InterProScan (Hunter et al., 2009) search engines. Queries of characterized PTS general carrier proteins and sugar-specific permeases from *E. coli* as well as *B. subtilis* were used for the identification of PTS components in archaea. Archaeal homologs of *B. subtilis* HprK were also analyzed. DHAK distribution in archaea was searched using *E. coli* or *C. freundii* DHAK as a query for BLASTP. For construction of phylogenetic trees and protein alignments, protein sequences were retrieved from the

NCBI database (Benson et al., 2010) and were N- and C-terminally trimmed within the BioEdit sequence editor software v7.0.4.1(Hall, 1999) prior to pairwise and multiple sequence alignments that were performed using CLUSTAL W (Thompson et al., 1994). Phylogenetic and molecular evolutionary analyses of the primary amino acid sequences were conducted using MEGA v3.1 (Kumar et al., 2004). The mean evolutionary distances were estimated from the protein sequences using the p-distance substitution model. Consensus trees were generated using the neighbor-joining method of construction (Saitou and Nei, 1987) and validated with the bootstrap phylogeny test (Felsenstein, 1985) (1,000 replicates; 64,238 seed) and pairwise gap deletion. Interior branch test values or bootstrap values greater than the 50% cutoff are indicated at the internal nodes. Due to space constraints within the figure legends, accession numbers for the following figures are listed below: Figures 3-3, 4-2, 5-4, 6-1, and 6-7.

Accession numbers for Figure 3-3 (alignment of haloarchaeal and bacterial GKs): are as follows: *E. coli* (Eco), YP_543453; *S. flexneri* (Sfl), NP_838952; *Bacillus cereus* (Bce), ZP_03103890; *Natrialba magadii* (Nma), ZP_03694006; *H. salinarum* (Hsa), NP_280665; *H. marismortui* (Hma), YP_135274; *H. lacusprofundi* (Hla), ZP_02016760; *H. walsbyi* (Hwa), YP_657499; *H. volcanii* (Hvo), YP_003535588.1; *E. faecalis* (Efa), NP_815610.1; *M. pneumoniae* (Mpn), NP_109738.1; and *B. subtilis* (Bsu), NP_388810.2.

Accession numbers for trimmed sequences for Figure 4-2 (phylogenetic distribution of GKs) are as follows: *Thermoanaerobacter sp*. X514, YP_001662655; *Thermoanaerobacter pseudethanolicus*, YP_001664537; *Thermoanaerobacter tengcongensis*, NP_6235761; *Clostridium hiranonis*, ZP_032922601; *Clostridium*

*difficile*, YP_001087882; *Thermotoga neapolitana*, YP_002534606; *Thermotoga sp.* RQ2, YP_001739349; *Marinitoga piezophila*, YP_002615530; *Thermotoga petrophila*, YP_001244954; *Petrotoga mobilis*, YP_001567349; *Desulfotomaculum reducens*, YP_001114174; *Carboxydothermus hydrogenoformans*, YP_360659; *Mannheimia succiniciproducens*, YP_089180; *Actinobacillus succinogenes*, YP_001344893; *Haemophilus influenzae*, NP_438851; *Haemophilus parasuis*, ZP_02478129; *Salmonella enterica*, ZP_02345174; *S. typhimurium*, NP_462967; *Citrobacter koseri*, YP_001454599; *K. pneumoniae*, YP_002235969; *Escherichia albertii*, ZP_02904065; *Shigella boydii*, YP_001882621; *E. coli*, YP_543453; *S. flexneri*, NP_838952; *Oceanobacillus iheyensis*, NP_693396; *Staphylococcus aureus*, NP_646000; *Exiguobacterium sibiricum*, YP_001813587; *Exiguobacterium sp*. , ZP_02991677; *Anoxybacillus flavithermus*, YP_002315832; *Bacillus weihenstephanensis* , YP_001643829; *B. cereus*, ZP_03103890; *Bacillus thuringiensis*, YP_035286; *Bacillus anthracis*, NP_843527; *Rubrobacter xylanophilus*, YP_643841; *Nitrosococcus oceani*, YP_344681; *Burkholderia xenovorans*, YP_560348; *Burkholderia multivorans*, YP_001578811; *Burkholderia ubonensis*, ZP_02377911; *N. magadii*, ZP_03694006; *H. salinarum*, NP_280665; *H. marismortui*, YP_135274; *H. lacusprofundi*, ZP_02016760; *H. walsbyi*, YP_657499; *S. cerevisiae*, CAA48791; and *H. volcanii*, YP_003535588.1

Accession numbers for protein sequences for Figure 5-4 (distribution of GpdA homologs in archaea and *E. coli*) are as follows: i) members of Gene organization I include *Halorhabdus utahensis* Huta_1471 (YP_003130380.1); *Halomicrobium mukohataei* Hmuk_2516 (YP_003178331.1), *H. walsbyi* HQ1734A (YP_657500.1), *H. marismortui* rrnAC0554 (YP_135276.1), *H. salinarum* VNG1969G (NP_280666.1), *H.*

*lacusprofundi* Hlac_1123 (YP_002565787.1), *N. magadii* Nmag_0933 (YP_003479079.1), *Halogeometricum borinquense* HborDRAFT_0007 (ZP_03997215.1), *H. volcanii* HVO_1538 (GpdA1) (YP_003535585.1) and HVO_A0269 (GpdA2) (YP_003533725.1), and *E. coli* EcGlpA (AP_002838.1) and (ii) members of Gene Organization II include *H. utahensis* Huta_0683 (YP_003129602.1), *H. mukohataei* Hmuk_2572 (YP_003178385.1), *H. borinquense* HborDRAFT_3500 (ZP_04000658.1), *H. marismortui* rrnAC1955 (YP_136529.1), *Sulfolobus islandicus* LS215_0342 (YP_002831137.1), *H. walsbyi* HQ2675A (YP_658392.1), *H. salinarum* OE2553R (YP_001689097.1), *T. pendens* Tpen_1127 (YP_920528.1), *Metallosphaera sedula* Msed_1177 (YP_001191262.1), *Caldivirga maquilingensis* Cmaq_1799 (YP_001541610.1), *Sulfolobus solfataricus* SSO2526 (NP_343866.1), *Sulfolobus acidocaldarius* Saci_2032 (YP_256621.1) and Saci_1118 (YP_255763.1), *Picrophilus torridus* PTO1486 (YP_024264.1), *Thermoplasma volcanium* TVN0840 (NP_111359.1), and *Thermoplasma acidophilum* Ta0633 (NP_394105.1).

Genomic sequences for Fig. 6-1B (genomic clustering of DeoR/GlpR-transcriptional regulators and PFK genes in haloarchaea and Gram-positive bacteria) are as follows: i) members of Group I include *H. volcanii* (NC_013967.1)*, Haloterrigena turkmenica* (NC_013743.1) and *Morella thermoacetica* (NC_007644.1); ii) members of Group II include *T. tengcongensis* (NC_003869.1)*, Symbiobacterium thermophilum* (NC_006177.1)*, B. cereus* (NC_003909.8)*, Lactobacillus sakei* (NC_007576.1) and *E. faecalis* (NC_004668.1); and iii) members of Group III include *H. marismortui* (NC_006396.1) and *H. mukohataei* (NC_013202.1).

Accession numbers for trimmed protein sequences in Figure 6-1 (phylogenetic distribution of repressor proteins of the DeoR/GlpR family from Bacteria and Archaea) are as follows: *E. coli* SrlR (NP_417187.1), UlaR (NP_290821.1), DeoT (NP_415800.1), SgcR (NP_418720.1), DeoR (NP_286606.1), AgaR (NP_289702.1), GlpR (NP_417881.1), b1770 (NP_416284.1) and c4824 (AAN83253.1); *P. aeruginosa* GlmR (NP_254237.1); *Leuconostoc citreum* FruR (YP_001728489.1); *Staphylococcus aureus* LacR (NP_372720.1); *L. lactis* LacR (NP_267113.1) and FruR (YP_001032855.1); *Corynebacterium glutamicum* SugR (NP_601141.1) and cgR_1764 (YP_001138660.1); *Lactobacillus casei* IolR (YP_001986205.1) and SorC (YP_001986411.1); *B. subtilis* IolR (NP_391856.1) and DeoR (NP_391822.1); *S. flexneri* SFV_3430 (YP_690777.1) and SFV_2884 (YP_690265.1); *H. influenza* HI1009 (NP_439170.1) and HI0615 (NP_438773.1); *Streptococcus mutans* LacR (NP_721845.1); *K. pneumoniae* SorC (YP_002241037.1); *Salmonella enterica* Sty0448 (NP_455005.1) *Arabidopsis thaliana* F-box protein (NP_566421.1); *Rhizobium leguminosarum* AraC (YP_768464.1); *T. tengcongensis* TTE2588 (AAM25712.1); *Heliobacterium modesticaldum* HM1_2674 (YP_001681214.1); *S. thermophilum* STH793 (YP_074622.1); *Clostridium botulinum* CBC_0871 (ZP_02620452.1); *H. volcanii* HVO_1501 (YP_003535550.1); *H. turkmenica* Htur_2761 (YP_003404307.1); *H. borinquense* HborDRAFT_0052 (ZP_03997260.1); *H. marismortui* rrnAC0341 (YP_135095.1); and *H. mukohataei* Hmuk_2660 (YP_003178473.1).

Finally, gene name or locus tag and accession numbers for trimmed sequences used in Figure 6-7 (distribution of PFK and KDGK in Bacteria and Archaea) are as follows: *H. volcanii* HVO_0549 (YP_003534614.1), HVO_A0328 (YP_003533784.1),

HVO_1500 (YP_003535549.1) and HVO_2612 (YP_003536628.1); *H. borinquense* HborDRAFT_0980 (ZP_03998188.1), HborDRAFT_0358 (ZP_03997566.1) and HborDRAFT_2235 (ZP_03999442.1); *H. lacusprofundi* Hlac_0463 (YP_002565135.1), Hlac_2870 (YP_002564316.1), Hlac_2162 (YP_002566809.1) and Hlac_2117 (YP_002566764.1); *H. marismortui* rrnAC0545 (YP_135269.1), rrnAC2551 (YP_137055.1) and rrnAC0342 (YP_135096.1); *H. turkmenica* Htur_3215 (YP_003404753.1), Htur_3911 (YP_003405439.1), Htur_1630 (YP_003403189.1), Htur_4085 (YP_003405592.1), Htur_0569 (YP_003402140.1) and Htur_2760 (YP_003404306.1); *H. mukohataei* Hmuk_2509 (YP_003178324.1), Hmuk_0377 (YP_003176221.1), Hmuk_2764 (YP_003178576.1) and Hmuk_2661 (YP_003178474.1); *Halalkalicoccus jeotgali* HacjB3_14395 (ADJ16260.1), HacjB3_09545 (ADJ15292.1) and HacjB3_10180 (ADJ15419.1); *N. magadii* Nmag_1292 (YP_003479434.1), Nmag_3485 (YP_003481597.1) and Nmag_2964 (YP_003481078.1); *H. salinarum* VNG0158G (NP_279296.1) and VNG1851G (NP_280577.1); *H. walsbyi* HQ1455A (YP_657227.1); *H. utahensis* Huta_2283 (YP_003131183.1), Huta_0006 (YP_003128929.1), Huta_0501 (YP_003129421.1); Huta_0650 (YP_003129570.1) and Huta_1103 (YP_003130015.1); *Natronomonas pharaonis* NP3184A (YP_327240.1); *S. solfataricus* KdgK (158431173); *Thermotoga maritima*, KdgK (90108697); *Sulfolobus tokodaii* KdgK (88192770); *E. coli* KdgK (NP_417983.2) and FruK (YP_003500240.1); *Thermus thermophilus* KdgK (48425860); *B. subtilis* KdgK (NP_390093.1); *Erwinia chrysanthemi* KdgK (CAA52961.1); *Thermoproteus tenax* KdgK (CAF18464.1); *C. maquilingensis* Cmaq_0369 (YP_001540205.1); *S. boydii* SBO_3525 (YP_409837.1); *H. influenzae* HI0049

(NP_438222.1) and HIAG_00717 (ZP_05850080.1); *Clostridium acetobutylicum* CA_C0395 (NP_347035.1); *L. casei* LCABL_28640 (YP_001988772.1); *S. flexneri* FruK (NP_708065.1); *L. lactis* FruB (YP_003353441.1); *Spiroplasma citri* FruK (AAF08321.1); *Borrelia burgdorferi* PfkB (EEF56173.1); *Pseudomonas putida* FruK (YP_001751248.1); *Homo sapiens* PfkM (AAA60068.1); *Mus musculus* PfkB (AAA20076.1); and *Bacillus licheniformis* FruK (YP_078830.1).

Table 2-1. Strains and plasmids used in Chapter 3.

| Strain or Plasmid | Description[α] | Source or Reference |
|---|---|---|
| *E. coli* | | |
| GM2163 | F⁻ *ara-14 leuB6 fhuA31 lacY1 tsx78 glnV44 galK2 galT22 mcrA dcm-6 hisG4 rfbD1 rpsL136 dam13*::Tn*9 xylA5 mtl-1 thi-1 mcrB1 hsdR2* | New England Biolabs |
| *H. volcanii* | | |
| DS70 | Wild-type isolate DS2 cured of plasmid pHV2 | (Oren, 1994) |
| H26 | DS70 *pyrE2* | (Allers et al., 2004) |
| KS3 | H26 *fruB ptsI* (devoid of FruB start codon and EI ORF) | This study |
| Plasmids | | |
| pTA131 | $Ap^r$; pBluescript II containing $P_{fdx}$-*pyrE2* | (Allers et al., 2004) |
| pJAM202 | $Ap^r$ $Nv^r$; pBAP5010 containing $P2_{rrnA}$-*psmB-his*$_6$; β-$His_6$ expressed in *H. volcanii* | (Kaczowka and Maupin-Furlow, 2003) |
| pJAM202c | $Ap^r$ $Nv^r$; control plasmid derived from pJAM202 | (Zhou et al., 2008) |
| pJAM809 | $Ap^r$ $Nv^r$; pJAM202 containing $P2_{rrnA}$-*hvo1862-strepII* (KpnI site inserted upstream of StrepII coding sequence) | (Humbard et al., 2009) |
| pJAM2055 | $Ap^r$ $Nv^r$; pJAM202c-derived expression plasmid including HpaI site for C-terminal fusion to StrepII tag | This study |
| pJAM2657 | $Ap^r$; pTA131 containing *ptsI* with ~ 700 bp of genomic DNA flanking 5' and 3' of the *ptsI* coding region | This study |
| pJAM2660 | $Ap^r$; pJAM2657-derived *ptsI fruB* suicide plasmid | This study |
| pJAM2663 | $Ap^r$ $Nv^r$; pJAM2055 containing $P2_{rrnA}$-*ptsI-fruB-strepII* | This study |
| pJAM2664 | $Ap^r$ $Nv^r$; pJAM2055 containing $P2_{rrnA}$-*ptsI-strepII* | This study |
| pJAM2665 | $Ap^r$ $Nv^r$; pJAM809 containing $P2_{rrnA}$-*fruB-strepII* | This study |

[α] The StrepII tag is a peptide that binds to the biotin binding site of streptavidin. $Ap^r$, ampicillin resistance; $Nv^r$, novobiocin resistance.

Table 2-2. Primers used in Chapter 3.

| Primer Names (paired as used) | PCR/Product descriptions | Primer Sequences[α] |
|---|---|---|
| *fruB* and *ptsI* (Hvo 1495; Hvo 1496) | | |
| HindIII Forward | ~500 bp of genomic DNA flanking 5' and 3' of *ptsI* generated using *H. volcanii* DS70 genomic DNA as a template; includes XbaI and HindIII sites for cloning into pTA131 to generate pJAM2657 | 5'- TCATGAAGCTTATCGAGTTCCTCCTCGACC-3' |
| XbaI Reverse | | 5'-GATGTCTAGAAATCCTTCGTCGAGC-3' |
| Inverse Forward | *ptsI*-suicide plasmid pJAM2660 generated by inverse PCR using pJAM2657 as template to generate pJAM2660; the start codon of *fruB* was also deleted during construction of pJAM2660 | 5'-AACTCGTCGCAGTCACATCCTGTCCGA-3' |
| Inverse Reverse | | 5'-AGCTTACTGTTTGGCTTCAGGCGTGGAAAG-3' |
| Negative Forward | ~1700 bp within *ptsI* coding region; used to screen Δ*ptsI* mutants | 5'-ATGACCGAACGAACCCTCTC-3' |
| Negative Reverse | | 5'-GCGACTTCAGCCTTCGT-3' |
| Positive Forward | ~700 bp of genomic DNA flanking 5' and 3' of *ptsI*; used to confirm Δ*ptsI* mutation by PCR | 5'-TCCGACGACTGACCACACCGAA-3' |
| Positive Reverse | | 5'-CAGGAGGTCCGAGTCCATCCG-3' |
| *fruB* Complimentary Forward | Coding region of *fruB* generated using *H. volcanii* DS70 genomic DNA as a template; includes NdeI and KpnI sites for cloning into pJAM809 to generate pJAM2665 | 5'-ATTACATCCATATGAAACTCGTCGCAGTCAC-3' |
| *fruB* Complimentary Reverse | | 5'-GTAGGTACCCGAGAACAGCTTCTTCAG -3' |
| *ptsI* Complimentary Forward | Coding region of *ptsI* generated using *H. volcanii* DS70 genomic DNA as a template; includes NdeI and HpaI sites for cloning into pJAM2055 to generate pJAM2664 | 5'-AACAGTAACATATGACCGAACCGAACCCTCT-3 |
| *ptsI* Complimentary Reverse | | 5'-ATGGCGCTGTTAACTTGGTCTAGTGTAAG-3' |

Table 2-2. Continued

| Primer Names (paired as used) | PCR/Product descriptions | Primer Sequences[α] |
|---|---|---|
| *ptsI-fruB* Complimentary Forward | Coding region of *ptsI-fruB* generated using *H. volcanii* DS70 genomic DNA as a template; | 5'-AACAGTAACATATGACCGAACCGAACCCTCT-3 |
| *ptsI-fruB* Complimentary Reverse | includes NdeI and HpaI sites for cloning into pJAM2066 to generate pJAM2663 | 5'- ATGGCGCTGTTAACCGAGAACAGCTTCTTCAG -3' |
| HindIII Forward | ~700 bp probe generated using pJAM2658 as template, used to confirm Δ*ptsI* mutation by Southern blot | 5'- TCATGAAGCTTATCGAGTTCCTCCTCGACC-3' |
| Inverse Reverse | | 5'-AGCTTACTGTTTGGCTTCAGGCGTGGAAAG-3' |

[α] Restriction enzyme recognition sequences are underlined.

Table 2-3. Strains and plasmids used in Chapter 4.

| Strain or Plasmid | Description[α] | Source or Reference |
|---|---|---|
| *E. coli* strains | | |
| DH5α | $F^-$ *recA1 endA1 hsdR17*($rK^-mK^+$) *supE44 thi-1 gyrA relA1* | Life Technologies |
| GM2163 | $F^-$ *ara-14 leuB6 fhuA31 lacY1 tsx78 glnV44 galK2 galT22 mcrA dcm-6 hisG4 rfbD1 rpsL136 dam13*::Tn*9 xylA5 mtl-1 thi-1 mcrB1 hsdR2* | New England Biolabs |
| *H. volcanii* strains | | |
| DS70 | Wild-type isolate DS2 cured of plasmid pHV2 | (Oren, 1994) |
| H26 | DS70 *pyrE2* | (Allers et al., 2004) |
| KS4 | H26 *glpK* (devoid of GlpK) | This study |
| Plasmids | | |
| pTA131 | $Ap^r$; pBluescript II containing P*fdx-pyrE2* | (Allers et al., 2004) |
| pJAM202c | $Ap^r$ $Nv^r$; control plasmid derived from pBAP5010 | (Zhou et al., 2008) |
| pJAM2055 | $Ap^r$ $Nv^r$; pJAM202c-derived expression plasmid including HpaI site for C-terminal fusion to StrepII tag | This study |
| pJAM2658 | $Ap^r$; pTA131-derived presuicide plasmid containing *glpK* with ~500-bp genomic DNA sequences flanking 5' and 3' ends of *glpK* | This study |
| pJAM2675 | $Ap^r$; pJAM2658-derived *glpK* suicide plasmid | This study |
| pJAM2666 | $Ap^r$ $Nv^r$; pJAM2055-derived expression plasmid containing $P2_{rrn}$-*glpK*-StrepII tag | This study |

[α] The StrepII tag is a peptide that binds to the biotin binding site of streptavidin. $Ap^r$, ampicillin resistance; $Nv^r$, novobiocin resistance.

Table 2-4. Primers used in Chapter 4.

| Primer Names (paired as used) | PCR/Product descriptions | Primer Sequences[α] |
|---|---|---|
| *glpK* (Hvo 1541) | | |
| XbaI Forward | ~500 bp of genomic DNA flanking 5' and 3' of *glpK* generated using *H. volcanii* DS70 genomic DNA as a template; includes XbaI and HindIII sites for cloning into pTA131 to generate pJAM2658 | 5'-GATCTTCTAGATCGACGACCAGGCGT-3' |
| HindIII Reverse | | 5'-GACTGCTAAGCTTCGATGACAACGATGT-3' |
| Inverse Forward | *glpK*-suicide plasmid pJAM2675 generated by inverse PCR using pJAM2658 as template | 5'-CACGTGTTTGAAGCATTCGCACTCCAGATTCC-3' |
| Inverse Reverse | | 5'-TTCTAACCAACCTCGATACGAACTCTCGGTGTGAGA-3' |
| Negative Forward | ~500 bp within *glpK* coding region; used to screen Δ*glpK* mutants | 5'-CGACGCCGAGCAGTTAGAAGCCA-3' |
| Negative Reverse | | 5'-GGAGTTCGTCGAGCGTCTCCCAG-3' |
| Positive Forward | ~700 bp of genomic DNA flanking 5' and 3' of *glpK*; used to confirm Δ*glpK* mutation by PCR | 5'-CGTCGTGTACCTCCTGTTCGATG-3' |
| Positive Reverse | | 5'-GCGACGATGATGAGCGGTTC-3' |
| Complimentary Forward | Coding region of *glpK* generated using *H. volcanii* DS70 genomic DNA as a template; includes NdeI and HpaI sites for cloning into pJAM2055 to generate pJAM2666 | 5'-TACGTTGGCATATGTCAGGAGAAACTTACGTCG-3' |
| Complimentary Reverse | | 5'-ATTGTTGTTAACTTCCTCCCGTGCCCA-3' |
| Inverse Forward | ~500 bp probe generated using pJAM2658 as template, used to confirm Δ*glpK* mutation by Southern blot | 5'-CACGTGTTTGAAGCATTCGCACTCCAGATTCC-3' |
| HindIII Reverse | | 5'-GACTGCTAAGCTTCGATGACAACGATGT-3' |
| (q)RT-PCR Primers | | |
| RT Forward | ~200 bp probe for cDNA of 3' end of *gpdA* (Hvo 1540) and 5' end of *glpK* with intergenic region; used to determine if *glpK* and *gpdA* are transcriptionally linked | 5'-GGCTACGACATCAAGCACCC-3' |
| RT Reverse | | 5'-TGGTCGATGGCACCGAC-3' |

Table 2-4. Continued

| Primer Names (paired as used) | PCR/Product descriptions | Primer Sequences[α] |
|---|---|---|
| (q)RT-PCR Primers | | |
| qRT 1541 Forward | ~200 bp probe within *glpK* coding region; used to quantify transcript levels of *glpK* by qRT-PCR; AT=52.5ºC | 5'-GTACCATCGTCGGTATGAC-3' |
| qRT 1541 Reverse | | 5'-TCGACTGGAGCTGACA-3' |
| qRT 1538 Forward | ~200 bp probe within *gpdA* coding region; used to quantify transcript levels of chromosomally encoded *gpdA* (Hvo 1538) by qRT-PCR AT=58.0ºC | 5'-CAGGTGGACACGGTCGTC-3' |
| qRT 1538 Reverse | | 5'-CGAGAGCGTCTCTATCATCAGGTC-3' |
| qRT A0269 Forward | ~200 bp probe within *gpdA*; used to quantify transcript levels of megaplasmid encoded *gpdA* (Hvo A0269) by qRT-PCR; AT=55.0ºC | 5'-GACTACGTTGTCAGTGCGAC-3' |
| qRT A0269 Reverse | | 5'-GGATGATGGTATCGCCCTC-3' |
| qRT 0484 Forward | ~200 bp probe within *ribL* coding region; used to quantify transcript levels of *ribL* (internal standard) by qRT-PCR AT=57.5ºC | 5'-CCGGCGCCTGCTTGTTCTCGCG-3' |
| qRT 0484 Reverse | | 5'-CCGAGGACTACCCCGTCCAGATTAGC-3' |

[α] Restriction enzyme recongnition sequences are underlined.

Table 2-5. Strains and plasmids used in Chapter 5.

| Strain or Plasmid | Description[a] | Source or reference |
|---|---|---|
| Strains | | |
| *E. coli* | | |
| Top10 | $F^-$ *recA1 endA1 hsdR17*($r_K^-$ $m_K^+$) *supE44 thi-1 gyrA relA1* | Invitrogen |
| GM2163 | $F^-$ *ara-14 leuB6 fhuA31 lacY1 tsx78 glnV44 galK2 galT22 mcrA dcm-6 hisG4 rfbD1 rpsL136 dam13*::Tn*9 xylA5 mtl-1 thi-1 mcrB1 hsdR2* | New England Biolabs |
| *H. volcanii* | | |
| DS70 | Wild-type isolate DS2 cured of plasmid pHV2 | (Oren, 1994) |
| H26 | DS70 *pyrE2* | (Allers et al., 2004) |
| KS4 | H26 *glpK* (devoid of GlpK) | (Sherwood et al., 2009) |
| KS12 | H26 *gpdA1* (devoid of chromosomal GpdA1) | This study |
| KS11 | H26 *gpdA2* (devoid of pHV4-carried GpdA2) | This study |
| Plasmids | | |
| pTA102 | $Ap^r$ $Nv^r$; pGB70 containing *H. alicantei bgaH* derived from pMLH32 | (Delmas et al., 2009) |
| pTA131 | $Ap^r$; pBluescript II containing $P_{fdx}$-*pyrE2* | (Allers et al., 2004) |
| pJAM202 | $Ap^r$ $Nv^r$; pBAP5010 containing $P2_{rrnA}$-*psmB-his*$_6$; β-$His_6$ expressed in *H. Volcanii* | (Kaczowka and Maupin-Furlow, 2003) |
| pJAM202c | $Ap^r$ $Nv^r$; control plasmid derived from pJAM202 | (Zhou et al., 2008) |
| pJAM809 | $Ap^r$ $Nv^r$; pJAM202 containing $P2_{rrnA}$-*hvo1862-strepII* (*KpnI* site inserted upstream of StrepII coding sequence) | (Humbard et al., 2009) |
| pJAM2658 | $Ap^r$; pTA131-derived presuicide plasmid containing *glpK* with ~ 500-bp genomic DNA sequences flanking 5' and 3' ends of *glpK* | (Sherwood et al., 2009) |
| pJAM2678 | $Ap^r$ $Nv^r$; pJAM202-derived plasmid containing $P2_{rrnA}$-*bgaH* from pTA102 | (Rawls et al., 2010) |
| pJAM2679 | $Ap^r$ $Nv^r$; pJAM2678 containing $P_{glpK\text{-}354\ bp}$-*bgaH* | This study |
| pJAM2680 | $Ap^r$ $Nv^r$; pJAM2678 containing $P_{gpdA1\text{-}310\ bp}$-*bgaH* | This study |
| pJAM2684 | $Ap^r$ $Nv^r$; pJAM809 containing $P2_{rrnA}$-*ptsH2-strepII* | This study |
| pJAM2693 | $Ap^r$ $Nv^r$; pJAM809 containing $P2_{rrnA}$-*glpF-strepII* | This study |
| pJAM2694 | $Ap^r$; pTA131 containing ~ 500 bp of genomic DNA flanking 5' and 3' of the *gpdA1* coding region | This study |
| pJAM2695 | $Ap^r$; pTA131-derived chromosomal *gpdA1* suicide plasmid | This study |
| pJAM2696 | $Ap^r$ $Nv^r$; pJAM809 containing $P2_{rrnA}$-*gpdA1-strepII* | This study |

Table 2-5. Continued

| Strain or Plasmid | Description[a] | Source or reference |
|---|---|---|
| pJAM2697 | $Ap^r$; pTA131 with ~ 500 bp of genomic DNA flanking 5' and 3' of the *gpdA2* coding region | This study |
| pJAM2698 | $Ap^r$; pTA131-derived pHV4-encoded *gpdA2* suicide plasmid | This study |
| pJAM2711 | $Ap^r$ $Nv^r$; pJAM809 containing $P2_{rrnA}$-*gpdA2-strepII* | This study |
| pJAM2712 | $Ap^r$ $Nv^r$; pJAM2678 containing $P_{trpA\text{-}321\ bp}$-*bgaH* | This study |
| pJAM2715 | $Ap^r$ $Nv^r$; pJAM2678-derived plasmid devoid of $P2_{rrnA}$ from pTA102 | (Rawls et al., 2010) |

[α] $Ap^r$, ampicillin resistance; $Nv^r$, novobiocin resistance; SD,Shine-Dalgarno sequence.

Table 2-6. Primers used in Chapter 5.

| Primer Name (paired as used) | PCR/Product Description[a] | Primer Sequence (5' to 3') |
|---|---|---|
| Knockout of *gpdA1* (HVO_1538): | | |
| BamHI Forward | 0.5 kb of genomic DNA flanking 5' and 3' of *gpdA1* generated using genomic DNA as a template; includes BamHI and HindIII sites for cloning into pTA131 to generate pJAM2694 | 5'-AGGATCCGAACACCGGGTCGAGA-3' |
| HindIII Reverse | | 5'-TTAAGCTTCGCGTCGAAGTCCGTGAGA-3' |
| Inverse Forward | *gpdA1*-suicide plasmid pJAM2695 generated by inverse PCR using pJAM2694 as template | 5'-ATGGCGATAACTGACGA -3' |
| Inverse Reverse | | 5'-CTGTCTTTCGTGAGGTAG -3' |
| Negative Forward | 1.2 kb within *gpdA1* coding region; used to screen Δ*gpdA1* mutants | 5'-AAGGAGTGTATCGAAGAGAACCG-3' |
| Negative Reverse | | 5'-CCTGACAGTTGCCCATCG-3' |
| Positive Forward | 0.7 kb of genomic DNA flanking 5' and 3' of *gpdA1* used to confirm Δ*gpdA1* mutation by PCR | 5'-TCGACGTAGGCGAACGAGG-3' |
| Positive Reverse | | 5'-GGATGTCTTCGAGCTTGAGTCCG-3' |
| Complimentary Forward | coding region of *gpdA1* generated using genomic DNA as a template; includes NdeI and KpnI sites for cloning into pJAM809 to generate pJAM2696 | 5'-GTACGACATATGAAAAAATCGCCGAGCG-3' |
| Complimentary Reverse | | 5'-ATGGTACCGTTATCGCCATCTGC-3' |
| Inverse Forward | 0.45 kb probe generated using pJAM2694 as template, used to confirm Δ *gpdA1* mutation by Southern blot | 5'-ATGGCGATAACTGACGA -3' |
| HindIII Reverse | | 5'- TTAAGCTTCGCGTCGAAGTCCGTGAGA -3 |
| Knockout of *gpdA2* (HVO_A0269): | | |
| BamHI Forward | 0.5 kb of genomic DNA flanking 5' and 3' of *gpdA2* generated using genomic DNA as a template; includes BamHI and HindIII sites for cloning into pTA131 to generate pJAM2697 | 5'-TGGATCCCACTACCTCATCGCCTTTG-3' |
| HindIII Reverse | | 5'-TGAAGCTTTCCTCGGCGAACTCGATTTC-3' |

Table 2-6. Continued

| Primer Name (paired as used) | PCR/Product Description[a] | Primer Sequence (5' to 3') |
|---|---|---|
| Inverse Forward | *gpdA2*-suicide plasmid pJAM2698 generated by inverse PCR using pJAM2697 as template | 5'-ATGGCGATTGAGAGCGAC-3' |
| Inverse Reverse | | 5'-ATAATTATGAAGAACCATGGGTAGCG-3' |
| Negative Forward | 1.3 kb within *gpdA2* coding region; used to screen Δ*gpdA2* mutants | 5'-TCGTCCAGTTGGAGGGCGA-3' |
| Negative Reverse | | 5'-CGTGACGCTGACCCTTCCAG-3' |
| Positive Forward | 0.6 kb and 0.7 kb of genomic DNA flanking 5' and 3' of *gpdA2*, respectively, used to confirm Δ*gpdA2* mutation by PCR | 5'-GGCGCGGTAGTCCACAATCACT-3' |
| Positive Reverse | | 5'-GCGGTCGACGTACGGCTTCA-3' |
| Complimentary Forward | coding region of *gpdA2* generated using genomic DNA as a template; includes BspHI and KpnI sites for cloning (by generating blunt ends using Vent Polymerase) into pJAM809 cut with NdeI and KpnI to generate pJAM2711 | 5'-CCGGCTTCATGAGCTACTCAGTCGTC-3' |
| Complimentary Reverse | | 5'-ATGGTACCATCGCCATGGCTGCC-3' |
| Inverse Forward | 0.6 kb probe generated using pJAM2697 as template, used to confirm Δ *gpdA2* mutation by Southern blot | 5'-ATGGCGATTGAGAGCGAC-3' |
| HindIII Reverse | | 5'-TGAAGCTTTCCTCGGCGAACTCGATTTC-3' |
| RT-PCR Primers | | |
| *gpdAB* RT Forward | anneals to 3'-end of *gpdB* and 5'-end of *gpdA* coding regions; used to determine if *gpdA* and *gpdB* are transcriptionally linked (annealing at 56 ºC) | 5'-CGACGCCGACATCGACT-3' |
| *gpdAB* RT Reverse | | 5'-GCCGATGACGAGCACG-3' |
| *gpdBC* RT Forward | Anneals to 3'-end of *gpdC* and 5'-end of *gpdB* coding regions; used to determine if *gpdB* and *gpdC* are transcriptionally linked (annealing at 60.5 ºC) | 5'-ACTCCGACCGACCGA -3 |
| *gpdBC* RT Reverse | | 5'-AAGTCGGGTTGCCTGG -3' |

Table 2-6. Continued

| Primer Name (paired as used) | PCR/Product Description[a] | Primer Sequence (5' to 3') |
|---|---|---|
| *gpdCglpK* RT Forward | anneals to 3'-end of *gpdC* and 5'-end of *glpK* coding regions; used to determine if | 5'-GGCTACGACATCAAGCACCC-3' |
| *gpdCglpK* RT Reverse | *gpdC* and *glpK* are transcriptionally linked (annealing at 61 ºC) | 5'-TGGTCGATGGCACCGAC-3' |
| *glpKX* RT Forward | anneals to 3'-end of *glpX* and 5'-end of *glpK* coding regions; used to determine if | 5'-GAACTCCGCGAGAACTGGCAGGT-3' |
| *glpKX* RT Reverse | *glpK* and *glpX* are transcriptionally linked (annealing at 66.4 ºC) | 5'-CCTTCGAACTGTCGGATGACGATGCC-3' |
| *glpXptsH2* RT Forward | anneals to 3'-end of *ptsH2* and 5'-end of *glpX* coding regions; used to determine if | 5'-GGGTCATCCCGAACTCG-3' |
| *glpXptsH2* RT Reverse | *glpX* and *ptsH2* are transcriptionally linked (annealing at 55 ºC) | 5'-CGTGCAGGCCGTCTT-3' |
| Promoter Fusion Primers | | |
| *bgaH* Forward | *bgaH* encoding β-galactosidase from *H. alicantei* was amplified using pTA102 as | 5'- CAGCGACCATATGACAGTTGGTGTCTGCT– 3' |
| *bgaH* Reverse | template; includes NdeI and BlpI sites for cloning into pJAM202 to generate pJAM2678 | 5'- TATGTAGCTCAGCTCACTCGGACGCGA– 3' |
| $P_{gpdA1\text{-}310\ bp}$ Forward | Putative *gpdA1* promoter generated using genomic DNA template; has XbaI and NdeI sites for cloning into | 5'-ATCTAGACCGACCACTACCGA-3' |
| $P_{gpdA1\text{-}310\ bp}$ Reverse | pJAM2678 to generate pJAM2679. Promoter region is 310-bp of genomic DNA upstream of the *gpdA1* start codon | 5'-ACGATCATATGTCTTTCGTGAGGT- 3' |
| $P_{glpK\text{-}354\ bp}$ Forward | Putative *glpK* promoter generated using genomic DNA template; has XbaI and | 5'-ATCTAGACGCACAACTGACGAACG-3' |
| $P_{glpK\text{-}354\ bp}$ Reverse | NdeI sites for cloning into pJAM2678 to generate pJAM2680. Promoter region includes 354-bp of genomic DNA upstream of the *glpK* start codon | 5'-ACGGACATATGTAACCAACCTCGATAC- 3' |

Table 2-6. Continued

| Primer Name (paired as used) | PCR/Product Description[α] | Primer Sequence (5' to 3') |
|---|---|---|
| $P_{trpA\text{-}321\ bp}$ Forward | Promoter of *trpA* generated using genomic DNA as a template; includes XbaI and NdeI sites for cloning into pJAM2678 to generate pJAM2712. Promoter region includes 321-bp of genomic DNA upstream of the start codon of *trpA* | 5'-GCTCTAGAACGACGCCATCACCTCC- 3' |
| $P_{trpA\text{-}321\ bp}$ Reverse | | 5'-ACGATTTCATATGGCCGCCAATAGGTCCG-3' |

[α]Restriction enzyme recognition sequences are underlined.

Table 2-7. Strains and plasmids used in Chapter 6.

| Strain or Plasmid | Description[a] | Source or reference |
|---|---|---|
| Strains | | |
| *E. coli* | | |
| Top10 | $F^-$ *recA1 endA1 hsdR17*($r_K^-$ $m_K^+$) *supE44 thi-1 gyrA relA1* | Invitrogen |
| GM2163 | $F^-$ *ara-14 leuB6 fhuA31 lacY1 tsx78 glnV44 galK2 galT22 mcrA dcm-6 hisG4 rfbD1 rpsL136 dam13*::Tn*9 xylA5 mtl-1 thi-1 mcrB1 hsdR2* | New England Biolabs |
| *H. volcanii* | | |
| DS70 | Wild-type isolate DS2 cured of plasmid pHV2 | (Oren, 1994) |
| H26 | DS70 *pyrE2* | (Allers et al., 2004) |
| KS8 | H26 *glpR* (devoid of GlpR) | This study |
| KS4 | H26 *glpK* (devoid of GlpK) | (Sherwood et al., 2009) |
| KS10 | H26 *glpK glpR* (devoid of GlpR and GlpK) | This study |
| Plasmids | | |
| pTA102 | $Ap^r$ $Nv^r$; pGB70 containing *H. alicantei bgaH* derived from pMLH32 | (Delmas et al., 2009) |
| pTA131 | $Ap^r$; pBluescript II containing $P_{fdx}$-*pyrE2* | (Allers et al., 2004) |
| pJAM202 | $Ap^r$ $Nv^r$; pBAP5010 containing $P2_{rrnA}$-*psmB-his*$_6$; β-$His_6$ expressed in *H. volcanii* | (Kaczowka and Maupin-Furlow, 2003) |
| pJAM202c | $Ap^r$ $Nv^r$; control plasmid derived from pJAM202 | (Zhou et al., 2008) |
| pJAM809 | $Ap^r$ $Nv^r$; pJAM202 containing $P2_{rrnA}$-*hvo1862-strepII* (*KpnI* site inserted upstream of StrepII coding sequence) | (Humbard et al., 2009) |
| pJAM2676 | $Ap^r$; pTA131 containing *glpR* with ~ 700 bp of genomic DNA flanking 5' and 3' of the *glpR* coding region | This study |
| pJAM2677 | $Ap^r$; pJAM2676-derived *glpR* suicide plasmid | This study |
| pJAM2678 | $Ap^r$ $Nv^r$; pJAM202-derived plasmid containing $P2_{rrnA}$-*bgaH* from pTA102 | This study |
| pJAM2682 | $Ap^r$ $Nv^r$; pJAM809 containing $P2_{rrnA}$-*glpR-strepII* | This study |
| pJAM2689 | $Ap^r$ $Nv^r$; pJAM2678 containing $P_{glpR\text{-}pfkB\text{-}188\ bp}$-*bgaH* | This study |

Table 2-7. Continued

| Strain or Plasmid | Description[a] | Source or reference |
|---|---|---|
| pJAM2702 | $Ap^r$ $Nv^r$; pJAM2678 containing $P_{kdgK2\text{-}232\ bp}$-*bgaH* | This study |
| pJAM2703 | $Ap^r$ $Nv^r$; pJAM2678 containing $P_{HVO\_A0327\text{-}kdgK2\text{-}122\ bp}$-*bgaH* | This study |
| pJAM2705 | $Ap^r$ $Nv^r$; pJAM2678 containing $P_{kdgK1\text{-}89\ bp}$-*bgaH* | This study |
| pJAM2706 | $Ap^r$ $Nv^r$; pJAM2678 containing $P_{kdgK1\text{-}524\ bp}$-*bgaH* | This study |
| pJAM2714 | $Ap^r$ $Nv^r$; pJAM2678-derived plasmid devoid of $P2_{rrnA}$ from pTA102 and SD | This study |
| pJAM2715 | $Ap^r$ $Nv^r$; pJAM2678-derived plasmid devoid of $P2_{rrnA}$ from pTA102 | This study |

[a] $Ap^r$, ampicillin resistance; $Nv^r$, novobiocin resistance; SD,Shine-Dalgarno sequence.

Table 2-8. Primers used in Chapter 6.

| Primer Name (paired as used) | PCR/Product Description[a] | Primer Sequence (5' to 3') |
|---|---|---|
| Knockout of *glpR* (HVO_1501): | | |
| BamHI Forward | 0.7 kb of genomic DNA flanking 5' and 3' of *glpR* generated using genomic DNA as a template; includes BamHI and HindIII sites for cloning into pTA131 to generate pJAM2676 | 5'-TGGATCCCACAAGGCGAACGTGAT-3' |
| HindIII Reverse | | 5'-TTAAGCTTGCACCTCGTCGTCGGTGA-3' |
| Inverse Forward | *glpR*-suicide plasmid pJAM2677 generated by inverse PCR using pJAM2676 as template | 5'-CGGTGGCGATTCCTCGTTACGA-3' |
| Inverse Reverse | | 5'-CGGAGTCGCACGATGATTCTCACA-3' |
| Negative Forward | 0.75 kb within *glpR* coding region; used to screen Δ*glpR* mutants | 5'-TGTTACCAGCAGAGCGC-3' |
| Negative Reverse | | 5'-CATCGTGCGACTCCGT-3' |
| Positive Forward | 0.8 kb of genomic DNA flanking 5' and 3' of *glp*R used to confirm Δ*glpR* mutation by PCR | 5'-ACCTCTCGACGCTCACGC-3' |
| Positive Reverse | | 5'-GGCGCGGAGAGCACC-3' |
| Complimentary Forward | coding region of *glpR* generated using genomic DNA as a template; includes NdeI and KpnI sites for cloning into pJAM809 to generate pJAM2682 | 5'-ATGCGACATATGTTACCAGCAGAGCGC-3' |
| Complimentary Reverse | | 5'-ATGGTACCTCGTGCGACTCCGTC-3' |
| Inverse Reverse | 0.7 kb probe generated using pJAM2676 as template, used to confirm Δ*glpR* mutation by Southern blot | 5'-CGGAGTCGCACGATGATTCTCACA-3' |
| HindIII Reverse | | 5'-TTAAGCTTGCACCTCGTCGTCGGTGA-3 |
| (q)RT-PCR Primers | | |

Table 2-8. Continued

| Primer Name (paired as used) | PCR/Product Description[a] | Primer Sequence (5' to 3') |
|---|---|---|
| RT Forward | anneals to 3'-end of *glpR* and 5'-end of *pfkB* coding regions; used to determine if *glpR* and *pfkB* are transcriptionally linked | 5'- GAGCTCTCGAAGCTC -3' |
| RT Reverse | | 5'- GGTTCGTC AAGTGA -3' |
| qRT 1500 Forward | 0.2 kb probe within *pfkB* coding region; used to quantify transcript levels of *pfkB* by qRT-PCR (annealing at 53 ºC) | 5'-GCAAGGGTATCAACGTCG-3 |
| qRT 1500 Reverse | | 5'-GAGCACAGTCGTGTTCAG-3' |
| qRT 1501 Forward | 0.2 kb probe within *glpR* coding region; used to quantify transcript levels of *glpR* by qRT-PCR (annealing at 49 ºC) | 5'-GTGACGCCGAGTATC-3' |
| qRT 1501 Reverse | | 5'-CGTAGACGCCCTGTTCG-3' |
| qRT 0549 Forward | 0.2 kb probe within *kdgK1* coding region; used to quantify transcript levels of *kdgK1* by qRT-PCR (annealing at 63 ºC) | 5'-ACCTGCTCGACTCGGT-3' |
| qRT 0549 Reverse | | 5'-CGTAGACGCCCTGTTCG-3' |
| qRT A0328 Forward | 0.2 kb probe within *kdgK2* coding region; used to quantify transcript levels of *kdgK2* by qRT-PCR (annealing at 53 ºC) | 5'-GCAGAACGAGACATCCG-3' |
| qRT A0328 Reverse | | 5'-GTTGCTCGTACACCGTTC-3' |
| qRT 0484 Forward | 0.2 kb probe within *ribL* coding region; used to quantify transcript levels of *ribL* (internal standard) by qRT-PCR (annealing at 57.5 ºC) | 5'-CCGGCGCCTGCTTGTTCTCGCG-3' |
| qRT 0484 Reverse | | 5'-CCGAGGACTACCCCGTCCAGATTAGC-3' |
| Promoter Fusion Primers | | |
| *bgaH* Forward | *H. alicantei bgaH* (β-galactosidase) amplified from pTA102; includes NdeI and BlpI sites for cloning into pJAM202 to generate pJAM2678 | 5'- CAGCGACCATATGACAGTTGGTGTCTGCT- 3' |
| *bgaH* Reverse | | 5'-TATGTAGCTCAGCTCACTCGGACGCGA- 3' |

Table 2-8. Continued

| Primer Name (paired as used) | PCR/Product Description[a] | Primer Sequence (5' to 3') |
|---|---|---|
| P *kdgK2*-232 bp Forward | Putative *kdgK2* promoter generated using genomic DNA as a template; includes XbaI and NdeI sites for cloning into pJAM2678 to generate pJAM2702. Promoter region includes 232-bp of genomic DNA upstream of the *kdgK2* start codon | 5'-CGCCGCTCTAGAACACAATGATCAACGTGGTGA-3' |
| P *kdgK2*-232 bp Reverse | | 5'- AATAGTCATATGCGCCCCTCGGCGGCT– 3' |
| P *HVO_A0327-kdgK2*-122 bp Forward | Putative *HVO_A0327-kdgK2* promoter generated using genomic DNA template; includes XbaI and NdeI sites for cloning into pJAM2678 to generate pJAM2703. Promoter region includes 122-bp of genomic DNA upstream of the HVO_A0327 start codon | 5'-GCGCCGCTCTAGAACACAATGATCAACGTGGTGA-3' |
| P *HVO_A0327-kdgK2*-122 bp Reverse | | 5'- AATAGTCATATGTGCGGGCGGTGGGGC– 3' |
| *P kdgK1*-89 bp Forward | Putative *kdgK1* promoter generated using genomic DNA template; includes XbaI and NdeI sites for cloning into pJAM2678 to generate pJAM2705. Promoter region includes 89-bp of genomic DNA upstream of the *kdgK1* start codon | 5'-ATCTAGAGCCGGCCGGAAGGGC– 3' |
| P *kdgK1*-89 bp Reverse | | 5'- AATAGTCATATGCGGCCGTTCGCAGGC- 3' |
| P *kdgK1*-524 bp Forward | Putative *kdgK1* promoter generated from genomic DNA template; includes XbaI and NdeI sites for cloning into pJAM2678 to generate pJAM2706. Promoter region includes 524-bp of genomic DNA upstream of the *kdgK1* start codon | 5'-ATCTAGATCCGAGCGGGTCGCGT– 3' |
| P *kdgK1*-524 bp Reverse | | 5'-ATGGTACCTCGTGCGACTCCGTC-3' |

Table 2-8. Continued

| Primer Name (paired as used) | PCR/Product Description[a] | Primer Sequence (5' to 3') |
|---|---|---|
| P *glpR-pfkB*-188 bp Forward | Putative promoter region of *glpR-pfkB* operon generated using genomic DNA as a template; includes XbaI and NdeI sites for cloning into pJAM2678 to generate pJAM2689. Promoter region includes 188-bp of genomic DNA upstream of the start codon of *glpR* | 5'- ATCTAGACGAACCGG CGATTCG – 3' |
| P *glpR-pfkB*-188 bp Reverse | | 5'- ACGATCATATGTGGCGATTCCTCG – 3' |

[a]Restriction enzyme recognition sequences are underlined.

# CHAPTER 3
# DISTRIBUTION OF PHOSPHOENOLPYRUVATE-LINKED PHOSPHOTRANSFERASE SYSTEM HOMOLOGS IN ARCHAEA AND IMPLICATIONS AS TO THEIR BIOLOGICAL FUNCTION

## Introduction

The PTS catalyzes the group translocation and concomitant phosphorylation of sugar substrates across the biological membrane in bacteria. PTS components include two soluble general energy-coupling proteins, EI and Hpr, which lack sugar specificity and membrane-associated EII permease complexes which are sugar-specific (Postma et al., 1993). The sugar-specific EII complexes generally consist of three proteins or protein domains (EIIA, EIIB, and EIIC); however, the mannose permease family consists of an additional membrane-spanning domain (EIID). Phosphorelay proceeds from PEP to the N3 position of histidine-189 of EI (Weigel et al., 1982a), to the N1 position of histidine-15 of Hpr (Weigel et al., 1982b), to a phosphorylatable histidine residue in the family-specific EIIA, to a phosphorylatable histidine residue within the permease-specific EIIB, and finally to the sugar substrate transported by the sugar-specific permease EIIC. All phosphoryl transfer reactions between PTS proteins are reversible and the phosphorylation status of various PTS proteins is determined by both PTS transport activity and the PEP to pyruvate ratio, reflecting flux through glycolysis (Kotrba et al., 2001). As a result, the dynamic phosphorylation status of PTS proteins in response to nutritional conditions and the metabolic state of the cell serves as the basis for PTS-mediated regulation of diverse metabolic processes including the transport and metabolism of non-PTS carbon sources, cell division, chemoreception, carbon storage and metabolism, non-carbon compound transport, cellular motility, cell physiology, gene expression, and switching between fermentative and respiratory metabolism (Barabote

and Saier, Jr., 2005; Deutscher et al., 2006). In addition to group translocation of sugars in bacteria, the PTS is also responsible for DHA metabolism (but not transport) in many bacteria (Erni et al., 2006). Many Gram-negative bacterial genomes also encode a nitrogen PTS which does not transport carbohydrates, but exerts regulatory functions implicated in metabolism of nitrogen and carbon, virulence, and potassium homeostasis (Barabote and Saier, Jr., 2005; Deutscher et al., 2006).

Until the recent examination of archaeal genomes (Comas et al., 2008), PTS proteins were believed to be exclusive to bacteria (Barabote and Saier, Jr., 2005; Lee et al., 2007). Current analysis of the PTS distribution in archaea has been severely limited, as only 19 archaeal genomes have been analyzed for PTS homologs, and only one has been reported to encode bacterial PTS homologs (Comas et al., 2008). With the increasing availability of archaeal genome sequences, this study sought to critically re-evaluate the presence of bacterial PTS homologs and their biological function in archaea. Ninety-two archaeal genomes (Benson et al., 2010) were searched for homologs of PTS proteins with search engines such as BLASTP (Altschul et al., 1997) and InterProScan (Hunter et al., 2009) using queries of characterized proteins from *E. coli, B. subtilis*, or *C. freundii*. PTS homologs are found in many halophilic Euryarchaeota, some methanogenic Euryarchaeota, and at least one Crenarchaeon. Furthermore, six archaeons encode a complete PTS, consisting of homologs of general carrier proteins EI and Hpr as well as membrane-associated permeases specific for mannose, fructose, and galactitol. DHAK homologs which cluster near PTS homologs and may function in DHA utilization were also identified. Overall, this study is expected to provide insight into the function and evolution of sugar transport in archaea.

## Results and Discussion

### Distribution of PTS Components in Archaea

Although the PTS is widely distributed in bacteria, its distribution in archaea is much more scattered. Ninety-two archaeal genomes (Benson et al., 2010) were searched for homologs of PTS general carrier and sugar-specific proteins using the search engines BLASTP (Altschul et al., 1997) and InterProScan (Hunter et al., 2009). Queries of characterized PTS proteins from *E. coli* as well as *B. subtilis* were used for BLASTP. Archaeal homologs of HprK were analyzed using *B. subtilis* as a query for BLASTP. The majority of archaeal genomes examined did not encode homologs of *E. coli* or *B. subtilis* PTS proteins. However, many halophilic and some methanogenic Euryarchaeota as well as at least one Crenarchaeon encoded PTS-like components (Table 3-1). Homologs for Hpr and EI proteins were identified in six of the 92 archaeal genomes analyzed: *T. pendens*, *H.* volcanii, *H. lacusprofundi*, *H. marismortui*, *H. turkmenica*, and *H. walsbyi*. In each case, these general carrier components were also accompanied with sugar-specific permeases (Table 3-1, Figure 3-1). Interestingly, the *H. volcanii* genome encodes three homologs of Hpr which cluster on the genome with additional PTS homologs (Table 3-1, Figure 3-1). In Gram-positive bacteria, Hpr phosphorylation at serine-46 is catalyzed by homohexameric ATP-dependent HprK, which is triggered by the availability of glycolytic intermediates such as FBP (Deutscher et al., 1995). In the presence of inhibitory molecules such as inorganic phosphate (Reizer et al., 1998), HprK can also serve as a phosphorylase, catalyzing the dephosphorylation of serine-46 (Galinier et al., 1998). Serine-46 phosphorylation is not directly implicated in sugar translocation, however the modification can inhibit EI-dependent histidine-15 phosphorylation up to 600-fold (Stülke et al., 1998). Although

many haloarchaeal Hpr homologs contain a conserved serine-46 residue, bioinformatics only predicts homologs of *B. subtilis* HprK in two haloarchaea, *H. marismortui* (at 27% to 39% amino acid identity) and *H. borinquense* (at 40% amino acid identity), the latter of which does not contain any detectable PTS homologs (Table 3-1). Homologs of *B. subtilis* HprK are also found in *Methanosarcina thermophila* (at 37% amino acid identity) and *Methanoregula boonei* (at 45% amino acid identity), despite the absence of additional PTS homologs. *H. volcanii* possesses the most versatile PTS of all the archaeal genomes analyzed based on the presence of both fructose- and galactitol-specific permeases (Table 3-1, Figure 3-1). Sugar-specific PTS permeases are additionally found in *T. pendens* (mannose-type), *H. marismortui* (fructose-type), and *H. turkmenica* (fructose-type) (Table 3-1, Figure 3-1).

**Distribution of DHAK Homologs in Archaea**

DHAKs (glycerone kinases, EC 2.7.1.29) are a family of amino acid sequence-conserved enzymes which utilize either ATP (eukaryotes and bacteria) or PEP (bacteria) as the source of the high-energy phosphoryl group (Bächler et al., 2005a). PEP-dependent DHAKs rely on the PTS general carrier components EI and Hpr as well as a tri-partite DHAK consisting of DhaK, DhaL, and DhaM subunits to phosphorylate DHA for its subsequent use. Unlike traditional PTS substrates, however, DHA is not transported into the cell by DHA-specific PTS permeases. The PTS instead serves to phosphorylate intracellular DHA in a phosphorelay proceeding from PEP to EI to Hpr to DhaM to ADP-bound DhaL and finally to DHA which is bound by DhaK.

Ninety-two archaeal genomes (Benson et al., 2010) were searched for the presence of DHAK using BLASTP (Altschul et al., 1997) and InterProScan (Hunter et al., 2009) search engines. DHAK homologs were identified using *E. coli* and *C. freundii*

DHAKs as a query for BLASTP. Out of the 92 available archaeal genome sequences, DHAK homologs were identified in only three haloarchaea. Specifically, only *H. volcanii*, *H. walsbyi*, and *H. lacusprofundi* encoded complete DHAKs (Table 3-1, Figure 3-1). The *H. volcanii* and *H. lacusprofundi* DHAK genes clustered chromosomally with genes encoding general carrier protein homologs Hpr (*ptsH*) and/or EI (*ptsI*) (Figure 3-1). The presence of DHAKs in haloarchaea may arise from the biological significance of DHA as an organic carbon source for haloarchaea. Although the permeability of DHA to the biological membrane is currently unknown, DHA derived from the glycerol cycle of *Dunaliella sp.* or as an overflow product of glycerol metabolism in *Salinibacter sp.* may serve as a putative energy source for haloarchaea (Elevi Bardavid and Oren, 2008).

**PTS Components and Haloarchaeal Glycerol Kinases**

Glycerol is an important organic carbon and energy source for haloarchaea and other members of halophilic, heterotrophic communities as a result of its large scale production by the halotolerant green alga *Dunaliella sp.* (Elevi Bardavid et al., 2008). As a result, GKs are widely distributed in haloarchaea and often cluster chromosomally with additional glycerol utilization enzymes including G3PDH and a putative glycerol facilitator protein (Figure 3-2). In Gram-positive bacteria such as *Enterococcus sp.* (Charrier et al., 1997), Hpr serves as an activator of GK activity through reversible phosphorylation (Deutscher and Sauerwald, 1986). In the presence of PTS substrates, EI phosphorylates Hpr which transfers the phosphate moiety to sugar-specific permeases which, in turn, phosphorylate the incoming PTS substrate. However, in the absence of preferable PTS substrates such as glucose, a phosphoryl residue is transferred from the N3-position of histidine-15 of Hpr to GlpK, allowing for subsequent 10-15 fold activation (Yeh et al., 2004). The site of GlpK phosphorylation in *E. faecalis*

was determined as a conserved histidine-232 (Charrier et al., 1997) (Figure 3-3). This conserved histidine-residue is noticeably absent from GKs of Gram-negative bacteria such as *E. coli* which employ a different mode of regulation of GK activity (Figure 3-3) and haloarchaeal GKs (Figure 3-3). The absence of the conserved histidine residue in haloarchaea may be due to the fact that glycerol is an important organic carbon sources for heterotrophic prokaryotes in hypersaline ecosystems as a result of its production and release by the halotolerant green alga *Dunaliella sp.* (Wegmann et al., 1980; Fujii and Hellebust, 1992; Elevi Bardavid et al., 2008). Thus, haloarchaeal GKs may not be subject to activation as glycerol is likely a preferred carbon source for members of the halophilic, heterotrophic microbial community (Sherwood et al., 2009). Although Hpr-dependent phosphorylation is a dominant form of GK regulation for many Gram-positive bacteria, not all members are subject to its regulation. Glycerol is one of the few carbon sources that *M. pneumoniae* is able to metabolize (Hames et al., 2009); thus, *M. pneumoniae* GK enzyme activity is constitutive and is not subject to activation by Hpr-dependent phosphorylation (Hames et al., 2009).

$EIIA^{Glc}$ (also called $III^{Glc}$ in older literature) is the central regulatory element of the PEP:PTS in enteric bacteria, serving as a signal for the availability of extracellular glucose. $EIIA^{Glc}$ recognizes and binds in a phosphorylation status-dependent manner to metabolic enzymes and transporters of secondary carbon sources, leading to their inactivation (Postma et al., 1993). Specifically in *E. coli*, $EIIA^{Glc}$ binds to GK, interacting with several amino acid residues including arginine-402 and glutamate-479 (the primary site of interaction). Many of these binding residues including glutamate-479 are conserved in haloarchaeal GKs (Figure 3-3); however, bioinformatics does not predict

any haloarchaeal genomes to encode a homolog of *E. coli* $EIIA^{Glc}$ (Figure 3-1). Previous studies have shown that when *E. coli* GK is modified at glycine-230 to aspartic acid by site-directed mutagenesis, the enzymatic activity of GK increases and allosteric regulation by the glycolytic pathway intermediate FBP decreases significantly (Anderson et al., 2007). In all haloarchaeal GK homologues analyzed, this glycine-230 to aspartic acid point mutation has occurred, possibly allowing for increased GK activity (Figure 3-3).

### Preliminary Evidence for the Involvement of *H. volcanii* EI and $EIIB^{Fru}$ in Fructose Metabolism

Given the versatility of the PTS components encoded by the *H. volcanii* genome, this haloarchaeon was selected as a model for preliminary examination of the biological function of PTS homologs. The open reading frame of *ptsI* (EI) as well as the start codon of *fruB* ($EIIB^{Fru}$) were deleted from the chromosome of H26 using a markerless deletion method (Bitan-Banin et al., 2003; Allers et al., 2004). The subsequent gene knockout was confirmed by DNA sequencing, Southern Blot, and PCR using primers which annealed external to the recombinatory region (Figure 3-4). While parent H26 readily utilized both fructose and glycerol, KS3 cells deficient in *ptsI* and *fruB* were unable to metabolize fructose in minimal medium containing glycerol and fructose as sole carbon sources (Figure 3-5). A plasmid containing both *fruB* and *ptsI* under the control of the constitutive *H. salinarum* rRNA P2 promoter fully complimented the mutation, however the mutation was not complemented by providing either gene alone *in trans* (data not shown). The PTS deletions did not appear to affect glycerol metabolism of the mutant strain KS3 based on HPLC analysis of glycerol utilization (Figure 3-5). These results are consistent with glycerol transport by a facilitator protein

and not by the PTS as in *E. coli* (Sanno et al., 1968). Interestingly, when mutant strain KS3 was grown in minimal medium containing glucose and glycerol, consumption of glucose and glycerol was not affected by the PTS mutations based on HPLC analysis of carbon utilization (Figure 3-6). In bacteria, glucose is transported and concomitantly phosphorylated by the PTS (Barabote and Saier, Jr., 2005). Given that *H. volcanii* lacks homologs for the PTS glucose-specific permease present in many bacteria such as *E. coli* and that a glucose-specific sodium transporter has been characterized in *H. volcanii* (Tawara and Kamo, 1991), it is not surprising that glucose metabolism does not appear affected by deletion of PTS components. The data here demonstrate that both EI and $EIIB^{Fru}$ are needed for *H. volcanii* fructose metabolism, and suggest a role for these proteins in the concomitant transport and phosphorylation of fructose by bacterial PTS homologs in *H. volcanii*.

## Conclusion

In conclusion, this study examined 92 published, archaeal genomes for homologs of characterized PTS proteins from both Gram-positive and Gram-negative bacteria. PTS homologs were identified in halophilic Euryarchaeota, methanogenic Euryarchaeota, and one Crenarchaeon. From the genomes analyzed, six archaeal genomes encoded a complete PTS consisting of homologs of general carrier proteins EI and Hpr as well as membrane-associated permeases specific for mannose, fructose, and galactitol. Preliminary examination of an *H. volcanii* mutant deficient in both $EIIB^{Fru}$ and EI demonstrated that these PTS homologs are needed for fructose metabolism and suggest a biological function of these proteins for group translocation of fructose in this haloarchaeon. Homologs of DHAKs which cluster near PTS homologs were also identified in three out of the 92 archaeal genomes analyzed. Overall, this study has

expanded the knowledge concerning sugar transport in archaea and is expected to serve as a guideline for understanding the biological function and evolution of the PTS within the third domain of life.

Table 3-1. Distribution of PTS homologs in archaea

| Organism | EI | Hpr | EIIA | EIIB | EIIC | EIID | DhaK | DhaL | DhaM | HprK |
|---|---|---|---|---|---|---|---|---|---|---|
| Crenarchaeota | | | | | | | | | | |
| *Thermofilum pendens* | Tpen_ 1092 | Tpen_ 1091 | Tpen_ 1098 (Man) | Tpen_ 1097 (Man) | | Tpen_ 1100 (Man) | | | | |
| Euryarchaeota | | | | | | | | | | |
| *Haloferax volcanii* | HVO_ 1496 | HVO_ 1497 | HVO_ 1498 (Fru) | HVO_ 1495 (Fru) | HVO_ 1499 (Fru) | | | | | |
| | HVO_ 2101 | HVO_ 2102 (Gat) | HVO_ 2104 (Gat) | HVO_ 2103 (Gat) | | | | | | |
| | HVO_ 1543 | | | | | | HVO_ 1546 | HVO_ 1545 | HVO_ 1544 | |
| *Halorubrum lacusprofundi* | Hlac_ 1461 | Hlac_ 1462 | | | | | Hlac_ 1458 | Hlac_ 1459 | Hlac_ 1460 | |
| *Haloarcula marismortui* | pNG 7391 | pNG 7389 | pNG 7388 (Fru) | pNG 7392 (Fru) | pNG 7387 (Fru) | | | | rrnAC 0402 | rrnAC0623, rrnAC2379 |
| *Halogeometricum borinquense DSM11551* | | | | | | | | | | HborDRAFT _2433 |
| *Haloterrigena turkmenica* | Htur_ 2756 | Htur_ 2757 | Htur_ 2758 (Fru) | Htur_ 2755 (Fru) | Htur_ 2759 (Fru) | | | | | |
| *Haloquadratum walsbyi* | HQ 2709A | HQ 2708A | | | | | HQ 2672A | HQ 2673A | HQ 2674A | |
| *Methanocaldococcus fervens AG86* | | | | Mefer_ 1365* | | | | | | |
| *Methanocaldococcus sp. FS406-22* | | | | MFS40622 __1559* | | | | | | |
| *Methanocaldococcus jannaschii DSM2661* | | | | MJ0581* | | | | | | |
| *Methanosarcina thermophila* | | | | | | | | | | Mthe_1685 |
| *Methanoregula boonei* | | | | | | | | | | Mboo_1155 |

* Indicates a truncated EII protein in which an EIIB domain is contained within a hypothetical protein

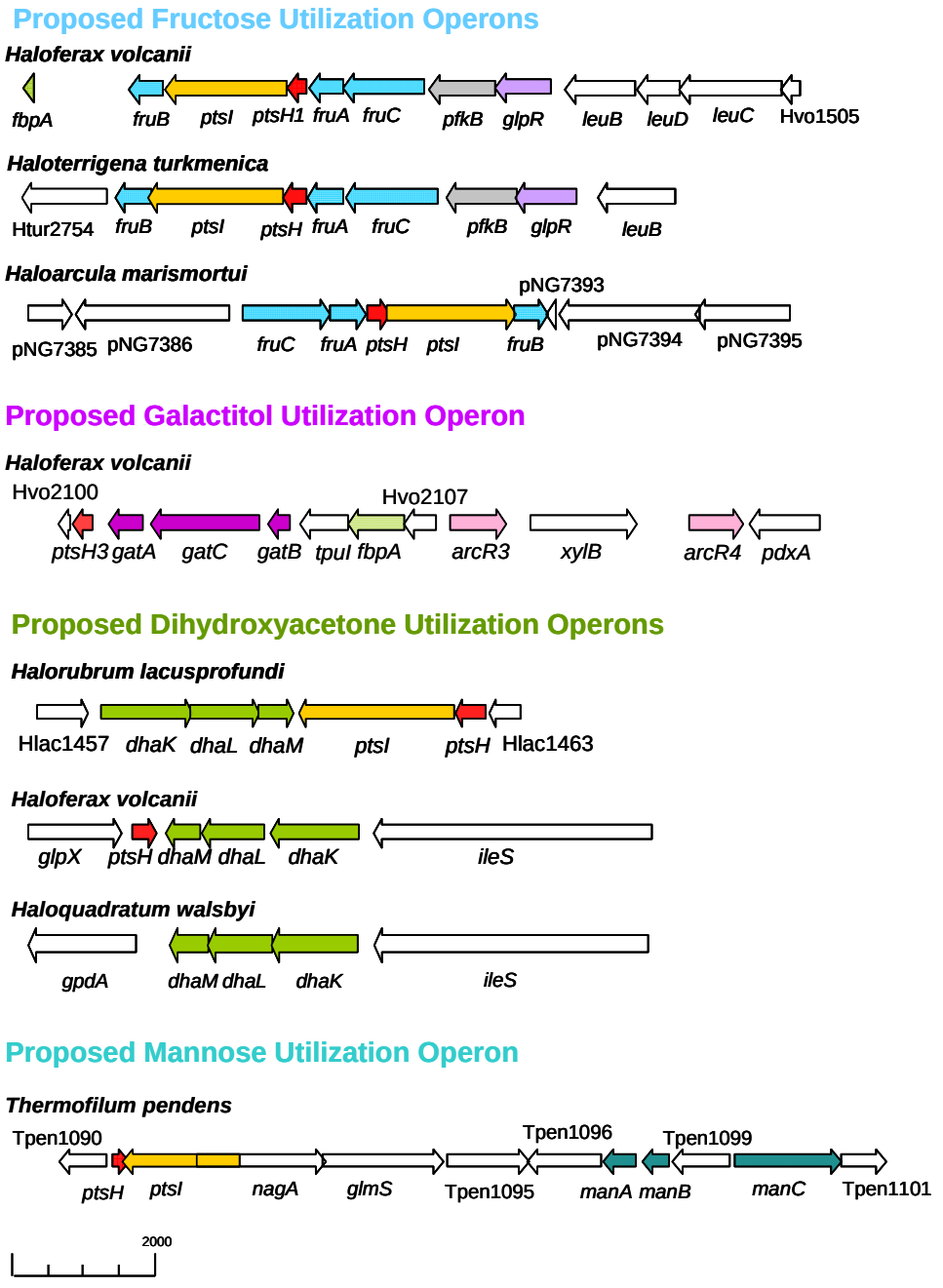


Figure 3-1. Genomic organization of complete phosphoenolpyruvate:phosphotransferase system utilization operons in archaea. Genes which are conserved across multiple species have been highlighted as follows: DeoR/GlpR-type transcriptional regulator (*glpR*, purple), DHAK (*dhaKLM*, green), PTS general carrier protein Hpr (*ptsH*, red), PTS general carrier protein EI (*ptsI*, gold), sugar-specific mannose permease $EII^{Man}$ (*manABC*, dark blue), PFK (*pfkB*, grey), leucine biosythesis genes (*leuBCD*, peach), sugar-specific fructose permease $EII^{Fru}$ (*fruABC*, bright blue), and sugar-specific galactitol permease $EII^{Gat}$ (*gatABC*, plum).

## Proposed Haloarchaeal Glycerol Utilization Operons

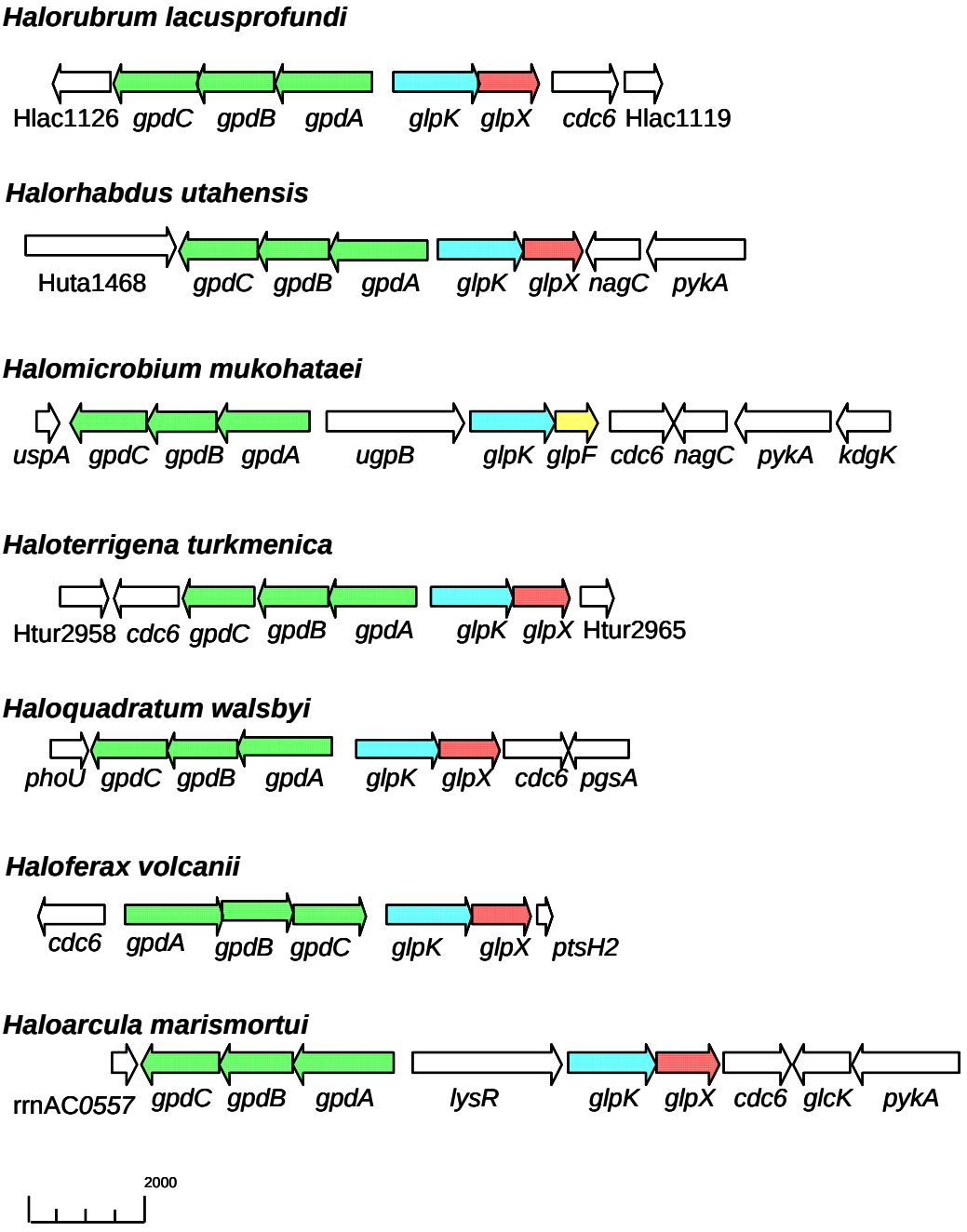


Figure 3-2. Organization of glycerol utilization operons from haloarchaea whose genome sequences have been completed. Genes that are conserved across multiple species are as follows: G3PDH (*gpdABC*, green), GK (*glpK*, blue), GlpF-like glycerol facilitator (*glpF*, yellow), and non-GlpF like glycerol facilitator (*glpX*, red).

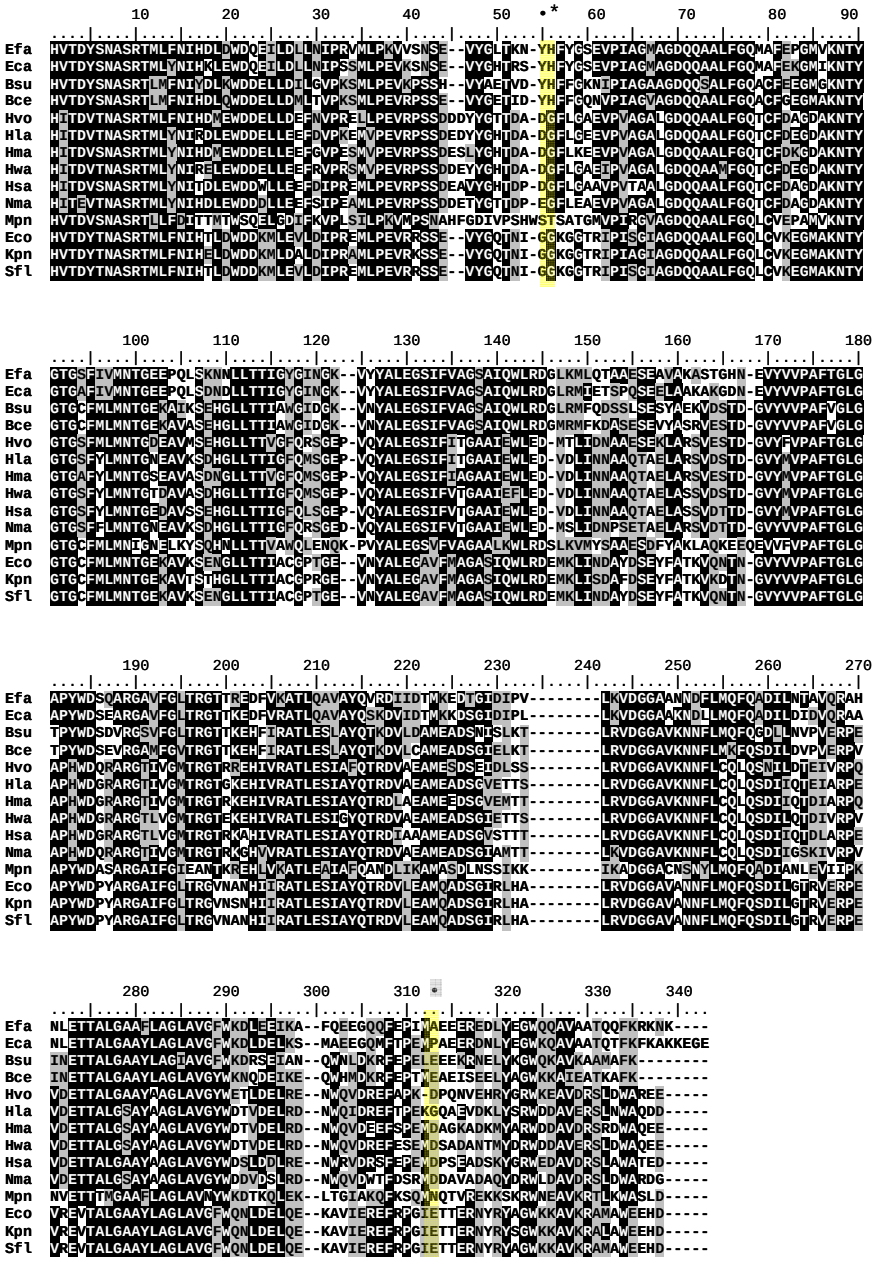


Figure 3-3. Alignment of haloarchaeal glycerol kinases and biochemically characterized bacterial glycerol kinases. Protein sequences were retrieved using the NCBI database and subsequently N- and C-terminally trimmed and aligned using CLUSTAL W (Thompson et al., 1994). Conserved regulatory sites are highlighted in yellow. The site of Hpr-dependent phosphorylation in Firmicutes is indicated by *. The primary site of EIIA$^{Glc}$ interaction is indicated as ●. A point mutation (G230D) known to increase enzymatic activity of *E. coli* GlpK is indicated by •. Accession numbers for the alignment can be found in Chapter 2.

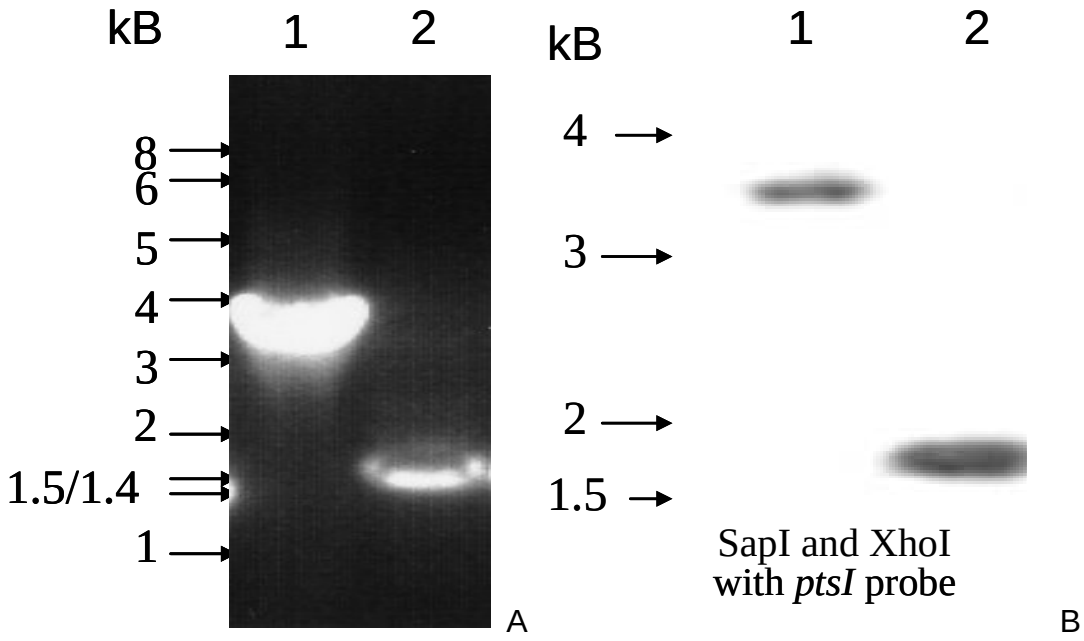


Figure 3-4. PCR and Southern blot confirmation of *H. volcanii fruB ptsI* mutant strain KS3 (H26 Δ*fruB*Δ*ptsI*). A) Confirmation of the *fruB ptsI* mutant strain KS3 by PCR. Primer pairs that annealed outside the genomic region cloned in suicide plasmid pJAM2660 were used for confirmation of the *fruB ptsI* gene deletions by PCR. Hi-Lo DNA markers and molecular masses are indicated on left. Genomic DNA from the following strains served as template: Lane 1. Parent strain H26, Lane 2. KS3 (H26 Δ*fruB*Δ*ptsI*). B) Southern blot confirmation of the *fruB ptsI* mutant strain KS3 (H26 Δ*fruB*Δ*ptsI*). Genomic DNA was digested with SapI and XhoI and hybridized with a DIG-labeled probe specific for *ptsI*. The following strains served as the source of genomic DNA: Lane 1. Parent strain H26, Lane 2. KS3 (H26 Δ*fruB*Δ*ptsI*).

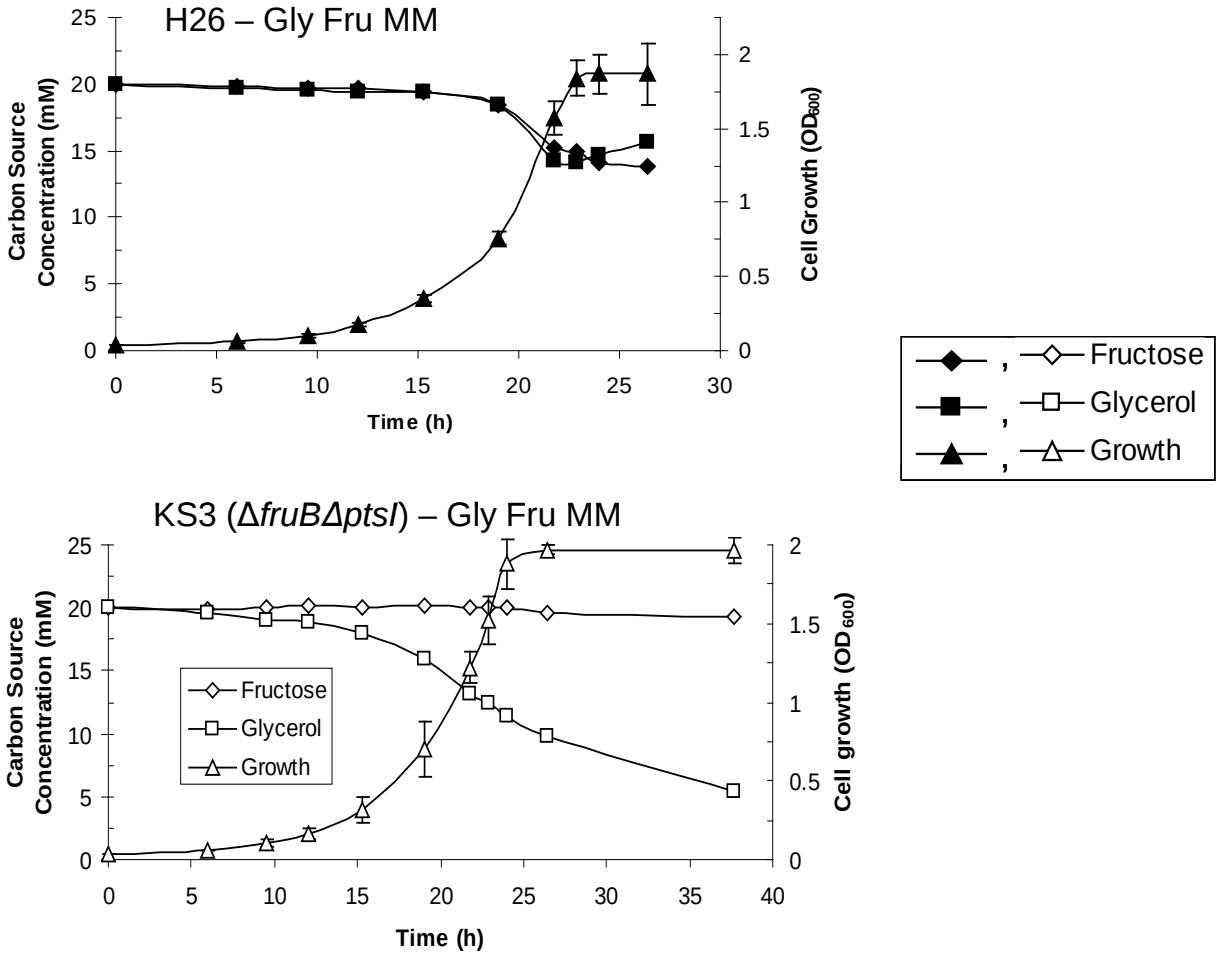


Figure 3-5. *H. volcanii* strain KS3 deficient in both PTS components EI and EIIB$^{Fru}$ (H26 Δ*fruB*Δ*ptsI*) is unable to metabolize fructose. The growth rates of and levels of carbon utilization by parent strain H26 and mutant KS3 cells grown on Gly Fru MM are shown. Growth at 42°C (200 RPM) was monitored as an increase in $OD_{600}$, where 1 U was equivalent to approximately $10^9$ CFU per ml for both strains. At various time points, supernatant fractions were withdrawn from cultures and analyzed by HPLC for glycerol and fructose consumption. Experiments were performed in triplicate, and the means ± SD were calculated.

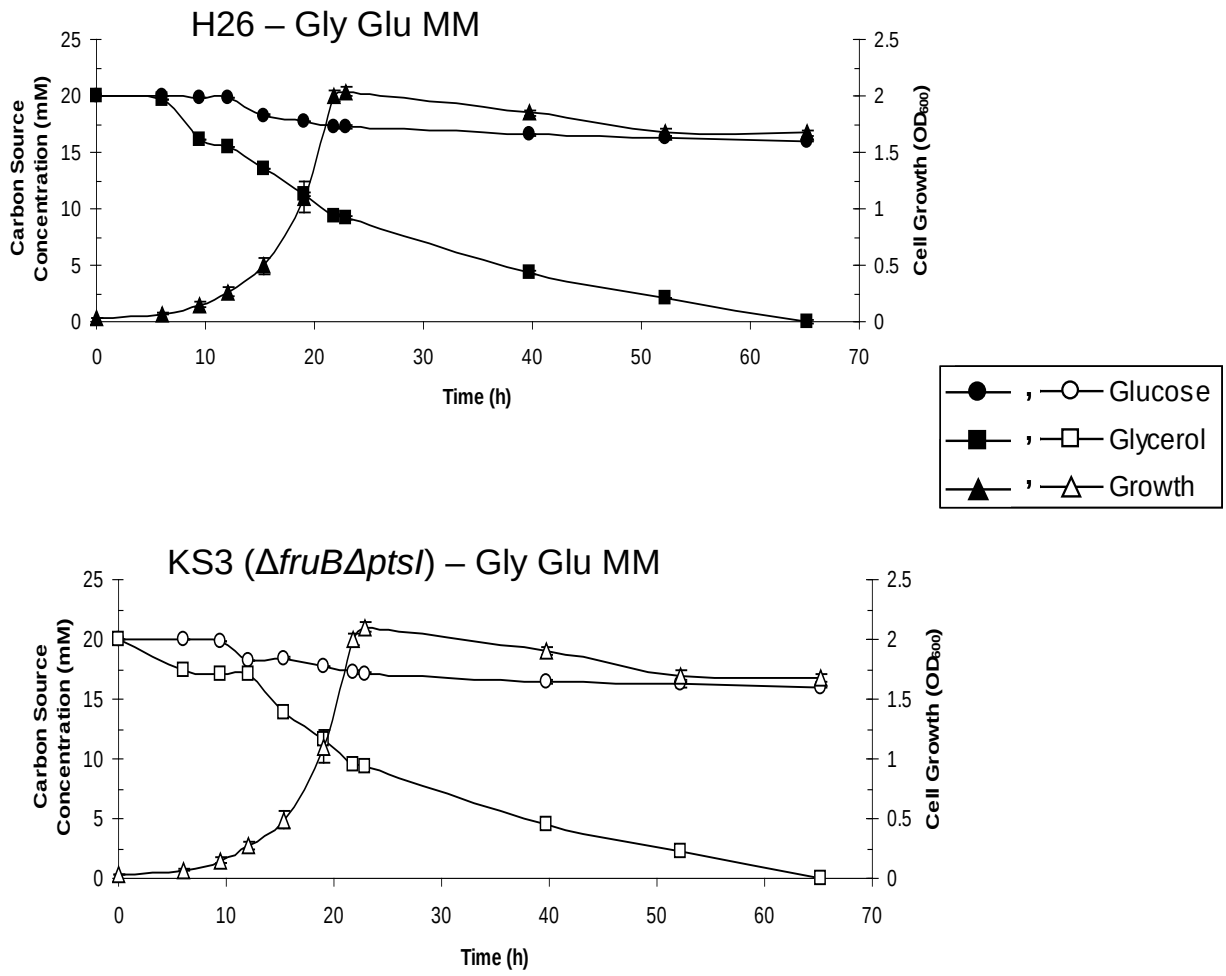


Figure 3-6. PTS components EI and EIIB$^{Fru}$ are not required for glucose metabolism in *H. volcanii*. The growth rates of and levels of carbon utilization by parent strain H26 and mutant KS3 cells grown on Gly Glu MM are shown. Growth at 42°C (200 RPM) was monitored by an increase in $OD_{600}$, where 1 U was equivalent to approximately $10^9$ CFU per ml for both strains. At various time points, supernatant fractions were withdrawn from cultures and analyzed by HPLC for glycerol and glucose consumption. Experiments were performed in triplicate, and the means ± SD were calculated.

# CHAPTER 4
# GLYCEROL KINASE AS THE SOLE ROUTE OF GLYCEROL CATABOLISM IN THE HALOARCHAEON *Haloferax volcanii*

## Introduction

Halophilic and halotolerant microorganisms have adapted different methods for withstanding the high osmotic pressure exerted by their surrounding hypersaline environment. Halophilic archaea (Christian and Waltho, 1962; Lanyi, 1974), as well as the halophilic bacterium *Salinibacter ruber* (Oren et al., 2002), maintain a high intracellular salt concentration by accumulating $K^+$ and $Cl^-$ ions and excluding $Na^+$ ions, thus requiring intracellular proteins to be active under high-salt conditions. Many halophilic bacteria (Ventosa et al., 1998), the halotolerant green alga *Dunaliella sp.* (Lanyi, 1974), and some haloarchaea (Lai et al., 1991) exclude cytoplasmic salts and rely on organic solutes such as ectoine, glycine betaine, and glycerol to provide osmotic balance. Glycerol, in particular, is accumulated in molar quantities by *Dunaliella* as an organic osmotic solute. Due to leakage from *Dunaliella* cells (Wegmann et al., 1980; Elevi Bardavid et al., 2008) and/or cellular lysis, glycerol is released into the surrounding environment, where it serves as a primary energy source for haloarchaea. Upon uptake, halophilic microorganisms assimilate glycerol into DHAP by one of two catabolic routes (Figure 4-1). In one route, glycerol is first phosphorylated by GK to form G3P, which is subsequently oxidized by G3PDH to produce DHAP. Alternatively, glycerol can be first oxidized by GDH to form DHA, which is subsequently phosphorylated by an ATP- or PEP:PTS-dependent DHAK to yield DHAP. Once generated from glycerol, DHAP can be channeled into pyruvate and other metabolic intermediates, including G1P, used as a phospholipid backbone in archaea (Nishihara et al., 1999).

Although glycerol is an important carbon and energy source for members of halophilic, heterotrophic communities, little is known regarding glycerol metabolism, especially in haloarchaea. Halophilic archaea such as *H. volcanii* have been previously shown to metabolize glycerol (Rawal et al., 1988), and specific activities of glycerol-metabolizing enzymes in various haloarchaea have been determined (Wassef et al., 1970; Rawal et al., 1988; Oren and Gurevich, 1994a); however, the metabolic pathways surrounding glycerol utilization at the molecular level have not been described. This study provides genetic and biochemical evidence that *H. volcanii* metabolizes glycerol through GK (encoded by *glpK*) and, most likely, a *glpK*-linked G3PDH (encoded by a *gpdA1B1C1* operon). These results provide insight into the central metabolic pathways of heterotrophic haloarchaea such as *H. volcanii*.

## Results and Discussion

### Glycerol is Metabolized through Glycerol Kinase

To analyze glycerol catabolism in *H. volcanii*, a gene encoding a GK homolog (HVO_1541; *glpK*) was targeted for knockout in a *pyrE2* mutant strain (H26). The deduced product of this gene, GlpK, was most closely related to (with 74 to 78% identity) and clustered in dendrograms with other putative GKs of haloarchaea, including those of *H. lacusprofundi*, *H. marismortui*, *H. walsbyi*, *N. magadii*, and *H. salinarum*, with the notable absence of GlpK homologs in the haloalkaliphilic archaeon *N. pharaonis* and other archaea (Figure 4-2). The *H. volcanii* and other haloarchaeal GlpK proteins also clustered with the bacterial GKs with the greatest degrees of identity (up to 58%) to those of the *Thermoanaerobacterales* and *Thermotogales* (Figure 4-2).

The *glpK* gene was deleted from the chromosome of *H. volcanii* by a markerless knockout strategy as described previously (Bitan-Banin et al., 2003; Allers et al., 2004).

Gene deletion was confirmed by PCR, Southern blotting, and sequencing analysis (Figure 4-3). The resultant GK mutant, H26 Δ*glpK* (KS4), was incapable of growth either on glycerol minimal medium plates (Figure 4-4) or in liquid culture (data not shown). A pHV2-based self-replicating plasmid containing the *glpK* gene under the control of a strong rRNA P2 promoter (pJAM2666) restored KS4 growth on glycerol, while the plasmid vector alone (pJAM202c) did not complement this *glpK* mutation (Figure 4-4). These results indicate that the GK homolog encoded by *glpK* is required for the growth of *H. volcanii* on glycerol. Previous studies have detected GK but not GDH activity in the lysate of *H. volcanii* cells grown in the presence of glycerol (Rawal et al., 1988). These findings are in agreement with the present results that in *H. volcanii*, glycerol metabolism proceeds through the *glpK*-encoded GK rather than through the conversion of glycerol to DHA by a GDH. These results also suggest that genes HVO_1546 to HVO_1544, which are predicted to encode putative DHAK subunits K, L, and M based on the *H. volcanii* genome sequence (Hartman et al., 2010), function in DHA metabolism and not glycerol metabolism. Consistent with this possibility, recent evidence suggests that *S. ruber* mediates the incomplete oxidation of glycerol to yield DHA as an overflow product which may then be taken up by heterotrophs present in hypersaline environments (Elevi Bardavid et al., 2008).

To biochemically confirm that the *glpK* homolog HVO_1541 codes for GK, the specific activities of GK in cell lysates from H26 and KS4 (H26 Δ*glpK*) were measured as described previously (Bublitz and Kennedy, 1954; Oren and Gurevich, 1994a). GK activity was readily detected in cells of the parent strain H26 grown in medium containing glycerol (Gly MM or Gly Glu MM), regardless of the presence of glucose

(Figure 4-5). Significant levels of GK activity were also detected in H26 cells grown on medium with glucose alone (Glu MM), although the levels were two-fold lower compared to those in H26 cells grown on media with glycerol (i.e., Gly MM and Gly Glu MM). GK activity was not detected in the GK mutant (KS4) or boiled cell lysate (the negative control) (Figure 4-5). The specific activity of GK in parent strain H26 grown in the presence of glycerol was 430 ± 30 nmol·min$^{-1}$mg protein$^{-1}$; although five-fold higher than previously reported specific activities of GKs in *S. ruber* (90 nmol·min$^{-1}$·mg protein$^{-1}$), *H. cutirubrum* (14 nmol·min$^{-1}$·mg protein$^{-1}$), and *H. volcanii* (31 nmol·min$^{-1}$·mg protein$^{-1}$ for cells grown in complex medium with peptides) determined in similar assays (Wassef et al., 1970; Oren and Gurevich, 1994a; Sher et al., 2004), this value was within a reasonable range of measurement for GK enzymes.

These results demonstrate that the *glpK* homolog HVO_1541 encodes a GK and that this gene is required for the catabolism of glycerol in *H. volcanii*. It should also be noted that GK activity is not universal among the archaea, unlike bacteria, and is absent in those organisms that cannot use glycerol as an energy source [e.g., autotrophic methanogens (Nishihara et al., 1999)]. Thus, GK is not thought to be involved in the synthesis of the backbone of archaeal phospholipids and is instead mediated by G1PDH, which generates G1P from DHAP. Therefore, glycerol does not appear to be channeled into DHA by a GDH for the growth of *H. volcanii*.

These results also reveal that GK activity in *H. volcanii*, although elevated by growth on glycerol, is not reduced by the presence of glucose in the growth medium. The detection of comparable levels of GK activity in *H. volcanii* cells grown on glycerol regardless of glucose supplementation contrasts with results for the *E. coli* model, in

which the *glpK* regulon encoding GK is subject to catabolite repression (Freedberg and Lin, 1973).

**Glycerol Metabolism is not Reduced in the Presence of Glucose**

To determine if the growth defect of the GK mutant (KS4) is exclusive to glycerol and to further investigate the observed differences in catabolite repression between *H. volcanii* and *E. coli*, the growth of and utilization of carbon by the *H. volcanii* H26 parent and KS4 mutant strains on minimal medium supplemented with either 20 mM glycerol and 20 mM glucose or 20 mM glucose alone (Gly Glu MM or Glu MM, respectively) were measured (Figure 4-6A and Figure 4-7A). Although there are other carbon sources [Tris buffer (30 mM), uracil (450 µM), biotin (0.41 µM), and thiamine (2.37 µM)] in the minimal medium, these alone do not support the growth of *H. volcanii* (data not shown). Thus, any observed growth would be due to glucose and/or glycerol in the medium.

The *glpK* mutant (KS4) and parent strain H26 grew and utilized glucose at nearly identical rates when cultured in minimal medium containing glucose as the sole carbon source (Glu MM) (Figure 4-6A). In both cases, roughly 85% of the glucose was metabolized within 60 h, contributing to an average overall $OD_{600}$ of 1.27 and a growth rate of 0.11 doublings per h when media was supplemented with 20 mM glucose (Figure 4-6A). The addition of 20 mM glycerol to 20 mM glucose (Gly Glu MM) enhanced the growth rate and cell yield of the parent H26 approximately two-fold, to 0.22 doublings per h and a final $OD_{600}$ of 2.0 (Figure 4-7A). Consistent with these results, H26 metabolized both of these carbon/energy sources but displayed a preference for glycerol, with 79% of the glycerol and only 16% of the glucose in the Gly Glu MM being metabolized (Figure 4-7A). Thus, H26 metabolized glucose at a reduced rate when glycerol was included in the growth medium. In contrast to H26, the *glpK*

mutant KS4 is unable to metabolize glycerol and does not induce glucose metabolism when grown in the presence of glycerol until approximately 30 h later than its parent, H26 (Figure 4-7A), and 20 h later than KS4 grown on medium with glucose alone (Figure 4-6A). Once KS4 initiated this delayed metabolism of glucose in glycerol-supplemented medium (Gly Glu MM), the growth rate (0.095 doublings per h) and final $OD_{600}$ (0.93) of these cells was only slightly lower compared to those of cells grown in medium with glucose alone. In addition to using 20 mM of each carbon source, a lower supplementation (5 mM) of glycerol and glucose was also used to examine both growth rates and carbon utilization. Both parent H26 and GK mutant KS4 (Δ*glpK*) metabolized glucose at similar rates (Figure 4-6B). For both strains, all of the glucose is metabolized within 35 hours and both cultures reached a maximum $OD_{600}$ of 0.75 (Figure 4-6B). Similar to the carbon preference observed in the minimal medium supplemented with 20 mM glycerol and 20 mM glucose, parent H26 metabolized the majority of the glycerol prior to induction of glucose metabolism in minimal medium supplemented with 5 mM glucose and 5 mM glycerol (Figure 4-7B).

Based on these results, *H. volcanii* glycerol metabolism is not reduced or delayed in the presence of glucose. The observed preference of *H. volcanii* for glycerol directly contrasts with that of *E. coli* which exhibits diauxic growth with glucose as the preferred carbon and energy source (Holtman et al., 2001). Preference for carbon compounds other than glucose is not novel. For example, members of the genus *Pseudomonas* exhibit organic acid-induced catabolite repression of glucose metabolism (Lynch and Franklin, 1978). However, preferential utilization of glycerol over glucose has not been reported previously.

**Levels of Glycerol-3-Phosphate Dehydrogenase and Glycerol Kinase Transcripts are Upregulated by the Addition of Glycerol**

Based on the genome sequence (Hartman et al., 2010), *H. volcanii* has two putative NAD(P) $^{+}$-linked G3PDH operons: one (*gpdA2B2C2*; HVO_A0269 to HVO_A0271) on the minichromosome pHV4 and one (*gpdA1B1C1*; HVO_1538 to HVO_1540) on the chromosome directly upstream of the GK gene (Figure 4-8A). The protein paralogs encoded by these two operons are closely related in amino acid sequence (58 to 74% identical and 67 to 85% similar). The products of both operons are distinct from the enantiomeric glycerophosphate synthase (EgsA), an NAD(P)$^{+}$-linked G1PDH responsible for the formation of the G1P backbone of archaeal phospholipids (Nishihara et al., 1999), most likely encoded by HVO_0822 in *H. volcanii*.

In order to determine whether either *gpd* operon is upregulated in the presence of glycerol, qRT-PCR was performed using gene-specific primers (Table 2-4). Primers were designed to correspond to the first gene (*gpdA2* [HVO_A0269] and *gpdA1* [HVO_1538]) in each of the two operons in order to achieve the strongest signal for transcriptional analysis (Figure 4-8A). In addition, qRT-PCR primers for *glpK* were designed to determine if the transcription of this gene was induced by glycerol. A transcript specific to the ribosomal protein L10 gene (*ribL*) was used as an internal control based on data from a previous study (Brenneis et al., 2007) and confirmation by qRT-PCR that the level of induction of transcripts specific for *ribL* in cells grown in the presence of glycerol and glucose was close to one-fold compared to transcript levels in cells grown in the presence of glucose alone.

By qRT-PCR analysis, transcripts specific for *glpK*, *gpdA1*, and *gpdA2* were detected at significant levels under all growth conditions examined (growth on Gly MM

and Gly Glu MM) (Figure 4-8B). In addition, transcripts specific for *gpdA1* and *glpK* were upregulated approximately 78- and 9-fold, respectively, in the presence of glycerol and glucose compared to those in the presence of glucose alone (Figure 4-8B). In contrast, *gpdA2* transcripts were not induced to significant levels (2.0- ± 1.0-fold) by glycerol (Figure 4-8B), indicating that the *gpdA2* operon is not likely to be involved in glycerol metabolism. These results reveal that transcripts specific for *glpK* and its gene neighbor *gpdA1* are significantly induced by glycerol, supporting the argument that both genes and their encoded enzymes (GK and G3PDH) are involved in glycerol metabolism in *H. volcanii*.

**Glycerol Kinase and Glycerol-3-Phosphate Dehydrogenase Genes are under the Control of a Common Promoter**

Due to the close proximity of *glpK* and *gpdA1B1C1* and the likely involvement of the encoded gene products in a common metabolic pathway (Lawrence, 1997; Overbeek et al., 1999), it was investigated whether these genes were co-transcribed in an operon. RT-PCR was performed using primers designed such that the forward primer would anneal to the 3'-coding region of *gpdC1* and the reverse primer would anneal to the 5'-coding region of *glpK*, amplifying a portion of each gene as well as the 364-bp intergenic region (Figure 4-8A). A single PCR product of the expected size was detected using synthesized cDNA (Figure 4-8C), and the sequence of the product was later confirmed. No product from the negative control reaction with RNA as a template was detected (Figure 4-8C). Thus, *glpK* and *gpdC1* are linked at the transcriptional level.

Although *glpK* and *gpdC1* of the putative *gpdA1B1C1* operon are transcriptionally linked, the reasons for the significant differences in the levels of induction of *glpK*- and

*gpdA1*-specific transcripts in the presence of glycerol (Figure 4-8B) remain to be determined. Multiple promoter elements may be involved in the transcription of this region of the chromosome and account for these differences in induction. Consistent with the possibility that multiple promoters control the expression of the *gpdA1B1C1-glpK* region, BRE and TATA box promoter consensus sequence elements were identified upstream of both *gpdA1* and *glpK* (Figure 4-8A, P1 and P2, respectively). Alternatively, the transcription of *glpK* (which is distal relative to *gpdA1*) may be reduced by transcriptional polarity, which leads to the premature termination of polycistronic mRNA translation, resulting in the reduced transcription of genes located distally from the operon (Wek et al., 1987). Another possibility is that the *glpK*-specific transcripts are more susceptible to degradation than those specific for *gpdA1*.

## Conclusion

This study demonstrates that glycerol metabolism in *H. volcanii* requires GK encoded by the *glpK* gene (HVO_1541) and that this gene is transcriptionally linked to a putative G3PDH operon (*gpdA1B1C1*; HVO_1538 to HVO_1540) located upstream of *glpK* on the chromosome. The levels of both *glpK*- and *gpdA1*-specific transcripts are significantly upregulated in the presence of glycerol, although not to the same extent, with the glycerol-dependent induction of *gpdA1*-specific transcripts being eight-fold greater that of *glpK*-specific transcripts. Promoter consensus elements upstream of both *gpdA1* and *glpK* suggest that, in addition to sharing a common promoter with *gpdA1*, *glpK* may be regulated independently of *gpdA1*. The present model is that *glpK* and *gpdA1* share a common P1 promoter immediately upstream of *gpdA1* that is tightly regulated in response to glycerol availability and that additional control of *glpK* transcription may be achieved through a *gpdA1*-independent P2 promoter immediately

upstream of *glpK*. This study also provides evidence that *H. volcanii* displays differential utilization of glycerol and glucose. Overall, the results not only shed light on glycerol metabolism in *H. volcanii*, but also add to the understanding of central metabolic pathways of haloarchaea.

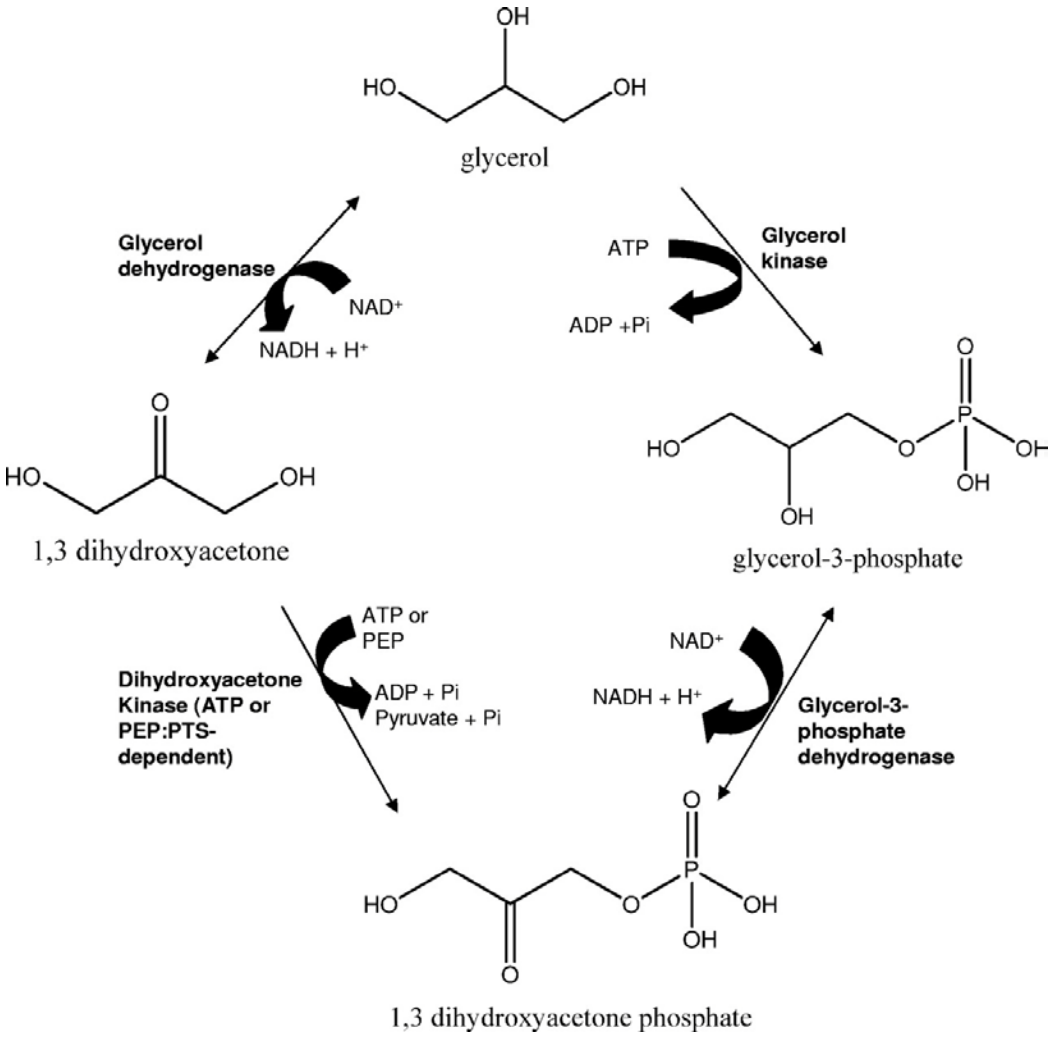


Figure 4-1. Halophilic microorganisms assimilate glycerol into DHAP by one of two catabolic routes. In the route depicted on the right, glycerol is phosphorylated by GK and subsequently converted into DHAP through G3PDH. In the route depicted on the left, glycerol is oxidized through GDH to form DHA, which is subsequently phosphorylated by an ATP- or PEP:PTS-dependent DHAK to yield DHAP. DHAP is channeled into pyruvate and other metabolic intermediates.

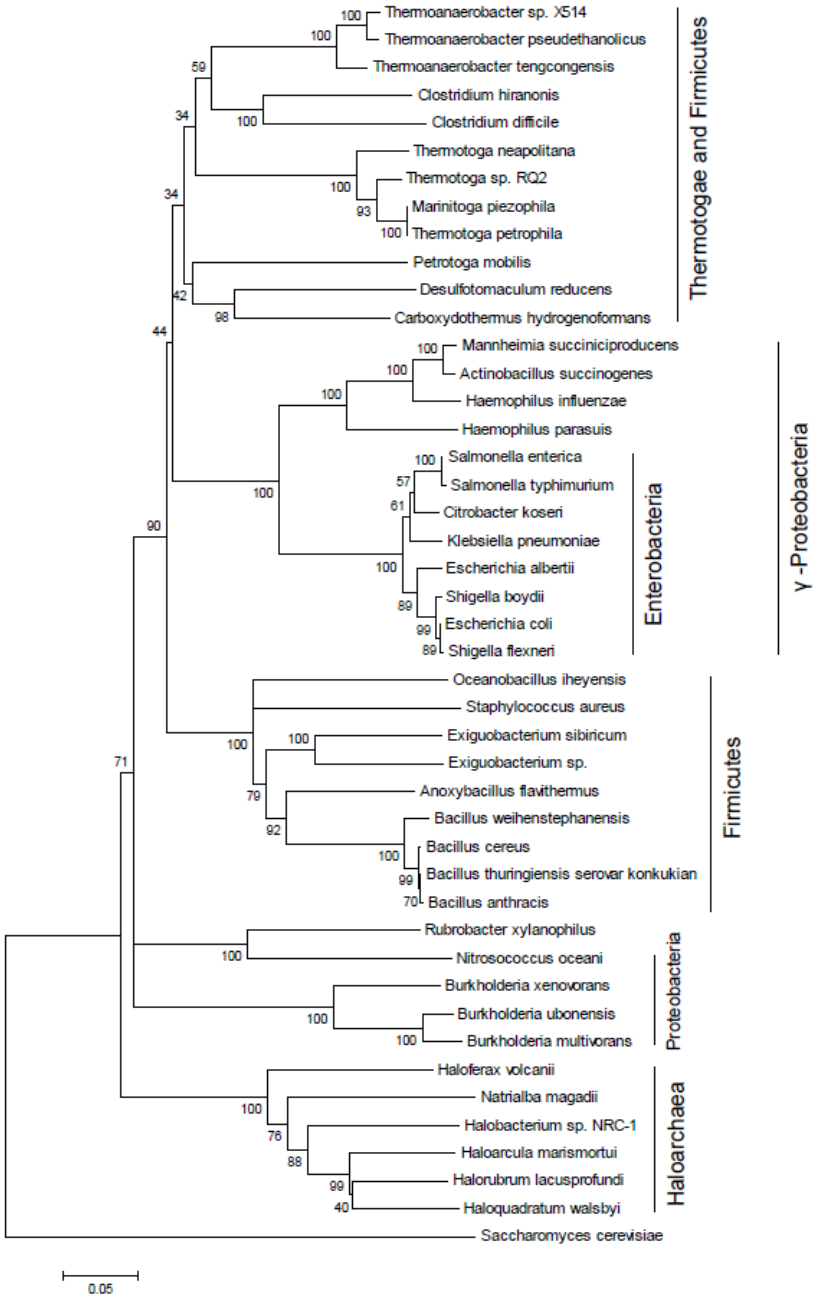


Figure 4-2. Phylogenetic distribution of glycerol kinases. Protein sequences were retrieved from the NCBI database, N- and C-terminally trimmed, and aligned using CLUSTAL W (Thompson et al., 1994). Pairwise comparisons were performed between sequences and mean genetic distance was evaluated using p-distance (gaps were analyzed using complete deletion). The best neighborhood-joining tree was then constructed using MEGA 4.0. Bootstrap support values are indicated at the internal nodes and were obtained by performing 1,000 replicates. Accession numbers for protein sequences are listed in Chapter 2.

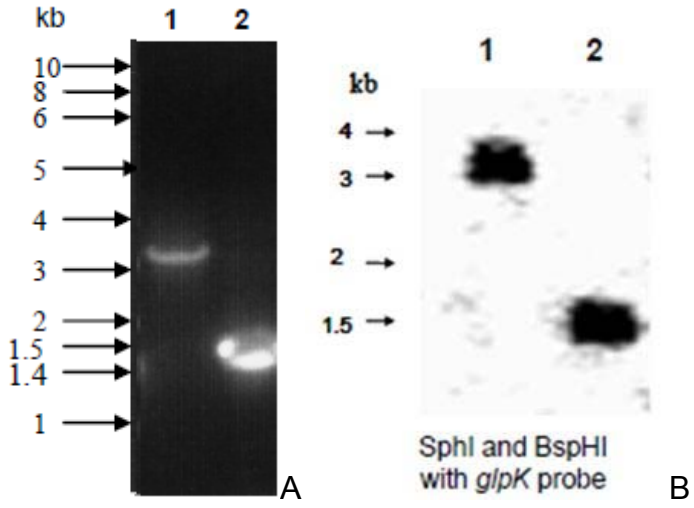


Figure 4-3. PCR and Southern blot confirmation of *H. volcanii* glycerol kinase mutant strain KS4 (H26 Δ*glpK*). A) Confirmation of the GK mutant strain KS4 (H26 Δ*glpK*) by PCR. Primer pairs that annealed outside of the recombinatory region were used for confirmation of the *glpK* gene knockout by PCR. Hi-Lo DNA markers and molecular masses are indicated on left. Genomic DNA from the following strains served as template: Lane 1. H26, Lane 2. H26 Δ*glpK.* B) Southern blot confirmation of the *glpK* (GK) gene knockout KS4. Genomic DNA was digested with SphI and BspHI and hybridized with a DIG-labeled probe specific for *glpK*. The following strains served as the source of genomic DNA: Lane 1. H26, Lane 2. KS4 (H26 Δ*glpK*).

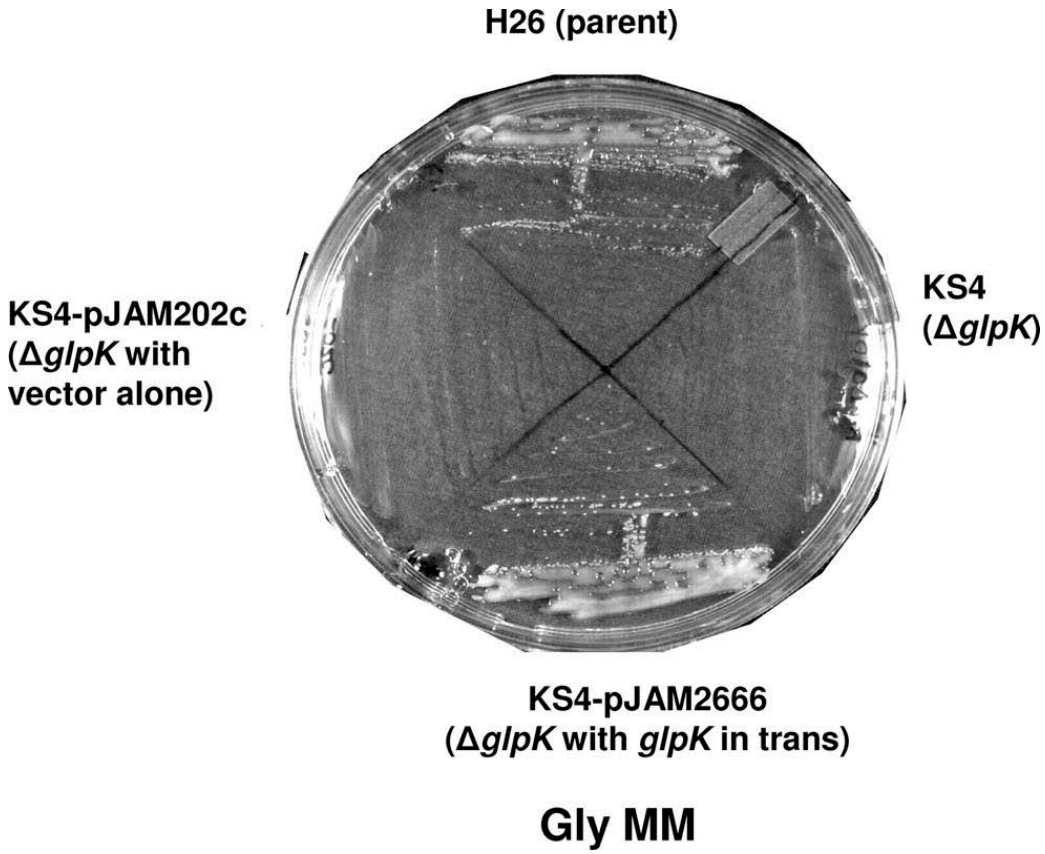


Figure 4-4. *H. volcanii* metabolizes glycerol through GlpK. Both the H26 parent strain and the H26 Δ*glpK* mutant KS4 transformed with a plasmid carrying *glpK* (pJAM2666) grew on Gly MM. In contrast, the *glpK* mutant strain (KS4) and KS4 transformed with vector alone (pJAM202c) were unable to grow on Gly MM. Cells were transferred with a loop from liquid Glu MM cultures onto plates of solid Gly MM, and the plates were incubated at 42°C for 3.5 days.

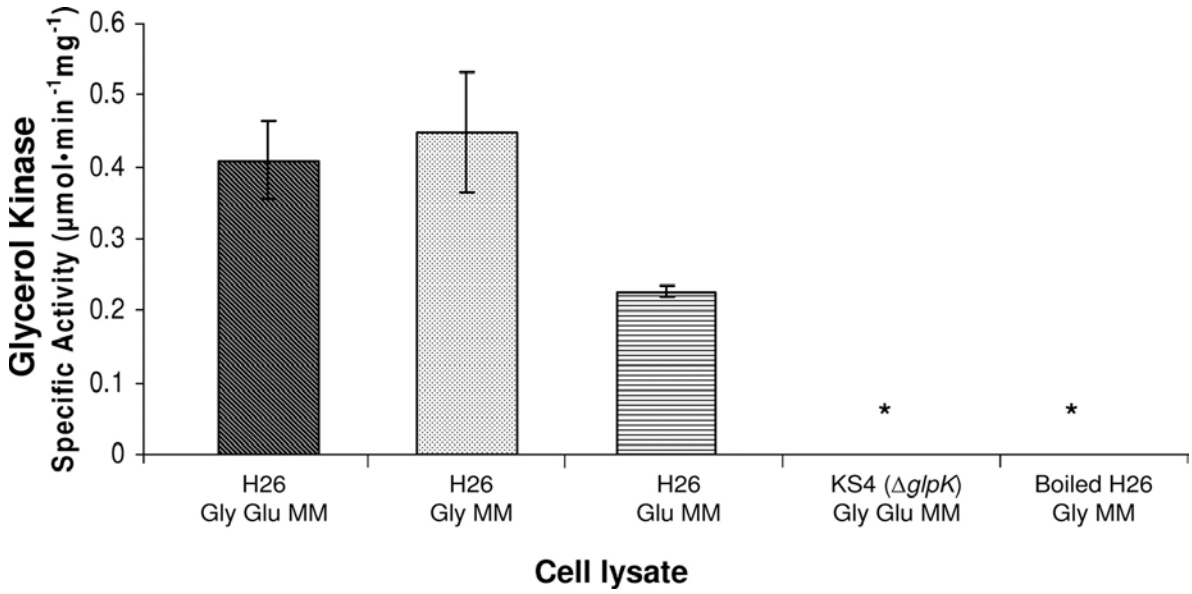


Figure 4-5. *H. volcanii* GK activity is dependent on *glpK* (HVO_1541), stimulated by growth on glycerol, and is detectable in the presence of glucose. *H. volcanii* H26 (parent) and KS4 (*glpK* mutant) cells were grown in Gly Glu MM, Gly MM, or Glu MM. Measurements of GK activities were performed using lysates prepared from log-phase cells as specified in Materials and Methods. * indicates that enzyme activity was not detected. Experiments were performed in triplicate, and the means ± SD were calculated.

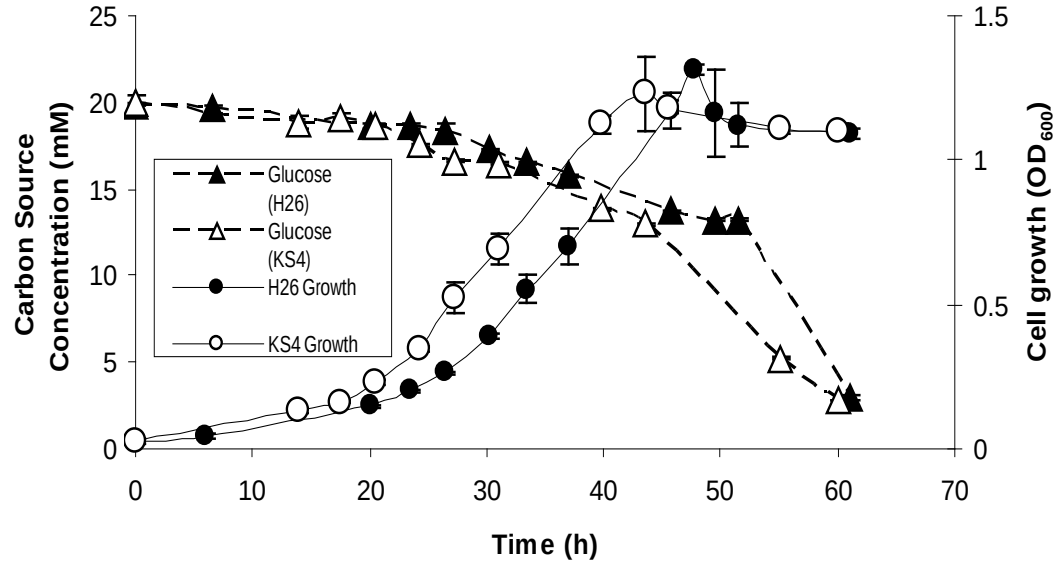


A

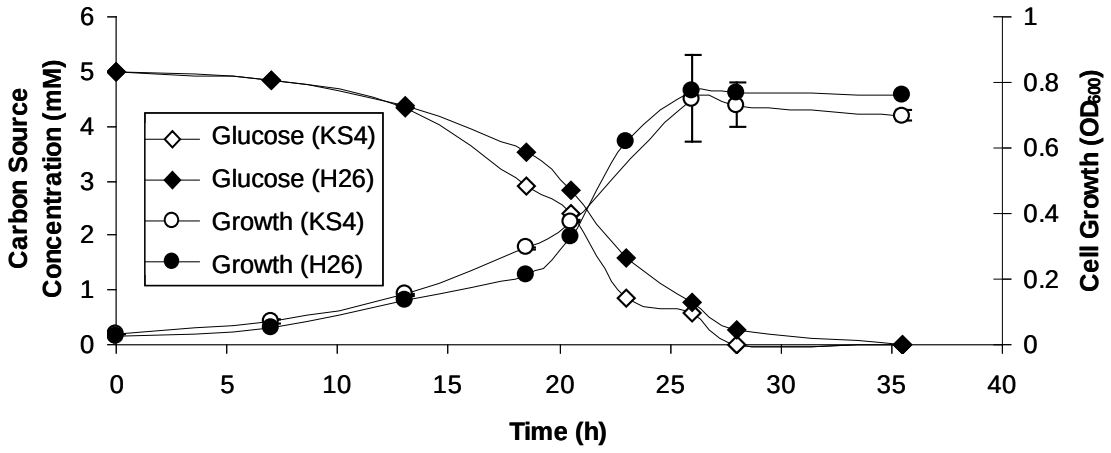


B

Figure 4-6. Parent strain H26 and glycerol kinase mutant strain KS4 (H26 Δ*glpK*) exhibit similar growth rates, cell yields, and carbon utilization patterns when grown in glucose minimal medium. Minimal medium was supplemented with either 20 mM Glu (A) or 5 mM Glu (B). Growth at 42°C (200 RPM) was monitored as an increase in $OD_{600}$, where 1 U was equivalent to approximately $10^9$ CFU per ml for all strains. At various time points, supernatant fractions were withdrawn from both parent H26 and KS4 cultures and analyzed by HPLC for glucose consumption. Experiments were performed in triplicate, and the means ± SD were calculated. Cell growth and glucose utilization levels are indicated.

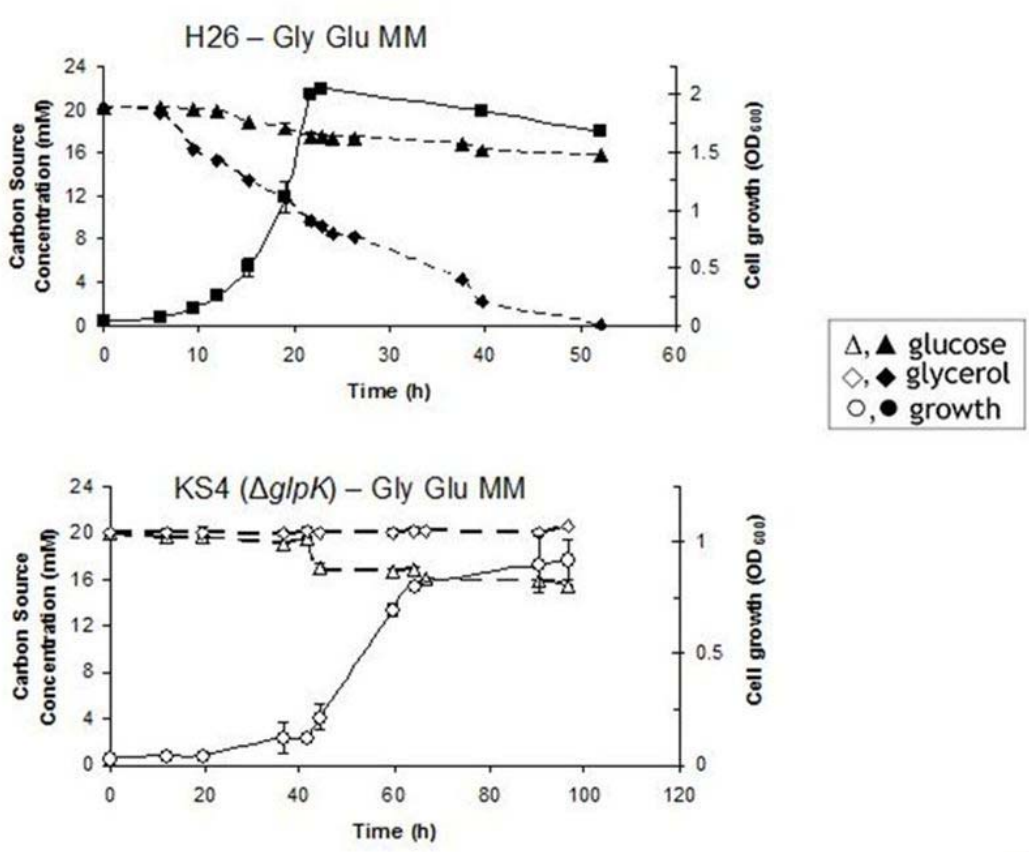


A

Figure 4-7. Parent strain H26 and GK mutant KS4 (H26 Δ*glpK*) exhibit differential utilization of glycerol and glucose. The growth rates of and levels of carbon utilization by parent strain H26 and mutant KS4 cells grown on Gly Glu MM with carbon sources supplemented at either 20 mM each (A) or 5 mM each (B) are shown. Growth at 42°C (200 RPM) was monitored by an increase in $OD_{600}$, where 1 U was equivalent to approximately $10^9$ CFU per ml for all strains. At various time points, 1 ml culture volumes were withdrawn, and supernatant fractions were analyzed by HPLC for glycerol and glucose consumption. Experiments were performed in triplicate, and the means ± SD were calculated.

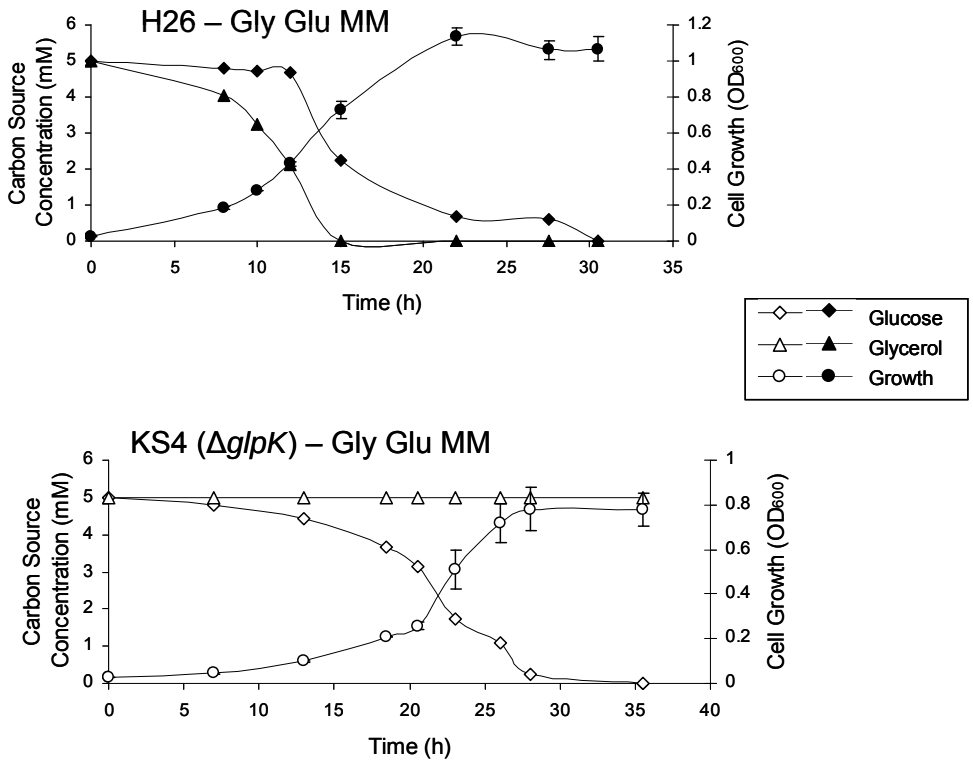


B

Figure 4-7. Continued.

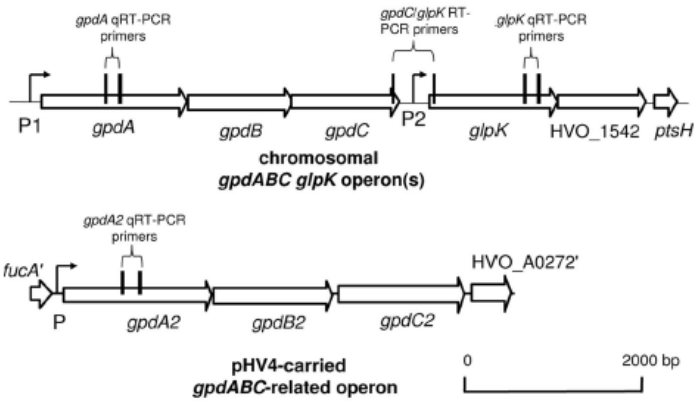


A

Figure 4-8. Genomic organization and transcript analysis of the GK gene and G3PDH-related operons of *H. volcanii*. (A) Schematic representations of the GK gene (*glpK*) and the G3PDH-related operons (*gpdA1B1C1* and *gpdA2B2C2*) of *H. volcanii* and location of annealing sites for (q)RT-PCRs. Representations of the chromosomally located *glpK* and *gpdA1B1C1* operon(s) and the pHV4-based *gpdA2B2C2* operon are presented. Vertical lines indicate annealing sites of primers used for (q)RT-PCR analyses. P1, P2, and P signify locations of BRE and TATA box archaeal promoter consensus elements. (B) Relative quantification of transcript levels specific for both the chromosomal *gpdA1* and pHV4-based *gpdA2* genes encoding G3PDH subunit A homologs (Hvo1538 and HvoA0269, respectively) and the GK *glpK* gene (Hvo1541). Transcripts for the chromosomal *glpK* and *gpdA1* genes are upregulated in the presence of glycerol. Transcript levels were derived by qRT-PCR as described in Materials and Methods. Calculations are based on the N-fold induction of transcription in the presence of Gly Glu MM compared to transcription in the presence of Glu MM. Results were normalized to the N-fold induction of the internal control, *ribL*. Experiments were performed in triplicate, and the means ± SD were calculated. (C) Chromosomal GK (*glpK*) and G3PDH (*gpdA1B1C1*) genes are under the control of a common promoter. An RT-PCR primer pair based on the 5' and 3' ends of *glpK* and *gpdC1*, respectively, was designed. Hi-Lo DNA markers and molecular sizes are indicated to the left. Total RNA from parent H26 was extracted and reverse transcribed to generate cDNA, which was used as a template for PCR (lane 1). RNA which had not undergone reverse transcription was used as a negative control template for PCR (lane 2).

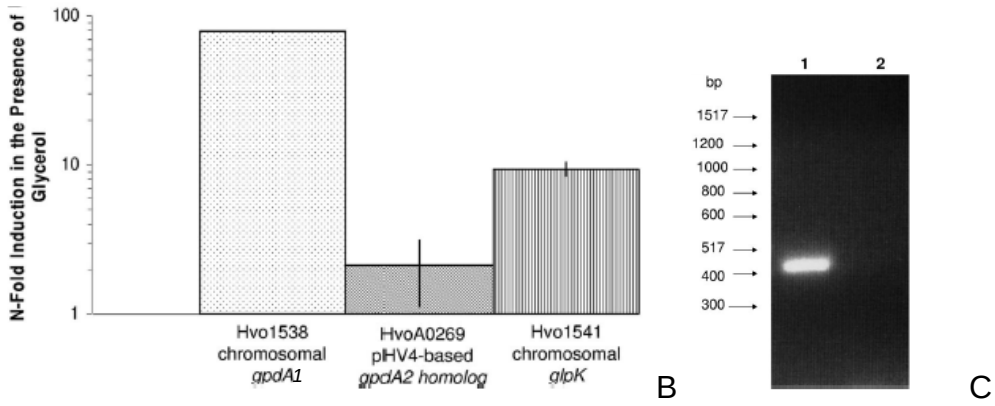


Figure 4-8. Continued.

# CHAPTER 5
# CHARACTERIZATION OF THE PRIMARY GLYCEROL METABOLIC OPERON IN THE HALOARCHAEON *Haloferax volcanii*

## Introduction

Glycerol is a highly abundant energy source in hypersaline environments as a result of leakage from and lysis of *Dunaliella sp.* which accumulate glycerol in molar quantities as a organic, osmotic solute (Ben Amotz and Avron, 1973b; Borowitzka and Brown, 1974; Wegmann et al., 1980; Elevi Bardavid et al., 2008). Glycerol is aerobically catabolized by heterotrophic community members by one of two routes: i) through GK and G3PDH or ii) through GDH and DHAK. In *H. volcanii*, glycerol metabolism proceeds solely through *glpK* encoding GK (Sherwood et al., 2009). In this study, the subsequent steps in glycerol metabolism was determined through biochemical and genetic characterization of two homologs of the bacterial, catalytic G3PDH subunit A. Both chromosomal *gpdA1* and pHV4-carried *gpdA2* of *H. volcanii* were investigated for their role, if any, in conversion of G3P to DHAP. This study confirms that G3P is metabolized primarily through *gpdA1* and provides evidence that the *H. volcanii* primary glycerol metabolic operon is under the control of a strong, glycerol-inducible *gpdA1* promoter ($P_{gpdA1}$, P1).

## Results and Discussion

### *H. volcanii* Glycerol Metabolic Operon is under the Control of an Inducible Promoter

In *H. volcanii*, *gpdC1* and *glpK* are linked at the transcriptional level (Sherwood et al., 2009). Due to the close chromosomal proximity of genes encoding a GK (*glpK*) to a G3PDH homolog (*gpdA1B1C*1), a putative non-GlpF glycerol facilitator protein (*glpX*), and bacterial PTS component Hpr homolog (*ptsH2*), the putative operon(s) of this

genomic region were investigated by performing a series of RT-PCRs. Primers were designed to amplify a portion of the coding region of neighboring genes *gpdA1* and *gpdB1* (13 bp overlap in coding sequence), *gpdB1* and *gpdC1* (3 bp overlap in coding sequence), *glpK* and *glpF* (4 bp intergenic region), and *glpF* and *ptsH2* (2 bp overlap in coding sequence) (Figure 5-1A). In each case, a single PCR product of expected size was detected (Figure 5-1B) and confirmed by DNA sequencing. No product was detected in the negative control reactions containing RNA as a template for PCR (Figure 5-1B). Thus, the genes encoded in the primary glycerol metabolic operon (*gpdA1B1C1glpKXptsH2*) are linked at the level of transcription (Figure 5-1B).

Although the primary glycerol metabolic operon (*gpdA1B1C1glpKXptsH2*) is transcriptionally-linked, the reasons for the significant differences in the levels of induction of *glpK*- and *gpdA1*-specific transcripts in the presence of glycerol (Figure 3-8 A) (Sherwood et al., 2009) remain to be determined. Possible explanations for the differences in abundance of *glpK*- and *gpdA1*-specific transcripts include: i) multiple promoter elements, ii) reduced transcription of *glpK* (which is distal relative to *gpdA1*) due to transcriptional polarity (Wek et al., 1987), and iii) differences in transcript susceptibility to degradation.

To determine if the differences in transcript induction was the existence of multiple promoter elements, transcriptional promoter-reporter fusion assays were performed using reporter constructs containing the 310-bp *gpdA1* and 354-bp *glpK* promoter DNA upstream of their translational start codons. These promoter regions were amplified, fused to the *H. alicantei bgaH*-based transcriptional reporter, and transformed into wild-type strain H26. Transcription of the promoter constructs was monitored by assay of β-

galactosidase activity of cells grown on various carbon sources. Using this approach, significant levels of transcription were detected for the *gpdA1* (38 to 310 mU·mg protein$^{-1}$) promoter construct compared to negative controls lacking promoter elements which were less than or equal to 8.1 mU·mg protein$^{-1}$ for all conditions tested (Table 5-1). The *gpdA1* promoter construct was highly inducible in glycerol medium [at least 7-fold up-regulated in cells grown on glycerol (± glucose) compared to glucose alone]. In contrast, transcription from the *glpK* promoter was weak and constitutive for all conditions tested (14 to 22 mU·mg protein$^{-1}$) (Table 5-1). The inducible *gpdA1* promoter was very strong compared to the weaker, non-glycerol-inducible *glpK* promoter for all conditions tested, except when cells were grown in glucose alone, for which it exhibited only slightly increased specific activity compared to the *glpK* promoter (38 mU·mg protein$^{-1}$ for $P_{gpdA1}$ compared to 22 mU·mg protein$^{-1}$ for $P_{glpK}$) (Table 5-1). It should be noted that when cells were grown on glycerol, the *gpdA1* promoter was relatively robust at driving expression of the heterologous *bgaH* reporter with activities greater than that of the *H. cutirubrum* rRNA P2 promoter (Table 5-1), used routinely for high-level production of proteins in *H. volcanii* (Kaczowka et al., 2005; Uthandi et al., 2010). Although the glycerol-responsive *gpdA1* promoter was not as inducible as the tryptophan-responsive *trpA* promoter (7-fold induction for $P_{gpdA1}$ versus 45-fold induction for $P_{trpA}$) (Table 5-1), the *gpdA1* promoter can serve as an alternative for experiments requiring differential gene regulation. In contrast, the *glpK* promoter was relatively weak (14-22 mU·mg protein$^{-1}$) at driving the expression of the heterologous *bgaH* reporter compared to the constitutive rRNA P2 promoter (230-260 mU·mg protein$^{-1}$) (Table 5-1). Overall, the data suggests that the *H. volcanii* glycerol metabolic operon is regulated by a tightly-controlled,

glycerol-inducible *gpdA1* promoter (P1) that drives the robust expression of the operon in the presence of glycerol.

**Glycerol Metabolism Proceeds Primarily through GpdA1**

Glycerol is metabolized solely through GK in *H. volcanii* (*glpK*, HVO_1541) (Sherwood et al., 2009). To analyze the subsequent step in glycerol catabolism, two genes encoding homologs of bacterial G3PDH subunit A, *gpdA1* (HVO_1538) and *gpdA2* (HVO_A0269), were deleted from the *H. volcanii* H26 genome using a markerless deletion strategy as previously described (Bitan-Banin et al., 2003; Allers et al., 2004). Subunit A of the G3PDH complex was targeted for gene knockout since this subunit is required for G3PDH activity in *E. coli* (Cole et al., 1988). The *gpdA1* and *gpdA2* gene deletions were confirmed by PCR, Southern Blot, and sequencing analysis (Figure 5-2). The resulting *gpdA1* mutant (KS12) was incapable of growth of glycerol minimal medium (Figure 5-3). In contrast, cells deficient in *gpdA2* (KS11) grew at a similar rate to wild type H26 on glycerol as the sole carbon source (Figure 5-3). The glycerol-dependent phenotype displayed by KS12 could be complimented by providing either *gpdA1* or *gpdA2 in trans*, under the control of the strong, constitutive *H. cutirubrum* rRNA P2 promoter (Figure 5-3). The ability of *gpdA2 in trans* to compliment cells deficient in *gpdA1* suggests that GpdA2 may be a functional isoform of GpdA1 whose intracellular levels are insufficient to impact glycerol metabolism.

To determine whether the difference in phenotype between the *gpdA* mutants was due to a difference in cellular levels, G3PDH activity was assessed in various strains. In parent H26, G3PDH activity was upregulated at least 2-fold when cells were grown in the presence of glycerol (± glucose) when compared to glucose alone (Table 5-2). Upon deletion of *gpdA1*, G3PDH activity was no longer induced by growth in the presence of

glycerol. This was evidenced by a 4-fold reduction in G3PDH activity of the *gpdA1* mutant KS12 compared to parent H26 during growth on glycerol and glucose. G3PDH activity in the *gpdA1* background was restored to parental levels by providing either *gpdA1* or *gpdA2 in trans*. A mutant deficient in *glpK* displayed a similar level of G3PDH activity compared to *gpdA1* when grown in minimal medium containing glycerol and glucose which could be complemented by providing *glpK in trans* (Table 5-2). The loss of activity in the *glpK* mutant suggests that G3P serves as the inducer of the chromosomal glycerol regulon, similar to *E. coli* (Hayashi and Lin, 1965). Deletion of *gpdA2* resulted in a slight, yet significant reduction in G3PDH activity compared to parent H26 when cells were grown in glycerol (± glucose) which could be fully complimented by providing *gpdA2 in trans* (Table 5-2). No activity was detected for negative controls containing either no substrate or boiled cell lysate. It is worth noting that similar to *E. coli* (Cole et al., 1988), GpdA is required for catalytic activity of the *H. volcanii* G3PDH complex based on the fact that activity was greatly reduced in *gpdA1*-deficient cells compared to parent H26 under all of the conditions tested (Table 5-2). Furthermore, *gpdA2* encodes a functional subunit of G3PDH based on the observed reduction in activity upon deletion of *gpdA2* (Table 5-2) and the ability of *gpdA2 in trans* to restore both growth phenotype (Figure 5-3) and G3PDH specific activity to parental levels in a *gpdA1*-deficient background (Table 5-2).

**Distribution of Archaeal GpdA Homologs**

Interestingly, many haloarchaeal genomes encode two *gpdA* genes, although these homologs have marked differences from the *H. volcanii gpdA* genes. Similar to *H. volcanii*, other haloarchaeal *gpdA1* genes often cluster chromosomally with additional glycerol metabolic genes including *gpdBC*, *glpK*, and a putative glycerol facilitator (*glpF*

or *glpX*) (Figure 3-2). However, unlike *H. volcanii gpdA2* which is pHV4-carried and appears to be co-transcribed with *gpdB2C2, gpdA2* from other haloarchaea is chromosomally-located and does not cluster with additional *gpdBC* subunits (Figure 5-4). Furthermore, unlike *H. volcanii* GpdA1 and GpdA2 which are equal in amino acid length, other haloarchaeal GpdA2s appear to have undergone a C-terminal truncation event. Specifically, these truncated GpdA2s are missing the C-terminal bacterioferritin-associated ferredoxin (BFD)-like [2Fe-2S] center common to GpdA proteins (Figure 5-5). Although the physiological role of BFD [2Fe-2S] remains unclear, it is thought to be a general redox and/or regulatory component involved in the iron storage or mobilization functions of bacterioferritin in bacteria (Garg et al., 1996). Despite differences with protein length and genomic organization, haloarchaeal GpdA homologs cluster phylogenetically (Figure 5-4). Within the haloarchaeal phylogenetic node, GpdA1 and GpdA2 are separated into distinctive lineages for which the atypical *H. volcanii* GpdA2 is the only exception to date (Figure 5-4). GpdA homologs are also found in other Euryarchaeota (*Thermoplasmata*) as well as Crenarchaeota (*Thermoprotei*), although additional GpdBC subunits are absent from these archaea (Figure 5-4). The absence of these additional subunits may be explained by the fact that glycerol is not commonly encountered as a primary carbon source by these microorganisms. Similar to GlpK, GpdA is noticeably absent from methanogenic archaea and other archaea who are unable to metabolize glycerol as the primary carbon source.

**Distribution of Archaeal Hpr Homologs and Putative Glycerol Facilitator Proteins**

Along with *glpK* and *gpdA1B1C1*, the glycerol metabolic operon of *H. volcanii* was also found to encode a homolog of the PTS general carrier protein Hpr (*ptsH2*) as well as a putative glycerol facilitator protein (*glpX*). Interestingly, *H. volcanii* contains three

homologs of Hpr, each of which clusters on the genome with additional PTS homologs (Figure 3-1) and has conserved histidine-15 and serine-46 residues (Figure 5-6). In *B. subtilis,* histidine-15 is the phosphorylation site of the phosphorelay reaction mediating sugar translocation and serine-46 is the regulatory residue which serves as a co-repressor for CcpA, respectively.

In addition to Hpr, a putative glycerol facilitator (*glpX*) is also encoded within the glycerol metabolic regulon of *H. volcanii*. Although this putative glycerol facilitator does not exhibit sequence homology with characterized glycerol facilitator proteins, it is distributed throughout haloarchaea and often clusters chromosomally with glycerol metabolic enzymes (Figure 3-2). GlpX may function as a glycerol facilitator based on genomic clustering and the presence of seven transmembrane domains as predicted by the SOSUI server (Table 5-3, Figure 5-7) (Hirokawa et al., 1998).

## Conclusion

This study reports the organization and regulation of the primary glycerol metabolic operon of *H. volcanii*. RT-PCR analyses demonstrated that *gpdA1B1C1* encoding G3PDH, *glpK* encoding GK, *glpF* encoding a putative glycerol facilitator and *ptsH2* encoding a homolog of bacterial PTS general carrier protein Hpr are transcriptionally linked. Furthermore, transcription of this glycerol metabolic operon proceeds through a glycerol-inducible *gpdA1* promoter as evidenced by a transcriptional promoter-reporter system.

The *H. volcanii* genome encodes two homologs of GpdA or GlpA, the catalytic subunit of bacterial G3PDH. Phenotypic and biochemical characterization of mutants deficient in either chromosomal *gpdA1* or pHV4-carried *gpdA2* has demonstrated that G3P is primarily catabolized through GpdA1 in *H. volcanii*. Although the *gpdA1* mutant

strain was unable to grow on glycerol as a sole carbon source, this phenotype could be restored by providing either *gpdA1* or *gpdA2 in trans*, suggesting that GpdA2 encodes a functional G3PDH isoform. Furthermore, G3PDH activity is glycerol-inducible, and this activity is reduced to basal levels in both *glpK* and *gpdA1* mutant strains when grown in the presence of glycerol. The dramatic loss of enzyme activity in *gpdA1*-deficient cells could be restored to parental levels by providing either *gpdA1* or *gpdA2 in trans*, confirming that the majority of G3PDH enzyme activity under glycerol-rich conditions derives from GpdA1. These results also suggest that G3P is needed for induction of G3PDH based on the reduced level of G3PDH activity in the *glpK* mutant. The results presented here provide the first genetic and biochemical characterization of a G3PDH in haloarchaea. Overall, the results not only shed light on glycerol metabolism in *H. volcanii*, but also add to the understanding of central metabolic pathways of haloarchaea.

Table 5-1. Transcription of a *bgaH* β-galactosidase reporter gene from the genomic region upstream of *gpdA1, glpK* and *trpA*.

| | β-Galactosidase Specific Activity (mU·mg protein$^{-1}$)[a] | | | | |
|---|---|---|---|---|---|
| Carbon Source | *gpdA1* (310 bp) | *glpK* (354 bp) | *trpA* (321 bp) | *rrnA* (551 bp) | None (SD only) |
| Gly | 310 ± 5 | 16 ± 2 | n.d. | 260 ± 10 | 8.1 ± 0.1 |
| Glu | 38 ± 0.001 | 22 ± 0.7 | n.d. | 250 ± 7 | 7.3 ± 0.9 |
| Gly Glu | 280 ± 8 | 14 ± 2 | n.d. | 260 ± 7 | 8.1 ± 0.05 |
| Suc Trp | n.d. | n.d. | 1700 ± 50 | 230 ± 30 | 7.4 ± 0.07 |
| Suc | n.d. | n.d. | 38 ± 6 | 260 ± 20 | 8.0 ± 0.08 |

[a]β-galactosidase activities were determined from the lysate of cells carrying transcriptional fusion constructs of promoters grown to log-phase in MM with Gly, Glu, Gly Glu, Suc Trp, and Suc as indicated. Promoter fusions included the start codon and genomic region (indicated in bp) immediately upstream of each target gene. Experiments were performed in triplicate, and the means ± SD were calculated. Abbreviation: n.d. not determined.

Table 5-2. G3PDH activity in various glycerol metabolic mutants.

| Glycerol-3-Phosphate Dehydrogenase Specific Activity (mU·mg protein$^{-1}$)[a] | | | | | | | | |
|---|---|---|---|---|---|---|---|---|
| Carbon Source | H26 | Δ *gpdA1* | Δ *gpdA2* | Δ *glpK* | Δ *gpdA1* + *gpdA1* | Δ *gpdA1* + *gpdA2* | Δ *gpdA2* + *gpdA2* | Δ *glpK* + *glpK* |
| Gly | 76 ± 10 | no growth | 55 ± 6 | no growth | 70 ± 9 | 67 ± 3 | 73 ± 9 | 72 ± 8 |
| Glu | 28 ± 4 | 19 ± 1 | 24 ± 2 | 19 ± 4 | 26 ± 6 | 28 ± 5 | 28 ± 5 | 27 ± 3 |
| Gly Glu | 67 ± 10 | 18 ± 1 | 47 ± 6 | 21 ±1 | 68 ± 9 | 67 ± 4 | 72 ± 7 | 67 ± 5 |

[a] G3PDH activities were determined from the lysate of cells deficient in genes encoding glycerol metabolic enzymes GlpK, GpdA1 or GpdA2 as well as parent H26 and strains containing *glpK*, *gpdA1* or *gpdA2 in trans*. Cells were grown to log-phase in MM with Gly, Glu and Gly Glu as indicated. Experiments were performed in triplicate, and the means ± SD were calculated.

Table 5-3. Predicted locations of transmembrane domains of *H. volcanii* GlpX.

| TM Helix Number | N-terminal Residue | Primary Sequence | C-terminal Residue | TM Helix Type | Length (AA) |
|---|---|---|---|---|---|
| 1 | Ala-4 | AFALQIPVIGVSTERFIVLLLAA | Ala-26 | 1º | 23 |
| 2 | Leu-26 | LGALPSFIFTGFVVLLGETAGIV | Val-58 | 1º | 23 |
| 3 | Ile-123 | ITYAFGTQPDILAVGGLFGVLGL | Leu-145 | 2º | 23 |
| 4 | Phe-157 | PLDSVALSVMTTAFIARIAFGYP | Phe-179 | 2º | 23 |
| 5 | Ala-230 | AGILGGWTWLITESFFLAYGISA | Ala-252 | 1º | 23 |
| 6 | Ala-282 | AAPMVGGSEPLIIVAAAVGGLIG | Gly-304 | 2º | 23 |
| 7 | Met-328 | MSITIYSLLIGVLFLLGVIPNSA | Ala-350 | 1º | 23 |

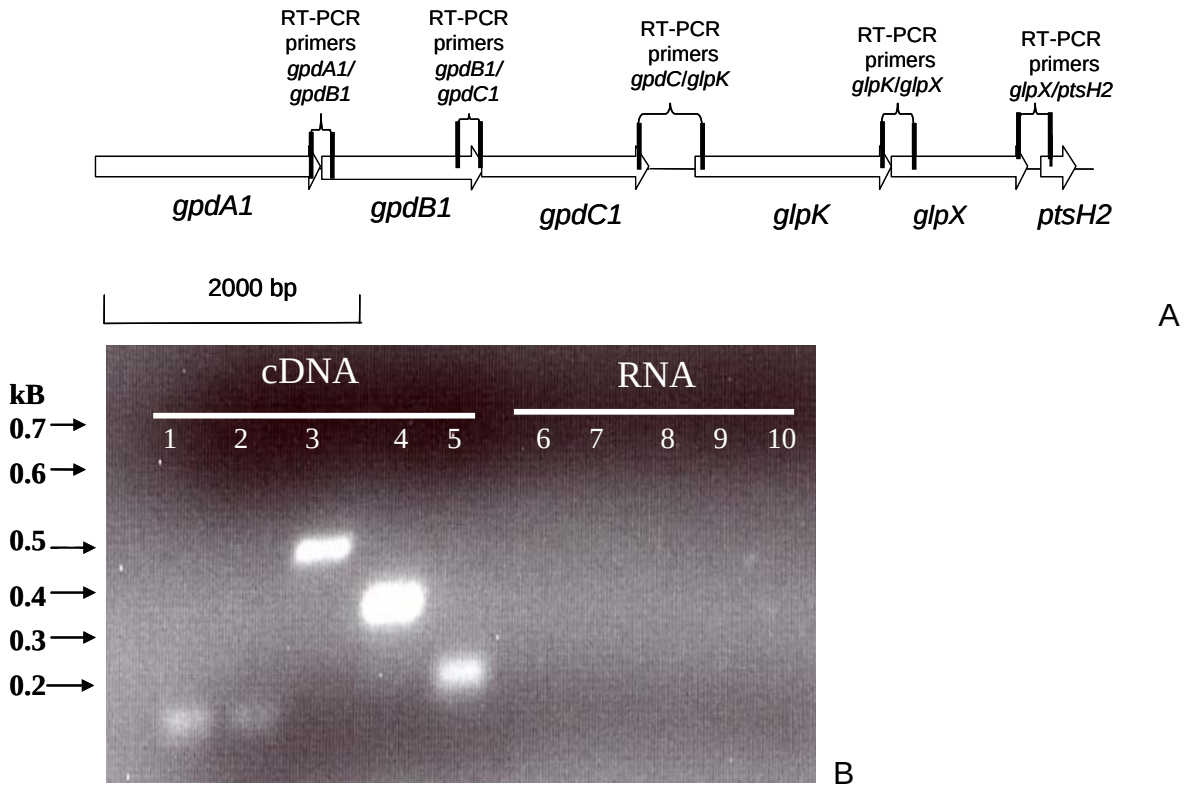


Figure 5-1. Genomic organization of the primary glycerol metabolic operon in *H. volcanii*. A) Schematic representation of the chromosomally- encoded *gpdA1B1C1glpKXptsH2* glycerol metabolic operon and the related pHV4-carried *gpdA2B2C2* operon on the *H. volcanii* genome and location of annealing sites (represented as vertical lines) for (q)RT-PCR primers. B) RT-PCR reveals genes within the *gpdA1B1C1glpKXptsH2* are co-transcribed. Total RNA from parent H26 was extracted and reverse transcribed to generate cDNA, which was used as a template for PCR amplifying the 3' and 5' ends of: *gpdA1* and *gpdB1* (lane 1), *gpdB1* and *gpdC1* (lane 2), *gpdC1* and *glpK* (lane 3), *glpK* and *glpF* (lane 4) and *glpF* and *ptsH2* (lane 5), respectively. RNA which had not undergone reverse transcription was used as a negative control template for each PCR reaction (lanes 6-10). 100 bp Quick Load DNA markers and molecular sizes are indicated on left.

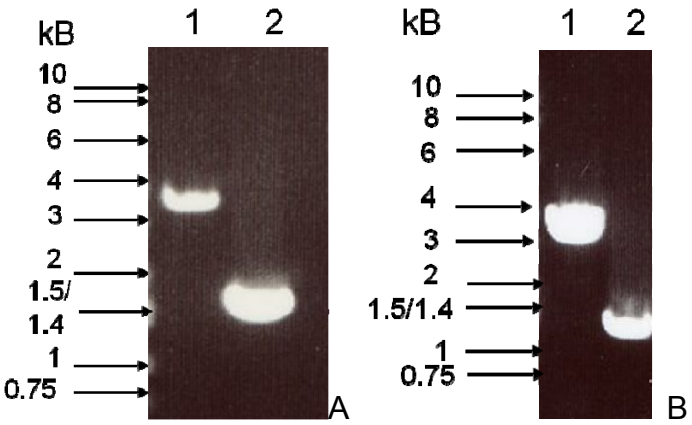


Figure 5-2. PCR and Southern blot confirmation of *H. volcanii gpdA1* and *gpdA2* mutant strains KS12 (H26 ∆*gpdA1*) and KS11 (H26 Δ*gpdA2*). (A) Confirmation of the *gpdA1* mutant KS12 by PCR. Primer pairs that annealed outside the genomic region cloned in suicide plasmid pJAM2695 were used for confirmation of the *gpdA1* gene knockout by PCR. Hi-Lo DNA markers and molecular masses are indicated on left. Genomic DNA from the following strains served as template: Lane 1. Parent strain H26, Lane 2. KS12 (H26 Δ*gpdA1*). (B) Confirmation of the *gpdA2* knockout KS11 by PCR. Primer pairs that annealed outside the genomic region cloned in suicide plasmid pJAM2697 were used for confirmation of the *gpdA2* gene knockout by PCR. Hi-Lo DNA markers and molecular masses are indicated on left. Genomic DNA from the following strains served as template: Lane 1. Parent strain H26, Lane 2. KS11 (H26 Δ*gpdA2*). (C) Southern blot confirmation of the *gpdA1* knockout in strain KS12 (H26 Δ*gpdA1*). Genomic DNA was digested with MluI and hybridized with a DIG-labeled probe specific for *gpdA1*. The following strains served as the source of genomic DNA: Lane 1. Parent strain H26, Lane 2. KS12 (H26 Δ*gpdA1*). (D) Southern blot confirmation of the *gpdA2* knockout in strain KS11 (H26 Δ*gpdA2*). Genomic DNA was digested with ClaI and BpuI and hybridized with a DIG-labeled probe specific for *gpdA2*. The following strains served as the source of genomic DNA: Lane 1. Parent strain H26, Lane 2. KS11 (H26 Δ*gpdA2*).

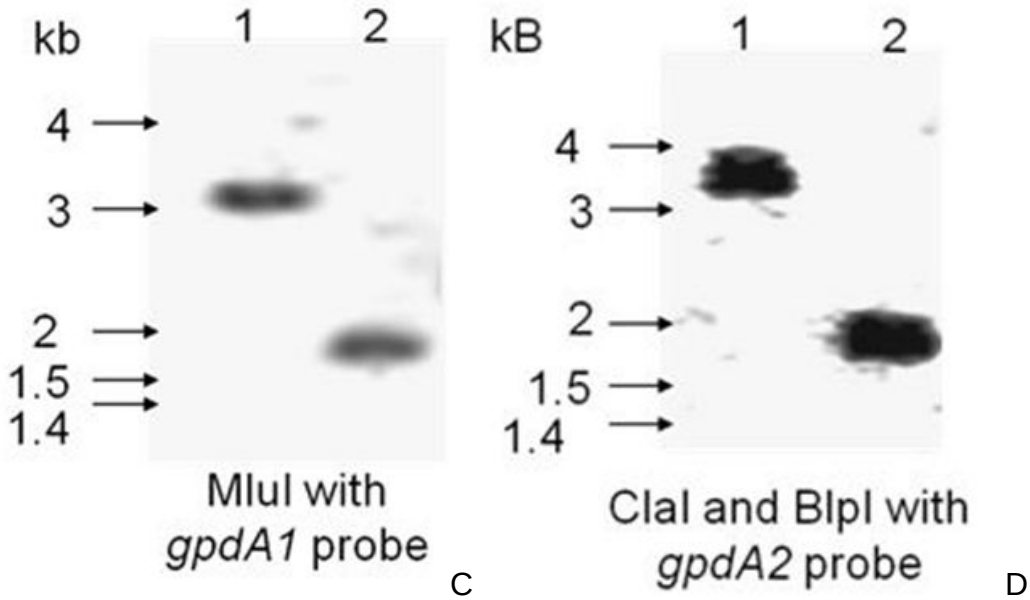


Figure 5-2. Continued

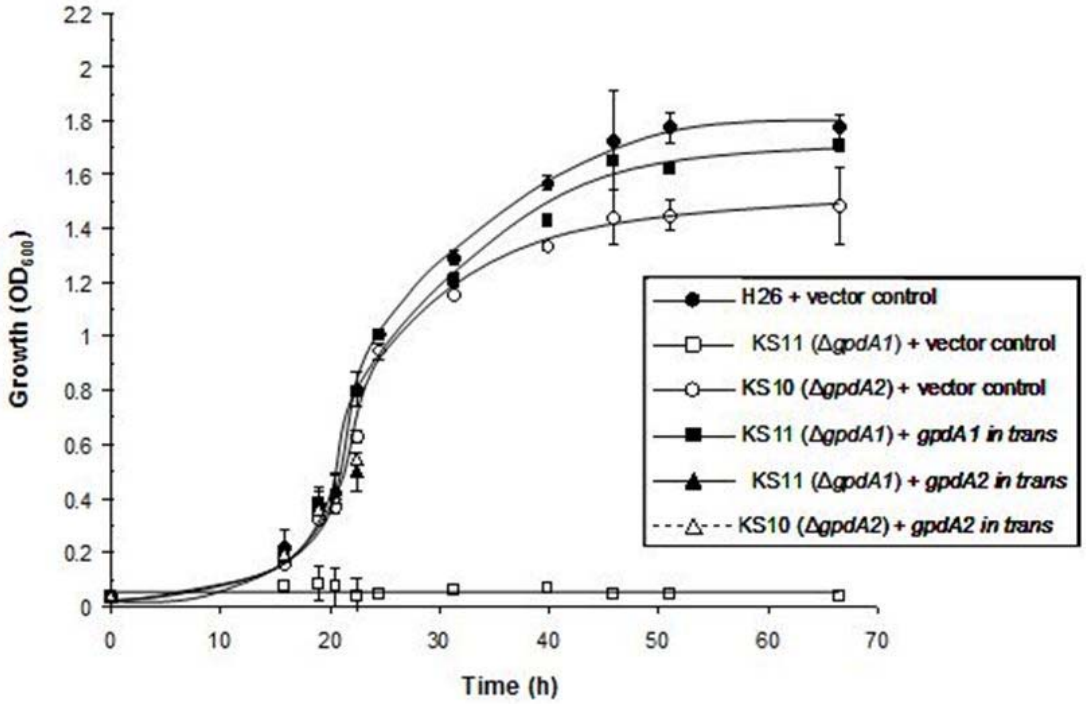


Figure 5-3. Glycerol is primarily catabolized through GpdA1 and not GpdA2 in *H. volcanii*. The parent strain H26 and GpdA2-deficient strain KS10 exhibit similar growth rates and cell yields when grown in Gly MM. In contrast, GpdA1-deficient strain KS11 is unable to utilize glycerol as a sole carbon source. However, the KS11 phenotype could be restored to parental levels by providing either *gpdA1* or *gpdA2* in trans. Growth at 42°C (200 RPM) was monitored by an increase in $OD_{600}$, where 1 U was equivalent to approximately $10^9$ CFU per ml for all strains. Experiments were performed in triplicate, and the means ± SD were calculated. Cell growth and carbon utilization levels are indicated. For simplicity, H26, KS10 and KS11 without vector control grown in Gly MM was not included in Figure 5-3, however, these strains exhibited identical growth rates and cell yields as those strains with vector control shown in Figure 5-3.

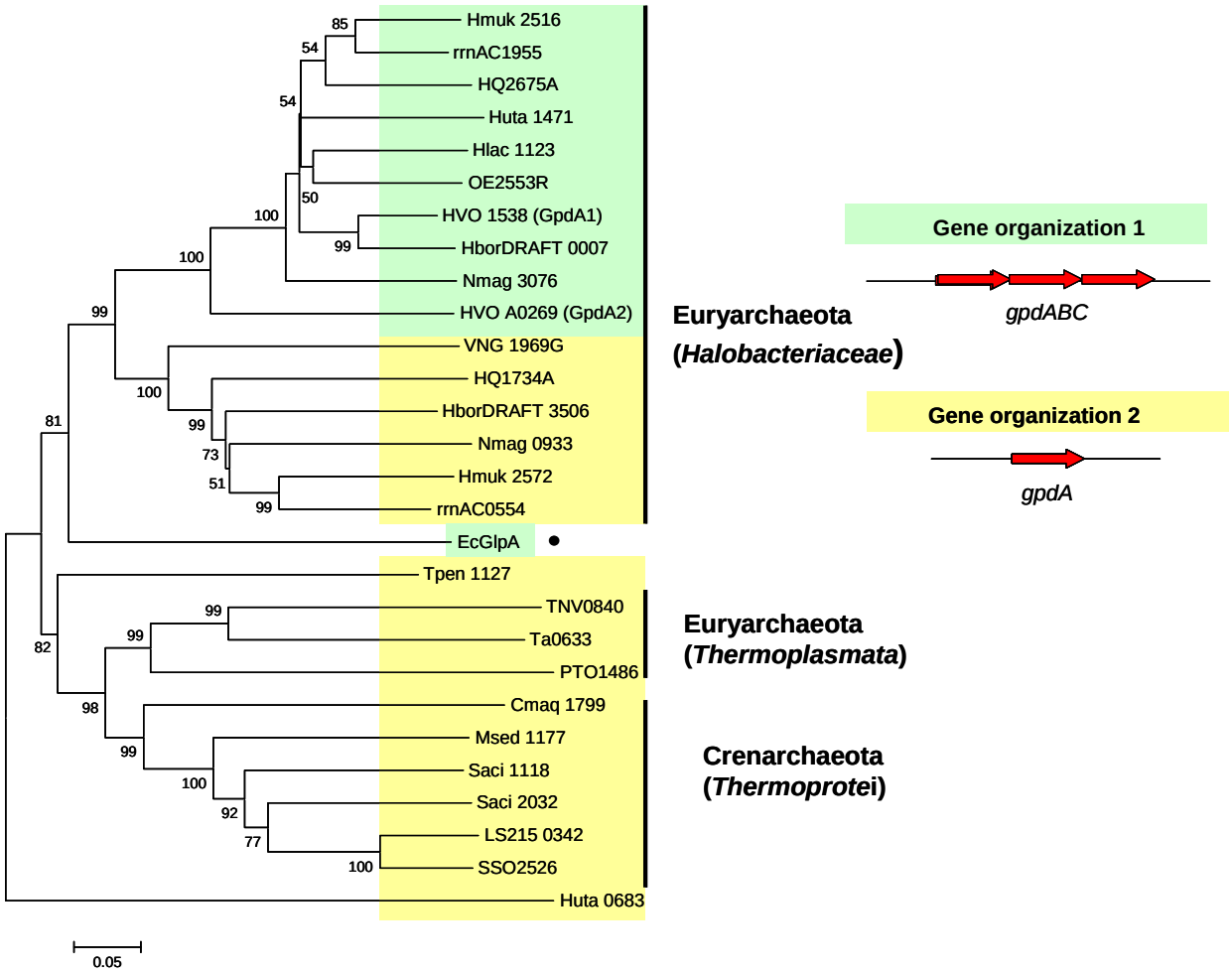


Figure 5-4. Phylogenetic distribution and genomic organization of GpdA homologs in Archaea and *E. coli*. Protein sequences were retrieved using the NCBI database and aligned using CLUSTAL W (Thompson et al., 1994) after N- and C-terminal trimming. Pairwise comparisons were performed between sequences and mean genetic distance was evaluated using p-distance (gaps were analyzed using pairwise deletion). The best neighborhood-joining tree was then constructed using MEGA 4.0. Bootstrap values are indicated at the internal nodes and were obtained by performing 1,000 replicates. Biochemically characterized proteins are indicated by ●. Genomic organizations of archaeal *gpdA* are indicated to the right. Two major gene neighborhood organizations for *gpdA* are noted: i) Gene Organization I (*gpdA* members belonging to this organization are highlighted in green) in which *gpdA* is encoded in the operon *gpdABC* and ii) Gene Organization II (*gpdA* members belonging to this organization are highlighted in yellow) in which *gpdA* does not cluster on the genome with *gpdBC*. Accession numbers for protein sequences are included in Chapter 2.

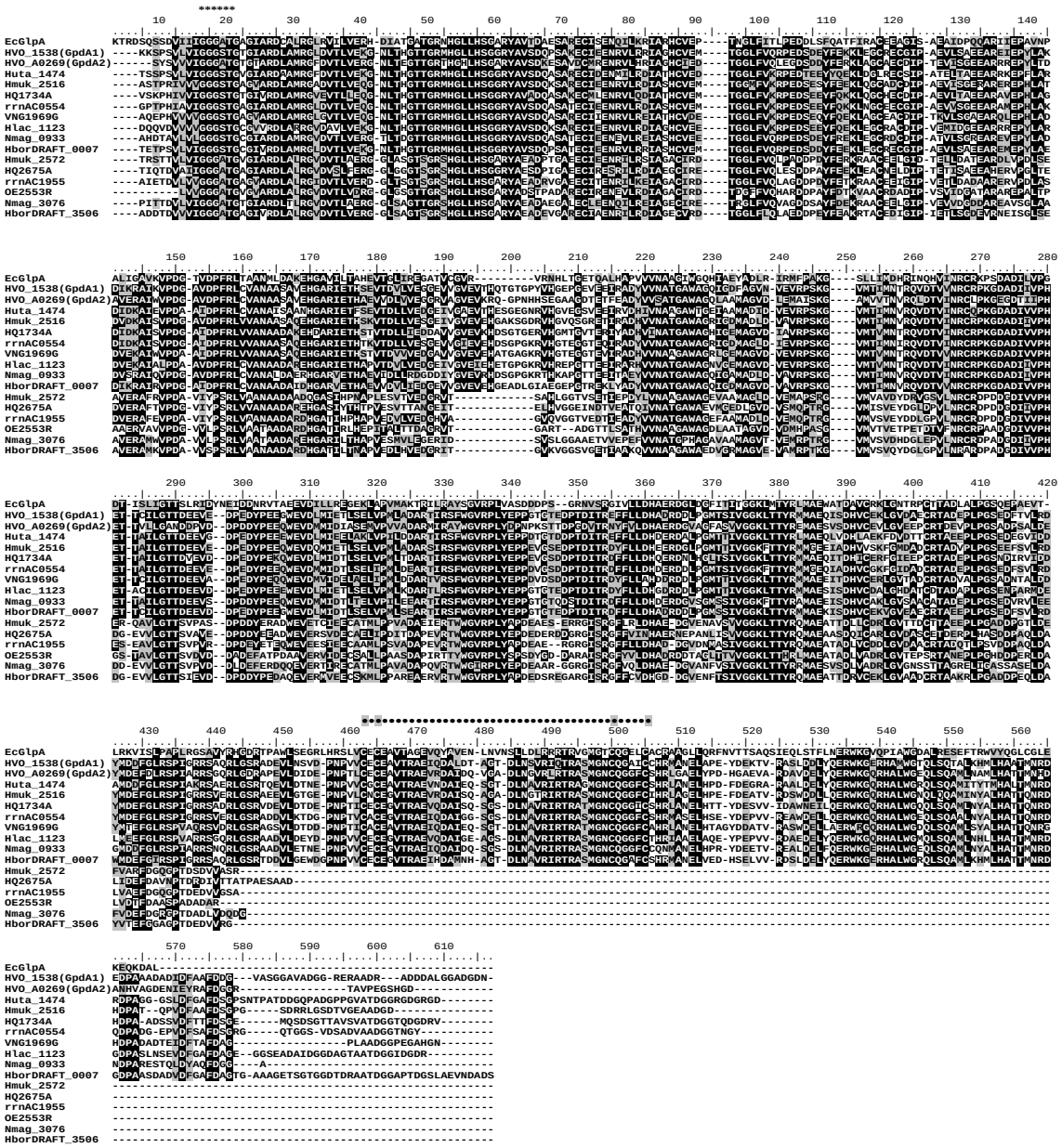

Figure 5-5. Many haloarchaeal genomes encode a full-length GpdA1 and a C-terminally truncated GpdA2. *H. volcanii* GpdA1 and GpdA2 were aligned with *E. coli* EcGlpA along with additional haloarchaeal GpdA1 and GpdA2 proteins using CLUSTAL W (Thompson et al., 1994). The N-terminal methionine was trimmed for alignment purposes. The conserved N-terminal NAD$^+$ binding domain typical of EcGlpA (GXGXXG) is indicated with ***** above the binding motif as predicted by alignments with previously characterized GpdA proteins. The BFD-like [2Fe-2S] motif ($CXCX_{34}CX_4C$) is indicated by ● placed above the sequence containing the binding motif. The [2Fe-2S]-coordinated cysteine residues within the binding motif are indicated as ● Accession numbers for protein sequences obtained are listed in Chapter 2.

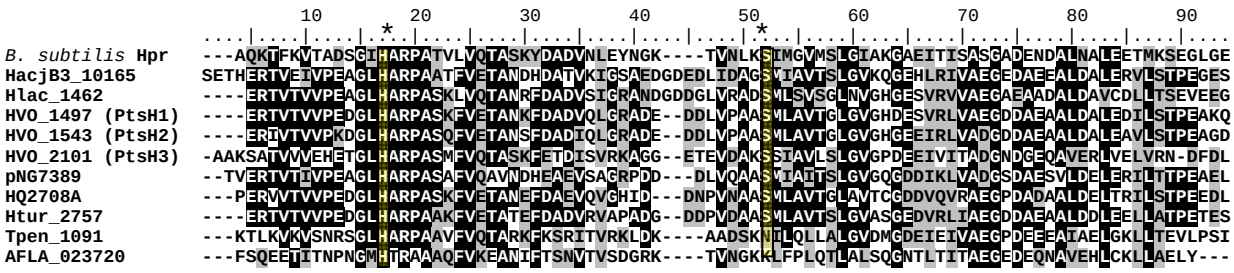


Figure 5-6. *B. subtilis* Hpr phosphorylative residues histidine-15 and serine-46 are conserved in haloarchaeal Hpr homologs. Phosphorylative residues histidine-15 and serine-46 are highlighted and additionally are indicated by *. Protein sequences were retrieved using the NCBI database and aligned using CLUSTAL W (Thompson et al., 1994) after N- and C-terminal trimming. Accession numbers for protein sequences are as follows: *B. subtilis* Hpr (CA31317.1); *H. jeotgali* HacjB3_10165 (YP_003737208); *H. lacusprofundi* Hlac_1462 (YP_002566120.1); *H. volcanii* HVO_2101 (YP_003536125.1), HVO_1497 (YP_003535546.1), HVO_1543 (YP_003535590.1); *H. marismortui* pNG7389 (YP_134785.1); *H. walsbyi* HQ2708A (YP_658421.1); *H. turkmenica* Htur_2757 (YP_003404303.1); *T. pendens* Tpen_1091 (YP_920493.1); *Aspergillus flavis* AFLA_023720 (XP_002373883.1); and *E. coli* Hpr (NP_416910.1).

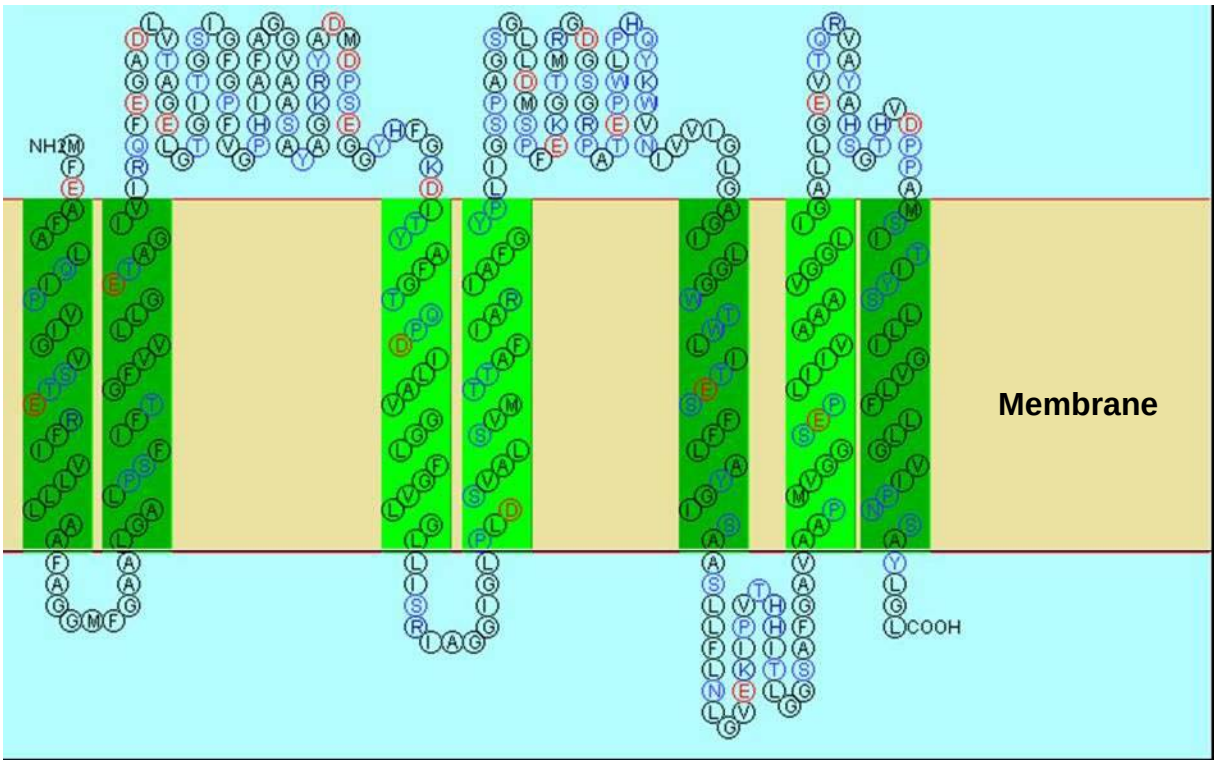


Figure 5-7. GlpX is a putative glycerol facilitator protein based on the presence of predicted transmembrane domains. The SOSUI server predicts seven transmembrane helices for *H. volcanii* GlpX by examination of the amphilicity of the primary amino acid sequence.

# CHAPTER 6
# GlpR REPRESSES FRUCTOSE AND GLUCOSE METABOLIC ENZYMES AT THE LEVEL OF TRANSCRIPTION IN THE HALOARCHAEON *Haloferax volcanii*

## Introduction

The archaeal basal transcriptional machinery closely resembles the eukaryotic RNA polymerase (RNAP) II apparatus. Along with a multi-subunit RNAP (Zillig et al., 1979), archaea encode two basal transcription factors, TBP and TFB, which are homologues of the eukaryotic TBP and general transcription factor TFIIB, respectively (Soppa, 1999; Bell and Jackson, 2001). Although archaeal transcriptional components are fundamentally eukaryotic-like in nature (Reeve et al., 1997), the majority of candidate transcriptional regulators are homologous to bacterial activators and repressors (Kyrpides and Ouzounis, 1999; Aravind and Koonin, 1999). Only a few archaeal candidate regulators resemble eukaryotic gene-specific transcription factors, one of the best characterized of which is GvpE, an activator of gas vesicle biosynthesis in haloarchaea which resembles the eukaryotic basic leucine zipper proteins (Offner and Pfeifer, 1995; Krüger et al., 1998). While bioinformatics analysis predicts many candidate archaeal regulators, only a limited number have been characterized at the molecular level, most of which are from hyperthermophiles (Lee et al., 2003; Xie and Reeve, 2005; Bell, 2005; Kanai et al., 2007; Fiorentino et al., 2007; Keese et al., 2010). Molecular data pertaining to haloarchaeal transcriptional regulation, specifically regulators of carbon utilization, are severely limited. Only a few global regulators, namely transcription factors (Facciotti et al., 2007; Coker and DasSarma, 2007; Schmid et al., 2009), have been implicated in regulating sugar metabolism in haloarchaea. Specifically, in *H. salinarum*, pairs of general transcription factors TBP and TFB control gene clusters (Facciotti et al., 2007; Coker and DasSarma, 2007), and transcription

factor TrmB regulates diverse metabolic pathways in response to nutrient limitation (Schmid et al., 2009). No transcriptional regulators of sugar metabolism have been characterized in the model haloarchaeon *H. volcanii* to date, although homologs of transcription factors can be predicted based on primary sequence. Furthermore, DeoR/GlpR-type regulators have yet to be characterized in archaea.

In this study, biochemical and genetic approaches were used to characterize GlpR, a putative transcriptional regulator of glycerol and/or sugar metabolism in *H. volcanii*. This study presents evidence that GlpR is not only autoregulatory, but also regulates transcription of the downstream *pfkB* gene encoding PFK as well as a distant chromosomal KDGK gene *kdgK1*. Taken together, these results provide the first example of a DeoR/GlpR-type repressor protein that controls key enzymes of sugar metabolism in haloarchaea, and allow valuable insight into haloarchaeal metabolic transcriptional regulation.

## Results and Discussion

### Identification of GlpR as a Putative Repressor of Metabolic Enzymes

In order to provide insight into the regulation of haloarchaeal central metabolism, the *H. volcanii* genome (Hartman et al., 2010) was searched for ORFs encoding proteins with DNA binding domains that clustered near sugar metabolic operons. One such ORF (HVO_1501; designated *glpR*), when searched against the NCBI protein database, clustered with the DeoR/GlpR family of transcriptional regulators of sugar metabolism (COG1349) (Figure 6-1A). The DeoR/GlpR protein family is widespread among bacteria and its members often serve as transcriptional repressors (Munch-Petersen and Jensen, 1990; Weissenborn et al., 1992; Zeng and Saxild, 1999; Ray and Larson, 2004; Barrière et al., 2005; Haghjoo and Galán, 2007) or activators (Zhu and

Lin, 1986; Gaurivaud et al., 2001) of either sugar or nucleoside metabolism. DeoR/GlpR-type repressors are comprised of approximately 250 amino acids, possess a helix-turn-helix DNA-binding motif near the N-terminus and generally bind a sugar phosphate effector molecule of the relevant metabolic pathway in the C-terminal portion of the protein which can also contain oligomerization domains (Zeng et al., 1996). In *H. volcanii* as well as in some haloarchaea and many Gram-positive bacteria, *glpR* clusters on the genome with *pfkB* encoding PFK (Figure 6-1B), a key enzyme of fructose metabolism in haloarchaea such as *H. volcanii* (Johnsen et al., 2001; Falb et al., 2008). Dendrogram analysis revealed that *H. volcanii* GlpR clusters to the DeoR/GlpR family of transcriptional regulators with closest relationship to uncharacterized proteins of haloarchaea and Firmicutes (Figure 6-1B and Figure 6-1C). This result suggested that GlpR may be involved in regulating sugar metabolic enzymes at the level of transcription in *H. volcanii* and was thus targeted for further analyses.

**Transcripts Encoding GlpR and PFK are under the Control of a Common Promoter and are Reduced in the Absence of Fructose**

In haloarchaea, PFK is involved in the metabolism of fructose through a modified Embden–Meyerhof–Parnas (EMP) pathway (Falb et al., 2008). Due to the close proximity of *glpR* and *pfkB* on the chromosome (4-bp overlap in coding sequence) (Figure 6-2A), it was investigated whether these genes were co-transcribed in an operon. RT-PCR was performed using primers designed to amplify a portion of each coding region (Figure 6-2A). A single PCR product of expected size (0.2 kb) was detected using cDNA as a template for PCR (Figure 6-2B). The primer specificity was confirmed by DNA sequencing. No product was detected in the negative control

reaction containing RNA as a template for PCR (Figure 6-2B). Thus, *glpR* and *pfkB* are linked at the level of transcription.

Since *glpR* and *pfkB* are co-transcribed and PFK activity is largely fructose-inducible and to some extent glucose-inducible in haloarchaea (Johnsen et al., 2001), it was investigated whether this regulation was controlled at the level of *pfkB*-transcript and whether *glpR* was also induced by sugars. RNA was extracted from parent H26 grown in minimal medium supplemented with different carbon sources including fructose, glucose, glycerol, and various combinations thereof, and was subjected to qRT-PCR using primers specific for the 200-bp coding region of *glpR* and *pfkB* (Table 2-8). Quantification was performed for each transcript. The internal standard, ribosomal protein L10 gene (*ribL)* transcript, was chosen based on previous use (Brenneis et al., 2007) and confirmation by qRT-PCR that the N-fold induction of transcripts specific for *ribL* was close to 1.0 when parent H26 was grown in minimal medium. Using this approach, transcripts were found to be up-regulated for both *glpR* (> 20 ± 7-fold) and *pfkB* (> 10 ± 3-fold) in the presence of fructose regardless of glycerol supplementation compared to glycerol alone (Figure 6-2C). Transcripts for *glpR* were also up-regulated (> 10 ± 4-fold) during growth on glucose regardless of glycerol supplementation compared to glycerol alone (Figure 6-2C). Thus, the data reveal that *glpR* and *pfkB* are co-transcribed from a common promoter and that the transcript levels of this operon are increased by fructose and, to a lesser extent, by glucose. These results are consistent with the observed sugar-dependent alterations in PFK activity for *H. saccharolyticus* (Johnsen et al., 2001), in which the addition of fructose to peptide-rich media stimulated

the level of PFK activity, and suggest that PFK is regulated at the level of transcription in haloarchaea.

**GlpR Represses PFK Transcription in the Absence of Fructose**

To analyze the role of GlpR in regulating sugar metabolism, the *glpR* gene (HVO_1501) was targeted for knockout in *H. volcanii* to generate *glpR* mutant strain KS8. Gene deletion was confirmed by PCR, Southern blotting, and sequencing analysis (Figure 6-3). qRT-PCRs were used to compare transcript levels of KS8 to parent strain H26 on various carbon sources. Using this approach, a *pfkB*-specific transcript was found to be significantly increased by the *glpR* knockout (10 to 12-fold) compared to parent H26 when cells were grown in the absence of fructose (in Gly MM) (Figure 6-2D). The abundance of *pfkB*-specific transcript in the presence of glycerol was restored to wildtype levels at least in part by providing a copy of *glpR in trans*, thus, ruling out polar effects of the markerless deletion of *glpR* on the *glpR-pfkB* operon (Figure 6-2D). In contrast to growth on glycerol alone, the *glpR* knockout had little if any impact on *pfkB*-transcript levels when cells were grown in the presence of fructose with or without glycerol (Figure 6-2D). Transcript levels remained high for *pfkB* in fructose-containing media for all strains analyzed (Figure 6-2D) and were not significantly altered by the *glpR* mutation (Figure 6-2D). Thus, while GlpR was required for repression of *pfkB*-specific transcripts in glycerol minimal medium, GlpR was not needed for the high-levels of *pfkB*-transcript present when cells were grown on fructose.

Based on the qRT-PCR findings showing that GlpR may serve as a repressor of *pfkB*-specific transcription in the absence of fructose, PFK activity was tested in both parent and *glpR*-deficient strains to determine if enzyme activity was altered. Consistent with the qRT-PCR results, PFK activity was increased in ‘wild-type’ cells grown in media

supplemented with fructose (versus glycerol alone) (Figure 6-4). Also consistent with the qRT-PCR results, PFK specific activity was significantly increased by the *glpR* knockout (2-fold compared to parent and *glpR*-complemented strains) when cells were grown on media with glycerol alone (Figure 6-4). Deletion of *glpR* also resulted in a 1.5-fold increase in PFK activity compared to parent and *glpR*-complemented strains when cells were grown in the presence of both fructose and glycerol (Figure 6-4). In contrast to media with glycerol (± fructose), PFK activity was decreased during growth on fructose by deletion of *glpR* (Figure 6-4). The reason for this latter finding remains to be determined but does not appear to be at the level of transcription based on the qRT-PCR results.

The PFK activity of *H. volcanii* was also measured after growth on peptide rich YPC medium ± fructose or glucose. Similar to minimal media, PFK activity was reduced when YPC was not supplemented with hexose sugars (Figure 6-5). GlpR, however, was not required for this decrease, which is in contrast to the GlpR-dependent reduction in PFK activity observed when sugars were excluded from glycerol minimal medium (Figure 6-4 and Figure 6-5). It should be noted that the range of PFK activity values determined for the *H. volcanii* strains under the various conditions (140 to 650 mU·mg protein$^{-1}$) was in agreement with PFK activities reported for other haloarchaea [22 mU·mg protein$^{-1}$ for *H. saccharolyticus* (Johnsen et al., 2001) and 1,300 mU·mg protein$^{-1}$ for *H. vallismortis* (Rangaswamy and Altekar, 1994) in peptide media with 25 - 28 mM fructose].

To determine whether the *glpR-pfkB* operon is regulated by GlpR at the level of transcription: i) the 188-bp genomic region upstream of the start codon of *glpR* was

fused to the coding region of the *H. alicantei bgaH* reporter and ii) the β-galactosidase activity of this reporter was monitored in parent and *glpR* mutant strains grown on various carbon sources. Using this approach, significant and comparable levels of reporter activity were detected for both parent and *glpR* mutant strains when cells were grown in the presence of fructose, regardless of glycerol supplementation (Table 6-1). Under these conditions, the β-galactosidase specific activity measured for the *glpR-pfkB* promoter was 25 to 34 mU·mg protein$^{-1}$ compared to the negative controls which lacked promoter elements that were less than or equal to 12 mU·mg protein$^{-1}$ for all conditions tested (Table 6-1). In contrast, when cells were grown on glycerol alone, the promoter activity of the *glpR-pfkB* operon was reduced in parent strain H26 to levels comparable to the vector control, while deletion of *glpR* increased promoter activity to levels similar to growth on fructose (Table 6-1). Overall, the data obtained with the promoter fusions are consistent with the qRT-PCR and PFK specific activity data, and reveal that GlpR is required for transcriptional repression of the *glpR-pfkB* operon during growth in the absence of fructose, possibly by interacting with promoter elements within the 188-bp region upstream of this operon. The results also reveal that the *glpR-pfkB* promoter is relatively moderate at driving the expression of heterologous genes such as *bgaH* compared to the strong and constitutive *H. cutirubrum* rRNA P2 promoter which reached levels of up to 260 mU·mg protein$^{-1}$ of β-galactosidase activity for the reporter fusion (Table 6-1).

**GlpR Represses KDGK Transcription during Growth in the Absence of Glucose**

To address whether GlpR is involved in the repression of other sugar catabolic pathways, qRT-PCR primers were designed for analysis of the transcript levels of genes encoding homologs of KDGK including chromosomally-encoded *kdgK1* (HVO_0549)

and pHV4-encoded *kdgK2* (HVO_A0328) (Figure 6-6A). In haloarchaea, KDGK is involved in the metabolism of glucose through a modified ED pathway (Falb et al., 2008). In *H. volcanii*, both *kdgK1* and *kdgK2* are predicted to encode active KDGK enzymes based on their conservation of active site residues and their close relationship to KDGKs from other microbes that have been characterized at the biochemical level (Figure 6-7). Since KdgK1 and KdgK2 are close homologs (62% identity and 74% similarity in amino acid sequence), DNA sequencing was used to confirm qRT-PCR product specificity. Based on qRT-PCRs, the transcripts of both *kdgK* genes were significantly up-regulated (4 to 12-fold) when parent strain H26 was grown on media containing glucose (± glycerol) compared to glycerol alone (Figure 6-6B). Furthermore, chromosomally-encoded *kdgK1* was significantly up-regulated in the *glpR* mutant compared to parent H26 when cells were grown on glycerol minimal medium (14-fold) but was relatively unaltered when cells were grown on media with glucose [*i.e*., 0.38 ± 0.02-fold lower in the presence of glucose alone and 2.4 ± 0.14-fold higher on glucose plus glycerol] (Figure 6-6C). Unlike *kdgK1*, the *glpR* mutation had little if any impact on *kdgK2* transcript levels compared to parent H26 on all media examined (*i.e*., Glu MM, Gly Glu MM and Gly MM) (Figure 6-6C).

Based on the qRT-PCR finding that GlpR may serve as a repressor of *kdgK1* transcript levels during growth in the absence of glucose, KDGK enzyme activity was monitored in both parent and *glpR* mutant strains to determine the role of GlpR at the protein level. Similar to transcript levels, KDGK activity was reduced when cells were grown on glycerol compared to glucose (Figure 6-8). Likewise, deletion of *glpR* resulted in significant increases in KDGK activity on glycerol, with the increase on glycerol and

glucose modest (2-fold) compared to glycerol alone (7-fold) (Figure 6-8). These levels were reduced to parental levels by providing *glpR in trans* (Figure 6-8). The *glpR* knockout did not impact KDGK activity when cells were grown with glucose as the sole carbon source (Figure 6-8) or on peptide-rich YPC media with or without glucose or fructose (Figure 6-9). Based on these results, the KDGK activity of *H. volcanii* was consistent with the qRT-PCR data in which *glpR* was needed for repression of *kdgK1* transcript levels on glycerol. Furthermore, KDGK specific activity (7.1 to 45 mU·mg protein$^{-1}$), although higher, was within a reasonable range observed for other haloarchaea (*i.e.*, *H. saccharolyticus* at 2 to 5 mU·mg protein$^{-1}$) (Johnsen et al., 2001).

To further investigate the role of GlpR at the level of KDGK transcription, *kdgK1* and *kdgK2* promoter regions were fused to a *bgaH*-based transcriptional reporter (as described above). Reporter fusions of various lengths and start sites were generated to ensure that the entire promoter and potential regulatory elements were included for analysis, and transcription of the *kdgK* promoter constructs was monitored by assay of β-galactosidase activity. Although β-galactosidase activities of the *kdgK1-* and *kdgK2-bgaH* transcriptional fusions were somewhat high on glycerol alone (Gly MM), these activities increased significantly upon glucose supplementation (Table 6-1). Furthermore, the β-galactosidase activity of both *kdgK1-bgaH* fusions was higher in the *glpR* mutant compared to the parent when the cells were grown on glycerol alone (Table 6-1). In contrast to *kdgK1*, deletion of *glpR* did not impact transcription of the *kdgK2*-promoter fusions as measured using the reporter constructs (Table 6-1). Thus, GlpR appears to reduce KDGK activity and *kdgK1* transcript levels through transcriptional repression of *kdgK1* when cells are grown in the absence of glucose (on

glycerol). It should be noted that both the 89- and 524-bp *kdgK1* and 122-bp HVO_A0327-*kdgK2* promoters are relatively robust at driving expression of the heterologous *bgaH* reporter. β-galactosidase activity for the *kdgK* promoters was greater than that of the *H. cutirubrum* rRNA P2 promoter (Table 6-1), used routinely for high-level production of proteins in *H. volcanii* (Kaczowka et al., 2005; Uthandi et al., 2010).

While the data reveal that GlpR is required for the transcriptional repression of *kdgK1* and the reduction of KDGK enzyme activity when the cells are grown in the absence of glucose, it remains to be determined why the levels of β-galactosidase activity are relatively high for both *kdgK1-bgaH* reporter fusions on glycerol compared to the nearly baseline level of transcripts detected for *kdgK1* by qRT-PCR during growth on this same medium. Post-transcriptional mechanisms and/or insufficient levels of GlpR needed to repress transcription of the *kdgK1-bgaH* reporter fusion on the multicopy plasmids, pJAM2705 and pJAM2706, may explain these findings.

**GlpR and Sugar Metabolism**

The data presented here indicate that GlpR represses transcription of the *glpR-pfkB* operon and *kdgK1* in the presence of glycerol, and that GlpR is no longer an active repressor of these operons when cells are grown on media with fructose and glucose. It is unclear, however, whether GlpR and/or these operons are responsible for the differential utilization of glucose and glycerol by *H. volcanii* (Sherwood et al., 2009) (Figure 6-10). To directly examine the role of GlpR in this phenomenon and determine whether glycerol and fructose are differentially metabolized, the *glpR* deletion was introduced into a previously described glycerol kinase (*glpK*) mutant strain KS4 (Sherwood et al., 2009) for phenotypic analysis. Since both *glpR* and *glpK* deletions are

in separate operons and markerless, this double mutant strain was readily generated. Parent and *glpK* mutant strains were analyzed as a replicate of previous experiments (Sherwood et al., 2009) along with single *glpR* and double *glpR glpK* mutant strains for growth and carbon utilization on minimal media including fructose, glucose and/or glycerol. Interestingly, glycerol and fructose are co-utilized when provided at equimolar concentrations (Figure 6-11). Furthermore, GlpR did not appear to mediate the differential rate at which glycerol and glucose are metabolized (Figure 6-10).

**Promoter Regions for *kdgK1* and *glpR-pfkB* Include a Putative GlpR Binding Motif**

Based on the finding that GlpR likely controls *pfkB* and *kdgK1* transcription within the 188-bp and 89-bp region upstream of the translational start codon for each gene, respectively, these regions were analyzed to determine putative promoter elements and GlpR binding motif(s). Shine-Dalgarno sites and promoter elements including the TFB responsive element (BRE) and TATA box were predicted based on consensus sequences (Gregor and Pfeifer, 2005). Next, inverted repeats located near these elements were aligned to identify potential GlpR binding site(s). Using this approach, an inverted hexameric repeat TCSNCN$_{(3\text{-}4)}$SSNGGA (where S is G or C and N is any nucleotide) was identified that overlaps the putative *kdgK1* promoter and is downstream of the putative *glpR-pfkB* promoter (Figure 6-12). This motif was not found within the *kdgK2* promoter region, consistent with the findings that GlpR regulates both *kdgK1* and *pfkB* but not *kdgK2.* Future investigation is expected to provide insight as to whether GlpR binds this motif and represses transcription from the *kdgK1* and *glpR-pfkB* promoters when cells are grown on glycerol (in the absence of glucose or fructose, respectively).

### GlpR Purifies as a Tetramer from Peptide-Rich Media under Both High and Low Salt

GlpR was C-terminally Strep-II tagged and the encoding gene was placed under the control of the constitutive rRNA P2 promoter from *H. cutirubrum* on plasmid pJAM2682. GlpR was purified from *H. volcanii* cells grown in rich, peptide based media and harvested for purification using StrepTactin and Superdex-200 gel filtration chromatography. GlpR-StrepII was purified under both high (2 M NaCl) and low (150 mM NaCl) salt conditions. Due to the fact that haloarchaea maintain a high intracellular cation concentration equal to that of the surrounding environment in order to reduce osmotic pressure, their proteins often require high concentrations of salt in order to retain activity (Lanyi, 1974), however, there are some notable exceptions (Uthandi et al., 2010). Under both high (data not shown) and low (Figure 6-13) salt, GlpR purified as a tetramer composed of monomeric subunits of approximately 30 kDa (Figure 6-14). Members from the DeoR/GlpR family of transcriptional repressors including *E. coli* GlpR are often tetramers (Larson et al., 1987). Both before and after gel filtration chromatography, the protein was confirmed to be homogenous by reducing 12% SDS-PAGE and subsequent staining with Coomassie Blue (Figure 6-14).

## Conclusion

This study demonstrates that the DeoR/GlpR-type GlpR represses the transcription of genes encoding both fructose and glucose metabolic enzymes when *H. volcanii* cells are grown in the absence of either fructose or glucose. Transcript levels and activities of key enzymes of fructose and glucose metabolism, PFK (*pfkB*) and KDGK (*kdgK1*), were reduced in the presence of glycerol alone compared to fructose and/or glucose. Analysis of the transcriptional fusions of the *pfkB* and *kdgK1* promoters

in a *glpR* mutant strain revealed that GlpR was required for transcriptional repression of these genes during growth on glycerol. In contrast, transcription of the megaplasmid pHV4-encoded *kdgK*2, although reduced by glycerol, was not significantly altered by the *glpR* mutation, suggesting that an additional regulator is used for *kdgK*2. The *glpR* and *pfkB* genes were co-transcribed under a common promoter based on RT-PCR analysis, suggesting that GlpR also serves as an autoregulator, and transcription of the *glpR-pfkB* operon was reduced during growth on glycerol alone compared to growth on fructose or glucose. The results presented here provide the first genetic and biochemical evidence of a DeoR/GlpR-type transcriptional repressor protein in haloarchaea. Future biochemical characterization of the GlpR regulon is expected to provide further insight into the transcriptional regulation of sugar metabolism in *H. volcanii* as well as other microorganisms with similar gene organizations. Further analysis will also provide new insight into how DeoR/GlpR family members can interact with and regulate archaeal basal-transcriptional machineries composed of eukaryotic-like RNAP and TBP and TFB proteins.

Table 6-1. Transcription of a *bgaH* β-galactosidase reporter gene from the genomic regions upstream of *glpR-pfkB*, *kdgK1*, and *kdgK2* in parent and *glpR* mutant strains grown on various carbon sources

| | | β-Galactosidase Specific Activity (mU·mg protein$^{-1}$)[a] | | | | | | |
|---|---|---|---|---|---|---|---|---|
| | Promoter: | *glpR-pfkB* (188 bp) | *kdgK1* (524 bp) | *kdgK1* (89 bp) | *HvoA0327-kdgK2* (122 bp) | *kdgK2* (232 bp) | *rrnA* (551 bp) | none (SD only) |
| Carbon Source | Mutation | | | | | | | |
| Gly | — | 9.2 ± 2 | 160 ± 3 | 180 ± 3 | 85 ± 0.01 | 14 ± 0.01 | 260 ± 10 | 8.1 ± 0.1 |
| | Δ*glpR* | 32 ± 3 | 270 ± 10 | 250 ± 8 | 99 ± 0.8 | 14 ± 0.01 | 250 ± 1 | 8.2 ± 0.2 |
| Fru | — | 27 ± 1 | n.d. | n.d. | n.d. | n.d. | 160 ± 7 | 8.2 ± 0.1 |
| | Δ*glpR* | 25 ± 0.3 | n.d. | n.d. | n.d. | n.d. | 150 ± 5 | 7.9 ± 0.2 |
| Gly Fru | — | 27 ± 0.2 | n.d. | n.d. | n.d. | n.d. | 190 ± 10 | 7.3 ± 0.9 |
| | Δ*glpR* | 34 ± 0.1 | n.d. | n.d. | n.d. | n.d. | 180 ± 9 | 8.2 ± 0.2 |
| Glu | — | n.d. | 300 ± 4 | 280 ± 0.01 | 190 ± 0.01 | 41 ± 0.1 | 250 ± 7 | 7.3 ± 0.9 |
| | Δ*glpR* | n.d. | 250 ± 2 | 280 ± 3 | 160 ± 0.01 | 39 ± 0.02 | 250 ± 0.01 | 12.0 ± 0.02 |
| Gly Glu | — | n.d. | 230 ± 5 | 200 ± 0.01 | 150 ± 4 | 33 ± 0.01 | 260 ± 7 | 8.1 ± 0.05 |
| | Δ*glpR* | n.d. | 300 ± 4 | 280 ± 1 | 160 ± 0.01 | 34 ± 0.01 | 260 ± 0.01 | 8.2 ± 0.2 |

[a]β-galactosidase activities were determined from the lysate of cells carrying transcriptional fusion constructs of promoters grown to log-phase in minimal media (MM) with Fru, Glu and Gly as indicated. Promoter fusions included the start codon and genomic region (indicated in bp) immediately upstream of each target gene. Note that *glpR-pfkB* and *HvoA0327- kdgK2* are operons most likely transcribed from these promoters. β-galactosidase activities increased by *glpR* mutation are shaded. Experiments were performed in triplicate, and the means ± SD were calculated. Abbreviations: SD, Shine-Dalgarno site, n.d. not determined.

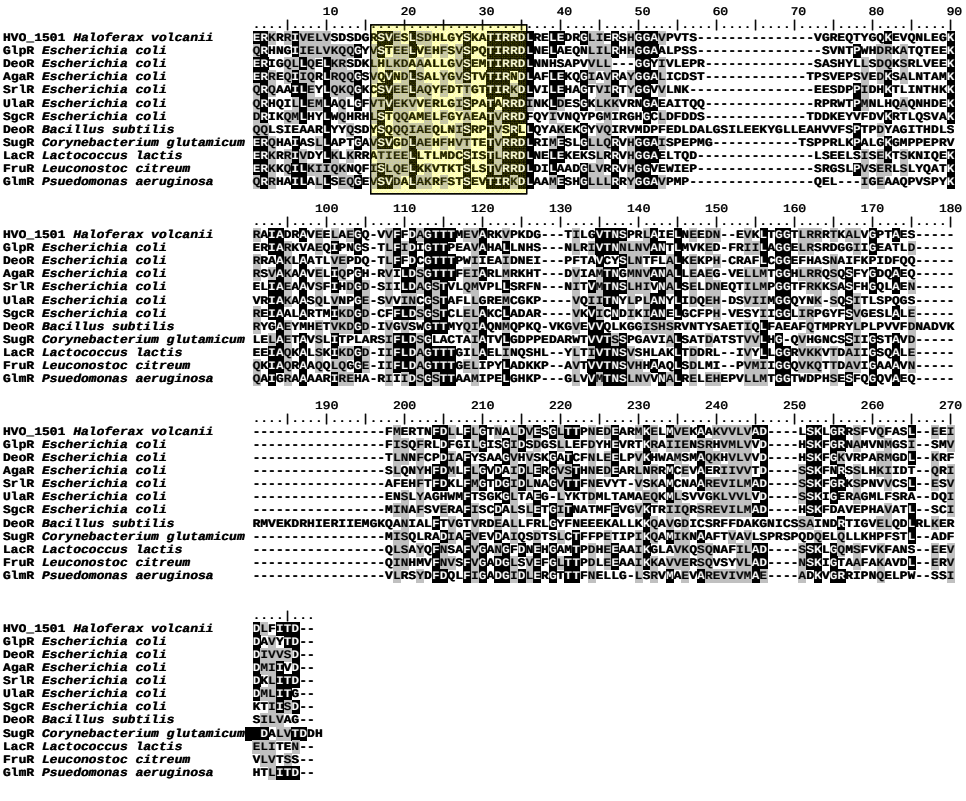


Figure 6-1. *H. volcanii glpR* (HVO_1501) encodes a homolog of DeoR/GlpR-type transcriptional regulators and is linked on the chromosome with genes of sugar metabolism. A) *H. volcanii* GlpR protein was searched against the NCBI protein database using BLASTP (Altschul et al., 1997) and found to be significantly related to COG1349, the DeoR/GlpR family of transcriptional regulators of sugar and nucleoside metabolism. *H. volcanii* GlpR was aligned with DeoR/GlpR family members using CLUSTAL W (Thompson et al., 1994) after N- and C-terminal trimming. The conserved N-terminal DNA binding domain typical of DeoR/GlpR proteins is shown in yellow. (B) Genomic clustering of DeoR/GlpR-transcriptional regulator (red) and PFK (green) genes is conserved in some haloarchaea and many Gram-positive bacteria. Group I: *glpR* clusters with *pfkB* and genes encoding a complete fructose PTS; Group II: *glpR* clusters with *pfkB* and genes encoding a partial fructose PTS; Group III: *glpR* clusters with *pfkB* as well as *fbpA* encoding fructose 1,6-bisphosphate aldolase. (C) Phylogenetic distribution of the DeoR/GlpR family from Bacteria and Archaea. Pairwise comparisons were performed between protein sequences and the mean genetic distance was evaluated using p-distance (gaps were analyzed using pairwise deletion). The best neighborhood-joining tree was then constructed using MEGA 4.0. Interior branch test values are indicated at the internal nodes and were obtained by performing 1,000 replicates. Biochemically characterized proteins are indicated by ●. Accession numbers for protein sequences are listed in Chapter 2.

**Group I**: *Haloferax volcanii, Haloterrigena turkmenica, Moorella thermoacetica*

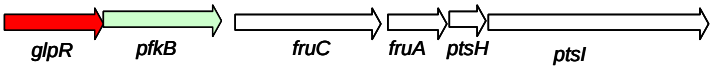


**Group II**: *Thermoanaerobacter tengcongensis, Symbiobacterium thermophilum, Bacillus cereus, Lactobacillus sakei, Enterococcus faecalis*

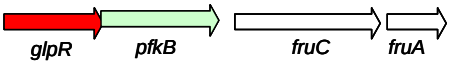


**Group III**: *Haloarcula marismortui, Halomicrobium mukohataei*

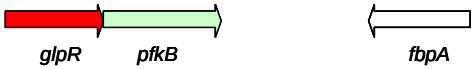


B

Figure 6-1. Continued

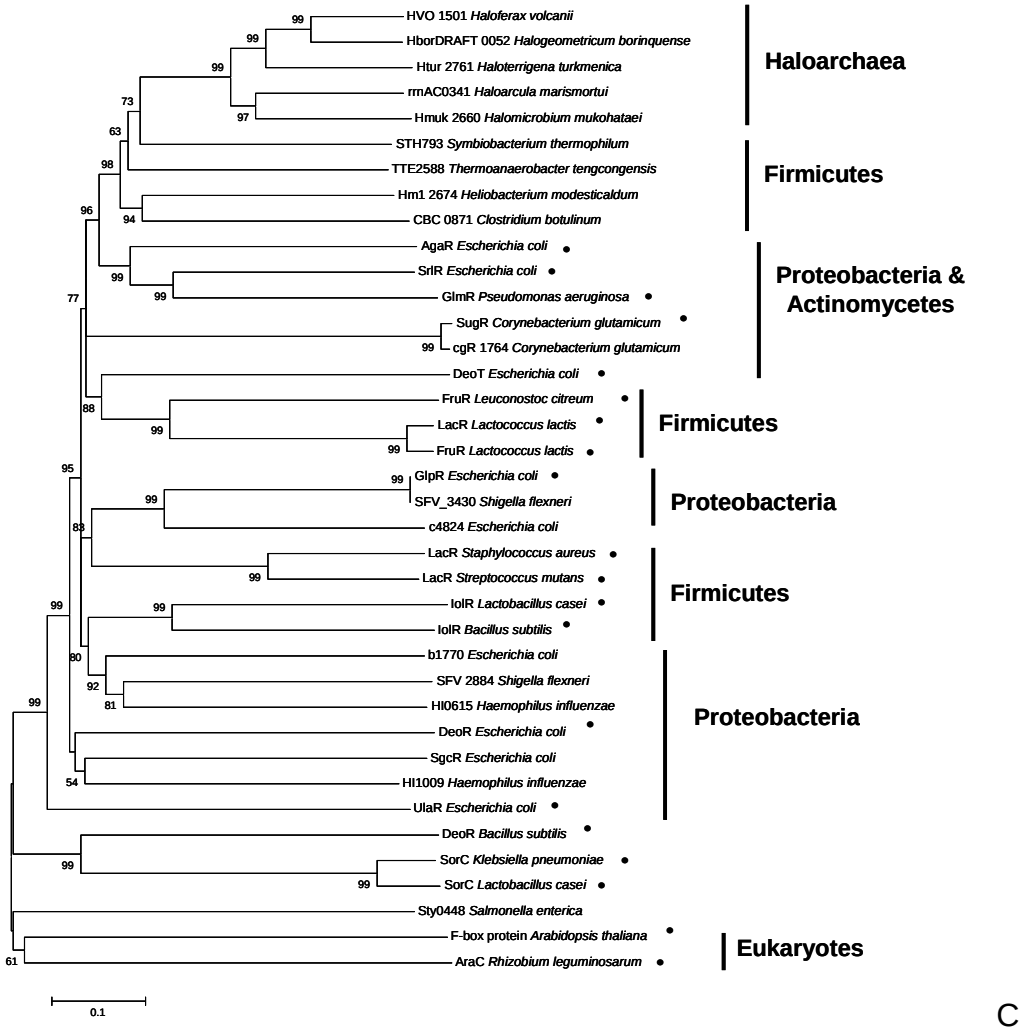


C

Figure 6-1. Continued

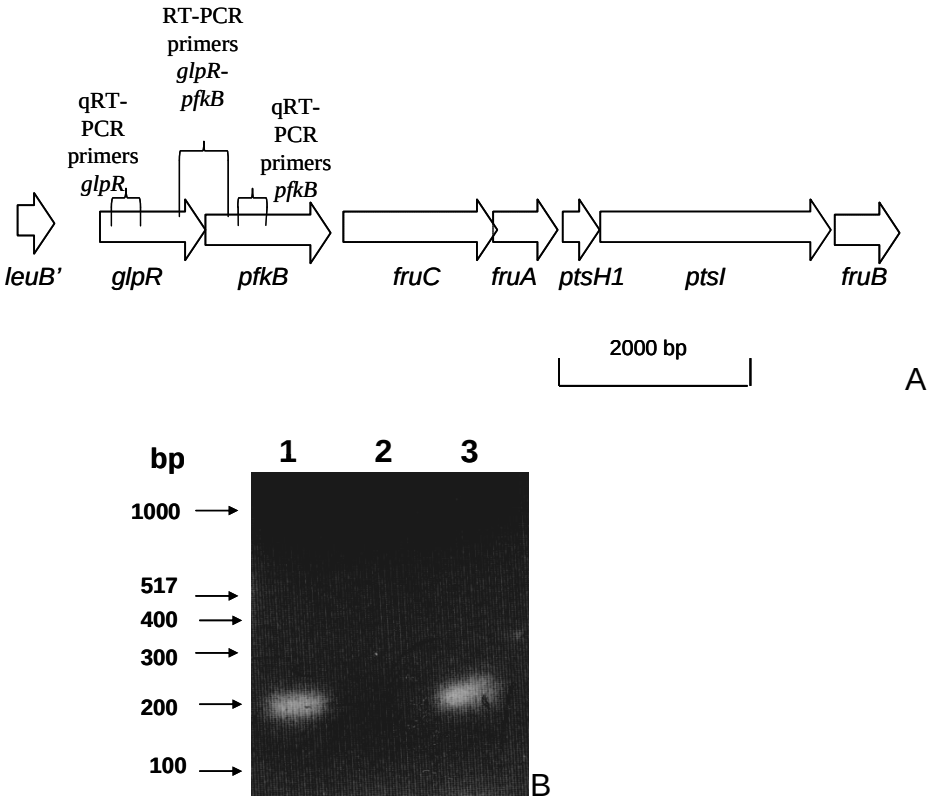


Figure 6-2. Genomic organization and transcript analysis of *pfkB* encoding phosphofructokinase (PFK) and *glpR* encoding GlpR, a putative transcriptional repressor of the DeoR/GlpR family in *H. volcanii*. A) Schematic representation of *glpR* and *pfkB* on the *H. volcanii* genome and location of annealing sites (represented as vertical lines) for (q)RT-PCR primers. B) qRT-PCR reveals *pfkB* and *glpR* are co-transcribed from a common promoter. Total RNA from parent H26 was extracted and reverse transcribed to generate cDNA, which was used as a template for PCR (lane 1). RNA which had not undergone reverse transcription was used as a negative control template for PCR (lane 2). Genomic DNA was used as a positive control template for PCR (lane 3). 100 bp Quick Load DNA markers and molecular sizes are indicated on left. C) Absolute quantification of transcripts specific for *pfkB* and *glpR* reveal that both genes are fructose- and glucose-inducible. Transcript levels were derived from qRT-PCR. D) Relative quantification of transcript levels specific for *pfkB* in *glpR* mutant KS8, KS8 with plasmid vector control (pJAM202c) and KS8 with *glpR in trans* (pJAM2682) compared to parent H26. PFK transcript is increased in the absence of fructose (in Gly) in KS8 compared to H26. Transcript levels were derived by qRT-PCR. Calculations are based on the N-fold induction of transcript levels in KS8 (and subsequent control and complimentary strains) compared to parent H26. Results were normalized with the internal control, *ribL*. Experiments were performed in triplicate, and the means ± SD were calculated.

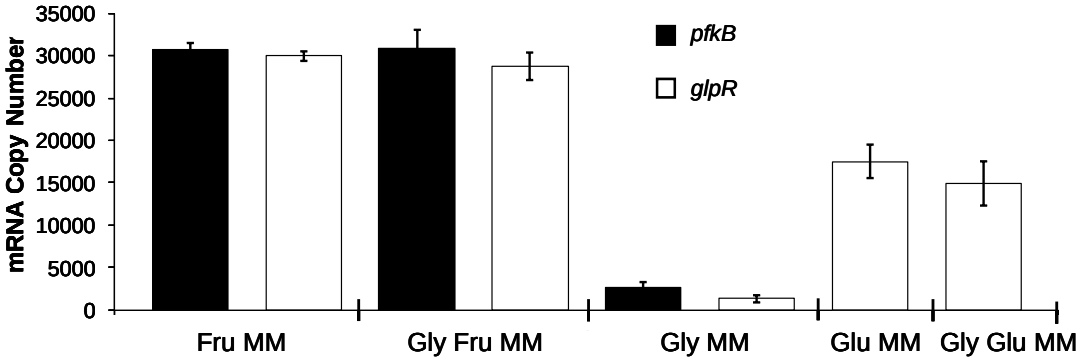


C

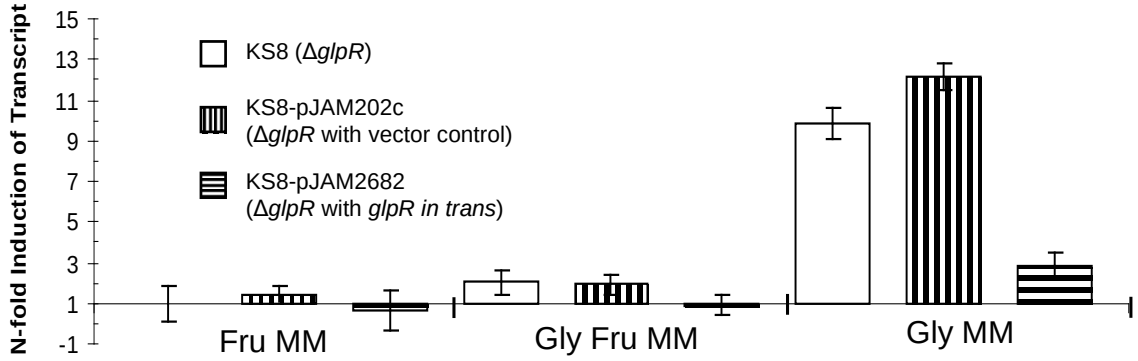


D

Figure 6-2. Continued

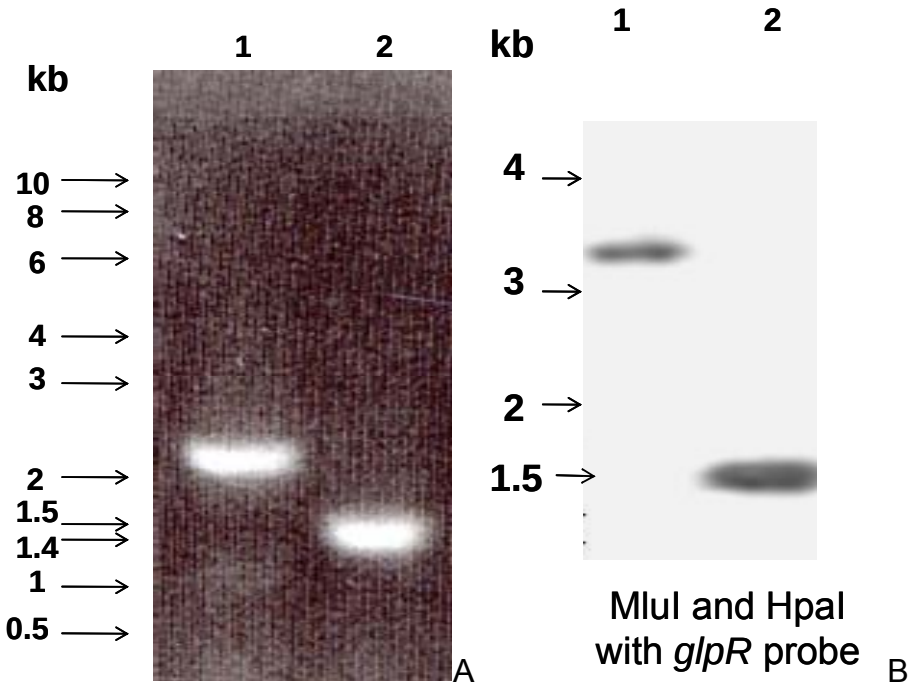


Figure 6-3. PCR and Southern blot confirmation of *H. volcanii glpR* mutant strain KS8 (H26 ∆*glpR*). A) Confirmation of the *glpR* knockout KS8 by PCR. Primer pairs that annealed outside the genomic region cloned in suicide plasmid pJAM2677 were used for confirmation of the *glpR* gene knockout by PCR. Hi-Lo DNA markers and molecular masses are indicated on left. Genomic DNA from the following strains served as template: Lane 1. Parent strain H26, Lane 2. KS8 (H26 Δ*glpR*). B) Southern blot confirmation of the *glpR* knockout in strain KS8 (H26 Δ*glpR*). Genomic DNA was digested with MluI and HpaI and hybridized with a DIG-labeled probe specific for *glpR*. The following strains served as the source of genomic DNA: Lane 1. Parent strain H26, Lane 2. KS8 (H26 Δ*glpR*).

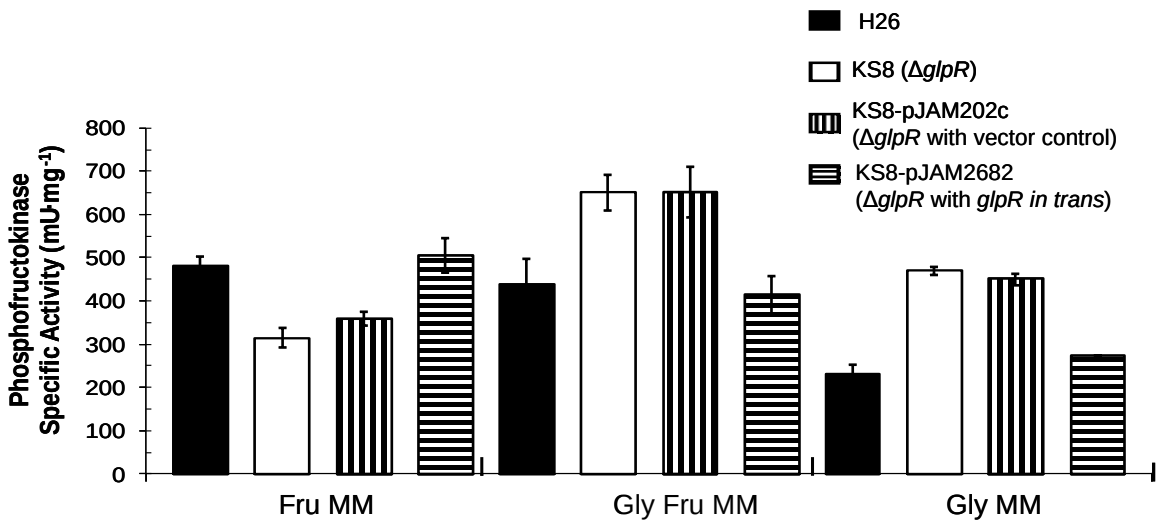


Figure 6-4. PFK activity increases when cells are grown on glycerol minimal medium after deletion of *glpR*. Specific activity of PFK was determined from cell lysate of *H. volcanii* H26 (parent), KS8 (*glpR* mutant), KS8-pJAM202c (*glpR* mutant with vector control) and KS8-pJAM2682 (*glpR* mutant with *glpR in trans*) cells grown to log-phase in Fru, Gly Fru and Gly as indicated. Experiments were performed in triplicate, and the means ± SD were calculated.

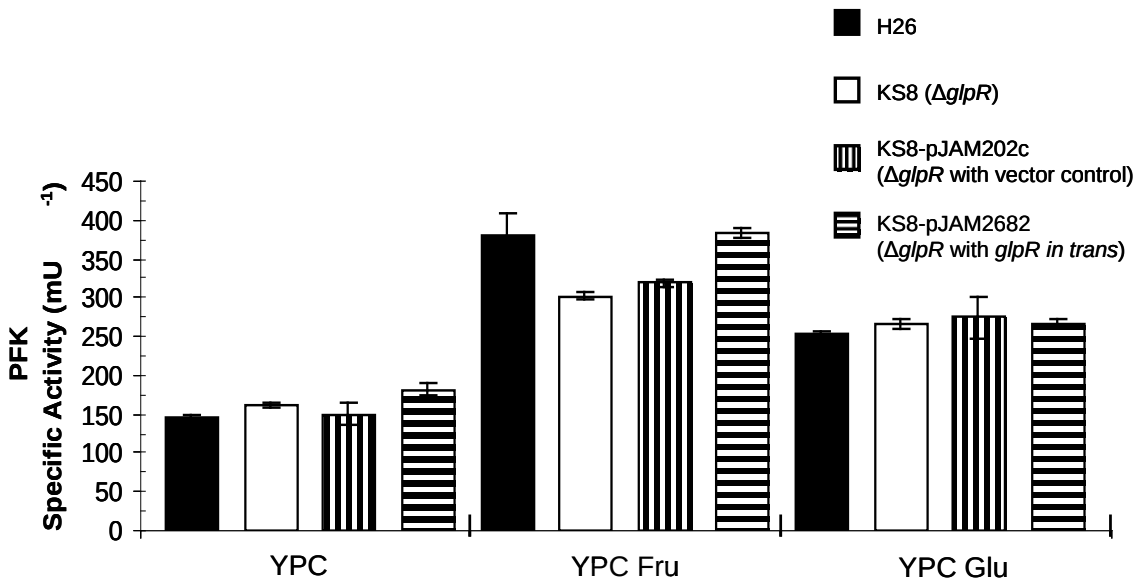


Figure 6-5. GlpR is not required for reduction of PFK activity on peptide media in the absence of fructose or glucose. PFK specific activity was determined as previously described for *H. volcanii* H26 (parent), KS8 (*glpR* deficient strain), KS8-pJAM202c (*glpR* mutant with vector control) and KS8-pJAM2682 (*glpR* deficient strain with *glpR in trans*) cells grown in YPC, YPC Fru and YPC Glu media.

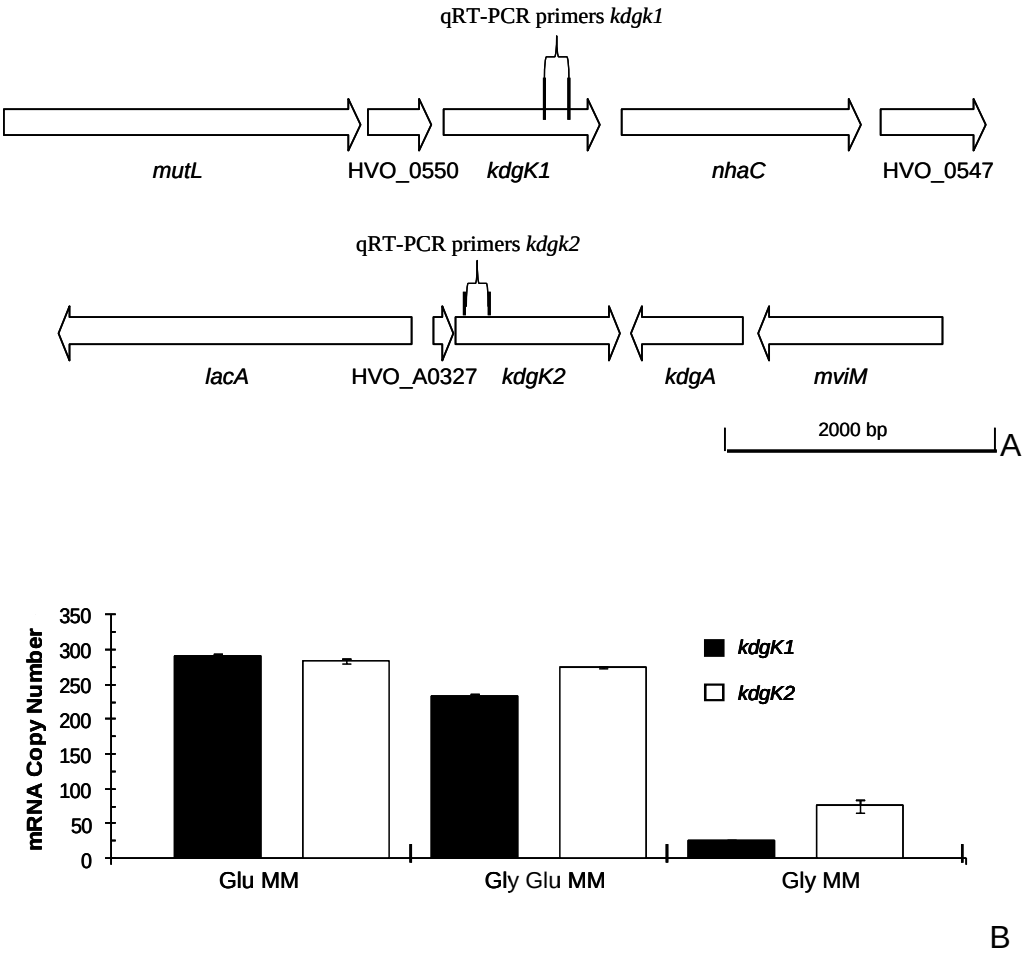


Figure 6-6. Genomic organization and transcript analysis of KDGK genes located on the chromosome and megaplasmid pHV4 of *H. volcanii*. A) Schematic representations of chromosomal *kdgK1* (upper) and related pHV4-carried *kdgK2* (lower) genes and their neighbors and location of annealing sites (represented as vertical lines) for qRT-PCR primers. B) Absolute quantification of transcripts specific for *kdgK1* and *kdgK2* reveals that both genes are glucose-inducible, regardless of glycerol supplementation. Transcript specific for *kdgK1* and *kdgK2* were up-regulated 12-fold and 4-fold, respectively, in the presence of glucose-containing media compared to glycerol alone. Transcript levels were derived from qRT-PCR as described in Methods and Materials. C) Relative quantification of transcript levels specific for *kdgK1* and *kdgK2*. Chromosomal *kdgK1* transcripts are increased in the presence of glycerol regardless of glucose supplementation in a *glpR* mutant (KS8) compared to parent H26. Transcript levels were derived by qRT-PCR. Calculations are based on the N-fold induction of transcription in the designated minimal media for *glpR*-deficient cells compared to parent H26. Results were normalized to the n-fold induction of the internal control, *ribL*. Experiments were performed in triplicate, and the means ± SD were calculated.

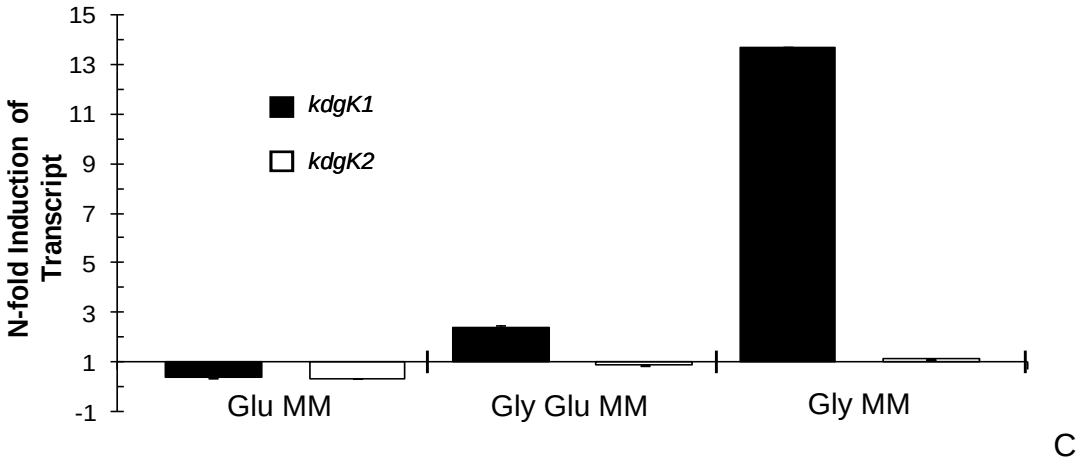


Figure 6-6. Continued

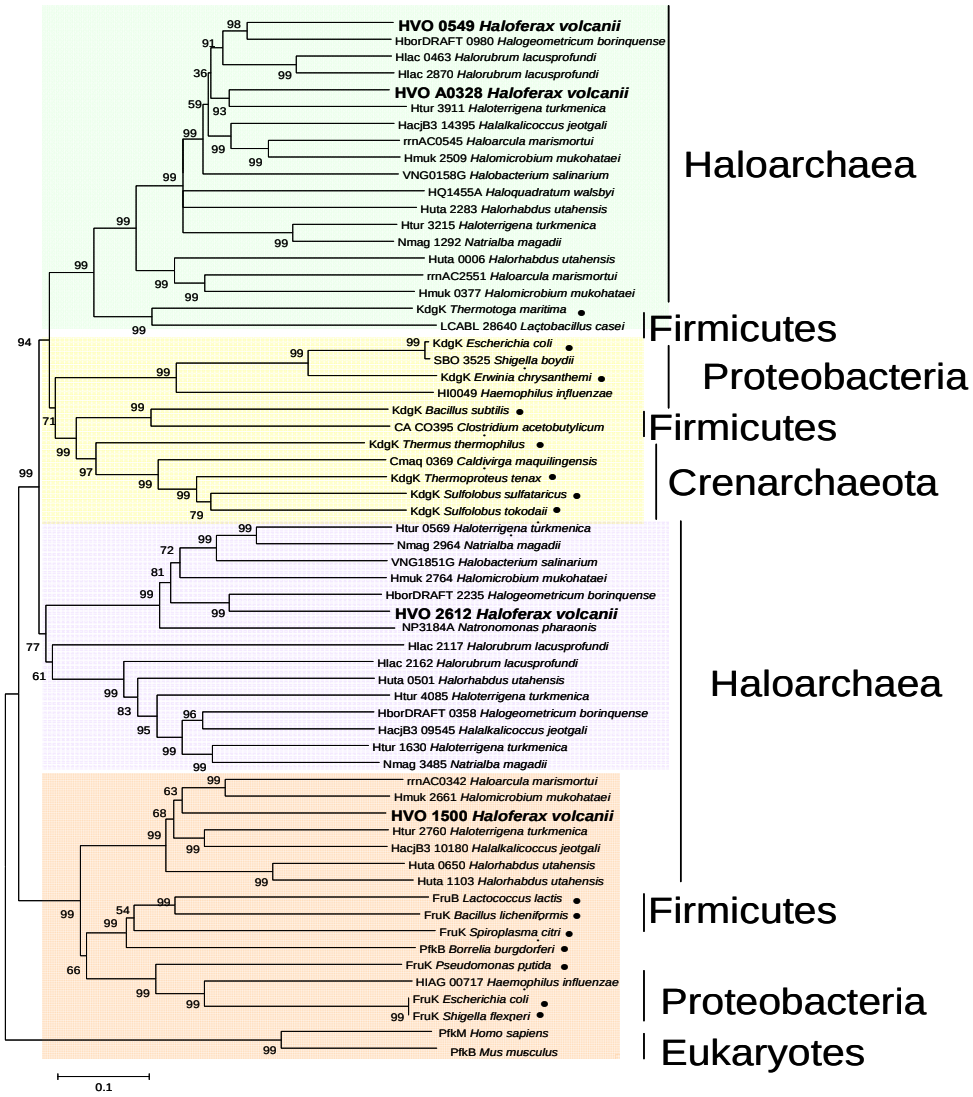


Figure 6-7. Phylogenetic distribution of PFK and KDGK in Bacteria and Archaea. Protein sequences were retrieved using the NCBI database (Benson et al., 2010) and subsequently N- and C-terminally trimmed and aligned using CLUSTAL W (Thompson et al., 1994). Pairwise comparisons were performed between sequences and mean genetic distance was evaluated using p-distance (gaps were analyzed using pairwise deletion). The best neighborhood-joining tree was then constructed using MEGA 4.0. Interior branch test values are indicated at the internal nodes and were obtained by performing 1,000 replicates. Biochemically characterized proteins are indicated by ●. Members belonging to each cluster are color-coded (green, Group I KDGK; yellow, Group II KDGK; purple, uncharacterized sugar kinases; red, PFK). *H. volcanii* proteins HVO_1500 (PfkB), HVO_A0328 (KdgK2), HVO_0549 (KdgK1), and HVO_2612 (sugar kinase) are indicated in bold, large font. Accession numbers for protein sequences are provided in Chapter 2.

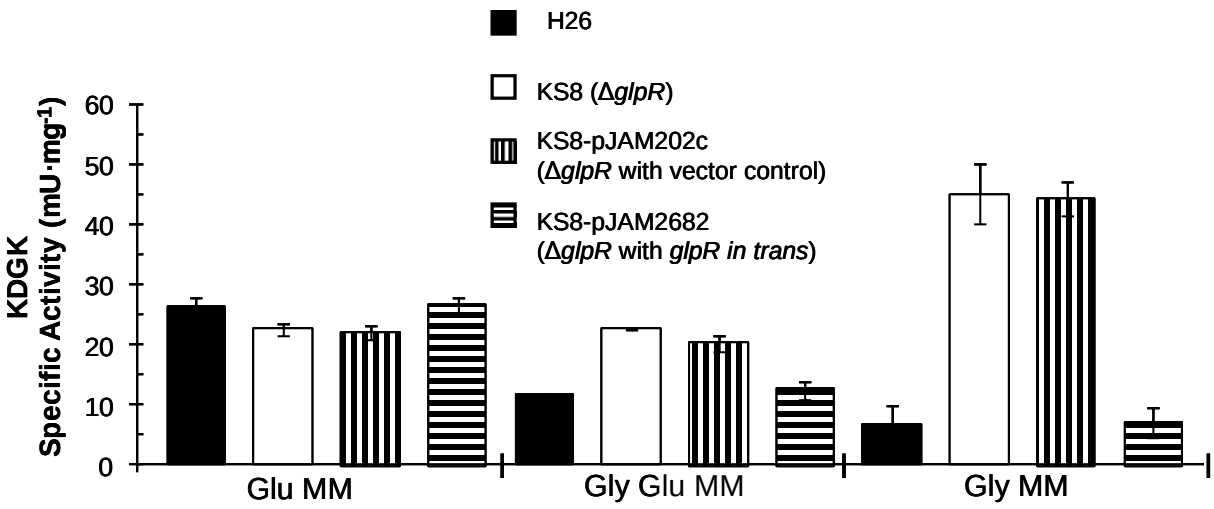


Figure 6-8. KDGK activity is increased by deletion of *glpR* in cells grown on glycerol minimal medium. KDGK specific activities were determined from cell lysate of log-phase *H. volcanii* H26 (parent), KS8 (*glpR* mutant), KS8-pJAM202c (*glpR* mutant with vector control) and KS8-pJAM2682 (*glpR* mutant with *glpR in trans*) grown on Glu , Gly Glu and Gly, as indicated. Experiments were performed in triplicate, and the means ± SD were calculated.

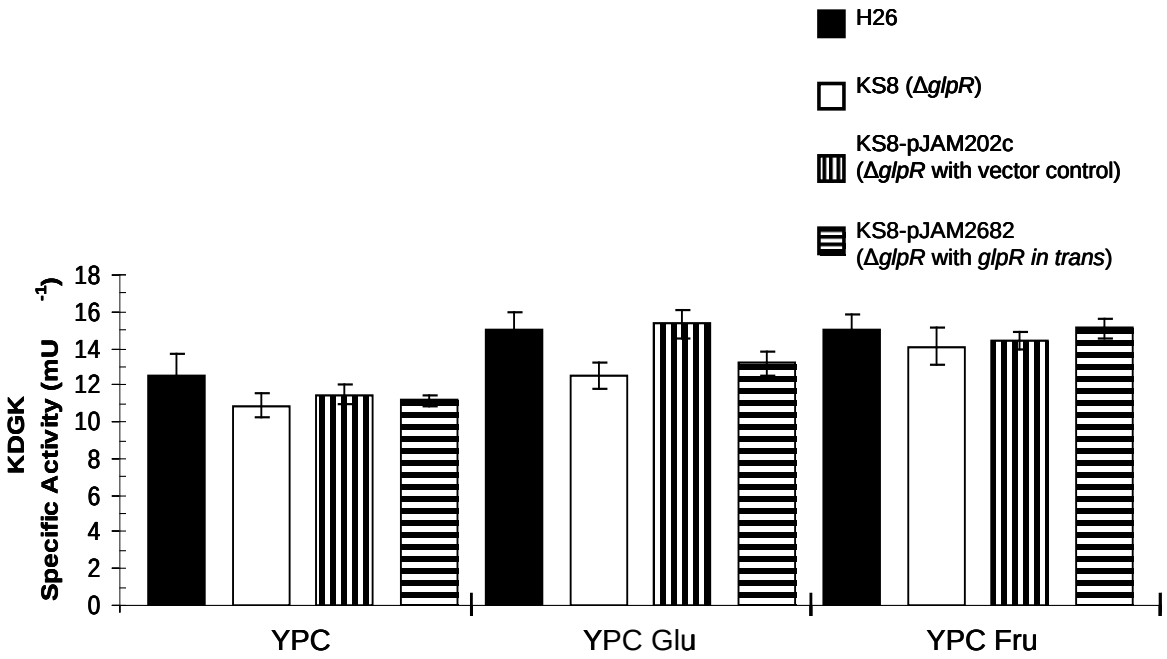


Figure 6-9. GlpR is not required for reduction of KDGK activity on peptide media in the absence of fructose or glucose. KDGK specific activity was determined as previously described for *H. volcanii* H26 (parent), KS8 (*glpR* mutant), KS8-pJAM202c (*glpR* mutant with vector control) and KS8-pJAM2682 (*glpR* mutant with *glpR in trans*) cells grown in YPC, YPC Fru and YPC Glu media.

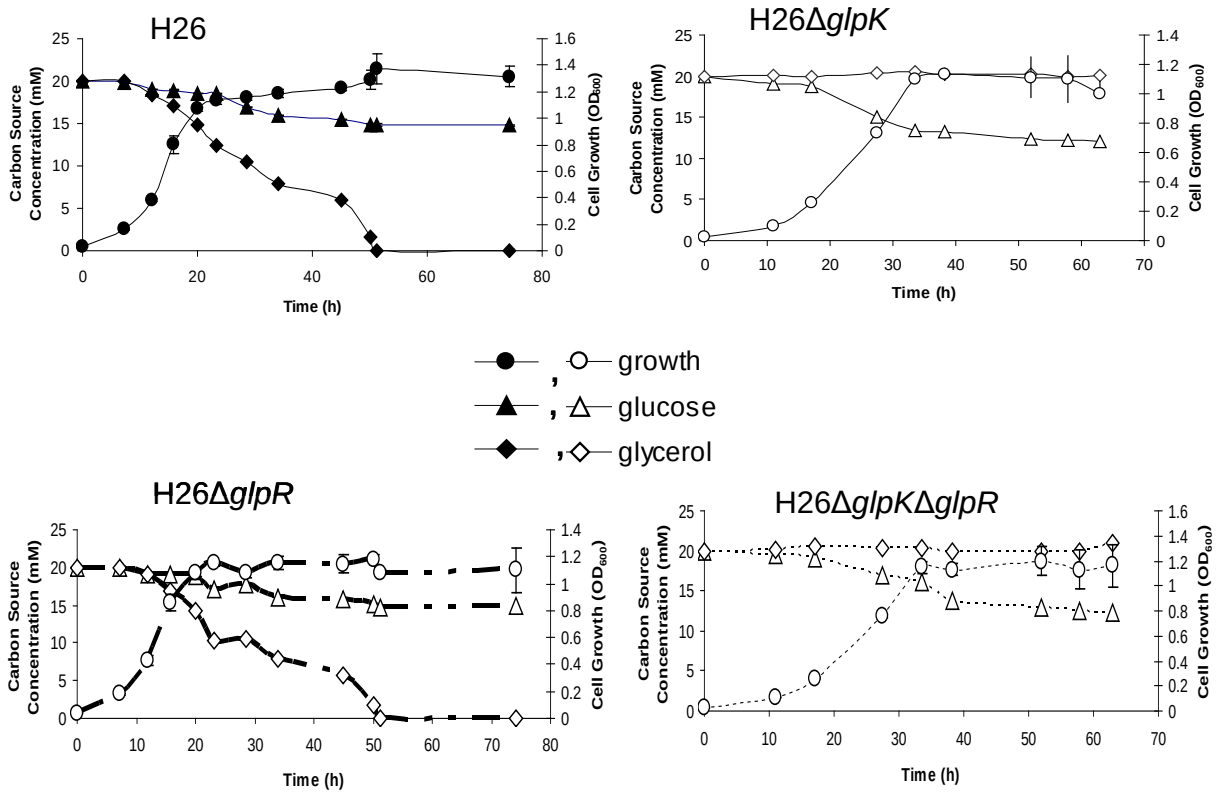


Figure 6-10. Deletion of GlpR does not impact glycerol or glucose utilization in *H. volcanii*. The parent strain H26 and GlpR-deficient strain KS8 exhibit similar growth rates, cell yields and carbon utilization patterns when grown in Gly Glu MM. Furthermore, GK (*glpK*) mutant KS4 and cells deficient in both GlpR and GK (H26 Δ*glpK* Δ*glpR*, KS10) exhibit similar growth rates, cell yields and carbon utilization patterns when grown in Gly Glu MM. Growth at 42°C (200 RPM) was monitored by an increase in $OD_{600}$, where 1 U was equivalent to approximately $10^9$ CFU per ml for all strains. At various time points, supernatant fractions were withdrawn from all cultures and analyzed by HPLC for glucose or glycerol consumption as previously described (Sherwood et al., 2009). Experiments were performed in triplicate, and the means ± SD were calculated. Cell growth and carbon utilization levels are indicated.

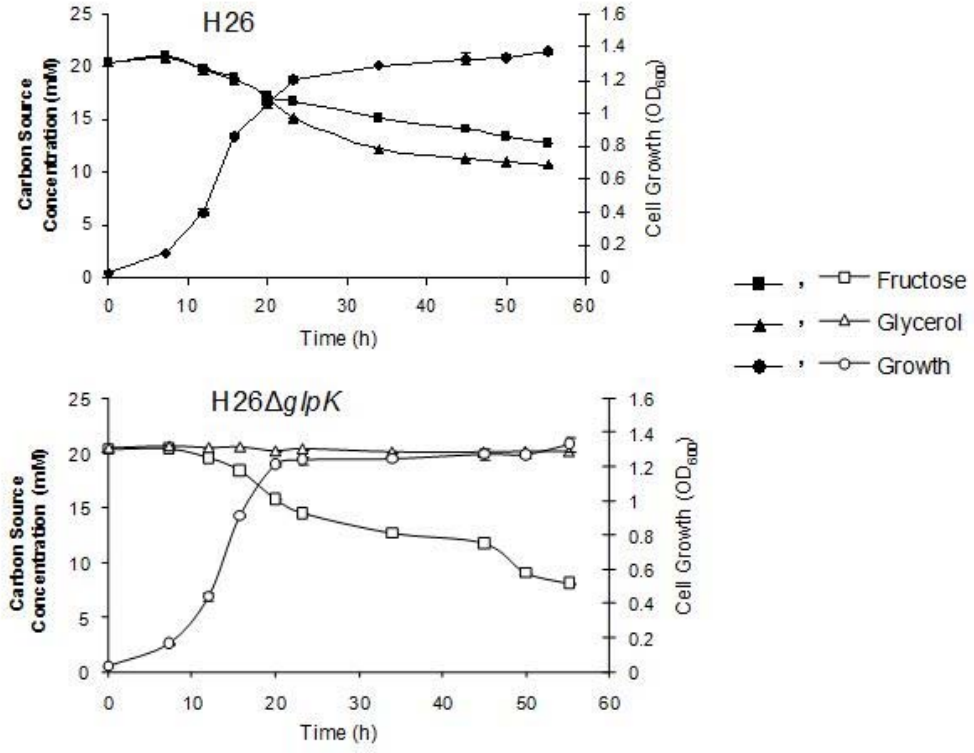


A

Figure 6-11. Glycerol and fructose are co-metabolized in *H. volcanii*. The parent strain H26 and glycerol kinase (*glpK*) mutant KS4 exhibit similar growth rates, cell yields and carbon utilization patterns when grown on Fru MM and Gly Fru MM with each carbon source supplemented at 20 mM (A) or 5 mM (B). Growth at 42°C (200 RPM) was monitored by an increase in $OD_{600}$, where 1 U was equivalent to approximately $10^9$ CFU per ml for all strains. At various time points, supernatant fractions were withdrawn from both parent H26 and KS4 cultures and analyzed by HPLC for fructose or glycerol consumption as previously described (Sherwood et al., 2009). Experiments were performed in triplicate, and the means ± SD were calculated. Cell growth and carbon utilization levels are indicated.

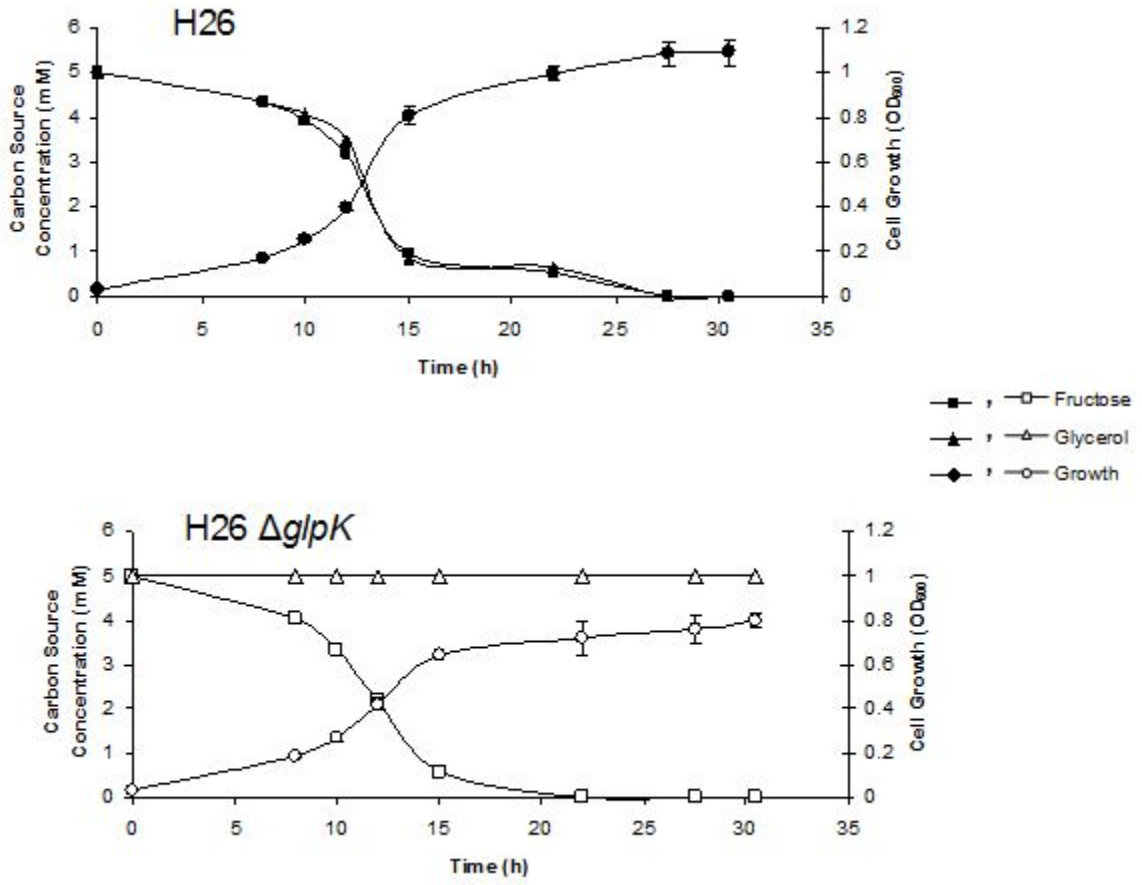


B

Figure 6-11. Continued


Figure 6-12. Genomic regions upstream of *glpR-pfkB* and *kdgK1* include a conserved inverted repeat that may serve in GlpR binding and transcriptional repression. Regions upstream of *glpR-pfkB* and *kdgK1* were analyzed for potential GlpR binding site(s) such as inverted repeats near putative Shine Dalgarno (SD) sites and promoter elements including the TFB responsive element (BRE) and TATA box (consensus sequence CRNAAT for BRE and TTTAWA for TATA box where W is A or T, R is A or G and N is any nucleotide base). Residues matching the consensus BRE/TATA box sequence are boxed and highlighted in grey. SD sites are indicated by a line above the DNA sequence, and the translational start codon is double underlined. An inverted hexameric repeat with a consensus sequence TCSNCN$_{(3-4)}$SSNGGA (where S is C or G and N is A, C, G, or T) was found common to the *glpR-pfkB* and *kdgK1* promoter regions. Inverted repeats are indicated with arrows displaying directionality.

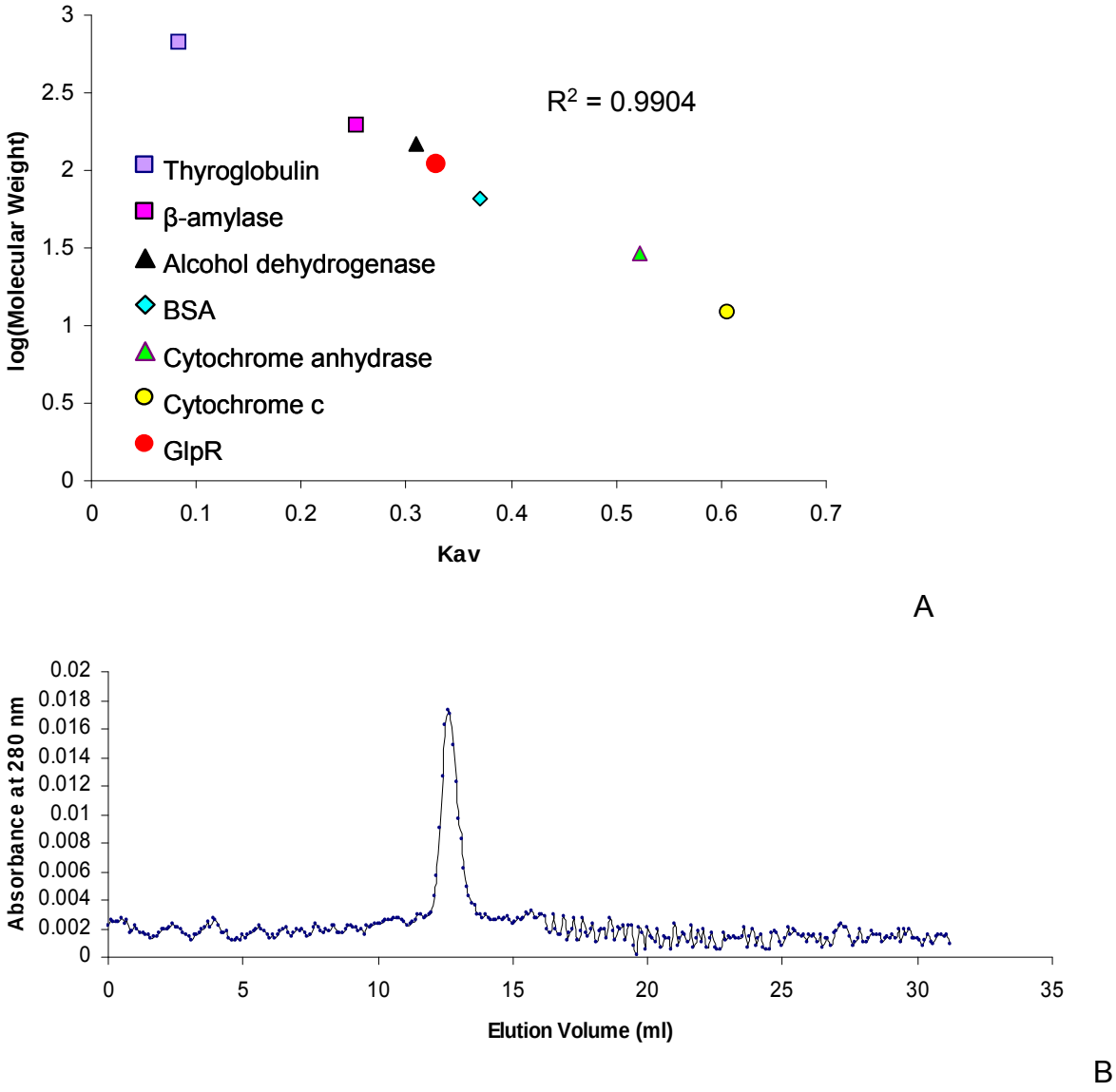


Figure 6-13. *H. volcanii* GlpR purifies as a tetramer by gel filtration. A) Standards of thyroglobulin, β-amylase, alcohol dehydrogenase, BSA, carbonic anhydrase, and cytochrome c were used determine the molecular weight of GlpR. The regression obtained upon plotting $K_{av}$ (x-axis) and log(molecular weight) (y-axis) was linear ($R^2$ = 0.9904). B) After StrepTactin chromatography, GlpR was purified to homogeneity by Superdex-200 chromatography using a low salt buffer (100 mM Tris pH 8.0 with 150 mM NaCl). GlpR eluted at a single peak consistent with a tetramer based on the molecular weight standards and the predicted molecular weight of GlpR.

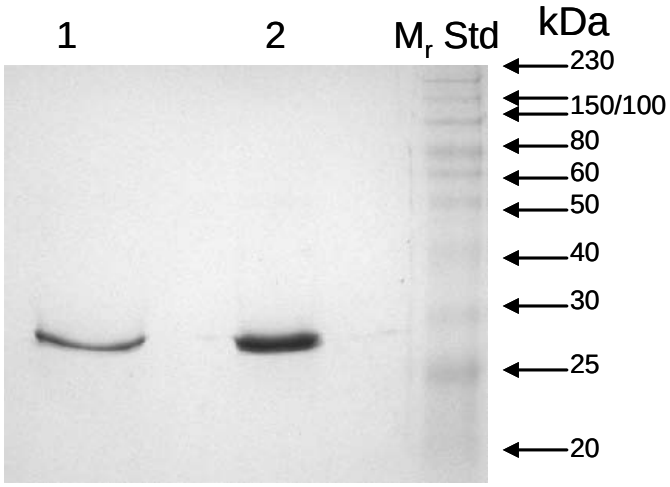


Figure 6-14. *H. volcanii* GlpR purifies to homogeneity after tandem StrepTactin and gel filtration chromatography. GlpR was C-terminally Strep-II tagged and purified by StrepTactin chromatography (Lane 1, 0.75 µg) followed by gel filtration chromatography (Lane 2, 2.3 µg). Purified fractions (20 µl) and Precision Plus Protein$^{TM}$ Kaleidoscope molecular mass marker ($M_r$ Std diluted at a ratio of 1:20 according to the Supplier's recommendations) were boiled for 10 min in 20 µl of SDS–PAGE buffer and were separated by 12% SDS–PAGE. Gels were stained with Coomassie Blue. Under denaturing conditions, the GlpR monomer was estimated to be approximately 30 kDa based on gel migration, consistent with the predicted size based on primary amino acid sequence analysis.

# CHAPTER 7
# SUMMARY AND CONCLUSIONS

## Summary of Findings

The goals of this study are to advance our understanding of the molecular mechanisms surrounding carbon metabolism and its regulation in haloarchaea using *H. volcanii* as a model organism. A combination of bioinformatic and molecular techniques were employed to identify and characterize the enzymes responsible for glycerol catabolism and the mechanisms controlling their regulation. A DeoR/GlpR-type transcriptional repressor of glucose and fructose metabolism was additionally identified and characterized.

This study demonstrated that *H. volcanii* glycerol metabolism proceeds primarily through an ATP-dependent GK and a chromosomally-encoded $NAD^+$-dependent G3PDH. Neither a mutant deficient in *glpK* or *gpdA1* was able to grow in minimal medium containing glycerol as the sole carbon source, although both knockout mutations could be complimented by providing the appropriate gene *in trans*. Interestingly, a *gpdA1* mutation could also be complimented by expressing *gpdA2 in trans* under the control of the constitutive rRNA P2 promoter from *H. cutirubrum*, suggesting that GpdA2 also encodes a functional G3PDH. The *glpK* and *gpdA1* transcripts as well as the specific enzymatic activity of their gene products were strongly induced by glycerol and not repressed by glucose. Rather, glycerol was preferentially metabolized over glucose when parent cells were grown in minimal media containing equimolar concentrations of glucose and glycerol. Although glycerol was preferentially used over glucose, glycerol and fructose were co-utilized in both parent and mutant strains. Both *glpK* and *gpdA1B1C1* were transcriptionally- linked in an operon which

also contains a putative glycerol facilitator, *glpX*, and a homolog of the bacterial PTS protein Hpr, *ptsH2*. This operon was further shown to be under the control of a glycerol-inducible *gpdA1* promoter.

This study has also provided evidence that a DeoR/GlpR-type transcriptional repressor regulates sugar metabolic enzymes in *H. volcanii*. GlpR repressed both *pfkB* encoding PFK and *kdgK1* encoding chromosomal KDGK in the presence of glycerol. Repression of *pfkB* and *kdgK1* was relieved when fructose or glucose was provided, respectively. The GlpR interaction site was limited to a 188-bp *glpR-pfkB* promoter region and an 89-bp *kdgK1* promoter region through transcriptional promoter-reporter fusion assays. A putative GlpR binding site was predicted within both interaction sites which consisted of an inverted hexameric repeat, $TCSnCn_{(3-4)}SSnGGA$ (where S is G or C and n is any nucleotide), which either overlaps or is downstream of putative promoter elements. GlpR has been purified to homogeneity as a tetramer whose monomeric subunits are approximately 30 kDa under both high and low salt from rich, peptide-containing media.

## Future Directions

Future investigation of *H. volcanii* glycerol metabolism will focus on its regulation and biotechnological application. Northern blot analysis will be employed to verify the regulation of the primary glycerol metabolic operon by the proposed promoter. As previously mentioned, glycerol-rich waste streams have been an attractive carbon source for bioconversion to more valuable chemicals. *H. volcanii* readily grows aerobically on biodiesel waste as a sole carbon source (Figure 7-1), however, anaerobic fermentation of glycerol has not been characterized. *H. volcanii* can grow anaerobically using external electron acceptors such as DMSO, trimethylamine-*N*-oxide, and nitrate

(Oren and Trüper, 1990; van Ooyen and Soppa, 2007). Thus, anaerobic glycerol metabolic pathways in *H. volcanii* will also be investigated, focusing on the bioindustrial applications. Although the EI and $EIIB^{Fru}$ homologs in *H. volcanii* are needed for fructose metabolism, a more detailed understanding of their roles along with additional PTS homologs such as Hpr will be crucial to understanding the evolution and biological function of the PTS in archaea. Future investigation of the GlpR repressor will focus on additional transcriptional targets using microarray analysis of parent and *glpR* mutant strains grown in the presence of glycerol. The mode of GlpR repression will also be characterized, specifically focusing on the promoter binding site using florescence anisotropy, electrophoretic mobility shift assays, and DNaseI footprinting assays. In addition, the effector molecule will be demonstrated using calorimetry.

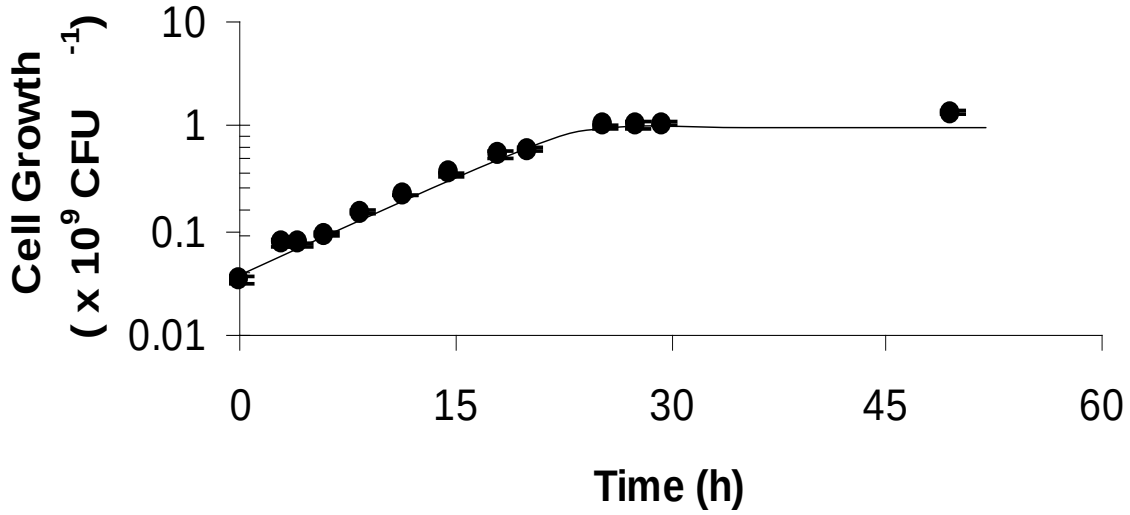


Figure 7-1. *H. volcanii* grows aerobically on biodiesel waste as a sole carbon source. Minimal media was prepared according to the Halohandbook (Dyall-Smith, 2008) and as detailed in Chapter 2, with biodiesel waste serving as a the sole carbon source. Glycerol content of the biodiesel waste was analyzed by HPLC and supplemented in the media to a final concentration of 20 mM. Growth at 42°C (200 RPM) was monitored by an increase in $OD_{600}$, where 1 U was equivalent to approximately $10^9$ CFU per ml. Experiments were performed in triplicate, and the means ± SD were calculated.

# LIST OF REFERENCES


Aaij, C. and Borst, P. (1972). The gel electrophoresis of DNA. Biochim. Biophys. Acta *269*, 192-200.

Abram, F., Su, W.L., Wiedmann, M., Boor, K.J., Coote, P., Botting, C., Karatzas, K.A., and O'Byrne, C.P. (2008). Proteomic analyses of a *Listeria monocytogenes* mutant lacking $\sigma^B$ identify new components of the $\sigma^B$ regulon and highlight a role for $\sigma^B$ in the utilization of glycerol. Appl. Environ. Microbiol. *74*, 594-604.

Adachi, O., Ano, Y., Shinagawa, E., and Matsushita, K. (2008). Purification and properties of two different dihydroxyacetone reductases in *Gluconobacter suboxydans* grown on glycerol. Biosci. Biotechnol. Biochem. *72*, 2124-2132.

Aiba, H. (1983). Autoregulation of the *Escherichia coli crp* gene: CRP is a transcriptional repressor for its own gene. Cell *32*, 141-149.

Albers, S.V., Elferink, M.G., Charlebois, R.L., Sensen, C.W., Driessen, A.J., and Konings, W.N. (1999). Glucose transport in the extremely thermoacidophilic *Sulfolobus solfataricus* involves a high-affinity membrane-integrated binding protein. J. Bacteriol. *181*, 4285-4291.

Albers, S.V., Koning, S.M., Konings, W.N., and Driessen, A.J. (2004). Insights into ABC transport in archaea. J. Bioenerg. Biomembr. *36*, 5-15.

Albertyn, J., Hohmann, S., Thevelein, J.M., and Prior, B.A. (1994). *GPD1*, which encodes glycerol-3-phosphate dehydrogenase, is essential for growth under osmotic stress in *Saccharomyces cerevisiae*, and its expression is regulated by the high-osmolarity glycerol response pathway. Mol. Cell Biol. *14*, 4135-4144.

Allers, T., Ngo, H.P., Mevarech, M., and Lloyd, R.G. (2004). Development of additional selectable markers for the halophilic archaeon *Haloferax volcanii* based on the *leuB* and *trpA* genes. Appl. Environ. Microbiol. *70*, 943-953.

Alpert, C.A. and Siebers, U. (1997). The *lac* operon of *Lactobacillus casei* contains *lacT*, a gene coding for a protein of the Bg1G family of transcriptional antiterminators. J. Bacteriol. *179*, 1555-1562.

Altekar, W. and Rangaswamy, V. (1990). Indication of a modified EMP pathway for fructose breakdown in a halophilic archaebacterium. FEMS Microbiol. Lett. *69*, 139-143.

Altekar, W. and Rangaswamy, V. (1992). Degradation of endogenous fructose during catabolism of sucrose and mannitol in halophilic archaebacteria. Arch. Microbiol. *158*, 356-363.

Altschul, S.F., Madden, T.L., Schaffer, A.A., Zhang, J., Zhang, Z., Miller, W., and Lipman, D.J. (1997). Gapped BLAST and PSI-BLAST: a new generation of protein database search programs. Nucleic Acids Res. *25*, 3389-3402.

Amouyal, M., Mortensen, L., Buc, H., and Hammer, K. (1989). Single and double loop formation when *deoR* repressor binds to its natural operator sites. Cell *58*, 545-551.

Amster-Choder, O. and Wright, A. (1992). Modulation of the dimerization of a transcriptional antiterminator protein by phosphorylation. Science *257*, 1395-1398.

Anderson, M.J., DeLabarre, B., Raghunathan, A., Palsson, B.O., Brunger, A.T., and Quake, S.R. (2007). Crystal structure of a hyperactive *Escherichia coli* glycerol kinase mutant Gly230 --> Asp obtained using microfluidic crystallization devices. Biochemistry *46*, 5722-5731.

Andrews, S., Reichow, S.L., and Gonen, T. (2008). Electron crystallography of aquaporins. IUBMB Life *60*, 430-436.

Ansell, R., Granath, K., Hohmann, S., Thevelein, J.M., and Adler, L. (1997). The two isoenzymes for yeast $NAD^+$-dependent glycerol 3-phosphate dehydrogenase encoded by *GPD1* and *GPD2* have distinct roles in osmoadaptation and redox regulation. EMBO J. *16*, 2179-2187.

Ánton, J., Peña, A., Santos, F., Martínez-García, M., Schmitt-Kopplin, P., and Rosselló-Mora, R. (2008). Distribution, abundance and diversity of the extremely halophilic bacterium *Salinibacter ruber*. Saline Systems *4*, 15.

Aono, S., Nakajima, H., Saito, K., and Okada, M. (1996). A novel heme protein that acts as a carbon monoxide-dependent transcriptional activator in *Rhodospirillum rubrum*. Biochem. Biophys. Res. Commun. *228*, 752-756.

Aravind, L. and Koonin, E.V. (1999). DNA-binding proteins and evolution of transcription regulation in the archaea. Nucleic Acids Res. *27*, 4658-4670.

Ayala, F.J., Barrio, E., and Kwiatowski, J. (1996). Molecular clock or erratic evolution? A tale of two genes. Proc. Natl. Acad. Sci. USA *93*, 11729-11734.

Bächler, C., Flükiger-Brühwiler, K., Schneider, P., Bähler, P., and Erni, B. (2005a). From ATP as substrate to ADP as coenzyme: functional evolution of the nucleotide binding subunit of dihydroxyacetone kinases. J. Biol. Chem. *280*, 18321-18325.

Bächler, C., Schneider, P., Bahler, P., Lustig, A., and Erni, B. (2005b). *Escherichia coli* dihydroxyacetone kinase controls gene expression by binding to transcription factor DhaR. EMBO J. *24*, 283-293.

Bachovchin, W.W., Eagar, R.G., Jr., Moore, K.W., and Richards, J.H. (1977). Mechanism of action of adenosylcobalamin: glycerol and other substrate analogues as substrates and inactivators for propanediol dehydratase--kinetics, stereospecificity, and mechanism. Biochemistry *16*, 1082-1092.

Baliga, N.S., Goo, Y.A., Ng, W.V., Hood, L., Daniels, C.J., and DasSarma, S. (2000). Is gene expression in *Halobacterium* NRC-1 regulated by multiple TBP and TFB transcription factors? Mol. Microbiol. *36*, 1184-1185.

Barabote, R.D. and Saier, M.H., Jr. (2005). Comparative genomic analyses of the bacterial phosphotransferase system. Microbiol. Mol. Biol. Rev. *69*, 608-634.

Barbirato, F., Astruc, S., Soucaille, P., Camarasa, C., Salmon, J.M., and Bories, A. (1997). Anaerobic pathways of glycerol dissimilation by *Enterobacter agglomerans* CNCM 1210: limitations and regulations. Microbiology *143*, 2423-2432.

Barrière, C., Veiga-da-Cunha, M., Pons, N., Guédon, E., van Hijum, S.A., Kok, J., Kuipers, O.P., Ehrlich, D.S., and Renault, P. (2005). Fructose utilization in *Lactococcus lactis* as a model for low-GC gram-positive bacteria: its regulator, signal, and DNA-binding site. J. Bacteriol. *187*, 3752-3761.

Bates, D.M., Popescu, C.V., Khoroshilova, N., Vogt, K., Beinert, H., Münck, E., and Kiley, P.J. (2000). Substitution of leucine 28 with histidine in the *Escherichia coli* transcription factor FNR results in increased stability of the $[4Fe\text{-}4S]^{(2+)}$ cluster to oxygen. J. Biol. Chem. *275*, 6234-6240.

Bayer, A.J., Pathy, M.S., and Newcombe, R. (1987). Double-blind randomised trial of intravenous glycerol in acute stroke. Lancet *1*, 405-408.

Becker, A., Fritz-Wolf, K., Kabsch, W., Knappe, J., Schultz, S., and Volker Wagner, A.F. (1999). Structure and mechanism of the glycyl radical enzyme pyruvate formate-lyase. Nat. Struct. Biol. *6*, 969-975.

Becker, L.A., Çetin, M.S., Hutkins, R.W., and Benson, A.K. (1998). Identification of the gene encoding the alternative sigma factor $\sigma^B$ from *Listeria monocytogenes* and its role in osmotolerance. J. Bacteriol. *180*, 4547-4554.

Beese, S.E., Negishi, T., and Levin, D.E. (2009). Identification of positive regulators of the yeast *fps1* glycerol channel. PLoS. Genet. *5*, e1000738.

Beijer, L., Nilsson, R.P., Holmberg, C., and Rutberg, L. (1993). The *glpP* and *glpF* genes of the glycerol regulon in *Bacillus subtilis*. J. Gen. Microbiol. *139*, 349-359.

Bell, S.D. (2005). Archaeal transcriptional regulation--variation on a bacterial theme? Trends Microbiol. *13*, 262-265.

Bell, S.D. and Jackson, S.P. (2001). Mechanism and regulation of transcription in archaea. Curr. Opin. Microbiol. *4*, 208-213.

Ben Amotz, A. and Avron, M. (1973a). NADP specific dihydroxyacetone reductase from *Dunaliella parva*. FEBS Lett. *29*, 153-155.

Ben Amotz, A. and Avron, M. (1973b). The role of glycerol in the osmotic regulation of the halophilic alga *Dunaliella parva*. Plant Physiol. *51*, 875-878.

Ben Amotz, A. and Avron, M. (1979). Osmoregulation in the halophilic algae *Dunaliella* and *Asteromonas*. Basic Life Sci. *14*, 91-99.

Benoff, B., Yang, H., Lawson, C.L., Parkinson, G., Liu, J., Blatter, E., Ebright, Y.W., Berman, H.M., and Ebright, R.H. (2002). Structural basis of transcription activation: the CAP-$\alpha$ CTD-DNA complex. Science *297*, 1562-1566.

Benson, D.A., Karsch-Mizrachi, I., Lipman, D.J., Ostell, J., and Sayers, E.W. (2010). GenBank. Nucleic Acids Res. *38*, D46-D51.

Bertani, G. (1951). Studies on lysogenesis. I. The mode of phage liberation by lysogenic *Escherichia coli*. J. Bacteriol. *62*, 293-300.

Bevers, L.E., Hagedoorn, P.L., Krijger, G.C., and Hagen, W.R. (2006). Tungsten transport protein A (WtpA) in *Pyrococcus furiosus*: the first member of a new class of tungstate and molybdate transporters. J. Bacteriol. *188*, 6498-6505.

Biebl, H. (2001). Fermentation of glycerol by *Clostridium pasteurianum*--batch and continuous culture studies. J. Ind. Microbiol. Biotechnol. *27*, 18-26.

Biebl, H., Zeng, A.P., Menzel, K., and Deckwer, W.D. (1998). Fermentation of glycerol to 1,3-propanediol and 2,3-butanediol by *Klebsiella pneumoniae*. Appl. Microbiol. Biotechnol. *50*, 24-29.

Bitan-Banin, G., Ortenberg, R., and Mevarech, M. (2003). Development of a gene knockout system for the halophilic archaeon *Haloferax volcanii* by use of the *pyrE* gene. J. Bacteriol. *185*, 772-778.

Bizzini, A., Zhao, C., Budin-Verneuil, A., Sauvageot, N., Giard, J.C., Auffray, Y., and Hartke, A. (2010). Glycerol is metabolized in a complex and strain-dependent manner in *Enterococcus faecalis*. J. Bacteriol. *192*, 779-785.

Björkqvist, S., Ansell, R., Adler, L., and Lidén, G. (1997). Physiological response to anaerobicity of glycerol-3-phosphate dehydrogenase mutants of *Saccharomyces cerevisiae*. Appl. Environ. Microbiol. *63*, 128-132.

Blake, T., Barnard, A., Busby, S.J., and Green, J. (2002). Transcription activation by FNR: evidence for a functional activating region 2. J. Bacteriol. *184*, 5855-5861.

Blaszczyk, U., Polit, A., Guz, A., and Wasylewski, Z. (2001). Interaction of cAMP receptor protein from *Escherichia coli* with cAMP and DNA studied by dynamic light scattering and time-resolved fluorescence anisotropy methods. J. Protein Chem. *20*, 601-610.

Blomberg, A. and Adler, L. (1989). Roles of glycerol and glycerol-3-phosphate dehydrogenase ($NAD^+$) in acquired osmotolerance of *Saccharomyces cerevisiae*. J. Bacteriol. *171*, 1087-1092.

Blomberg, A. and Adler, L. (1992). Physiology of osmotolerance in fungi. Adv. Microb. Physiol. *33*, 145-212.

Boël, G., Mijakovic, I., Mazé, A., Poncet, S., Taha, M.K., Larribe, M., Darbon, E., Khemiri, A., Galinier, A., and Deutscher, J. (2003). Transcription regulators potentially controlled by HPr kinase/phosphorylase in Gram-negative bacteria. J. Mol. Microbiol. Biotechnol. *5*, 206-215.

Bolhuis, H., Palm, P., Wende, A., Falb, M., Rampp, M., Rodriguez-Valera, F., Pfeiffer, F., and Oesterhelt, D. (2006). The genome of the square archaeon *Haloquadratum walsbyi* : life at the limits of water activity. BMC Genomics *7*, 169.

Borowitzka, L.J. and Brown, A.D. (1974). The salt relations of marine and halophilic species of the unicellular green alga, *Dunaliella*. The role of glycerol as a compatible solute. Arch. Mikrobiol. *96*, 37-52.

Borowitzka, L.J., Kessly, D.S., and Brown, A.D. (1977). The salt relations of *Dunaliella*. Further observations on glycerol production and its regulation. Arch. Microbiol. *113*, 131-138.

Bouvet, O.M., Lenormand, P., Ageron, E., and Grimont, P.A. (1995). Taxonomic diversity of anaerobic glycerol dissimilation in the *Enterobacteriaceae*. Res. Microbiol. *146*, 279-290.

Bradford, M.M. (1976). A rapid and sensitive method for the quantitation of microgram quantities of protein utilizing the principle of protein-dye binding. Anal. Biochem. *72*, 248-254.

Bräsen, C. and Schönheit, P. (2001). Mechanisms of acetate formation and acetate activation in halophilic archaea. Arch. Microbiol. *175*, 360-368.

Brenneis, M., Hering, O., Lange, C., and Soppa, J. (2007). Experimental characterization of *Cis*-acting elements important for translation and transcription in halophilic archaea. PLoS Genet. *3*, e229.

Brisson, D., Vohl, M.C., St Pierre, J., Hudson, T.J., and Gaudet, D. (2001). Glycerol: a neglected variable in metabolic processes? Bioessays *23*, 534-542.

Brown, A.D. and Simpson, J.R. (1972). Water relations of sugar-tolerant yeasts: the role of intracellular polyols. J. Gen. Microbiol. *72*, 589-591.

Brown, F.F., Sussman, I., Avron, M., and Degani, H. (1982). NMR studies of glycerol permeability in lipid vesicles, erythrocytes and the alga *Dunaliella*. Biochim. Biophys. Acta *690*, 165-173.

Bublitz, C. and Kennedy, E. (1954). Synthesis of phosphatides in isolated mitochondria. III. The enzymatic phosphorylation of glycerol. J. Biol. Chem. *211*, 951-961.

Cameron, A.D., Roper, D.I., Moreton, K.M., Muirhead, H., Holbrook, J.J., and Wigley, D.B. (1994). Allosteric activation in *Bacillus stearothermophilus* lactate dehydrogenase investigated by an X-ray crystallographic analysis of a mutant designed to prevent tetramerization of the enzyme. J. Mol. Biol. *238*, 615-625.

Chan, S., Giuroiu, I., Chernishof, I., Sawaya, M.R., Chiang, J., Gunsalus, R.P., Arbing, M.A., and Perry, L.J. (2010). Apo and ligand-bound structures of ModA from the archaeon *Methanosarcina acetivorans*. Acta Crystallogr. Sect. F Struct. Biol. Cryst. Commun. *66*, 242-250.

Charrier, V., Buckley, E., Parsonage, D., Galinier, A., Darbon, E., Jaquinod, M., Forest, E., Deutscher, J., and Claiborne, A. (1997). Cloning and sequencing of two *Enterococcal glpK* genes and regulation of the encoded glycerol kinases by phosphoenolpyruvate-dependent, phosphotransferase system-catalyzed phosphorylation of a single histidyl residue. J. Biol. Chem. *272*, 14166-14174.

Chaumont, F., Moshelion, M., and Daniels, M.J. (2005). Regulation of plant aquaporin activity. Biol. Cell *97*, 749-764.

Chauvin, F., Brand, L., and Roseman, S. (1994). Sugar transport by the bacterial phosphotransferase system. Characterization of the *Escherichia coli* enzyme I monomer/dimer equilibrium by fluorescence anisotropy. J. Biol. Chem. *269*, 20263-20269.

Chauvin, F., Brand, L., and Roseman, S. (1996). Enzyme I: the first protein and potential regulator of the bacterial phosphoenolpyruvate: glycose phosphotransferase system. Res. Microbiol. *147*, 471-479.

Cheek, S., Ginalski, K., Zhang, H., and Grishin, N.V. (2005). A comprehensive update of the sequence and structure classification of kinases. BMC Struct. Biol. *16*, 5-6.

Chen, X., Fang, H., Rao, Z., Shen, W., Zhuge, B., Wang, Z., and Zhuge, J. (2008). Cloning and characterization of a $NAD^+$-dependent glycerol-3-phosphate dehydrogenase gene from *Candida glycerinogenes*, an industrial glycerol producer. FEMS Yeast Res. *8*, 725-734.

Chitlaru, E. and Pick, U. (1991). Regulation of glycerol synthesis in response to osmotic changes in *Dunaliella*. Plant Physiol. *96*, 50-60.

Christian, J. and Waltho, J. (1962). Solute concentrations within cells of halophilic and non-halophilic bacteria. Biochim. Biophys. Acta *65*, 506-508.

Cline, S.W., Lam, W.L., Charlebois, R.L., Schalkwyk, L.C., and Doolittle, W.F. (1989). Transformation methods for halophilic archaebacteria. Can. J. Microbiol. *35*, 148-152.

Coker, J.A. and DasSarma, S. (2007). Genetic and transcriptomic analysis of transcription factor genes in the model halophilic Archaeon: coordinate action of TbpD and TfbA. BMC Genet. *8*, 61.

Cole, S.T., Eiglmeier, K., Ahmed, S., Honore, N., Elmes, L., Anderson, W.F., and Weiner, J.H. (1988). Nucleotide sequence and gene-polypeptide relationships of the *glpABC* operon encoding the anaerobic *sn*-glycerol-3-phosphate dehydrogenase of *Escherichia coli* K-12. J. Bacteriol. *170*, 2448-2456.

Comas, I., González-Candelas, F., and Zúñiga, M. (2008). Unraveling the evolutionary history of the phosphoryl-transfer chain of the phosphoenolpyruvate:phosphotransferase system through phylogenetic analyses and genome context. BMC Evol. Biol. *8*, 147.

Cozzarelli, N.R., Freedberg, W.B., and Lin, E.C. (1968). Genetic control of L-$\alpha$-glycerophosphate system in *Escherichia coli*. J. Mol. Biol. *31*, 371-387.

Craigie, J.S. and McLachlan, J. (1964). Glycerol as a photosynthetic product in *Dunaliella tertiolecta butcher*. Can. J. Bot. *42*, 777-778.

Crutz, A.M., Steinmetz, M., Aymerich, S., Richter, R., and Le Coq, D. (1990). Induction of levansucrase in *Bacillus subtilis*: an antitermination mechanism negatively controlled by the phosphotransferase system. J. Bacteriol. *172*, 1043-1050.

Cruz-Ramos, H., Crack, J., Wu, G., Hughes, M.N., Scott, C., Thomson, A.J., Green, J., and Poole, R.K. (2002). NO sensing by FNR: regulation of the *Escherichia coli* NO-detoxifying flavohaemoglobin, Hmp. EMBO J. *21*, 3235-3244.

Cymer, F. and Schneider, D. (2010). A single glutamate residue controls the oligomerization, function, and stability of the aquaglyceroporin GlpF. Biochemistry *49*, 279-286.

Daniel, R., Bobik, T.A., and Gottschalk, G. (1998). Biochemistry of coenzyme B12-dependent glycerol and diol dehydratases and organization of the encoding genes. FEMS Microbiol. Rev. *22*, 553-566.

Daniel, R., Boenigk, R., and Gottschalk, G. (1995). Purification of 1,3-propanediol dehydrogenase from *Citrobacter freundii* and cloning, sequencing, and overexpression of the corresponding gene in *Escherichia coli*. J. Bacteriol. *177*, 2151-2156.

de Boer, M., Broekhuizen, C.P., and Postma, P.W. (1986). Regulation of glycerol kinase by enzyme $III^{Glc}$ of the phosphoenolpyruvate:carbohydrate phosphotransferase system. J. Bacteriol. *167*, 393-395.

de Riel, J.K. and Paulus, H. (1978a). Subunit dissociation in the allosteric regulation of glycerol kinase from *Escherichia coli*. 1. Kinetic evidence. Biochemistry *17*, 5134-5140.

de Riel, J.K. and Paulus, H. (1978b). Subunit dissociation in the allosteric regulation of glycerol kinase from *Escherichia coli.* 2. Physical evidence. Biochemistry *17*, 5141-5146.

Delmas, S., Shunburne, L., Ngo, H.P., and Allers, T. (2009). Mre11-Rad50 promotes rapid repair of DNA damage in the polyploid archaeon *Haloferax volcanii* by restraining homologous recombination. PLoS Genet. *5*, e1000552.

Deutscher, J., Francke, C., and Postma, P.W. (2006). How phosphotransferase system-related protein phosphorylation regulates carbohydrate metabolism in bacteria. Microbiol. Mol. Biol. Rev. *70*, 939-1031.

Deutscher, J., Herro, R., Bourand, A., Mijakovic, I., and Poncet, S. (2005). P-Ser-HPr--a link between carbon metabolism and the virulence of some pathogenic bacteria. Biochim. Biophys. Acta *1754*, 118-125.

Deutscher, J., Küster, E., Bergstedt, U., Charrier, V., and Hillen, W. (1995). Protein kinase-dependent HPr/CcpA interaction links glycolytic activity to carbon catabolite repression in gram-positive bacteria. Mol. Microbiol. *15*, 1049-1053.

Deutscher, J., Reizer, J., Fischer, C., Galinier, A., Saier, M.H., Jr., and Steinmetz, M. (1994). Loss of protein kinase-catalyzed phosphorylation of HPr, a phosphocarrier protein of the phosphotransferase system, by mutation of the *ptsH* gene confers catabolite repression resistance to several catabolic genes of *Bacillus subtilis*. J. Bacteriol. *176*, 3336-3344.

Deutscher, J. and Sauerwald, H. (1986). Stimulation of dihydroxyacetone and glycerol kinase activity in *Streptococcus faecalis* by phosphoenolpyruvate-dependent phosphorylation catalyzed by enzyme I and HPr of the phosphotransferase system. J. Bacteriol. *166*, 829-836.

Dharmadi, Y., Murarka, A., and Gonzalez, R. (2006). Anaerobic fermentation of glycerol by *Escherichia coli*: a new platform for metabolic engineering. Biotechnol. Bioeng. *94*, 821-829.

Dihazi, H., Kessler, R., and Eschrich, K. (2004). High osmolarity glycerol (HOG) pathway-induced phosphorylation and activation of 6-phosphofructo-2-kinase are essential for glycerol accumulation and yeast cell proliferation under hyperosmotic stress. J. Biol. Chem. *279*, 23961-23968.

Dramsi, S., Kocks, C., Forestier, C., and Cossart, P. (1993). Internalin-mediated invasion of epithelial cells by *Listeria monocytogenes* is regulated by the bacterial growth state, temperature and the pleiotropic activator *prfA*. Mol. Microbiol. *9*, 931-941.

Duchesne, L., Deschamps, S., Pellerin, I., Lagree, V., Froger, A., Thomas, D., Bron, P., Delamarche, C., and Hubert, J.F. (2001). Oligomerization of water and solute channels of the major intrinsic protein (MIP) family. Kidney Int. *60*, 422-426.

Dyall-Smith, M. (2008). The Halohandbook: protocols for halobacterial genetics. http://www.haloarchaea.com/resources/halohandbook/Halohandbook_2008_v7.pdf.

Ebright, R.H., Ebright, Y.W., and Gunasekera, A. (1989). Consensus DNA site for the *Escherichia coli* catabolite gene activator protein (CAP): CAP exhibits a 450-fold higher affinity for the consensus DNA site than for the *E. coli lac* DNA site. Nucleic Acids Res. *17*, 10295-10305.

Ecelbarger, C.A., Terris, J., Frindt, G., Echevarria, M., Marples, D., Nielsen, S., and Knepper, M.A. (1995). Aquaporin-3 water channel localization and regulation in rat kidney. Am. J. Physiol. *269*, F663-F672.

Eiglmeier, K., Honoré, N., Iuchi, S., Lin, E.C., and Cole, S.T. (1989). Molecular genetic analysis of FNR-dependent promoters. Mol. Microbiol. *3*, 869-878.

Elevi Bardavid, R., Khristo, P., and Oren, A. (2008). Interrelationships between *Dunaliella* and halophilic prokaryotes in saltern crystallizer ponds. Extremophiles *12*, 5-14.

Elevi Bardavid, R. and Oren, A. (2008). Dihydroxyacetone metabolism in *Salinibacter ruber* and in *Haloquadratum walsbyi*. Extremophiles *12*, 125-131.

Elferink, M.G., Albers, S.V., Konings, W.N., and Driessen, A.J. (2001). Sugar transport in *Sulfolobus solfataricus* is mediated by two families of binding protein-dependent ABC transporters. Mol. Microbiol. *39*, 1494-1503.

Erni, B., Siebold, C., Christen, S., Srinivas, A., Oberholzer, A., and Baumann, U. (2006). Small substrate, big surprise: fold, function and phylogeny of dihydroxyacetone kinases. Cell Mol. Life Sci. *63*, 890-900.

Facciotti, M.T., Reiss, D.J., Pan, M., Kaur, A., Vuthoori, M., Bonneau, R., Shannon, P., Srivastava, A., Donohoe, S.M., Hood, L.E., and Baliga, N.S. (2007). General transcription factor specified global gene regulation in archaea. Proc. Natl. Acad. Sci. USA *104*, 4630-4635.

Falb, M., Müller, K., Königsmaier, L., Oberwinkler, T., Horn, P., von Gronau, S., Gonzalez, O., Pfeiffer, F., Bornberg-Bauer, E., and Oesterhelt, D. (2008). Metabolism of halophilic archaea. Extremophiles *12*, 177-196.

Felsenstein, J. (1985). Confidence limits on phylogenies: An apporach using the boostrap. Evolution *39*, 783-791.

Ferreira, A., O'Byrne, C.P., and Boor, K.J. (2001). Role of $\sigma^B$ in heat, ethanol, acid, and oxidative stress resistance and during carbon starvation in *Listeria monocytogenes*. Appl. Environ. Microbiol. *67*, 4454-4457.

Ferreira, C. and Lucas, C. (2007). Glucose repression over *Saccharomyces cerevisiae* glycerol/$H^+$ symporter gene *STL1* is overcome by high temperature. FEBS Lett. *581*, 1923-1927.

Ferreira, C., van Voorst, F., Martins, A., Neves, L., Oliveira, R., Kielland-Brandt, M.C., Lucas, C., and Brandt, A. (2005). A member of the sugar transporter family, Stl1p is the glycerol/$H^+$ symporter in *Saccharomyces cerevisiae*. Mol. Biol. Cell *16*, 2068-2076.

Fiorentino, G., Ronca, R., Cannio, R., Rossi, M., and Bartolucci, S. (2007). MarR-like transcriptional regulator involved in detoxification of aromatic compounds in *Sulfolobus solfataricus*. J. Bacteriol. *189*, 7351-7360.

Forsberg, C.W. (1987). Production of 1,3-propanediol from glycerol by *Clostridium acetobutylicum* and other *Clostridium* species. Appl. Environ. Microbiol. *53*, 639-643.

Freedberg, W.B., Kistler, W.S., and Lin, E.C. (1971). Lethal synthesis of methylglyoxal by *Escherichia coli* during unregulated glycerol metabolism. J. Bacteriol. *108*, 137-144.

Freedberg, W.B. and Lin, E.C. (1973). Three kinds of controls affecting the expression of the *glp* regulon in *Escherichia coli*. J. Bacteriol. *115*, 816-823.

Frey, M., Rothe, M., Wagner, A.F., and Knappe, J. (1994). Adenosylmethionine-dependent synthesis of the glycyl radical in pyruvate formate-lyase by abstraction of the glycine C-2 pro-*S* hydrogen atom. Studies of [$^2$H]glycine-substituted enzyme and peptides homologous to the glycine 734 site. J. Biol. Chem. *269*, 12432-12437.

Froger, A., Rolland, J.P., Bron, P., Lagrée, V., Le Cahérec, F., Deschamps, S., Hubert, J.F., Pellerin, I., Thomas, D., and Delamarche, C. (2001). Functional characterization of a microbial aquaglyceroporin. Microbiology *147*, 1129-1135.

Fu, D., Libson, A., Miercke, L.J., Weitzman, C., Nollert, P., Krucinski, J., and Stroud, R.M. (2000). Structure of a glycerol-conducting channel and the basis for its selectivity. Science *290*, 481-486.

Fujii, S. and Hellebust, J.A. (1992). Release of intracellular glycerol and pore formation in *Dunaliella tertiolecta* exposed to hypertonic stress. Can. J. Bot. *70*, 1313-1318.

Galinier, A., Haiech, J., Kilhoffer, M.C., Jaquinod, M., Stülke, J., Deutscher, J., and Martin-Verstraete, I. (1997). The *Bacillus subtilis crh* gene encodes a HPr-like protein involved in carbon catabolite repression. Proc. Natl. Acad. Sci. USA *94*, 8439-8444.

Galinier, A., Kravanja, M., Engelmann, R., Hengstenberg, W., Kilhoffer, M.C., Deutscher, J., and Haiech, J. (1998). New protein kinase and protein phosphatase families mediate signal transduction in bacterial catabolite repression. Proc. Natl. Acad. Sci. USA *95*, 1823-1828.

Gancedo, C., Llobell, A., Ribas, J.C., and Luchi, F. (1986). Isolation and characterization of mutants from *Schyzosaccharomyces pombe* defective in glycerol catabolism. Eur. J. Biochem. *159*, 171-174.

Garg, R.P., Vargo, C.J., Cui, X., and Kurtz, D.M., Jr. (1996). A [2Fe-2S] protein encoded by an open reading frame upstream of the *Escherichia coli* bacterioferritin gene. Biochemistry *35*, 6297-6301.

Garrett, D.S., Seok, Y.J., Peterkofsky, A., Gronenborn, A.M., and Clore, G.M. (1999). Solution structure of the 40,000 Mr phosphoryl transfer complex between the N-terminal domain of enzyme I and HPr. Nat. Struct. Biol. *6*, 166-173.

Gaurivaud, P., Laigret, F., Garnier, M., and Bové, J.M. (2001). Characterization of FruR as a putative activator of the fructose operon of *Spiroplasma citri*. FEMS Microbiol. Lett. *198*, 73-78.

Gee, R., Goyal, A., Byerrum, R.U., and Tolbert, N.E. (1989). Two isozymes of dihydroxyacetone phosphate reductase in *Dunaliella*. Plant Physiol. *91*, 345-351.

Gee, R., Goyal, A., Byerrum, R.U., and Tolbert, N.E. (1993). Two isoforms of dihydroxyacetone phosphate reductase from the chloroplasts of *Dunaliella tertiolecta*. Plant Physiol. *103*, 243-249.

Gee, R., Goyal, A., Gerber, D., Byerrum, R.U., and Tolbert, N.E. (1988a). Isolation of dihydroxyacetone phosphate reductase from *Dunaliella* chloroplasts and comparison with isozymes from spinach leaves. Plant Physiol. *88*, 896-903.

Gee, R.W., Byerrum, R.U., Gerber, D.W., and Tolbert, N.E. (1988b). Dihydroxyacetone phosphate reductase in plants. Plant Physiol. *86*, 98-103.

Geiduschek, E.P. and Ouhammouch, M. (2005). Archaeal transcription and its regulators. Mol. Microbiol. *56*, 1397-1407.

Georgellis, D., Kwon, O., De Wulf, P., and Lin, E.C. (1998). Signal decay through a reverse phosphorelay in the Arc two-component signal transduction system. J. Biol. Chem. *273*, 32864-32869.

Georgellis, D., Kwon, O., and Lin, E.C. (1999). Amplification of signaling activity of the *arc* two-component system of *Escherichia coli* by anaerobic metabolites. An *in vitro* study with different protein modules. J. Biol. Chem. *274*, 35950-35954.

Georgellis, D., Kwon, O., and Lin, E.C. (2001). Quinones as the redox signal for the *arc* two-component system of bacteria. Science *292*, 2314-2316.

Georgellis, D., Lynch, A.S., and Lin, E.C. (1997). *In vitro* phosphorylation study of the *arc* two-component signal transduction system of *Escherichia coli*. J. Bacteriol. *179*, 5429-5435.

Ghoshal, D., Mach, D., Agarwal, M., Goyal, A., and Goyal, A. (2002). Osmoregulatory isoform of dihydroxyacetone phosphate reductase from *Dunaliella tertiolecta*: purification and characterization. Protein Expr. Purif. *24*, 404-411.

Giard, J.C., Riboulet, E., Verneuil, N., Sanguinetti, M., Auffray, Y., and Hartke, A. (2006). Characterization of Ers, a PrfA-like regulator of *Enterococcus faecalis*. FEMS Immunol. Med. Microbiol. *46*, 410-418.

Glatz, E., Nilsson, R.P., Rutberg, L., and Rutberg, B. (1996). A dual role for the *Bacillus subtilis glpD* leader and the GlpP protein in the regulated expression of *glpD*: antitermination and control of mRNA stability. Mol. Microbiol. *19*, 319-328.

Glatz, E., Persson, M., and Rutberg, B. (1998). Antiterminator protein GlpP of *Bacillus subtilis* binds to *glpD* leader mRNA. Microbiology *144*, 449-456.

Gochnauer, M.B. and Kushner, D.J. (1969). Growth and nutrition of extremely halophilic bacteria. Can. J. Microbiol. *15*, 1157-1165.

Gonzalez, R., Murarka, A., Dharmadi, Y., and Yazdani, S.S. (2008). A new model for the anaerobic fermentation of glycerol in enteric bacteria: trunk and auxiliary pathways in *Escherichia coli*. Metab. Eng. *10*, 234-245.

González-Gil, G., Kahmann, R., and Muskhelishvili, G. (1998). Regulation of *crp* transcription by oscillation between distinct nucleoprotein complexes. EMBO J. *17*, 2877-2885.

González-Pajuelo, M., Andrade, J.C., and Vasconcelos, I. (2004). Production of 1,3-propanediol by *Clostridium butyricum* VPI 3266 using a synthetic medium and raw glycerol. J. Ind. Microbiol. Biotechnol. *31*, 442-446.

Görke, B. and Stülke, J. (2008). Carbon catabolite repression in bacteria: many ways to make the most out of nutrients. Nat. Rev. Microbiol. *6*, 613-624.

Gottfried, E.L. and Robertson, N.A. (1974). Glycerol lysis time as a screening test for erythrocyte disorders. J. Lab Clin. Med. *83*, 323-333.

Goyal, A. (2007). Osmoregulation in *Dunaliella*, Part II: Photosynthesis and starch contribute carbon for glycerol synthesis during a salt stress in *Dunaliella tertiolecta*. Plant Physiol. Biochem. *45*, 705-710.

Goyal, A., Brown, A.D., and Gimmler, H. (1987). Regulation of salt-induced starch degradation in *Dunaliella tertiolecta*. J. Plant Physiol. *127*, 77-96.

Green, J., Sharrocks, A.D., Green, B., Geisow, M., and Guest, J.R. (1993). Properties of FNR proteins substituted at each of the five cysteine residues. Mol. Microbiol. *8*, 61-68.

Gregor, D. and Pfeifer, F. (2005). *In vivo* analyses of constitutive and regulated promoters in halophilic archaea. Microbiology *151*, 25-33.

Gutknecht, R., Beutler, R., Garcia-Alles, L.F., Baumann, U., and Erni, B. (2001). The dihydroxyacetone kinase of *Escherichia coli* utilizes a phosphoprotein instead of ATP as phosphoryl donor. EMBO J. *20*, 2480-2486.

Haghjoo, E. and Galán, J.E. (2007). Identification of a transcriptional regulator that controls intracellular gene expression in *Salmonella typhi*. Mol. Microbiol. *64*, 1549-1561.

Hall, T.A. (1999). Bioedit: a user-friendly biological sequence alignment editor and analysis program for Windows 95/98/NT. Nucleic Acids Symp. Ser. *41*, 95-98.

Hames, C., Halbedel, S., Hoppert, M., Frey, J., and Stülke, J. (2009). Glycerol metabolism is important for cytotoxicity of *Mycoplasma pneumoniae*. J. Bacteriol. *191*, 747-753.

Hanamura, A. and Aiba, H. (1992). A new aspect of transcriptional control of the *Escherichia coli crp* gene: positive autoregulation. Mol. Microbiol. *6*, 2489-2497.

Hartman, A.L., Norais, C., Badger, J.H., Delmas, S., Haldenby, S., Madupu, R., Robinson, J., Khouri, H., Ren, Q., Lowe, T.M., Maupin-Furlow, J., Pohlschroder, M., Daniels, C., Pfeiffer, F., Allers, T., and Eisen, J.A. (2010). The complete genome sequence of *Haloferax volcanii* DS2, a model archaeon. PLoS One *5*, e9605.

Hayashi, S., Koch, J., and Lin, E. (1964). Active Tranport of L-$\alpha$-glycerophosphate in *Escherichia coli*. J. Biol. Chem. *239*, 3098-3105.

Hayashi, S.I. and Lin, E.C. (1965). Product induction of glycerol kinase in *Escherichia coli*. J. Mol. Biol. *14*, 515-521.

Hedfalk, K., Bill, R.M., Mullins, J.G., Karlgren, S., Filipsson, C., Bergstrom, J., Tamás, M.J., Rydström, J., and Hohmann, S. (2004). A regulatory domain in the C-terminal extension of the yeast glycerol channel Fps1p. J. Biol. Chem. *279*, 14954-14960.

Heller, K.B., Lin, E.C., and Wilson, T.H. (1980). Substrate specificity and transport properties of the glycerol facilitator of *Escherichia coli*. J. Bacteriol. *144*, 274-278.

Henkin, T.M., Grundy, F.J., Nicholson, W.L., and Chambliss, G.H. (1991). Catabolite repression of $\alpha$-amylase gene expression in *Bacillus subtilis* involves a *trans*-acting gene product homologous to the *Escherichia coli lacI* and *galR* repressors. Mol. Microbiol. *5*, 575-584.

Hirokawa, T., Boon-Chieng, S., and Mitaku, S. (1998). SOSUI: classification and secondary structure prediction system for membrane proteins. Bioinformatics *14*, 378-379.

Hochstein, L.I. (1974). The metabolism of carbohydrates by extremely halophilic bacteria: glucose metabolism via a modified Entner-Doudoroff pathway. Can. J. Microbiol. *20*, 1085-1091.

Hohmann, I., Bill, R.M., Kayingo, I., and Prior, B.A. (2000). Microbial MIP channels. Trends Microbiol. *8*, 33-38.

Hohmann, S. (2002). Osmotic stress signaling and osmoadaptation in yeasts. Microbiol. Mol. Biol. Rev. *66*, 300-372.

Holland, I.B. and Blight, M.A. (1999). ABC-ATPases, adaptable energy generators fuelling transmembrane movement of a variety of molecules in organisms from bacteria to humans. J. Mol. Biol. *293*, 381-399.

Holmberg, C. and Rutberg, B. (1991). Expression of the gene encoding glycerol-3-phosphate dehydrogenase (*glpD*) in *Bacillus subtilis* is controlled by antitermination. Mol. Microbiol. *5*, 2891-2900.

Holmes, M.L. and Dyall-Smith, M.L. (2000). Sequence and expression of a halobacterial beta-galactosidase gene. Mol. Microbiol. *36*, 114-122.

Holtman, C.K., Pawlyk, A.C., Meadow, N.D., and Pettigrew, D.W. (2001). Reverse genetics of *Escherichia coli* glycerol kinase allosteric regulation and glucose control of glycerol utilization *in vivo*. J. Bacteriol. *183*, 3336-3344.

Horlacher, R., Xavier, K.B., Santos, H., DiRuggiero, J., Kossmann, M., and Boos, W. (1998). Archaeal binding protein-dependent ABC transporter: molecular and biochemical analysis of the trehalose/maltose transport system of the hyperthermophilic archaeon *Thermococcus litoralis*. J. Bacteriol. *180*, 680-689.

Hu, Z.C., Liu, Z.Q., Zheng, Y.G., and Shen, Y.C. (2010). Production of 1,3-dihydroxyacetone from glycerol by *Gluconobacter oxydans* ZJB09112. J. Microbiol. Biotechnol. *20*, 340-345.

Humbard, M.A., Zhou, G., and Maupin-Furlow, J.A. (2009). The N-terminal penultimate residue of 20S proteasome $\alpha$1 influences its N$\alpha$ acetylation and protein levels as well as growth rate and stress response of *Haloferax volcanii* . J. Bacteriol. *191*, 3794-3803.

Hunter, S., Apweiler, R., Attwood, T.K., Bairoch, A., Bateman, A., Binns, D., Bork, P., Das, U., Daugherty, L., Duquenne, L., Finn, R.D., Gough, J., Haft, D., Hulo, N., Kahn, D., Kelly, E., Laugraud, A., Letunic, I., Lonsdale, D., Lopez, R., Madera, M., Maslen, J., McAnulla, C., McDowall, J., Mistry, J., Mitchell, A., Mulder, N., Natale, D., Orengo, C., Quinn, A.F., Selengut, J.D., Sigrist, C.J., Thimma, M., Thomas, P.D., Valentin, F., Wilson, D., Wu, C.H., and Yeats, C. (2009). InterPro: the integrative protein signature database. Nucleic Acids Res. *37*, D211-D215.

Hurley, J.H. (2003). GAF domains: cyclic nucleotides come full circle. Sci. STKE *2003*, E1.

Hurley, J.H., Faber, H.R., Worthylake, D., Meadow, N.D., Roseman, S., Pettigrew, D.W., and Remington, S.J. (1993). Structure of the regulatory complex of *Escherichia coli* $III^{Glc}$ with glycerol kinase. Science *259*, 673-677.

Hurtado-Gomez, E., Fernandez-Ballester, G., Nothaft, H., Gomez, J., Titgemeyer, F., and Neira, J.L. (2006). Biophysical characterization of the enzyme I of the *Streptomyces coelicolor* phosphoenolpyruvate:sugar phosphotransferase system. Biophys. J. *90*, 4592-4604.

Hutchings, M.I., Crack, J.C., Shearer, N., Thompson, B.J., Thomson, A.J., and Spiro, S. (2002). Transcription factor FnrP from *Paracoccus denitrificans* contains an iron-sulfur cluster and is activated by anoxia: identification of essential cysteine residues. J. Bacteriol. *184*, 503-508.

Ishibashi, K. (2009). New members of mammalian aquaporins: AQP10-AQP12. Handb. Exp. Pharmacol. 251-262.

Ishibashi, K., Yamauchi, K., Kageyama, Y., Saito-Ohara, F., Ikeuchi, T., Marumo, F., and Sasaki, S. (1998). Molecular characterization of human Aquaporin-7 gene and its chromosomal mapping. Biochim. Biophys. Acta *1399*, 62-66.

Ito, T., Nakashimada, Y., Senba, K., Matsui, T., and Nishio, N. (2005). Hydrogen and ethanol production from glycerol-containing wastes discharged after biodiesel manufacturing process. J. Biosci. Bioeng. *100*, 260-265.

Iuchi, S., Cameron, D.C., and Lin, E.C. (1989). A second global regulator gene (*arcB*) mediating repression of enzymes in aerobic pathways of *Escherichia coli*. J. Bacteriol. *171*, 868-873.

Iuchi, S., Cole, S.T., and Lin, E.C. (1990). Multiple regulatory elements for the *glpA* operon encoding anaerobic glycerol-3-phosphate dehydrogenase and the *glpD* operon encoding aerobic glycerol-3-phosphate dehydrogenase in *Escherichia coli*: further characterization of respiratory control. J. Bacteriol. *172*, 179-184.

Iuchi, S. and Lin, E.C. (1988). *arcA* (*dye*), a global regulatory gene in *Escherichia coli* mediating repression of enzymes in aerobic pathways. Proc. Natl. Acad. Sci. USA *85*, 1888-1892.

Iuchi, S. and Lin, E.C. (1992). Mutational analysis of signal transduction by ArcB, a membrane sensor protein responsible for anaerobic repression of operons involved in the central aerobic pathways in *Escherichia coli*. J. Bacteriol. *174*, 3972-3980.

Jackson, D.W., Simecka, J.W., and Romeo, T. (2002). Catabolite repression of *Escherichia coli* biofilm formation. J. Bacteriol. *184*, 3406-3410.

Jennings, D.H. (1984). Polyol metabolism in fungi. Adv. Microb. Physiol. *25*, 149-193.

Jeon, Y., Lee, Y.S., Han, J.S., Kim, J.B., and Hwang, D.S. (2001). Multimerization of phosphorylated and non-phosphorylated ArcA is necessary for the response regulator function of the Arc two-component signal transduction system. J. Biol. Chem. *276*, 40873-40879.

Johansson, J., Balsalobre, C., Wang, S.Y., Urbonaviciene, J., Jin, D.J., Sondén, B., and Uhlin, B.E. (2000). Nucleoid proteins stimulate stringently controlled bacterial promoters: a link between the cAMP-CRP and the (p)ppGpp regulons in *Escherichia coli*. Cell *102*, 475-485.

Johnsen, U., Selig, M., Xavier, K.B., Santos, H., and Schönheit, P. (2001). Different glycolytic pathways for glucose and fructose in the halophilic archaeon *Halococcus saccharolyticus*. Arch. Microbiol. *175*, 52-61.

Johnson, E.A. and Lin, E.C. (1987). *Klebsiella pneumoniae* 1,3-propanediol:$NAD^+$ oxidoreductase. J. Bacteriol. *169*, 2050-2054.

Jones, B.E., Dossonnet, V., Küster, E., Hillen, W., Deutscher, J., and Klevit, R.E. (1997). Binding of the catabolite repressor protein CcpA to its DNA target is regulated by phosphorylation of its corepressor HPr. J. Biol. Chem. *272*, 26530-26535.

Jovell, R.J., Macario, A.J., and Conway, d.M. (1996). ABC transporters in Archaea: two genes encoding homologs of the nucleotide-binding components in the methanogen *Methanosarcina mazei* S-6. Gene *174*, 281-284.

Kaczowka, S.J. and Maupin-Furlow, J.A. (2003). Subunit topology of two 20S proteasomes from *Haloferax volcanii*. J. Bacteriol. *185*, 165-174.

Kaczowka, S.J., Reuter, C.J., Talarico, L.A., and Maupin-Furlow, J.A. (2005). Recombinant production of *Zymomonas mobilis* pyruvate decarboxylase in the haloarchaeon *Haloferax volcanii*. Archaea *1*, 327-334.

Kanai, T., Akerboom, J., Takedomi, S., van de Werken, H.J., Blombach, F., van der, O.J., Murakami, T., Atomi, H., and Imanaka, T. (2007). A global transcriptional regulator in *Thermococcus kodakaraensis* controls the expression levels of both glycolytic and gluconeogenic enzyme-encoding genes. J. Biol. Chem. *282*, 33659-33670.

Kang, Y., Weber, K.D., Qiu, Y., Kiley, P.J., and Blattner, F.R. (2005). Genome-wide expression analysis indicates that FNR of *Escherichia coli* K-12 regulates a large number of genes of unknown function. J. Bacteriol. *187*, 1135-1160.

Karlgren, S., Filipsson, C., Mullins, J.G., Bill, R.M., Tamás, M.J., and Hohmann, S. (2004). Identification of residues controlling transport through the yeast aquaglyceroporin Fps1 using a genetic screen. Eur. J. Biochem. *271*, 771-779.

Karlgren, S., Pettersson, N., Nordlander, B., Mathai, J.C., Brodsky, J.L., Zeidel, M.L., Bill, R.M., and Hohmann, S. (2005). Conditional osmotic stress in yeast: a system to study transport through aquaglyceroporins and osmostress signaling. J. Biol. Chem. *280*, 7186-7193.

Kates, M. (1978). The phytanyl ether-linked polar lipids and isoprenoid neutral lipids of extremely halophilic bacteria. Prog. Chem. Fats Other Lipids *15*, 301-342.

Kayingo, G., Martins, A., Andrie, R., Neves, L., Lucas, C., and Wong, B. (2009). A permease encoded by *STL1* is required for active glycerol uptake by *Candida albicans*. Microbiology *155*, 1547-1557.

Keese, A.M., Schut, G.J., Ouhammouch, M., Adams, M.W., and Thomm, M. (2010). Genome-wide identification of targets for the archaeal heat shock regulator *phr* by cell-free transcription of genomic DNA. J. Bacteriol. *192*, 1292-1298.

Kets, E.P., Galinski, E.A., de Wit, M., de Bont, J.A., and Heipieper, H.J. (1996). Mannitol, a novel bacterial compatible solute in *Pseudomonas putida* S12. J. Bacteriol. *178*, 6665-6670.

Khoroshilova, N., Popescu, C., Münck, E., Beinert, H., and Kiley, P.J. (1997). Iron-sulfur cluster disassembly in the FNR protein of *Escherichia coli* by oxygen [4Fe-4S] to [2Fe-2S] conversion with loss of biological activity. Proc. Natl. Acad. Sci. USA *94*, 6087-6092.

Kimura, T., Takahashi, M., Yoshihara, K., Furuichi, T., Suzuki, K., Imai, K., Karita, S., Sakka, K., and Ohmiya, K. (1998). Cloning and characterization of two genes encoding dihydroxyacetone kinase from *Schizosaccharomyces pombe* IFO 0354. Biochim. Biophys. Acta *1442*, 361-368.

Klevit, R.E. and Waygood, E.B. (1986). Two-dimensional $^{1}$H NMR studies of histidine-containing protein from *Escherichia coli*. 3. Secondary and tertiary structure as determined by NMR. Biochemistry *25*, 7774-7781.

Kolb, A., Busby, S., Buc, H., Garges, S., and Adhya, S. (1993). Transcriptional regulation by cAMP and its receptor protein. Annu. Rev. Biochem. *62*, 749-795.

Koning, S.M., Elferink, M.G., Konings, W.N., and Driessen, A.J. (2001). Cellobiose uptake in the hyperthermophilic archaeon *Pyrococcus furiosus* is mediated by an inducible, high-affinity ABC transporter. J. Bacteriol. *183*, 4979-4984.

Koning, S.M., Konings, W.N., and Driessen, A.J. (2002). Biochemical evidence for the presence of two α-glucoside ABC-transport systems in the hyperthermophilic archaeon *Pyrococcus furiosus*. Archaea *1*, 19-25.

Kormann, A.W., Hurst, R.O., and Flynn, T.G. (1972). Purification and properties of an $NADP^+$ -dependent glycerol dehydrogenase from rabbit skeletal muscle. Biochim. Biophys. Acta *258*, 40-55.

Körner, H., Sofia, H.J., and Zumft, W.G. (2003). Phylogeny of the bacterial superfamily of Crp-Fnr transcription regulators: exploiting the metabolic spectrum by controlling alternative gene programs. FEMS Microbiol. Rev. *27*, 559-592.

Kotrba, P., Inui, M., and Yukawa, H. (2001). Bacterial phosphotransferase system (PTS) in carbohydrate uptake and control of carbon metabolism. J. Biosci. Bioeng. *92*, 502-517.

Krüger, K., Hermann, T., Armbruster, V., and Pfeifer, F. (1998). The transcriptional activator GvpE for the halobacterial gas vesicle genes resembles a basic region leucine-zipper regulatory protein. J. Mol. Biol. *279*, 761-771.

Kuchitsu, K., Katsuhara, M., and Miyachi, S. (1989). Rapid cytoplasmic alkalinization and dynamics of intracellular copmartmentation in inorganic phosphate during adaptation against salt stress in a halotolerant green alga *Dunaliella tertiolecta*: $^{31}P$ Nuclear Magnetic Resonance study. Plant Cell Physiol. *30*, 407-414.

Kumar, S., Tamura, K., and Nei, M. (2004). MEGA3: Integrated software for Molecular Evolutionary Genetics Analysis and sequence alignment. Brief. Bioinform. *5*, 150-163.

Kuritzkes, D.R., Zhang, X.Y., and Lin, E.C. (1984). Use of φ(*glp-lac*) in studies of respiratory regulation of the *Escherichia coli* anaerobic *sn*-glycerol-3-phosphate dehydrogenase genes (*glpAB*). J. Bacteriol. *157*, 591-598.

Kuriyama, H., Shimomura, I., Kishida, K., Kondo, H., Furuyama, N., Nishizawa, H., Maeda, N., Matsuda, M., Nagaretani, H., Kihara, S., Nakamura, T., Tochino, Y., Funahashi, T., and Matsuzawa, Y. (2002). Coordinated regulation of fat-specific and liver-specific glycerol channels, aquaporin adipose and aquaporin 9. Diabetes *51*, 2915-2921.

Kyrpides, N.C. and Ouzounis, C.A. (1999). Transcription in archaea. Proc. Natl. Acad. Sci. USA *96*, 8545-8550.

Laemmli, U.K. (1970). Cleavage of structural proteins during the assembly of the head of bacteriophage T4. Nature *227*, 680-685.

Lages, F. and Lucas, C. (1997). Contribution to the physiological characterization of glycerol active uptake in *Saccharomyces cerevisiae*. Biochim. Biophys. Acta *1322*, 8-18.

Lai, M.C., Sowers, K.R., Robertson, D.E., Roberts, M.F., and Gunsalus, R.P. (1991). Distribution of compatible solutes in the halophilic methanogenic archaebacteria. J. Bacteriol. *173*, 5352-5358.

Lamberg, K.E., Luther, C., Weber, K.D., and Kiley, P.J. (2002). Characterization of activating region 3 from *Escherichia coli* FNR. J. Mol. Biol. *315*, 275-283.

Landis, L., Xu, J., and Johnson, R.C. (1999). The cAMP receptor protein CRP can function as an osmoregulator of transcription in *Escherichia coli*. Genes Dev. *13*, 3081-3091.

Lanyi, J.K. (1974). Salt-dependent properties of proteins from extremely halophilic bacteria. Bacteriol. Rev. *38*, 272-290.

Larson, T.J., Cantwell, J.S., and Loo-Bhattacharya, A.T. (1992). Interaction at a distance between multiple operators controls the adjacent, divergently transcribed *glpTQ-glpACB* operons of *Escherichia coli* K-12. J. Biol. Chem. *267*, 6114-6121.

Larson, T.J., Ye, S.Z., Weissenborn, D.L., Hoffmann, H.J., and Schweizer, H. (1987). Purification and characterization of the repressor for the *sn*-glycerol 3-phosphate regulon of *Escherichia coli* K12. J. Biol. Chem. *262*, 15869-15874.

Larsson, C., Påhlman, I.L., Ansell, R., Rigoulet, M., Adler, L., and Gustafsson, L. (1998). The importance of the glycerol 3-phosphate shuttle during aerobic growth of *Saccharomyces cerevisiae*. Yeast *14*, 347-357.

Lawrence, J.G. (1997). Selfish operons and speciation by gene transfer. Trends Microbiol. *5*, 355-359.

Lazazzera, B.A., Beinert, H., Khoroshilova, N., Kennedy, M.C., and Kiley, P.J. (1996). DNA binding and dimerization of the Fe-S-containing FNR protein from *Escherichia coli* are regulated by oxygen. J. Biol. Chem. *271*, 2762-2768.

Lee, D.J., Wing, H.J., Savery, N.J., and Busby, S.J. (2000). Analysis of interactions between Activating Region 1 of *Escherichia coli* FNR protein and the C-terminal domain of the RNA polymerase $\alpha$ subunit: use of alanine scanning and suppression genetics. Mol. Microbiol. *37*, 1032-1040.

Lee, M.D., Bhakta, K.Y., Raina, S., Yonescu, R., Griffin, C.A., Copeland, N.G., Gilbert, D.J., Jenkins, N.A., Preston, G.M., and Agre, P. (1996). The human Aquaporin-5 gene. Molecular characterization and chromosomal localization. J. Biol. Chem. *271*, 8599-8604.

Lee, P.C., Lee, W.G., Lee, S.Y., and Chang, H.N. (2001). Succinic acid production with reduced by-product formation in the fermentation of *Anaerobiospirillum succiniciproducens* using glycerol as a carbon source. Biotechnol. Bioeng. *72*, 41-48.

Lee, S.J., Böhm, A., Krug, M., and Boos, W. (2007). The ABC of binding-protein-dependent transport in Archaea. Trends Microbiol. *15*, 389-397.

Lee, S.J., Engelmann, A., Horlacher, R., Qu, Q., Vierke, G., Hebbeln, C., Thomm, M., and Boos, W. (2003). TrmB, a sugar-specific transcriptional regulator of the trehalose/maltose ABC transporter from the hyperthermophilic archaeon *Thermococcus litoralis*. J. Biol. Chem. *278*, 983-990.

Lee, S.J., Moulakakis, C., Koning, S.M., Hausner, W., Thomm, M., and Boos, W. (2005). TrmB, a sugar sensing regulator of ABC transporter genes in *Pyrococcus furiosus* exhibits dual promoter specificity and is controlled by different inducers. Mol. Microbiol. *57*, 1797-1807.

Lee, S.J., Surma, M., Hausner, W., Thomm, M., and Boos, W. (2008). The role of TrmB and TrmB-like transcriptional regulators for sugar transport and metabolism in the hyperthermophilic archaeon *Pyrococcus furiosus*. Arch. Microbiol. *190*, 247-256.

Lerner, H.R. and Avron, M. (1977). Dihydroxyacetone kinase activity in *Dunaliella parva*. Plant Physiol. *59*, 15-17.

Lerner, H.R., Sussman, I., and Avron, M. (1980). Characterization and partial purification of dihydroxyacetone kinase in *Dunaliella salina*. Biochim. Biophys. Acta *615*, 1-9.

Lerner, J. (1987). Acidic amino acid transport in animal cells and tissues. Comp. Biochem. Physiol. B *87*, 443-457.

LiCalsi, C., Crocenzi, T.S., Freire, E., and Roseman, S. (1991). Sugar transport by the bacterial phosphotransferase system. Structural and thermodynamic domains of enzyme I of *Salmonella typhimurium*. J. Biol. Chem. *266*, 19519-19527.

Lin, E.C. (1977). Glycerol utilization and its regulation in mammals. Annu. Rev. Biochem. *46*, 765-795.

Liska, A.J., Shevchenko, A., Pick, U., and Katz, A. (2004). Enhanced photosynthesis and redox energy production contribute to salinity tolerance in *Dunaliella* as revealed by homology-based proteomics. Plant Physiol. *136*, 2806-2817.

Liu, W.Z., Faber, R., Feese, M., Remington, S.J., and Pettigrew, D.W. (1994). *Escherichia coli* glycerol kinase: role of a tetramer interface in regulation by fructose 1,6-bisphosphate and phosphotransferase system regulatory protein $III^{glc}$. Biochemistry *33*, 10120-10126.

Liu, Y., Zhang, Y.G., Zhang, R.B., Zhang, F., and Zhu, J. (2010). Glycerol/Glucose Co-Fermentation: One More Proficient Process to Produce Propionic Acid by *Propionibacterium acidipropionici*. Curr. Microbiol .

Liu, Z., Carbrey, J.M., Agre, P., and Rosen, B.P. (2004). Arsenic trioxide uptake by human and rat aquaglyceroporins. Biochem. Biophys. Res. Commun. *316*, 1178-1185.

Lu, M., Lee, M.D., Smith, B.L., Jung, J.S., Agre, P., Verdijk, M.A., Merkx, G., Rijss, J.P., and Deen, P.M. (1996). The human AQP4 gene: definition of the locus encoding two water channel polypeptides in brain. Proc. Natl. Acad. Sci. USA *93*, 10908-10912.

Lynch, W.H. and Franklin, M. (1978). Effect of temperature on diauxic growth with glucose and organic acids in *Pseudomonas fluorescens*. Arch. Microbiol. *118*, 133-140.

MacDonald, R.E., Greene, R.V., and Lanyi, J.K. (1977). Light-activated amino acid transport systems in *Halobacterium halobium* envelope vesicles: role of chemical and electrical gradients. Biochemistry *16*, 3227-3235.

Maciaszczyk-Dziubinska, E., Migdal, I., Migocka, M., Bocer, T., and Wysocki, R. (2010). The yeast aquaglyceroporin Fps1p is a bidirectional arsenite channel. FEBS Lett. *584*, 726-732.

Madigan, M.T., Martinko, J.M., and Parker, J. (2006). Cell Structure/Function. In Brock Biology of Microorganisms,(New York: Pearson Printing Hall, Inc.), pp. 66-101.

Mao, X.J., Huo, Y.X., Buck, M., Kolb, A., and Wang, Y.P. (2007). Interplay between CRP-cAMP and PII-Ntr systems forms novel regulatory network between carbon metabolism and nitrogen assimilation in *Escherichia coli*. Nucleic Acids Res. *35*, 1432-1440.

Matsuzawa, T., Ohashi, T., Hosomi, A., Tanaka, N., Tohda, H., and Takegawa, K. (2010). The *gld1*$^{+}$ gene encoding glycerol dehydrogenase is required for glycerol metabolism in *Schizosaccharomyces pombe*. Appl. Microbiol. Biotechnol. *87*, 715-727.

McCurdy, D.K., Schneider, B., and Scheie, H.G. (1966). Oral glycerol: the mechanism of intraocular hypotension. Am. J. Ophthalmol. *61*, 1244-1249.

Meadow, N.D. and Roseman, S. (1996). Rate and equilibrium constants for phosphoryltransfer between active site histidines of *Escherichia coli* HPr and the signal transducing protein III$^{Glc}$. J. Biol. Chem. *271*, 33440-33445.

Mellati, A.A., Yücel, M., Altinörs, N., and Gündüz, U. (1992). Regulation of M2-type pyruvate kinase from human meningioma by allosteric effectors fructose 1,6 diphosphate and L-alanine. Cancer Biochem. Biophys. *13*, 33-41.

Mettert, E.L. and Kiley, P.J. (2005). ClpXP-dependent proteolysis of FNR upon loss of its sensing oxygen [4Fe-4S] cluster. J. Mol. Biol. *354*, 220-232.

Miwa, Y., Nakata, A., Ogiwara, A., Yamamoto, M., and Fujita, Y. (2000). Evaluation and characterization of catabolite-responsive elements (*cre*) of *Bacillus subtilis*. Nucleic Acids Res. *28*, 1206-1210.

Mobasheri, A. and Marples, D. (2004). Expression of the AQP-1 water channel in normal human tissues: a semiquantitative study using tissue microarray technology. Am. J. Physiol. Cell Physiol. *286*, C529-C537.

Moore, L.J. and Kiley, P.J. (2001). Characterization of the dimerization domain in the FNR transcription factor. J. Biol. Chem. *276*, 45744-45750.

Morett, E. and Segovia, L. (1993). The $\sigma^{54}$ bacterial enhancer-binding protein family: mechanism of action and phylogenetic relationship of their functional domains. J. Bacteriol. *175*, 6067-6074.

Mori, K. and Toraya, T. (1999). Mechanism of reactivation of coenzyme B12-dependent diol dehydratase by a molecular chaperone-like reactivating factor. Biochemistry *38*, 13170-13178.

Mu, Y., Teng, H., Zhang, D.J., Wang, W., and Xiu, Z.L. (2006). Microbial production of 1,3-propanediol by *Klebsiella pneumoniae* using crude glycerol from biodiesel preparations. Biotechnol. Lett. *28*, 1755-1759.

Munch-Petersen, A. and Jensen, N. (1990). Analysis of the regulatory region of the *Escherichia coli nupG* gene, encoding a nucleoside-transport protein. Eur. J. Biochem. *190*, 547-551.

Murarka, A., Dharmadi, Y., Yazdani, S.S., and Gonzalez, R. (2008). Fermentative utilization of glycerol by *Escherichia coli* and its implications for the production of fuels and chemicals. Appl. Environ. Microbiol. *74*, 1124-1135.

Muro-Pastor, M.I., Reyes, J.C., and Florencio, F.J. (2001). Cyanobacteria perceive nitrogen status by sensing intracellular 2-oxoglutarate levels. J. Biol. Chem. *276*, 38320-38328.

Nelissen, B., De Wachter, R., and Goffeau, A. (1997). Classification of all putative permeases and other membrane plurispanners of the major facilitator superfamily encoded by the complete genome of *Saccharomyces cerevisiae*. FEMS Microbiol. Rev. *21*, 113-134.

Nevoigt, E. and Stahl, U. (1996). Reduced pyruvate decarboxylase and increased glycerol-3-phosphate dehydrogenase [$NAD^+$] levels enhance glycerol production in *Saccharomyces cerevisiae*. Yeast *12*, 1331-1337.

Ng, W.L., Yang, C.F., Halladay, J.T., Arora, P., and DasSarma, S. (1995). Isolation of genomic and plasmid DNAs from *Halobacterium halobium.* In Archaea: a Laboratory Manual 1, F.T. Robb, A.R. Place, S. DasSarma, and E.M. Fleischmann, eds. (Cold Spring Harbor: Cold Spring Harbor Laboratory Press), pp. 179-184.

Nilsson, R.P., Beijer, L., and Rutberg, B. (1994). The *glpT* and *glpQ* genes of the glycerol regulon in *Bacillus subtilis*. Microbiology *140*, 723-730.

Nishihara, M., Yamazaki, T., Oshima, T., and Koga, Y. (1999). *sn*-glycerol-1-phosphate-forming activities in Archaea: separation of archaeal phospholipid biosynthesis and glycerol catabolism by glycerophosphate enantiomers. J. Bacteriol. *181*, 1330-1333.

Nishino, K., Senda, Y., and Yamaguchi, A. (2008). CRP regulator modulates multidrug resistance of *Escherichia coli* by repressing the *mdtEF* multidrug efflux genes. J. Antibiot. (Tokyo) *61*, 120-127.

Nissen, T.L., Hamann, C.W., Kielland-Brandt, M.C., Nielsen, J., and Villadsen, J. (2000). Anaerobic and aerobic batch cultivations of *Saccharomyces cerevisiae* mutants impaired in glycerol synthesis. Yeast *16*, 463-474.

Niu, W., Kim, Y., Tau, G., Heyduk, T., and Ebright, R.H. (1996). Transcription activation at class II CAP-dependent promoters: two interactions between CAP and RNA polymerase. Cell *87*, 1123-1134.

Norbeck, J. and Blomberg, A. (1997). Metabolic and regulatory changes associated with growth of *Saccharomyces cerevisiae* in 1.4 M NaCl. Evidence for osmotic induction of glycerol dissimilation via the dihydroxyacetone pathway. J. Biol. Chem. *272*, 5544-5554.

Norbeck, J., Påhlman, A.K., Akhtar, N., Blomberg, A., and Adler, L. (1996). Purification and characterization of two isoenzymes of DL-glycerol-3-phosphatase from *Saccharomyces cerevisiae*. Identification of the corresponding *GPP1* and *GPP2* genes and evidence for osmotic regulation of Gpp2p expression by the osmosensing mitogen-activated protein kinase signal transduction pathway. J. Biol. Chem. *271*, 13875-13881.

Novotny, M.J., Frederickson, W.L., Waygood, E.B., and Saier, M.H., Jr. (1985). Allosteric regulation of glycerol kinase by enzyme $III^{glc}$ of the phosphotransferase system in *Escherichia coli* and *Salmonella typhimurium*. J. Bacteriol. *162*, 810-816.

O'Brien, J.R., Raynaud, C., Croux, C., Girbal, L., Soucaille, P., and Lanzilotta, W.N. (2004). Insight into the mechanism of the B12-independent glycerol dehydratase from *Clostridium butyricum*: preliminary biochemical and structural characterization. Biochemistry *43*, 4635-4645.

Oberholzer, A.E., Schneider, P., Baumann, U., and Erni, B. (2006). Crystal structure of the nucleotide-binding subunit DhaL of the *Escherichia coli* dihydroxyacetone kinase. J. Mol. Biol. *359*, 539-545.

Offner, S. and Pfeifer, F. (1995). Complementation studies with the gas vesicle-encoding p-vac region of *Halobacterium salinarium* PHH1 reveal a regulatory role for the p-*gvpDE* genes. Mol. Microbiol. *16*, 9-19.

Ohmiya, R., Yamada, H., Nakashima, K., Aiba, H., and Mizuno, T. (1995). Osmoregulation of fission yeast: cloning of two distinct genes encoding glycerol-3-phosphate dehydrogenase, one of which is responsible for osmotolerance for growth. Mol. Microbiol. *18*, 963-973.

Ohnishi, T., Ohnishi, K., Wang, X., Takahashi, A., and Okaichi, K. (1999). Restoration of mutant TP53 to normal TP53 function by glycerol as a chemical chaperone. Radiat. Res. *151*, 498-500.

Oliveira, R., Lages, F., Silva-Graça, M., and Lucas, C. (2003). Fps1p channel is the mediator of the major part of glycerol passive diffusion in *Saccharomyces cerevisiae*: artefacts and re-definitions. Biochim. Biophys. Acta *1613*, 57-71.

Oren, A. (1994). Enzyme diversity in halophilic archaea. Microbiologia *10*, 217-228.

Oren, A. (1999). Bioenergetic aspects of halophilism. Microbiol. Mol. Biol. Rev. *63*, 334-348.

Oren, A. (2008). Microbial life at high salt concentrations: phylogenetic and metabolic diversity. Saline Systems *4*, 2.

Oren, A. and Gurevich, P. (1994a). Distribution of glycerol dehydrogenase and glycerol kinase activity in halophilic archaea. FEMS Microbiol. Lett. *118*, 311-316.

Oren, A. and Gurevich, P. (1994b). Production of D-lactate, acetate, and pyruvate from glycerol in communities of halophilic archaea in the Dead Sea and in saltern crystallizer ponds. FEMS Microbiol. Ecol. *14*, 147-156.

Oren, A., Heldal, M., Norland, S., and Galinski, E.A. (2002). Intracellular ion and organic solute concentrations of the extremely halophilic bacterium *Salinibacter ruber*. Extremophiles *6*, 491-498.

Oren, A. and Trüper, H.S. (1990). Anaerobic growth of halophilic archaeobacteria by reduction of dimethysulfoxide and trimethylamine *N*-oxide. FEMS Microbiol. Lett. *70*, 33-36.

Ormö, M., Bystrom, C.E., and Remington, S.J. (1998). Crystal structure of a complex of *Escherichia coli* glycerol kinase and an allosteric effector fructose 1,6-bisphosphate. Biochemistry *37*, 16565-16572.

Overbeek, R., Fonstein, M., D'Souza, M., Pusch, G.D., and Maltsev, N. (1999). The use of gene clusters to infer functional coupling. Proc. Natl. Acad. Sci. USA *96*, 2896-2901.

Påhlman, A.K., Granath, K., Ansell, R., Hohmann, S., and Adler, L. (2001). The yeast glycerol 3-phosphatases Gpp1p and Gpp2p are required for glycerol biosynthesis and differentially involved in the cellular responses to osmotic, anaerobic, and oxidative stress. J. Biol. Chem. *276*, 3555-3563.

Papanikolaou, S., Muniglia, L., Chevalot, I., Aggelis, G., and Marc, I. (2002). *Yarrowia lipolytica* as a potential producer of citric acid from raw glycerol. J. Appl. Microbiol. *92*, 737-744.

Passner, J.M., Schultz, S.C., and Steitz, T.A. (2000). Modeling the cAMP-induced allosteric transition using the crystal structure of CAP-cAMP at 2.1 Å resolution. J. Mol. Biol. *304*, 847-859.

Passner, J.M. and Steitz, T.A. (1997). The structure of a CAP-DNA complex having two cAMP molecules bound to each monomer. Proc. Natl. Acad. Sci. USA *94*, 2843-2847.

Pelton, J.G., Torchia, D.A., Remington, S.J., Murphy, K.P., Meadow, N.D., and Roseman, S. (1996). Structures of active site histidine mutants of $III^{Glc}$, a major signal-transducing protein in *Escherichia coli.* Effects on the mechanisms of regulation and phosphoryl transfer. J. Biol. Chem. *271*, 33446-33456.

Petrov, K. and Petrova, P. (2009). High production of 2,3-butanediol from glycerol by *Klebsiella pneumoniae* G31. Appl. Microbiol. Biotechnol. *84*, 659-665.

Pettersson, N., Filipsson, C., Becit, E., Brive, L., and Hohmann, S. (2005). Aquaporins in yeasts and filamentous fungi. Biol. Cell *97*, 487-500.

Pettigrew, D.W. (2009). Oligomeric interactions provide alternatives to direct steric modes of control of sugar kinase/actin/hsp70 superfamily functions by heterotropic allosteric effectors: inhibition of *E. coli* glycerol kinase. Arch. Biochem. Biophys. *492*, 29-39.

Pettigrew, D.W., Meadow, N.D., Roseman, S., and Remington, S.J. (1998). Cation-promoted association of *Escherichia coli* phosphocarrier protein $IIA^{Glc}$ with regulatory target protein glycerol kinase: substitutions of a Zinc(II) ligand and implications for inducer exclusion. Biochemistry *37*, 4875-4883.

Pfaffl, M.W. (2001). A new mathematical model for relative quantification in real-time RT-PCR. Nucleic Acids Res. *29*, e45.

Pocalyko, D.J., Carroll, L.J., Martin, B.M., Babbitt, P.C., and Dunaway-Mariano, D. (1990). Analysis of sequence homologies in plant and bacterial pyruvate phosphate dikinase, enzyme I of the bacterial phosphoenolpyruvate: sugar phosphotransferase system and other PEP-utilizing enzymes. Identification of potential catalytic and regulatory motifs. Biochemistry *29*, 10757-10765.

Ponting, C.P. and Aravind, L. (1997). PAS: a multifunctional domain family comes to light. Curr. Biol. *7*, R674-R677.

Postma, P.W., Lengeler, J.W., and Jacobson, G.R. (1993). Phosphoenolpyruvate:carbohydrate phosphotransferase systems of bacteria. Microbiol. Rev. *57*, 543-594.

Powell, B.S., Court DL, Inada, T., Nakamura, Y., Michotey, V., Cui, X., Reizer, A., Saier, M.H., Jr., and Reizer, J. (1995). Novel proteins of the phosphotransferase system encoded within the *rpoN* operon of *Escherichia coli*. Enzyme IIA$^{Ntr}$ affects growth on organic nitrogen and the conditional lethality of an *era*$^{ts}$ mutant. J. Biol. Chem. *270*, 4822-4839.

Presper, K.A., Wong, C.Y., Liu, L., Meadow, N.D., and Roseman, S. (1989). Site-directed mutagenesis of the phosphocarrier protein. III$^{Glc}$, a major signal-transducing protein in *Escherichia coli*. Proc. Natl. Acad. Sci. USA *86*, 4052-4055.

Quiocho, F.A. and Ledvina, P.S. (1996). Atomic structure and specificity of bacterial periplasmic receptors for active transport and chemotaxis: variation of common themes. Mol. Microbiol. *20*, 17-25.

Rangaswamy, V. and Altekar, W. (1994). Characterization of 1-phosphofructokinase from halophilic archaebacterium *Haloarcula vallismortis*. Biochim. Biophys. Acta *1201*, 106-112.

Rappas, M., Schumacher, J., Beuron, F., Niwa, H., Bordes, P., Wigneshweraraj, S., Keetch, C.A., Robinson, C.V., Buck, M., and Zhang, X. (2005). Structural insights into the activity of enhancer-binding proteins. Science *307*, 1972-1975.

Rawal, N., Kelkar, S.M., and Altekar, W. (1988). Alternative routes of carbohydrate metabolism in halophilic archaebacteria. Indian J. Biochem. Biophys. *25*, 674-686.

Rawls, K.S., Yacovone, S.K., and Maupin-Furlow, J.A. (2010). GlpR represses fructose and glucose metabolic enzymes at the level of transcription in the haloarchaeon *Haloferax volcanii*. J. Bacteriol. *192*, 6251-6260.

Ray, W.K. and Larson, T.J. (2004). Application of AgaR repressor and dominant repressor variants for verification of a gene cluster involved in *N*-acetylgalactosamine metabolism in *Escherichia coli* K-12. Mol. Microbiol. *51*, 813-826.

Raynaud, C., Sarçabal, P., Meynial-Salles, I., Croux, C., and Soucaille, P. (2003). Molecular characterization of the 1,3-propanediol (1,3-PD) operon of *Clostridium butyricum*. Proc. Natl. Acad. Sci. USA *100*, 5010-5015.

Reeve, J.N., Sandman, K., and Daniels, C.J. (1997). Archaeal histones, nucleosomes, and transcription initiation. Cell *89*, 999-1002.

Reizer, J., Hoischen, C., Titgemeyer, F., Rivolta, C., Rabus, R., Stülke, J., Karamata, D., Saier, M.H., Jr., and Hillen, W. (1998). A novel protein kinase that controls carbon catabolite repression in bacteria. Mol. Microbiol. *27*, 1157-1169.

Reizer, J., Reizer, A., and Saier, M.H., Jr. (1993). The MIP family of integral membrane channel proteins: sequence comparisons, evolutionary relationships, reconstructed pathway of evolution, and proposed functional differentiation of the two repeated halves of the proteins. Crit. Rev. Biochem. Mol. Biol. *28*, 235-257.

Remize, F., Barnavon, L., and Dequin, S. (2001). Glycerol export and glycerol-3-phosphate dehydrogenase, but not glycerol phosphatase, are rate limiting for glycerol production in *Saccharomyces cerevisiae*. Metab. Eng. *3*, 301-312.

Riboulet-Bisson, E., Hartke, A., Auffray, Y., and Giard, J.C. (2009a). Ers controls glycerol metabolism in *Enterococcus faecalis*. Curr. Microbiol. *58*, 201-204.

Riboulet-Bisson, E., Le Jeune, A., Benachour, A., Auffray, Y., Hartke, A., and Giard, J.C. (2009b). Ers a Crp/Fnr-like transcriptional regulator of *Enterococcus faecalis*. Int. J. Food Microbiol. *131*, 71-74.

Richey, D.P. and Lin, E.C. (1972). Importance of facilitated diffusion for effective utilization of glycerol by *Escherichia coli*. J. Bacteriol. *112*, 784-790.

Richter, N., Neumann, M., Liese, A., Wohlgemuth, R., Eggert, T., and Hummel, W. (2009). Characterisation of a recombinant NADP-dependent glycerol dehydrogenase from *Gluconobacter oxydans* and its application in the production of L-glyceraldehyde. ChemBioChem *10*, 1888-1896.

Rutledge, R.G. and Côté, C. (2003). Mathematics of quantitative kinetic PCR and the application of standard curves. Nucleic Acids Res. *31*, e93.

Sabourin-Provost, G. and Hallenbeck, P.C. (2009). High yield conversion of a crude glycerol fraction from biodiesel production to hydrogen by photofermentation. Bioresour. Technol. *100*, 3513-3517.

Saier, M.H., Jr. (2000). Families of transmembrane sugar transport proteins. Mol. Microbiol. *35*, 699-710.

Saitou, N. and Nei, M. (1987). The neighbor-joining method: a new method for reconstructing phylogenetic trees. Mol. Biol. Evol. *4*, 406-425.

Sakai, S. and Yagishita, T. (2007). Microbial production of hydrogen and ethanol from glycerol-containing wastes discharged from a biodiesel fuel production plant in a bioelectrochemical reactor with thionine. Biotechnol. Bioeng. *98*, 340-348.

Sakasegawa, S., Hagemeier, C.H., Thauer, R.K., Essen, L.O., and Shima, S. (2004). Structural and functional analysis of the *gpsA* gene product of *Archaeoglobus fulgidus*: a glycerol-3-phosphate dehydrogenase with an unusual $NADP^+$ preference. Protein Sci. *13*, 3161-3171.

Salmon, K., Hung, S.P., Mekjian, K., Baldi, P., Hatfield, G.W., and Gunsalus, R.P. (2003). Global gene expression profiling in *Escherichia coli* K12. The effects of oxygen availability and FNR. J. Biol. Chem. *278*, 29837-29855.

Sanno, Y., Wilson, T.H., and Lin, E.C. (1968). Control of permeation to glycerol in cells of *Escherichia coli*. Biochem. Biophys. Res. Commun. *32*, 344-349.

Santa Anna, L.M., Sebastian, G.V., Pereira, N., Jr., Alves, T.L., Menezes, E.P., and Freire, D.M. (2001). Production of biosurfactant from a new and promising strain of *Pseudomonas aeruginosa* PA1. Appl. Biochem. Biotechnol. *91-93*, 459-467.

Schmid, A.K., Reiss, D.J., Pan, M., Koide, T., and Baliga, N.S. (2009). A single transcription factor regulates evolutionarily diverse but functionally linked metabolic pathways in response to nutrient availability. Mol. Syst. Biol. *5*, 282.

Schmidt, S., Pflüger, K., Kögl, S., Spanheimer, R., and Muller, V. (2007). The salt-induced ABC transporter Ota of the methanogenic archaeon *Methanosarcina mazei* Go1 is a glycine betaine transporter. FEMS Microbiol. Lett. *277*, 44-49.

Schneider, K.L., Pollard, K.S., Baertsch, R., Pohl, A., and Lowe, T.M. (2006). The UCSC archaeal genome browser. Nucleic Acids Res. *34*, D407-D410.

Schryvers, A., Lohmeier, E., and Weiner, J.H. (1978). Chemical and functional properties of the native and reconstituted forms of the membrane-bound, aerobic glycerol-3-phosphate dehydrogenase of *Escherichia coli*. J. Biol. Chem. *253*, 783-788.

Schumacher, M.A., Allen, G.S., Diel, M., Seidel, G., Hillen, W., and Brennan, R.G. (2004). Structural basis for allosteric control of the transcription regulator CcpA by the phosphoprotein HPr-Ser46-P. Cell *118*, 731-741.

Schütz, H. and Radler, F. (1984). Anaerobic reduction of glycerol to propanediol-1,3 by *Lactobacillus brevis* and *Lactobacillus buchneri*. Syst. Appl. Microbiol. *5*, 169-178.

Schweizer, H.P. and Po, C. (1996). Regulation of glycerol metabolism in *Pseudomonas aeruginosa*: characterization of the *glpR* repressor gene. J. Bacteriol. *178*, 5215-5221.

Seifert, C., Bowien, S., Gottschalk, G., and Daniel, R. (2001). Identification and expression of the genes and purification and characterization of the gene products involved in reactivation of coenzyme B12-dependent glycerol dehydratase of *Citrobacter freundii*. Eur. J. Biochem. *268*, 2369-2378.

Senior, B. and Loridan, L. (1968). Studies of liver glycogenoses, with particular reference to the metabolism of intravenously administered glycerol. N. Engl. J. Med. *279*, 958-965.

Seo, M.Y., Seo, J.W., Heo, S.Y., Baek, J.O., Rairakhwada, D., Oh, B.R., Seo, P.S., Choi, M.H., and Kim, C.H. (2009). Elimination of by-product formation during production of 1,3-propanediol in *Klebsiella pneumoniae* by inactivation of glycerol oxidative pathway. Appl. Microbiol. Biotechnol. *84*, 527-534.

Severina, L.O., Pimenov, N.V., and Plakunov, V.K. (1991). Glucose transport into the extremely halophilic archaebacteria. Arch. Microbiol. *155*, 131-136.

Sharma, H., Yu, S., Kong, J., Wang, J., and Steitz, T.A. (2009). Structure of apo-CAP reveals that large conformational changes are necessary for DNA binding. Proc. Natl. Acad. Sci. USA *106*, 16604-16609.

Sher, J., Elevi, R., Mana, L., and Oren, A. (2004). Glycerol metabolism in the extremely halophilic bacterium *Salinibacter ruber*. FEMS Microbiol. Lett. *232*, 211-215.

Sherwood, K.E., Cano, D.J., and Maupin-Furlow, J.A. (2009). Glycerol-mediated repression of glucose metabolism and glycerol kinase as the sole route of glycerol catabolism in the haloarchaeon *Haloferax volcanii*. J. Bacteriol. *191*, 4307-4315.

Siebers, B. and Schönheit, P. (2005). Unusual pathways and enzymes of central carbohydrate metabolism in Archaea. Curr. Opin. Microbiol. *8*, 695-705.

Siebold, C., Arnold, I., Garcia-Alles, L.F., Baumann, U., and Erni, B. (2003a). Crystal structure of the *Citrobacter freundii* dihydroxyacetone kinase reveals an eight-stranded $\alpha$-helical barrel ATP-binding domain. J. Biol. Chem. *278*, 48236-48244.

Siebold, C., Garcia-Alles, L.F., Erni, B., and Baumann, U. (2003b). A mechanism of covalent substrate binding in the x-ray structure of subunit K of the *Escherichia coli* dihydroxyacetone kinase. Proc. Natl. Acad. Sci. USA *100*, 8188-8192.

Soppa, J. (1999). Transcription initiation in Archaea: facts, factors and future aspects. Mol. Microbiol. *31*, 1295-1305.

Spiro, S., Gaston, K.L., Bell, A.I., Roberts, R.E., Busby, S.J., and Guest, J.R. (1990). Interconversion of the DNA-binding specificities of two related transcription regulators, CRP and FNR. Mol. Microbiol. *4*, 1831-1838.

Sprague, G.F. and Cronan, J.E. (1977). Isolation and characterization of *Saccharomyces cerevisiae* mutants defective in glycerol catabolism. J. Bacteriol. *129*, 1335-1342.

St Martin, E.J., Freedberg, W.B., and Lin, E.C. (1977). Kinase replacement by a dehydrogenase for *Escherichia coli* glycerol utilization. J. Bacteriol. *131*, 1026-1028.

Stülke, J., Arnaud, M., Rapoport, G., and Martin-Verstraete, I. (1998). PRD--a protein domain involved in PTS-dependent induction and carbon catabolite repression of catabolic operons in bacteria. Mol. Microbiol. *28*, 865-874.

Stülke, J. and Hillen, W. (1998). Coupling physiology and gene regulation in bacteria: the phosphotransferase sugar uptake system delivers the signals. Naturwissenschaften *85*, 583-592.

Stülke, J., Martin-Verstraete, I., Zagorec, M., Rose, M., Klier, A., and Rapoport, G. (1997). Induction of the *Bacillus subtilis ptsGHI* operon by glucose is controlled by a novel antiterminator, GlcT. Mol. Microbiol. *25*, 65-78.

Sui, H., Walian, P.J., Tang, G., Oh, A., and Jap, B.K. (2000). Crystallization and preliminary X-ray crystallographic analysis of water channel AQP1. Acta Crystallogr. D Biol. Crystallogr. *56*, 1198-1200.

Sutton, V.R., Stubna, A., Patschkowski, T., Munck, E., Beinert, H., and Kiley, P.J. (2004). Superoxide destroys the $[2Fe\text{-}2S]^{2+}$ cluster of FNR from *Escherichia coli*. Biochemistry *43*, 791-798.

Takano, J., Kaidoh, K., and Kamo, N. (1995). Fructose transport by *Haloferax volcanii*. Can. J. Microbiol. *41*, 241-246.

Talarico, T.L., Axelsson, L.T., Novotny, J., Fiuzat, M., and Dobrogosz, W.J. (1990). Utilization of glycerol as a hydrogen acceptor by *Lactobacillus reuteri:* purification of 1,3-propanediol:NAD oxidoreductase. Appl. Environ. Microbiol. *56*, 943-948.

Tamás, M.J., Karlgren, S., Bill, R.M., Hedfalk, K., Allegri, L., Ferreira, M., Thevelein, J.M., Rydstrom, J., Mullins, J.G., and Hohmann, S. (2003). A short regulatory domain restricts glycerol transport through yeast Fps1p. J. Biol. Chem. *278*, 6337-6345.

Tamás, M.J., Luyten, K., Sutherland, F.C., Hernandez, A., Albertyn, J., Valadi, H., Li, H., Prior, B.A., Kilian, S.G., Ramos, J., Gustafsson, L., Thevelein, J.M., and Hohmann, S. (1999). Fps1p controls the accumulation and release of the compatible solute glycerol in yeast osmoregulation. Mol. Microbiol. *31*, 1087-1104.

Tang, C.T., Ruch, F.E., Jr., and Lin, C.C. (1979). Purification and properties of a nicotinamide adenine dinucleotide-linked dehydrogenase that serves an *Escherichia coli* mutant for glycerol catabolism. J. Bacteriol. *140*, 182-187.

Tawara, E. and Kamo, N. (1991). Glucose transport of *Haloferax volcanii* requires the $Na(^{+})$-electrochemical potential gradient and inhibitors for the mammalian glucose transporter inhibit the transport. Biochim. Biophys. Acta *1070*, 293-299.

Thompson, J.D., Higgins, D.G., and Gibson, T.J. (1994). CLUSTAL W: improving the sensitivity of progressive multiple sequence alignment through sequence weighting, position-specific gap penalties and weight matrix choice. Nucleic Acids Res. *22*, 4673-4680.

Thorner, J.W. and Paulus, H. (1973). Catalytic and allosteric properties of glycerol kinase from *Escherichia coli*. J. Biol. Chem. *248*, 3922-3932.

Toews, C.J. (1967). The kinetics and reaction mechanism of the nicotinamide-adenine dinucleotide phosphate-specific glycerol dehydrogenase of rat skeletal muscle. Biochem. J. *105*, 1067-1073.

Tomlinson, G.A. and Hochstein, L.I. (1972). Studies on acid production during carbohydrate metabolism by extremely halophilic bacteria. Can. J. Microbiol. *18*, 1973-1976.

Toraya, T. (2000). Radical catalysis of B12 enzymes: structure, mechanism, inactivation, and reactivation of diol and glycerol dehydratases. Cell Mol. Life Sci. *57*, 106-127.

Toraya, T. (2003). Radical catalysis in coenzyme B12-dependent isomerization (eliminating) reactions. Chem. Rev. *103*, 2095-2127.

Toraya, T., Kuno, S., and Fukui, S. (1980). Distribution of coenzyme B12-dependent diol dehydratase and glycerol dehydratase in selected genera of *Enterobacteriaceae* and *Propionibacteriaceae*. J. Bacteriol. *141*, 1439-1442.

Uthandi, S., Saad, B., Humbard, M.A., and Maupin-Furlow, J.A. (2010). LccA, an archaeal laccase secreted as a highly stable glycoprotein into the extracellular medium by *Haloferax volcanii*. Appl. Environ. Microbiol. *76*, 733-743.

Van Aelst, L., Hohmann, S., Zimmermann, F.K., Jans, A.W., and Thevelein, J.M. (1991). A yeast homologue of the bovine lens fibre MIP gene family complements the growth defect of a *Saccharomyces cerevisiae* mutant on fermentable sugars but not its defect in glucose-induced RAS-mediated cAMP signalling. EMBO J. *10*, 2095-2104.

van Ooyen, J. and Soppa, J. (2007). Three 2-oxoacid dehydrogenase operons in *Haloferax volcanii*: expression, deletion mutants and evolution. Microbiology *153*, 3303-3313.

Van Spanning, R.J., Houben, E., Reijnders, W.N., Spiro, S., Westerhoff, H.V., and Saunders, N. (1999). Nitric oxide is a signal for NNR-mediated transcription activation in *Paracoccus denitrificans*. J. Bacteriol. *181*, 4129-4132.

Varga, M.E. and Weiner, J.H. (1995). Physiological role of GlpB of anaerobic glycerol-3-phosphate dehydrogenase of *Escherichia coli*. Biochem. Cell Biol. *73*, 147-153.

Veiga-da-Cunha, M. and Foster, M.A. (1992). 1,3-Propanediol:NAD+ oxidoreductases of *Lactobacillus brevis* and *Lactobacillus buchneri*. Appl. Environ. Microbiol. *58*, 2005-2010.

Ventosa, A., Nieto, J.J., and Oren, A. (1998). Biology of moderately halophilic aerobic bacteria. Microbiol. Mol. Biol. Rev. *62*, 504-544.

Voegele, R.T., Sweet, G.D., and Boos, W. (1993). Glycerol kinase of *Escherichia coli* is activated by interaction with the glycerol facilitator. J. Bacteriol. *175*, 1087-1094.

Wagner, A.F., Demand, J., Schilling, G., Pils, T., and Knappe, J. (1999). A dehydroalanyl residue can capture the 5'-deoxyadenosyl radical generated from *S*-adenosylmethionine by pyruvate formate-lyase-activating enzyme. Biochem. Biophys. Res. Commun. *254*, 306-310.

Wallace, I.S., Choi, W.G., and Roberts, D.M. (2006). The structure, function and regulation of the nodulin 26-like intrinsic protein family of plant aquaglyceroporins. Biochim. Biophys. Acta *1758*, 1165-1175.

Wallace, I.S., Wills, D.M., Guenther, J.F., and Roberts, D.M. (2002). Functional selectivity for glycerol of the nodulin 26 subfamily of plant membrane intrinsic proteins. FEBS Lett. *523*, 109-112.

Walz, A.C., Demel, R.A., de Kruijff, B., and Mutzel, R. (2002). Aerobic *sn*-glycerol-3-phosphate dehydrogenase from *Escherichia coli* binds to the cytoplasmic membrane through an amphipathic $\alpha$-helix. Biochem. J. *365*, 471-479.

Wang, G., Louis, J.M., Sondej, M., Seok, Y.J., Peterkofsky, A., and Clore, G.M. (2000). Solution structure of the phosphoryl transfer complex between the signal transducing proteins HPr and $IIA^{glucose}$ of the *Escherichia coli* phosphoenolpyruvate:sugar phosphotransferase system. EMBO J. *19*, 5635-5649.

Wang, Z.X., Kayingo, G., Blomberg, A., and Prior, B.A. (2002). Cloning, sequencing and characterization of a gene encoding dihydroxyacetone kinase from *Zygosaccharomyces rouxii* NRRL2547. Yeast *19*, 1447-1458.

Wang, Z.X., Zhuge, J., Fang, H., and Prior, B.A. (2001). Glycerol production by microbial fermentation: a review. Biotechnol. Adv. *19*, 201-223.

Wanner, C. and Soppa, J. (1999). Genetic identification of three ABC transporters as essential elements for nitrate respiration in *Haloferax volcanii*. Genetics *152*, 1417-1428.

Wassef, M.K., Sarner, J., and Kates, M. (1970). Stereospecificity of the glycerol kinase and the glycerophosphate dehydrogenase in *Halobacterium cutirubrum*. Can. J. Biochem. *48*, 69-73.

Weaver, C.D. and Roberts, D.M. (1992). Determination of the site of phosphorylation of nodulin 26 by the calcium-dependent protein kinase from soybean nodules. Biochemistry *31*, 8954-8959.

Wegmann, K., Ben Amotz, A., and Avron, M. (1980). Effect of temperature on glycerol retention in the halotolerant algae *Dunaliella* and *Asteromonas*. Plant Physiol. *66*, 1196-1197.

Weigel, N., Kukuruzinska, M.A., Nakazawa, A., Waygood, E.B., and Roseman, S. (1982a). Sugar transport by the bacterial phosphotransferase system. Phosphoryl transfer reactions catalyzed by enzyme I of *Salmonella typhimurium*. J. Biol. Chem. *257*, 14477-14491.

Weigel, N., Powers, D.A., and Roseman, S. (1982b). Sugar transport by the bacterial phosphotransferase system. Primary structure and active site of a general phosphocarrier protein (HPr) from *Salmonella typhimurium*. J. Biol. Chem. *257*, 14499-14509.

Weissenborn, D.L., Wittekindt, N., and Larson, T.J. (1992). Structure and regulation of the *glpFK* operon encoding glycerol diffusion facilitator and glycerol kinase of *Escherichia coli* K-12. J. Biol. Chem. *267*, 6122-6131.

Wek, R.C., Sameshima, J.H., and Hatfield, G.W. (1987). Rho-dependent transcriptional polarity in the *ilvGMEDA* operon of wild-type *Escherichia coli* K12. J. Biol. Chem. *262*, 15256-15261.

Wiedmann, M., Arvik, T.J., Hurley, R.J., and Boor, K.J. (1998). General stress transcription factor $\sigma^B$ and its role in acid tolerance and virulence of *Listeria monocytogenes*. J. Bacteriol. *180*, 3650-3656.

Wing, H.J., Williams, S.M., and Busby, S.J. (1995). Spacing requirements for transcription activation by *Escherichia coli* FNR protein. J. Bacteriol. *177*, 6704-6710.

Wistow, G.J., Pisano, M.M., and Chepelinsky, A.B. (1991). Tandem sequence repeats in transmembrane channel proteins. Trends Biochem. Sci. *16*, 170-171.

Woodson, J.D., Reynolds, A.A., and Escalante-Semerena, J.C. (2005). ABC transporter for corrinoids in *Halobacterium sp*. strain NRC-1. J. Bacteriol. *187*, 5901-5909.

Xavier, K.B., Martins, L.O., Peist, R., Kossmann, M., Boos, W., and Santos, H. (1996). High-affinity maltose/trehalose transport system in the hyperthermophilic archaeon *Thermococcus litoralis*. J. Bacteriol. *178*, 4773-4777.

Xie, Y. and Reeve, J.N. (2005). Regulation of tryptophan operon expression in the archaeon *Methanothermobacter thermautotrophicus*. J. Bacteriol. *187*, 6419-6429.

Yang, B., Gerhardt, S.G., and Larson, T.J. (1997). Action at a distance for *glp* repressor control of *glpTQ* transcription in *Escherichia coli* K-12. Mol. Microbiol. *24*, 511-521.

Yang, B. and Larson, T.J. (1996). Action at a distance for negative control of transcription of the *glpD* gene encoding *sn*-glycerol 3-phosphate dehydrogenase of *Escherichia coli* K-12. J. Bacteriol. *178*, 7090-7098.

Yang, B. and Larson, T.J. (1998). Multiple promoters are responsible for transcription of the *glpEGR* operon of *Escherichia coli* K-12. Biochim. Biophys. Acta *1396*, 114-126.

Yazdani, S.S. and Gonzalez, R. (2007). Anaerobic fermentation of glycerol: a path to economic viability for the biofuels industry. Curr. Opin. Biotechnol. *18*, 213-219.

Ye, S.Z. and Larson, T.J. (1988). Structures of the promoter and operator of the *glpD* gene encoding aerobic *sn*-glycerol-3-phosphate dehydrogenase of *Escherichia coli* K-12. J. Bacteriol. *170*, 4209-4215.

Yeh, J.I., Charrier, V., Paulo, J., Hou, L., Darbon, E., Claiborne, A., Hol, W.G., and Deutscher, J. (2004). Structures of Enterococcal glycerol kinase in the absence and presence of glycerol: correlation of conformation to substrate binding and a mechanism of activation by phosphorylation. Biochemistry *43*, 362-373.

Yeh, J.I., Chinte, U., and Du, S. (2008). Structure of glycerol-3-phosphate dehydrogenase, an essential monotopic membrane enzyme involved in respiration and metabolism. Proc. Natl. Acad. Sci. USA *105*, 3280-3285.

Yu, P. and Pettigrew, D.W. (2003). Linkage between fructose 1,6-bisphosphate binding and the dimer-tetramer equilibrium of *Escherichia coli* glycerol kinase: critical behavior arising from change of ligand stoichiometry. Biochemistry *42*, 4243-4252.

Zaigler, A., Schuster, S.C., and Soppa, J. (2003). Construction and usage of a onefold-coverage shotgun DNA microarray to characterize the metabolism of the archaeon *Haloferax volcanii*. Mol. Microbiol. *48*, 1089-1105.

Zardoya, R. (2005). Phylogeny and evolution of the major intrinsic protein family. Biol. Cell *97*, 397-414.

Zeilstra-Ryalls, J.H. and Kaplan, S. (1996). Control of *hemA* expression in *Rhodobacter sphaeroides* 2.4.1: regulation through alterations in the cellular redox state. J. Bacteriol. *178*, 985-993.

Zeng, G., Ye, S., and Larson, T.J. (1996). Repressor for the *sn*-glycerol 3-phosphate regulon of *Escherichia coli* K-12: primary structure and identification of the DNA-binding domain. J. Bacteriol. *178*, 7080-7089.

Zeng, X. and Saxild, H.H. (1999). Identification and characterization of a DeoR-specific operator sequence essential for induction of *dra-nupC-pdp* operon expression in *Bacillus subtilis*. J. Bacteriol. *181*, 1719-1727.

Zhang, Z., Gosset, G., Barabote, R., Gonzalez, C.S., Cuevas, W.A., and Saier, M.H., Jr. (2005). Functional interactions between the carbon and iron utilization regulators, Crp and Fur, in *Escherichia coli*. J. Bacteriol. *187*, 980-990.

Zhao, N., Oh, W., Trybul, D., Thrasher, K.S., Kingsbury, T.J., and Larson, T.J. (1994). Characterization of the interaction of the *glp* repressor of *Escherichia coli* K-12 with single and tandem *glp* operator variants. J. Bacteriol. *176*, 2393-2397.

Zhou, G., Kowalczyk, D., Humbard, M.A., Rohatgi, S., and Maupin-Furlow, J.A. (2008). Proteasomal components required for cell growth and stress responses in the haloarchaeon *Haloferax volcanii*. J. Bacteriol. *190*, 8096-8105.

Zhou, Y., Zhang, X., and Ebright, R.H. (1993). Identification of the activating region of catabolite gene activator protein (CAP): isolation and characterization of mutants of CAP specifically defective in transcription activation. Proc. Natl. Acad. Sci. USA *90*, 6081-6085.

Zhu, M.M., Lawman, P.D., and Cameron, D.C. (2002). Improving 1,3-propanediol production from glycerol in a metabolically engineered *Escherichia coli* by reducing accumulation of *sn*-glycerol-3-phosphate. Biotechnol. Prog. *18*, 694-699.

Zhu, Y. and Lin, E.C. (1986). An evolvant of *Escherichia coli* that employs the L-fucose pathway also for growth on L-galactose and D-arabinose. J. Mol. Evol. *23*, 259-266.

Zillig, W., Stetter, K.O., and Janekovic, D. (1979). DNA-dependent RNA polymerase from the archaebacterium *Sulfolobus acidocaldarius*. Eur. J. Biochem. *96*, 597-604.

Zubay, G., Schwartz, D., and Beckwith, J. (1970). Mechanism of activation of catabolite-sensitive genes: a positive control system. Proc. Natl. Acad. Sci. USA *66*, 104-110.

Zurbriggen, A., Jeckelmann, J.M., Christen, S., Bieniossek, C., Baumann, U., and Erni, B. (2008). X-ray structures of the three *Lactococcus lactis* dihydroxyacetone kinase subunits and of a transient intersubunit complex. J. Biol. Chem. *283*, 35789-35796.

# BIOGRAPHICAL SKETCH

Katherine Sherwood Rawls was born to Stephen and Frances Sherwood at the Indian River Memorial Hospital in Vero Beach, Florida. From August of 1998 to June of 2002, Katherine attended Vero Beach High School during which time she competed at local, state, and international levels of science fair competition in the category of Microbiology. After graduating as Salutatorian of her high school class in June of 2002, she received scholarships from the Florida Bright Futures Foundation, the Gator Boosters Foundation, the First Baptist Church of Vero Beach, Florida, and the Daughters of the American Revolution to pursue a Bachelor's of Science degree in Microbiology and Cell Science at the University of Florida. During her undergraduate career at the University of Florida, she performed research in Dr. Julie Maupin-Furlow's laboratory under the guidance of Gosia Gil-Ramadas where she examined the genomic organization of proteasomal genes in *H. volcanii*, resulting in her first publication. In 2004, Katherine received the University of Florida Presidential Scholar award and was inducted into the Golden Key International Honor Society. In 2005, she received the University of Florida Institute of Food and Agricultural Sciences (IFAS) Research Internship Award, allowing her to perform research in Dr. Julie Maupin-Furlow's lab, where she focused on the overproduction of *H. volcanii* TrmA in *E. coli*. She graduated *Cum Laude* from the University of Florida in May of 2006, after which she received an Alumni Fellowship Award to continue her graduate studies in Dr. Julie Maupin-Furlow's laboratory. As a graduate student, Katherine has attended numerous conferences including the American Society of Microbiology (ASM) Florida Branch and National Annual Meetings, the Florida Genetics Institute Research Symposium, and the Gordon Research Conference. She has additionally served as the graduate conference

organizer for the first, annual Department of Microbiology and Cell Science Undergraduate Research Symposium and as an organizer for the Department of Microbiology and Cell Science Fall 2007 and Spring 2008 seminar series. She has received various graduate honors including the Grand Speaker Award (at the 2007 and 2008 Florida Branch ASM Meetings), the first place poster award (at the 2010 University of Florida Departments of Microbiology and Cell Science and Molecular Genetics and Microbiology Joint Graduate Research Symposium), a nomination for the 2007 University of Florida Jack L. Fry Excellence in Teaching award, the Richard and Mary Finkelstein Student Travel Grant (at the 2008 National ASM Meeting), the 2008 IFAS Travel Grant Scholarship, and the 2009-2010 Doris Lowe and Earl and Verna Lowe Graduate Scholarship. The work presented in this dissertation has resulted in the publication of two, peer-reviewed primary author research articles with a third research article and a review in preparation.

On October 24, 2009, Katherine married Colin Douglas Rawls, who recently received a Master's degree in Economics from the University of Florida. Upon completion of her degree, Katherine plans to pursue a government or academic career in molecular biology.